Catalytic Production of Biodiesel

Madsen, Anders Theilgaard

Publication date:
2011

Document Version
Publisher's PDF, also known as Version of record

Catalytic Production of Biodiesel






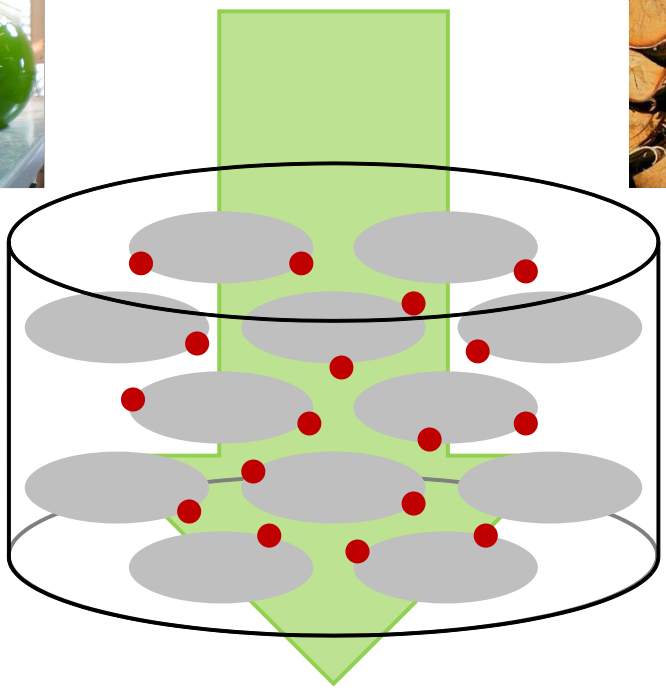
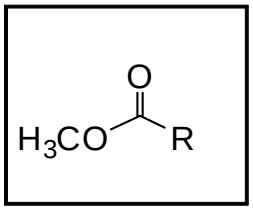

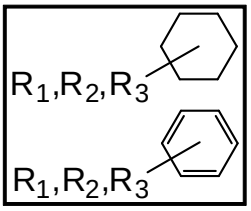

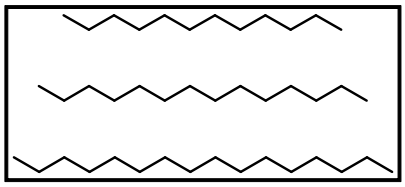
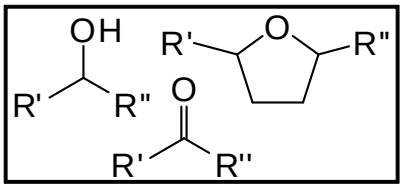

Anders Theilgaard Madsen

Ph.D. Thesis
Technical University of Denmark
Department of Chemistry

June 2011

Centre for Catalysis and Sustainable Chemistry

DTU

Catalytic Production of Biodiesel

Anders Theilgaard Madsen

Ph.D. Thesis
Technical University of Denmark
Department of Chemistry
June 2011

WASTE 2 VALUE
2. generations biodiesel til transportsektoren

Danish National Research Foundation's
Center for Sustainable and Green Chemistry

Preface

The present thesis is submitted in candidacy for obtaining the Ph.D.-degree from the Technical University of Denmark (DTU). The Ph.D.-project has been carried out from January 2008 to June 2011, initially under the supervision of professor Claus Hviid Christensen at the Center for Sustainable and Green Chemistry (CSG). When Claus sought new career opportunities professor Rasmus Fehrmann took over supervision of the project in the current Centre for Catalysis and Sustainable Chemistry (CSC).

The topic of the project has been the production of diesel oil from biomass, which may me produced via a number of different heterogeneous catalytic routes. The experimental work have focused on two of these methods, both starting from fats and oils, namely the esterification and transesterification with methanol over acid and base catalysts to yield fatty acid methyl esters, and the hydrodeoxygenation over supported transition-metal catalysts to yield straight-chain alkanes.

Financial support from the Danish Research and Innovation Council under the innovation consortium "Waste-2-value" is gratefully acknowledged. Of the participants in Waste-2-value special mention and thanks are due to Jakob S. Engbæk, Jesper Bøgelund, Sune D. Nygaard, and Jens Christiansen from the chemistry and materials groups at the Danish Technological Institute for spending effort and time in preparing esterification catalysts and supports as well as for scientific and technical discussions. It has been inspiring and instructive to work together with Danish companies having an practical interest in catalysis research.

I have had the pleasure of working together with a number of people to whom I wish to express my sincere thanks: El Hadi Ahmed for performing many of the batch hydrodeoxygenation experiments and synthesising a range of catalysts for that purpose; Olivier Nguyen van Buu for synthesising a lot of the catalysts for the esterification and transesterification experiments; Lene Fjerbæk from the University of Southern Denmark (SDU) for performing catalyst activity tests; Johannes Due-Hansen and Uffe Vie Mentzel for an endless number of fruitful discussions on all technical matters arising during the years as well as moral and scientific support. I wish to stress my thankfulness to all the students and employees from both CSG and CSC for a helpful, social, and supportive working environment.

I finally wish to express my utmost gratitude towards the Catalysis group at the Process Chemistry Centre, Åbo Akademi, Finland, for hosting my research stay there and helping to make it indeed memorable. Especially professor Dmitry Murzin, associate professor Päivi Mäki-Arvela, and Kari Eränen for their assistance and dedicated supervision. Special thanks go to Bartosz Rozmysłowizc, Toni Riittonen, and Atte Aho for good companionship, help, and fruitful discussions.

Anders Theilgaard Madsen

Abstract

The focus of this thesis is the catalytic production of diesel from biomass, especially emphasising catalytic conversion of waste vegetable oils and fats.

In chapter 1 an introduction to biofuels and a review on different catalytic methods for diesel production from biomass is given. Two of these methods have been used industrially for a number of years already, namely the transesterification (and esterification) of oils and fats with methanol to form fatty acid methyl esters (FAME), and the hydrodeoxygenation (HDO) of fats and oils to form straight-chain alkanes. Other possible routes to diesel include upgrading and deoxygenation of pyrolysis oils or aqueous sludge wastes, condensations and reductions of sugars in aqueous phase (aqueous-phase reforming, APR) for monofunctional hydrocarbons, and gasification of any type of biomass followed by Fischer-Tropsch-synthesis for alkane biofuels. These methods have not yet been industrialised, but may be more promising due to the larger abundance of their potential feedstocks, especially waste feedstocks.

Chapter 2 deals with formation of FAME from waste fats and oils. A range of acidic catalysts were tested in a model fat mixture of methanol, lauric acid and trioctanoin. Sulphonic acid-functionalised ionic liquids showed extremely fast convertion of lauric acid to methyl laurate, and trioctanoate was converted to methyl octanoate within 24 h. A catalyst based on a sulphonated carbon-matrix made by pyrolysing (or carbonising) carbohydrates, so-called sulphonated pyrolysed sucrose (SPS), was optimised further. No systematic dependency on pyrolysis and sulphonation conditions could be obtained, however, with respect to esterification activity, but high activity was obtained in the model fat mixture. SPS impregnated on opel-cell Al_2O_3 and microporous SiO_2 (ISPS) was much less active in the esterification than the orignal SPS powder due to low loading and thereby low number of strongly acidic sites on the real catalyst. The ISPS-packed-bed catalysed conversion of rapeseed oil revealed low activity but advantageous flow properties. A number of functionalised, organic bases have been tested for their activity in transesterification of trioctanoate with methanol, especially guanidines. The activity for trioctanoate conversion was promising, however, hygroscopic catalysts be may lead to saponification of the triglyceride.

Hydrodeoxygenation is treated in chapter 3. The reaction routes and activity in batch hydrodeoxygenation are strongly dependent on the supported noble metal catalyst and temperature used for the conversion to alkanes. Generally, Pt and Pd were the most active metals and have highest selectivity for decarboxylation reaction. Stearic or oleic acid were converted much faster than tripalmitin. The deoxygenation was performed in a continuous trickle-bed reactor over 2 wt% Pd/Sibunit at 300°C. 10 wt% stearic acid yielded almost complete and selective conversion to heptadecane in 5% H_2/Ar at 20 bar, however pure Ar gas led to deactivation. A deactivation profile by coking builds up as a function of the distance from the reactor inlet. A constant conversion of 12% was obtained with neat stearic acid in 7 days time-on-stream of the spent catalyst. The activity for deoxygenation in continuous mode decreased as stearic acid > ethyl stearate > tristearin under 5 % H_2 in Ar, while lack of H_2 in the feed quickly led to complete deactivation of the catalysts in all feeds.

The work is concluded with a summary and an outlook in chapter 4.

Dansk Resumé

Hovedemnet i denne afhandling er katalytisk fremstilling af diesel fra biomasse, med særligt fokus på katalytisk omdannelse af affaldsfedtstoffer som slagteriaffald, brugte stegeolier o.a.

Kapitel 1 giver en kort introduktion til biobrændstof og en redegørelse for publicerede metoder til dieselfremstilling fra biomasse. Homogent katalyseret forestring og omestring af fedtstoffer med methanol til såkaldt FAME og hydrodeoxygeneringen af fedtstoffer til alkaner er de to metoder, der er udbredt i industriel skala til dato. Diesel fra biomasse kan dog også fremstilles ved opgradering og deoxygenering af tjære og slam og pyrolyse-olier, ved raffinering af kulhydrater via kondensationer og reduktion i vandfase til monofunktionaliserede kulbrinter og ved komplet forgasning og efterfølgende Fischer-Tropsch-syntese til alkaner. De sidste metoder er endnu ikke blevet opskaleret til industriel skala, men kan blive betydende i fremtiden grundet billigere og lettere tilgængelige råstoffer.

Kapitel 2 omhandler fremstillingen af FAME fra affaldsfedt. En række forskellige sure katalysatorer er blevet testet i en modelblanding af methanol, laurinsyre og trioctanoin. Et antal sulfonsyrefunktionaliserede ioniske væsker viste nærmest omgående omsætning af laurinsyre til methyllaurat, mens trioctanoat var fuldt omdannet til methylcaprylat efter et døgn. En type katalysatorer baseret på sulfatiserede pyrolyserede kulhydrater (SPS), primært sukrose, blev i batch-forsøg fundet velegnede baseret på høj aktivitet grundet høj surhed og er derfor blevet yderligere optimeret. Der er ikke fundet nogen systematisk afhængighed på aktiviteten for forestring af pyrolyse- og sulfoneringsbetingelserne. SPS imprægneret på et åben-cellet Al_2O_3-ekstrudat og mikroporøse SiO_2-piller (ISPS) var langt mindre aktiv i forestringen end SPS grundet et lavt antal stærke sure centre. ISPS anvendt som pakket katalysatorleje i kontinuerte reaktorer for forestringen af methanol og laurinsyre eller oliesyre viste tilsvarende moderat eller lav aktivitet. Forskellige organiske baser som f.eks. guanidiner er blevet anvendt som katalysatorerer til omestringen af trioctanoin med methanol. Aktiviteten for omdannelse til methyloctanoat er lovende for de stærke baser, men forsæbningen af fedtstofferne er en uønsket sidereaktion, som kan finde sted ved brug af hygroskopiske baser.

Hydrodeoxygenering behandles i kapitel 3. Reaktionsveje og aktivitet i batch-reaktor er stærkt afhængige af hvilket supporteret ædelmetal, der anvendes som katalysator, samt af reaktionstemperaturen. Pt og Pd er generelt de mest aktive ædelmetaller og har ligeledes højest selektivitet mod decarboxylering. Stearinsyre og oliesyre blev i de udførte forsøg omdannet væsentlig hurtigere end tripalmitin. Deoxygeneringen blev ligeledes undersøgt over et katalysatorleje af 2 wt% Pd/Sibunit i en kontinuert rørreaktor med ved 300°C. En 10 wt% opløsning af stearinsyre gav næsten fuld omsætning og selektivitet til n-heptadecan i 20 bar 5% H_2/Ar, mens ren Ar resulterede i deaktivering. En konstant omsætning på 12 % ren stearinsyre kunne efterfølgende opnås i 5% H_2/Ar. En deaktiveringsprofil opbyggedes i reaktoren som funktion af afstanden fra indløbet. I 5% H_2/Ar blev stearinsyre omsat hurtigere end ethylstearat, der blev omsat hurtigere end tristearin, men skifte til ren Ar gas førte til deaktivering af katalytsatoren indenfor kort tid med alle de tre reaktanter.

Afslutningsvis gives en perspektivering af arbejdet i kapitel 4.

Publications

List of published work and conference contributions during the Ph.D. project.

Scientific peer-reviewed articles in international journals

Anders Theilgaard Madsen, Bartosz Rozmysłowizc, Teuvo Kilpiö, Päivi Mäki-Arvela, Kari Eränen, Dmitry Murzin, "Step changes and deactivation behaviour in the continuous decarboxylation of stearic acid", (2011), submitted

Anders Theilgaard Madsen, El Hadi Ahmed, Claus Hviid Christensen, Anders Riisager, Rasmus Fehrmann, "Hydrodeoxygenation of Waste Fat for Diesel Production: Study on Model Feed with Pt/alumina Catalyst", *Fuel*, (2011), accepted

Anders Theilgaard Madsen, Helle Søndergaard, Anders Riisager, Rasmus Fehrmann, "Challenges and Perspectives in the Production of Diesel from Biomass", *Biofuels*, **2**(4), (2011)

Esben Taarning, Anders Theilgaard Madsen, Jorge Mario Marchetti, Kresten Egeblad, Claus Hviid Christensen, "Oxidation of Glycerol and Propanediols in Methanol over Heterogeneous Gold Catalysts", *Green Chem.* **10**, 408-414 (2008)

Poster presentations at international conferences

Anders Theilgaard Madsen, El Hadi Ahmed, Claus Hviid Christensen, "Biodiesel via Hydrotreating of Fat", *9th Netherlands' Catalysis and Chemistry Conference*, Noordwijkerhout, The Netherlands, March 3rd - 5th (2008)

Anders Theilgaard Madsen, El Hadi Ahmed, Claus Hviid Christensen, "Investigation of a model feed for hydrotreating of oils and fats", *INCA summerschool of Green Chemistry*, Venice, Italy, October 12th - 18th (2008)

Anders Theilgaard Madsen, Anders Riisager, Rasmus Fehrmann, "Model feed for catalytic hydrodeoxygenation and fats for biodiesel production", *inGAP-NanoCat summerschool*, Trondheim, Norway, June 21st - 26th (2009)

Anders Theilgaard Madsen, Anders Riisager, Rasmus Fehrmann, "Esterification of free fatty acids in biodiesel production with sulphonated pyrolysed carbohydrate catalysts", *EuropaCat IX*, Salamanca, Spain, August 30th - September 4th (2009)

Anders Theilgaard Madsen, Anders Riisager, Rasmus Fehrmann, "Understanding hydrodeoxygenation of oils and fats", *2nd International Biodiesel Conference*, Munich, Germany, November 15th - 17th (2009)

Oral presentations at international conferences

Anders Theilgaard Madsen, El Hadi Ahmed, Claus Hviid Christensen, "Model Feed for the Hydrotreating of Fat for Biodiesel Production", *2nd EuCheMS Chemistry Congress*, Turin, Italy, September 16th - 20th (2008)

Popular scientific articles (in Danish)

Anders Theilgaard Madsen, Sune Dowler Nygaard, Hans Ove Hansen, Lene Bonde, "Bæredygtigt Brændstof fra Affald", *Aktuel Naturvidenskab*, **6**, 30-33 (2008)

Anders Theilgaard Madsen, Esben Taarning, Claus Hviid Christensen, "Fremtidens Biodiesel: Kom fedtaffald i tanken", *LMFK-bladet*, **1**, 26-30 (2009)

Anders Theilgaard Madsen, Anders Riisager, Rasmus Fehrmann, "Udfordringer og strategier ved produktion af biodiesel", *Dansk Kemi*, **90**(8), 18-21 (2009)

Contents

Chapter 1

Catalysis, Biofuels, and Diesel

For most of the 20th century, mankind and especially the industrialised nations have relied heavily on the cheap and abundant availability of fossil carbonaceous feedstock for transportation fuels, chemicals and energy production (in the form of heat and electricity). However, towards the end of the 20th century and the start of the 21st it has become increasingly evident that humanity faces a number of unprecedented challenges in terms of future energy resources and consumption [1], which may be sketched as:

The environmental challenge: The combustion of fossil oil, gas and coal releases the greenhouse gas CO_2 to the atmosphere from carbonaceous resources that have not been part of the global atmosphere or biosphere for millions of years. The effect of greenhouse gases on the atmosphere are well acknowledged both in terms of global and local climate changes and by a mean global temperature increase [2]. But also the combustion-related emissions of nitrogen oxides, sulphur oxides and aromatic particulates from the consumption of fossil fuels have negative environmental effects as well as being harmful to the health of human beings. The massive human use of consumable goods af all kinds also leads to buildup of solid or liquid waste, which must be treated or disposed of in an ecologically safe and sustainable manner. This recognition is not always fulfilled.

The social challenge: The global population is increasing, and the increasing populations especially in the developing countries require a higher standard of living, thereby increasing the demand for electricity, housing, fuel, sanitation, consumables, clean water, and food.

The resource challenge: The projected gradual depletion of easily accessible fossile resources of oil, gas, and coal, especially mineral oil deposits, is leading to the search for and extraction of less accessible carbonaceous resources like tar sands, deep-water oil deposits or deposits in ecologically sensitive areas. These extraction methods will become more costly in terms of both energy, processing and labour, and will take place in increasingly inhabitable areas of the world like the Arctic, Canada, Siberia, or the like [1]. This happens while the global energy demand is increasing.

The ostensibly ever-increasing demand for fertiliser, plastics, consumables, electrical devices, chemicals, fuels and energy put pressure on the existing energy supply and infrastructure, but also spark search for sustainable alternatives and furthers the focus on energy and resource efficiency. This is especially the case for fuel-consuming vehicles.

The most critical feedstock in the chemical industry and refineries is oil, and transportation fuels constitute the largest part of the oil consumption [3]. This means that a global shift towards renewable feedstocks is necessary [4], and biomass is the only renewable carbonaceous material available apart from CO_2. Its use as a base for sustainable fuels and chemicals in the future is therefore indispensable.

In the European Union (EU), the 2003 fuel directive 2003/30/EC mandated that a share of 5.75% energy content should derive from biofuels in 2010, rising to 10% by 2020 [5]. This was enforced by the EU in the 2009 directive for promotion of energy from renewable resources 2009/28/EC. At the same time the EU has opted for a promotion of biofuel production from waste products and a discouragement of "bad biofuels systems" in the Renewable Energy Road Map - i.e., an exclusion of biofuels produced with a low or even negative displacement of CO_2 from the atmosphere, or where the production triggers deterioration of sensitive wild-life habitats and ecosystems [6, 7].

Furthermore, as transportation fuels based on fossil feedstocks are usually the cheapest type of chemicals at all, the production processes for sustainable biofuels must also be economically feasible and the feedstock as cheap as possible.

1.1 Catalysis - Setting the scene

Efficient, economical, and environmentally sound chemical production usually require the aid of catalysis to run at acceptable rates. Most of the western standard of living may be said to be based on the ability of the chemical industry to turn available raw materials efficiently into fuels, chemicals and applicable energy.

It is useful to notice the definition of catalysis: A catalyst is a substance that takes part in and enhances the rate of a chemical reaction without being consumed by the reaction. The science concerned with the rate of reactions is *chemical kinetics*, which also embodies catalysis.

However, reactions have to be thermodynamically favourable to occur, i.e. the reaction must be able to happen spontaneously - it must have a negative Gibbs-free energy. A catalyst does not change the position of chemical equilibrium, but it accelerates the tendence of the reaction towards equilibrium. Popularly coined thermodynamics defines what is possible, and catalysis and kinetics how and how fast it is possible.

Industrial catalysis as a discipline, especially heterogeneous catalysis, has developed largely concurrently with the modern methods of industrial petroleum refining and has steadily allowed more sophisticated use of feedstocks for a growing range of and demand for petroleum products [4, 8]. For instance, a large part of the current diesel and petrol is produced via respectively catalytic hydrocracking and fluid catalytic cracking of heavier fractions from the crude distillation; the hydrodesulphurisation of fuels to make sulphur-free fuels; or the production of hydrogen by steam reforming of natural gas [9].

The shift towards biomass as a feedstock for fuels and chemicals requires development of new catalytic chemistry [8]: Petroleum almost entirely lacks chemical functionalities that can be attacked easily. This is suitable for fuels for internal combustion engines. This also means that most refinery processes are run at high temperatures and with specific catalysts to activate the petroleum compounds. However, biomass is from a petrochemical viewpoint over-functionalised especially with respect to oxygen, and thus the conversion into applicable fuels or chemicals usually require removal or defunctionalisation of most or all of these functionalities, depending on feedstock type.

Catalysis will likely gain an even higher importance as a discipline, and a profound knowledge

of the science behind it, as well as harnessing it on a technical scale will be of utmost importance for the future chemical industry.

1.2 Diesel as a biofuel

The production of biomass diesel is growing. The different possibilites for producing diesel oils from biomass resources have undergone substantial research in the latter years, and a number of catalytic methods have now been established: Fats and oils can either be transesterified with alcohol to form fatty acid alkyl esters [10–15], deoxygenated with hydrogen to form n-alkanes [16–24], or cracked at elevated temperatures to form a hydrocarbon mixture [22, 25–27]. Carbohydrates may be converted by aqueous-phase-reforming to form unfunctionalised or monofunctional hydrocarbons [28–31]. Biomass in general may be gasified to syn-gas and undergo Fischer-Tropsch-synthesis [32–35], or bio-oils can be produced by flash pyrolysis and upgraded by cracking or hydrogenation [36–41]. The possibilities are sketched in Figure 1.1.

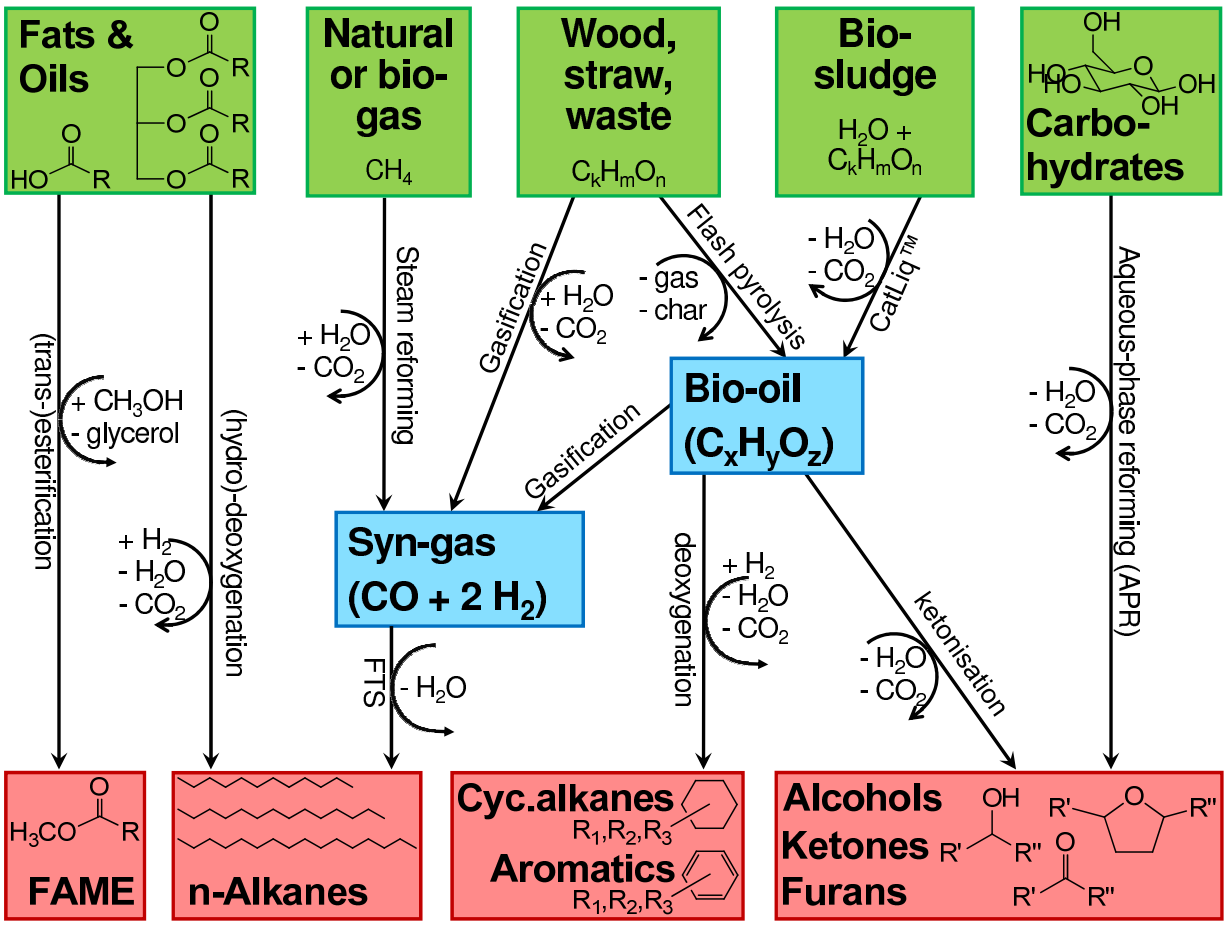

Figure 1.1: An overview of feedstocks, conversion routes and products as plausible components in the production of diesel from biomass.

The term "biodiesel" usually refers solely to as fatty acid alkyl esters, and again mostly the methyl esters (FAME) are considered [42]. However others have suggested wider definitions and raised points about too narrow focus regarding naming the fuels [43–45]. For the sake of clarity the term

"biodiesel" will be avoided in the present thesis and the technical-chemical terms for each fuel will be used instead. The market share of FAME is the largest of the diesel oils from biomass, but it is nonetheless not the only one.

Pure vegetable oils or fats are not biodiesel fuels and cannot be used as such. Engine and fuel system require modifications to be able to run on these fuels, and these changes are often illegal for road vehicles and lead to annulment of engine warranties and specifications for emissions. The combustion in the engine has a tendency to become incomplete, and both particle and NO_x emissions are reported to rise. Plant oils are also too viscous to be pumped in the fuel and injector systems [13, 46].

1.3 Fatty acid alkyl esters from fats and oils

The most applied method for producing diesel from biomass as well as the one which has received most attention the latter years is the alcoholysis or transesterification of fats and oils to yield fatty acid alkyl esters (FAAE). Usually the alcohol is methanol due to lowest cost, easiest separation and highest reaction rates obtained, whereby methyl esters of the fatty acids (FAME) result [47, 48]. FAME can be used directly in the engine without modification and can be mixed in all ratios with traditional diesel fuel.

1.3.1 Industrial production of fatty acid methyl esters

Fats and oils consist primarily of triglycerides (TG). These, as well as mono- and diglycerides, can be transesterified into FAMEs by methanol, see Figure 1.2. The sources of the TGs can be all types of vegetable oils, animal fats, or waste greases [48, 49]. A successful transesterification leads to two phases: a bottom phase containing the glycerol and an upper phase containing the FAME.

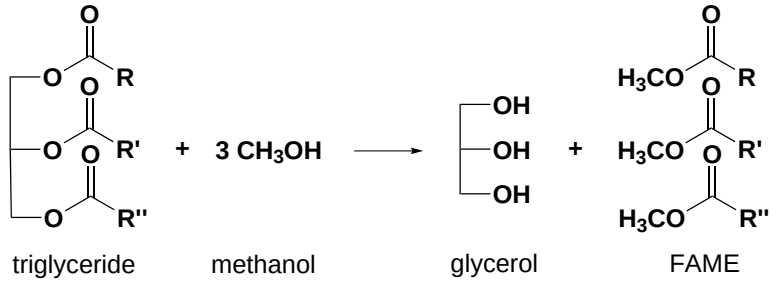

Figure 1.2: Transesterification of a triglyceride with methanol, yielding glycerol and fatty acid methyl esters.

1.3.1.1 Transesterification

In industrial practise, the reaction is performed at 60-70°C and is catalysed by a few wt% of a strong base - the hydroxides or methoxides of sodium or potassium are used as homogeneous catalyst, KOH being the norm due to its low price [48, 50, 51]. One molecule of glycerol is obtained as a by-product for every three FAME molecules produced.

The transesterification is equilibrium-driven and in fact reversible. However, due to use of 2-3 times molar excess of methanol and the immiscibility of FAME and alcohols, above 99% yield of FAME can usually be obtained within a few hours of reaction [47, 48]. The oil- and FAME-phase (non-polar) and the alcohol phase (polar) are not directly miscible with each other. This means that, initially, the reaction is slow and dependent on vigorous mixing of the two phases (e.g. by stirring) to get a large contact area between the two phases. During reaction, di- and mono-glycerides are formed, and these compounds act as emulsifiers for the reaction mixture. Once the transesterification is nearing completion, the two phases start to separate again (settling) [13]. Industrially the transesterification is normally performed in a stirred batch-reactor, and as sufficient settling often requires longer time than the transesterification reaction itself, the settling is often performed in a separate settling-tank [52].

1.3.1.2 Esterification

The homogeneous, base-catalysed transesterification is working efficiently, but it gives rise to a number of challenges. First and foremost oils and fats may contain free fatty acids (FFA). Most fresh vegetable oils usually do not contain problematic amounts of free fatty acids, but especially waste fats are challenging: 2 to 7 wt% FFA for used cooking oils, 5 to 30 wt% for waste animal fats and abattoir waste, and some trap greases can contain over 50 wt% FFA [12, 13]. The FFAs will react with the basic catalyst and form soap, and when the feedstock contains more than about 0.5-1 wt% the reaction becomes unacceptably slow due to consumption of base otherwise intended for transesterification, and the formed soap emulsifies the phases and hinders the settling and separation after reaction [48].

For this reason, the FFAs must first be reacted with methanol to form FAME. Esterifications are acid-catalysed, and in the industry a few wt% sulphuric acid, H_2SO_4 is often used for this purpose. An acidic esterification step is therefore performed prior to the basic transesterification. Sulphuric acid is the cheapest acid and has the advantage of being both strong and very hygroscopic. The mixture of methanol and fat is esterified for a few hours at 60-70°C , around the boiling point of methanol, with stirring so as to bring the content of free fatty acids below 0.5 wt% (as is shown in Figure 1.3) prior to the transesterification [48].

Thus, two consecutive reaction steps are needed. The esterification by homogeneous acid leads to a number of other challenges: First of all the acid solution from esterification must be neutralised and made alkaline with the addition of the base for the transesterification, and even by the end of transesterification acid must again be added to neutralise the alkaline alcohol-phase. This naturally yields large amounts of salts as by-products (usually K_2SO_4 and $KHSO_4$). This has no immediate use. Furthermore it is necessary to use new homogeneous catalysts for each FAME batch. Another issue with this is the purification of glycerol and excess methanol afterwards, which is often contaminated with water and salt [52]. An immediate decantation removing most of the salt can however be made after settling.

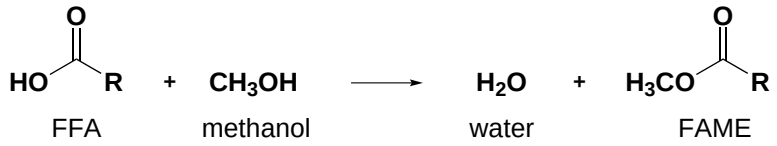

Figure 1.3: Esterification of a Free Fatty Acid (FFA) with methanol to yield FAME and water.

In principle, the transesterification can be catalyzed by both bases and acids leaving room for a one-step acid-catalysed process, but the base-catalysed reaction is 3-4 orders of magnitude faster than the acid-catalysed reaction [10, 47, 48, 53]. Heating the batch to at least 150-200°C must be performed for completion of the transesterification with acid catalyst within an acceptable time-scale. This requires working with pressurised equipment (due to the vapor pressure of methanol, which has a normal boiling-point of 64.6°C (STP)), and is therefore usually disregarded and considered uneconomical at least with sulphuric acid.

It is of major interest to substitute the homogeneous catalysts with heterogeneous catalysts. This

would avoid the formation of inapplicable salt by-products, lower the expenses for buying catalysts for each batch of FAME, and prevent the equipment corrosion by dissolved H_2SO_4 in the methanol. Water formed by the neutralisation of H_2SO_4 with KOH will contribute to soap formation of FFAs formed via basic hydrolysis of glycerides. Also, a solid catalyst would allow easier operation in a liquid-liquid-solid plug-flow-reactor with static mixers, which may be much more desirable with regards to labour demand, process control, -layout and -supervision, and optimisation of product quality [48, 54].

1.3.2 Basic catalysts for transesterification

1.3.2.1 Inorganic metal-oxide bases

A wide range of basic oxides have been investigated as catalysts for transesterification of oils and fats with methanol. Alkali or earth-alkali metal oxides or hydroxides are generally very basic and thus active, but usually the monometallic metal oxides tend to dissolve in the methanol over time [55]. Calcining MgO with ZrO_2, however, yielded a bimetallic oxide with high basicity almost unaffected by dissolution [56, 57]. CuO, CoO, and MnO supported on Al_2O_3 have been studied and yielded up to 97% FAME at room temperature, dependent on the calcination temperature [58]. ZnO and Al_2O_3–ZnO mixed oxide [59, 60] were investigated as well as rare-earth oxides [61], but both required high temperatures (at least 200°C) for conversion of vegetable oils and methanol to FAME. However, bimetallic oxides of calcium ($Ca_2Fe_2O_5$, $CaMnO_3$, $CaCeO_3$, $CaTiO_3$ and $CaZrO_3$) have also been investigated and catalysed transesterification with methanol at 60°C, usually with good reusability of the oxide [62].

Porous materials like zeolites BEA, USY, and FAU and mesoporous silicalites like KIT-6, ITQ-6, SBA-15, and MCM-41 have been ion-exchanged with La^{3+}, Mg^{2+}, or K^+ and tested [63–65], however, high activities for transesterification to FAME are usually only obtained at higher temperatures (>150°C) with some ion-exchanged porous silicalites, and it is a question if too small pores in the material is not a hindrance for reaction.

Basic hydrotalcites have been extensively tested. These are comprised of layered units of mixed Al_2O_3–MgO, and due to their basicity and special porosity they are potential catalysts for transesterification to form FAME. Compared to other inorganic porous bases hydrotalcites often have superior activities for transesterification [66, 67]. Several researchers have characterised their properties and catalytic activity in relation to composition and calcination conditions [68–72]. Activity enhancements of the hydrotalcites have as well been studied, for instance by doping with Cs, Ba, Sr, or La [73], by substitution of Al with Fe [74], or substitution of part of the Mg with Co [75]. Embedding hydrotalcite on a polymer-support was as well successful [76].

1.3.2.2 Organic amine bases

A number of different organic amines and derivatives functionalities have shown to be applicable for the transesterification of oils and fats: Earlier a number of alkylguanidines or cyclic guanidines have been suggested as very active catalysts for transesterification, and substituted tetramethyl guanidine (R-TMG) or substituted 1,5,7-triazabicyclo[4,4,0]dec-5-ene (R-TBD) nested on PS/PVB polymer

supports have been suggested as heterogenised analogoues - due to very strong Lewis-basic sites [77, 78]. Up to 90% yield after 1 h methanlysis over 1 wt% of the homogeneous guanidines was obtained, and almost the same could be achieved over the heterogenised analogues [77, 78]. Carbon nanotubes doped with amines or gem-diamines have recently shown activity in the transesterification of triglycerides, however, reaction times were longer even at slightly elevated temperatures (up to 115°C) [79, 80].

Methyl-substituted phosphazenium catalysts (based on units of P–(N–$(CH_3)_x)_4$) could be applied as a strongly basic catalyst, either unsupported or linked to silica support [81, 82]. The unsupported catalysts yielded over 90% FAME in 15 min [81] at 60°C, while the supported phosphazeium had much lower activity, dependent on the loading of active compound on SiO_2 [82].

Transesterification reactions to achieve various alkyl mono- and diesters have been performed with moderate success with amino-functionalised SBA-15, which however required 110°C and 24 h reaction time [83]. Base-functionalised metal-organic frameworks (MOF) and supported quarternary substituted ammonium groups for methanolysis of various esters have been investigated [84, 85], but the highest ester formation activity reported has been 60% after 4 h at 60°C over 1 wt% of quarternary substituted ammonium functionalities [85].

1.3.3 Acidic catalysts for esterification

1.3.3.1 Acidic inorganic oxides and derivatives

Metal-oxide supported and zirconium phosphate-supported tungstated catalysts ($WO_3/M(P)O_x$) have been investigated for the esterification of FFA, which readily takes place between 60 and 200°C - at the highest temperatures the transesterification reaction of the glycerides is also pronounced [86–90]. Related to the solid tungstated oxides are the so-called heteropolyacids, based most regularly on tungsten or molybdenum phosphate. They are strong acids in their protonated form, and may be supported on metal oxide or even carbon [91]. By substituting some protons with a cation, for instance $Zr_{0.7}H_{0.2}PW_{12}O_{40}$, the acids became even more acidic and catalysed both esterification and transesterification at 65°C within 4 to 8 h [92]. Completely protonated forms of tungstated and molybdated phosphate and silicates ($H_3PW_{12}O_{40}$, $H_4SiW_{12}O_{40}$, $H_3PMo_{12}O_{40}$, and $H_4SiMo_{12}O_{40}$) had different acidity, which however did correlate with transesterification activity: Molybdated samples where more active than tungstated ones [93]. This trend changed when supporting the catalysts on silica support [94]. A range of experiments were conducted with 12-tungstophosphoric acid ($H_3PW_{12}O_{40}$) supported on various materials, which easily catalysed the esterification of FFA in waste oils between 25°C and 60°C [95–97]. Also, a multifunctionalised mixture of $H_3PW_{12}O_{40}$ supported on Nb_2O_5 or Ta_2O_5 (and optionally SiO_2) was active for esterification at benign conditions [98, 99], and tuning this by adding non-polar alkyl groups to the structure enhanced reaction rates [100]. Some heteropolyacids may, however, suffer from leaching of the acidic species to methanol [101].

Related again to the tungstated oxides are sulphated metal oxides. For instance, the sulphated oxides of TiO_2, SnO_2 and ZrO_2 have been suggested as novel acidic catalysts for the esterification of FFA with methanol to form FAME, as well as for the simultaneous transesterification of the triglycerides

[102–107]. The same oxides were as well evaluated supported on or mixed with high-surface-area supports of Al_2O_3 or SiO_2 [102, 108–111]. It should be noted that some authors have reported leaching of sulphate species to the methanol solution from SO_4^{2-}/MO_x by hydrolysis due to formation of water by esterification. This is likely dependent on calcination conditions [107].

1.3.3.2 Acidic micro- and mesoporous silicalites

Various Brøndsted-acidic zeolites have been shown to remove FFA via esterification at 60°C [112]. Higher temperatures were, however, required for Brøndsted-acidic Al-MCM-41 to esterify FFA [113]. By functionalisation of MCM-41 and SBA-15 through impregnation and grafting with respectively acidic WO_3, Keggin- & Preyssler-type heteropolyacids and sulphonic acid functionalities, esterification of FFA with methanol could be achieved [114–116]. However, the grafted sulphonic acid had far more superior activity to the other grafted acids on mesoporous supports, providing 55% ester yield at 60°C after 6 h over 0.4 wt% catalyst. MCM-41 functionalised with organic linkers and tin-triflate functionalities have been tested for FAME synthesis from methanol and soybean oil at 65-70°C with ultrasonic or microwave activation and up to 74% yield at 70°C after 2 h were achieved [53] due to the use of microwaves.

1.3.3.3 Organic sulphonic acids

Amongst the acidic catalysts for esterification of FFA one type of organic acid has been studied most extensively, namely sulphonic acids ($R–SO_3H$). Simple sulphonic acids soluble in methanol include methanesulphonic acid ($MeSO_3H$) and p-toluenesulphonic acid, however solid sulphonic acids can be prepared by sulphonation in sulphuric acid and thus grafting the functionality onto polymeric supports; the resulting acid is often as strong as or stronger than sulphuric acid. Commercial resin-type sulphonic acids can be purchased even in amounts applicable on a technical scale, for instance ion-exchange resins [117], and some are specifically marketed as catalysts for esterification of FFA. Esterification was performed over various Amberlyst-resins and Dowex HCR-W2-resins between 30°C and 65°C [118, 119], and satisfactory lowering of the FFA amount was achieved within these conditions. Amberlyst BD20-resin was found superior to Amberlyst 15-resin, both with respect to recycling of the catalyst and tolerance to water [120]. A study between the commercial cation-exchange resins NKC-9, 001x7, and D61 proved the former to be superior with FFA and methanol, yielding about 90% conversion of FFA at 62°C after 2 h [121].

A number of polymer-based sulphonic-acids have been prepared for the esterification reaction and studied in the literature, for instance starting from PVA-PS/PVB [122], PS [123, 124], sulphonated PV and PS [125], or mesoporous silica with grafted functional groups [126], or polyanilines deposited on carbon [127]. The yields of sulphonic acid groups are usually between 0.6 and 6.0 mmol/g of the total supported catalyst mass. In all cases, esterification of FFA may be performed under normal operating conditions of 60°C with 1-2 times molar excess of methanol.

Another approach for obtaining a sulphonic acid-containing polymer was first proposed by Toda et al. [128]. Initially a carbohydrate source, eg. sucrose, glucose, starch, or cellulose is carbonised (or pyrolysed) under inert atmosphere at around 400°C for 4-24 h, then the resulting carbonated

carbohydrate (now consisting of small graphene layers [129]) is sulphonated with concentrated or fuming sulphuric acid at elevated temperatures (around 150°C) for 4-24 h. Low surface areas are obtained of the carbon material itself and its sulphonated derivative, which however increase upon swelling in hydrophilic solvent. Nonetheless the catalyst is very active in the esterification of FFA at 60°C [130, 131]. The sulphonic acid obtained by this scheme had comparable strength to that of H_2SO_4 [132]. By following this procedure, a carbohydrate-based sulphonic acid was obtained which was investigated for both esterification and transesterification in methanol at 150°C and 17 bar. While FAME did result from both reactions, leaching of sulphonic acid functionalities occured at these conditions [133]. If the carbohydrate source is first impregnated on mesoporous silicas, porosity and hydrophobicity can be tailored to the reaction desired [134], and esterification can take place at a faster rate due to an increased surface area induced by the support [135].

1.3.4 Alternative catalytic technologies for fatty acid methyl ester production

1.3.4.1 Ionic liquid (trans-)esterification

Brønsted-functionalised acidic ionic liquids (ILs) have recently been suggested as alternative esterification catalysts [136]. ILs are salts, usually organic, with a melting point below 100°C. Thus they can be used as catalysts and/or solvents for numerous reactions. Even though ionic liquids have been reported as a reaction medium for traditional catalysts [137–139], ILs can be functionalised by incorporating a sulphonic acid functionality, yielding a very strong acid which at the same time can be used as a liquid reaction medium or stirred/dissolved into the reaction mixture and afterwards separated [140]. This makes ionic liquids suitable catalysts for the esterification and transesterification reactions [136]. The cation may for instance be based on substituted imidazolium or pyridinium ions functionalised with a sulphonic acid, and anions should preferably be very weak bases such as bis-triflat or methyl sulfonate [136, 140, 141]. The melting point of the ILs must be below the reaction temperature for FAME synthesis, as the activity is otherwise too low [140]. By functionalising the IL with more sulphonic acid functionalities the IL may get an even higher catalytic activity [142].

1.3.4.2 Enzymatic (trans-)esterification

Besides chemical catalysts, lipases from different microorganisms can also be applied for esterification and transesterification. The conditions are often mild, usually around 25-50°C. Furthermore lipases may catalyse both the transesterification and the esterification [47]. For the lipases to be applied in industrial FAME production they must be immobilised on a carrier material, preferably porous to give a high surface area [143–146]. Unfortunately the catalytic activity is not to date reported to be of the same magnitude as the basic and acidic catalysts [10, 50]. Activity can sometimes be enhanced by using a co-colvent, though [147, 148]. Some lipases may as well be rendered inactive by too high concentrations of methanol, and continuous addition of methanol, genetically altering the lipases or switching alcohol can therefore be necessary [149, 150].

1.3.4.3 Supercritical (trans-)esterification

As an alternative to using catalysts, the esterification and transesterification may also be performed with supercritical methanol (P_{Cr} = 81 bar, T_{Cr} = 234.5°C) [151]. Adding for instance carbon dioxide or hexane as co-solvent or an inorganic base as catalyst to the supercritical methanol can furthermore improve the yield of FAME [152–155]. However, the super-critical conditions require equipment suitable for high pressures and temperatures, and the energy and economical balances for this may not be advantageous.

1.3.5 Glycerol

The main by-product of the transesterification of fats and oils with alcohol is glycerol, as seen in Figure 1.2 on page 13. Producing one ton of FAME yields about 100 kg of glycerol, and it has previously been estimated (in 2006) that the production of glycerol would be 6 times more than the demand in 2020 due to the production of fatty acid methyl esters [156]. While this figure may be exaggerated today as the growth in production of FAME has not been as explosive as projected, valorisation can still be an important contribution to the overall economy of the FAME process.

A few suggested reactions of glycerol into more valuable chemicals are seen in Figure 1.4, including reduction, dehydration, oxidation, or complete gasification into synthesis gas for production of for instance methanol. A number of reviews on glycerol conversion to value-added chemicals are available [157–159].

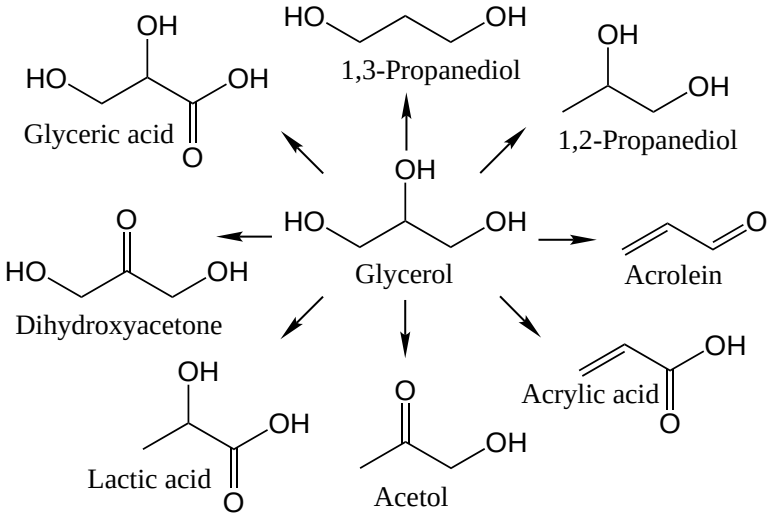

Figure 1.4: Overview of some of the reactions of glycerol.

1.3.5.1 Dehydration

Glycerol can be dehydrated into acrolein over acidic catalysts. Both acrolein and its oxidised derivatives (acid and esters) are industrial polymer building blocks produced annually on megaton-scale [160]. Various solid acids have been proposed as catalysts for this, eg. acidic zeolites in aqueous or gaseous phase [161–163], over silica-alumina or vanadium phosphate acids [164], Nb_2O_5 [165], HPAs [166], or even near-critical water dehydration to acrolein. Acrylic acid may afterwards be ob-

tained by oxidation of acrolein [167]. The dehydration intermediate acetol (hydroxyacetone) may also be employed. A scheme employing catalytic reactive distillation has been proposed to give high acetol yields in the gas-phase [168].

1.3.5.2 Reduction

Selective reduction of glycerol with hydrogen can yield either 1,2-propanediol (1,2-PD, propylene glycol) or 1,3-propanediol (1,3-PD), usually in a mixture dependent on the catalyst used while 1- or 2-pronanol may result as by-products. 1,3-PD can be used as a building block for polymers or as an antifreeze, while 1,2-DP has use as solvent or antifreeze [157, 158]. High selectivity towards either propanediol is challenging and difficult to obtain, while a resulting mixture of propanediols may be difficult to separate. High or complete selectivity towards 1,2-PD have been achieved by using Raney copper [169], Cu_2O or ZnO supported catalysts [170], or Ru/C possibly together with a cation exchange resin [171–173]. A selectivity of 49% for 1,3-PD has been achieved over $Re_yIr_{1-y}O_x/SiO_2$ in aqueous solution [174], while also tungstic acid improved the selectivity towards 1,3-PD [170]. It has been suggested that adding Brønsted acidic catalyst enhances selectivity towards 1,3-PD, for instance over $Pt/WO_3/ZrO_2$ [175].

1.3.5.3 Oxidation

Being a triol glycerol can undergo oxidation resulting in a network of various products. Dihydroxyacetone (DHA) and glyceric acid, the primary intermediates in the glycerol oxidation network find use in the pharmaceutical or food industry and must be obtained by selective oxidation - a challenging task for catalytic chemistry [157]. On an industrial scale the oxidant should preferably be atmospheric oxygen. Especially supported Pt, Pd or preferably Au have been shown effective for the aqueous conversion, often at high selectivities. In excess base and aqueous solvent 100% selectivity towards the glycerate anion was achieved over 1% Au/C [176]. Without added base and over acidic Au-Pt/H-MOR zeolite, 81% selectivity at full conversion has been achieved [177]. Glyceric acid can also be synthesized by anodic oxidation of glycerol using an Ag_2O electrode [178]. Oxidation is selective towards the DHA over supported Bi-Pt in acidic media [179, 180], while anodic oxidation yielded only 25% selectivity as optimum [181]. The alkaline alcohol mixture separated out from FAME production may also be oxidised directly over Au/TiO_2 to form methyl glycerate, dimethyl tartronate or dimethyl mesoxalate [182].

Polylactic acid has potential to become the green and biodegradable plastic of the future, and glycerol can be converted directly to lactic acid by fermentation. Recently the lactate anion was obtained by alkaline hydrothermal reaction of glycerol at 280°C, albeit by consuming equimolar amounts of base [183]. Conversion via DHA or glyceraldehyde may be more efficient, for instance by electrochemical oxidation and isomerisation [184], or as recently suggested via Lewis-acidic catalysts [185, 186].

Microorganisms can selectively perform some of the above-mentioned reduction or oxidation reactions by fermentation routes often with excellent selectivity [159], however these usually work only at low temperatures, low aqueous concentrations and reaction rates, while from an industrial

point of view concentrated streams and high turnovers with minimised reactor volumes and more tolerant chemical catalysts are preferred.

1.3.5.4 Derivatisation

Valorisation of glycerol could also be afforded by derivatisation of the molecule itself. Suggested reactions in the literature include etherification with iso-butenes to give octane enhancers for gasoline [156, 187, 188], acetalisation with ketones and aldehydes [189], or condensation with carbonic acid to afford monoglyceride carbonate as an oxygenated diesel additive [190]. The catalytic synthesis of etherified oligomers and polymers of glycerol have as well been described for upgrading of the compound [191].

1.3.5.5 Synthesis Gas

Glycerol may also be steam reformed into synthesis gas (syn-gas). This has been studied for instance over transition-metal catalysts of Pt, Pt-Re, Rh, or Co supported on for instance C, Al_2O_3 or CeO_2–Al_2O_3 [192–195]. Depending on conditions, by-production of tar-like compounds can interfere and lead to clogging of systems and deactivation of reforming catalysts [196]. The syn-gas obtained from steam reformed glycerol can furthermore be used for hydrogen production, for instance for use in fuel cells, or it can be converted into methanol via the methanol synthesis or hydrocarbons via the Fischer-Tropsch-synthesis (FTS) [197].

1.4 Hydrodeoxygenation of fats and oils

The hydrodeoxygenation of fats and oils is an alternative and a quite different approach for upgrading fatty feedstock. It was first industrialised by Finnish Neste Oil at their refinery in Porvoo, Finland, who refer to the product as "NExBTL" (Next generation Biomass-To-Liquids) as described by Koskinen et al. [43] and Mikkonen [45]. Other names suggested are "green diesel" or "renewable diesel", albeit the latter seem to be the preferred term [198]. The approach usually requires hydrogen, and may be idealised as shown in Figure 1.5. Based on recent literature the catalysts for upgrading fats and oils can be divided into three categories, namely 1) supported sulphided metals, 2) supported (noble) metals or 3) acid-base catalysts for cracking-type deoxygenation.

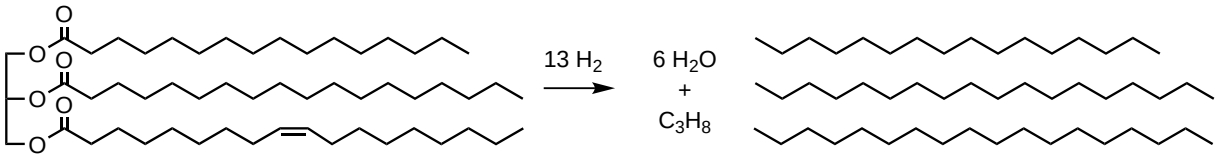

Figure 1.5: Hydrogenation (full reduction) of a triglyceride to yield propane, water and long-chain alkanes.

From literature it is evident, however, that not only a full reduction of the feedstock is possible, but other reactions compete as well, namely decarboxylation of the carboxylate functionality (ester or carboxylic acid) to yield an n-alkane and CO_2, and decarbonylation to yield a 1-n-alkene, water, and CO. The loss of the carboxylate functionality as CO or CO_2 results in shortening the fatty acid carbon chain by one carbon of the resulting alkane or 1-alkene, contrary to the full reduction which conserves the number of carbon atoms in the carbon chains.

The latter two routes are illustrated in Figure 1.6. The preferential reaction routes are largely determined by the conditions of the process and the specific catalyst used. Generelly noble-metal catalysts have notable preference for the decarboxylation and decarbonylation pathways, while the sulphided metal catalysts tend to favour the full reduction, although the picture is often more varied. The deoxygenation over cracking-type catalysts does, due to higher temperature and often high acidity, also yield cracking-type products (see Figure 1.8 on page 25).

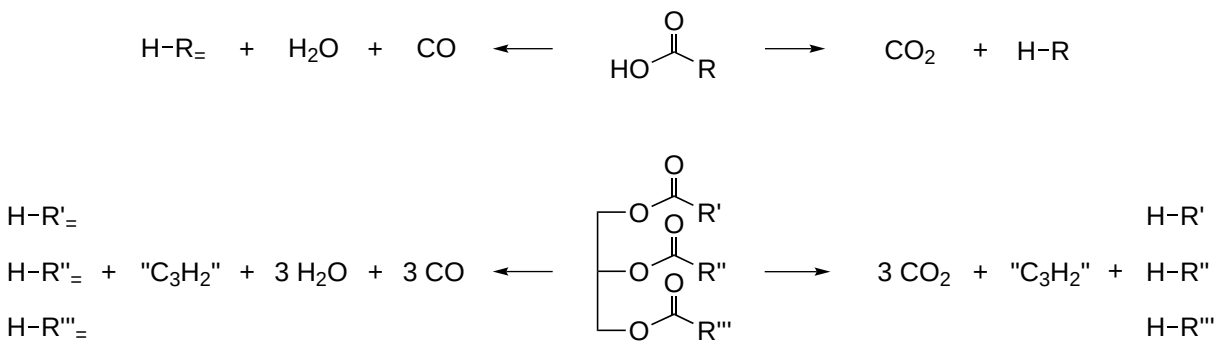

Figure 1.6: Decarbonylation *(left-hand side)* and decarboxylation *(right-hand side)* idealised reaction schemes for deoxygenation of free fatty acids and triglycerides in oils and fats. $R_=$ denotes a terminal double-bond.

1.4.1 Supported sulphided metal catalysts

Kubička and co-workers evaluated the conversion of rapeseed oil over sulphided CoMo and NiMo supported primarily on Al_2O_3, at 250-350°C and 7 to 110 bar H_2. The activity of sulphided $NiMo/Al_2O_3$ superseeded that of separate Mo/Al_2O_3 and Ni/Al_2O_3 in liquid phase HDO [199], and full conversion of rapeseed oil over three commercial sulphided $NiMo/Al_2O_3$ at 70 bar H_2 was only achieved at >310°C, while lower temperatures left free fatty acids and triglycerides in the product mixture [200]. At 20-110 bar H_2 and 300-320°C sulphided CoMo supported on mesoporous Al_2O_3 and MCM-41 it was observed that higher yields of alkanes were achieved with lewis-acidic Al_2O_3 as support, but building Al into the framework of MCM-41 to make the support acidic improved the yields [201, 202]. The primary reaction route of sulphided $NiMo/Al_2O_3$ was towards full reduction, which however decreased on behalf of decarbonylation/decarboxylation reaction with rising temperature and increasing conversion, while unsulphided Ni/Al_2O_3 had the highest selectivity towards decarbonylation/decarboxylation products [203].

The co-treating of sunflower oil and heavy vacuum oil (from petroleum distillation) over sulphided $NiMo/Al_2O_3$ was studied by Huber et al at 300-450°C at 50 bar in a tubular flow reactor, which yielded a maximum carbon yield of 71% of C_{15}-C_{18} n-alkanes from the oil. Cracking reactions rose with temperature, as did the isomerisation of resulting n-alkanes [18]. Co-treating was also evaluated by Šimáček et al. with respectively 0% or 5% rapeseed oil in vacuum-gas oil (from petroleum distillation) at 400-420°C, which yielded similar fuel properties [22].

Donnis and co-workers confirmed that both reduction and decarboxylation can take place in the hydrotreatment over sulphided $NiMo/\gamma$-Al_2O_3, and selectivity to decarboxylation products from rapeseed oil of as much as 64% at full conversion was obtained during deoxygenation in light gas oil at 45 bar H_2 and 350°C [41]. The treating of pure palm oil was recently performed by Guzman et al over $NiMo/Al_2O_3$ at 40-90 bar H_2 and 350°C. The selectivity to even-carbon n-alkanes (complete reduction) was observed to increase with H_2 pressure [21].

Krause et al studied the HDO of heptanoic acid, heptanol, methyl and ethyl heptanoate over sulphided $CoMo/Al_2O_3$ and $NiMo/Al_2O_3$ [204, 205]. The treatment was performed at 250°C and 15 or 75 bar H_2. NiMo, but not CoMo was very sensitive to the sulphidation conditions using either H_2S and CS_2, while the unsulphided catalysts were neither very active nor selective to C_6 and C_7 alkane formation. Acid functionalities on the catalysts mediate esterification and dehydration of some intermediates [205, 206].

Sulphided catalysts require that sulphur must be added as for instance H_2S or CS_2, or the feedstocks must be co-treated with sulphur-containing compounds like refinery gas oils - otherwise the sulphided catalysts deactivate (desulphidise) by incorporation of sulphur in the product stream [205]. The comsumption of hydrogen should optimally be minimised to save cost for the treatment, so higher selectivity for decarboxylation or decarbonylation as described by Donnis et al. is advantageous [41] - if methanation does not prove to be a problem. A great asset of this procedure is the absence of formed aromatics.

1.4.2 Supported transition-metal catalysts

The deoxygenation of fatty feedstock over supported transition metal catalysts has been studied mostly by the group of Murzin and Mäki-Arvela at Åbo Akademi. Usually conversion of saturated feedstock like stearic acid, ethyl stearate, and tristearine to alkanes have been studied, normally between 270-360°C in inert gas or in a mixture with H_2 at up to 40 bars.

In a screening of a range of active catalyst metals and supports Snåre et al. found that Pt or Pd supported on carbon were most active and had the highest selectivities for decarboxylation of stearic acid to n-heptadecane [17]. In connected works Pd/C was used as catalyst to convert tristearine, ethyl stearate, and stearic acid to alkanes, which was modelled by Snåre, Kubičková and co-workers [16, 207], as well as the kinetics for deoxygenation of other fatty acids [23, 208]. It could be concluded that conversion of the carboxylic acid itself took place almost exclusively via decarboxylation, but ester functionalities underwent more complicated mechanisms in the conversion to n-alkanes [16, 207].

In semibatch reaction-mode, Rosmysłowicz et al. studied deoxygenation of C_{18} tall oil fatty acid over Pd on Sibunit carbon and found considerable impact on the conversion to C_{17}-hydrocarbons from the concentration of hydrogen in the gasphase [20]. Crocker and co-authors studied conversion of triglycerides over carbon-supported Ni, Pd and Pt at 350°C without added hydrogen and observed CO_2, CO, CH_4 and small hydrocarbons in the gasphase, a range of liquid alkanes and heavier paraffins, as well as free fatty acids as intermediates [209]. By studying the transformation of methyl octanoate and methyl stearate over Pt/Al_2O_3 at 330°C in He and H_2 gas it was found by Do et al. that H_2 suppresses formation of higher self-condensates of both compounds and that decarbonylation is always the primary reaction route [210].

Palladium and platinum as catalysts have also been investigated on a number of nanoporous and microporous supports. Lestari et al. investigated deoxygenation of stearic acid over Pd on SBA-15 [211], Ping and co-authors used Pd on and in a mesocellular SiO_2-foam also to deoxygenate stearic acid [212], while Kikhtyanen and co-workers applied Pd/SAPO-31 for the conversion of sunflower oil [24]. Hancsók and co-authors deoxygenated saturated vegetable oil over Pt/H-ZSM-22/Al_2O_3 to isomerised alkanes [213]. These studies indicated that acidic functionalities of the support lead to modest isomerisation of the formed n-alkanes which improves the cold properties of the fuel, but undesired cracking and deactivation may also take place if the temperature gets too high [213].

From literature it appears that carboxylic acids deoxygenate via decarboxylation (- CO_2), while esters undergo decarbonylation (- CO) - this can however be hard to determine in an experimental setup due to the Water-Gas Shift-equilibrium (WGS), as shown in Figure 1.7 a). The noble metals used as catalysts usually have high selectivity towards decarboxylation or decarbonylation pathways, which minimises the immediate use of hydrogen. Hydrogen is, however, needed to avoid deactivation by aromatisation or CO poisoning. This leads to another problem, namely the formation of methane from CO or CO_2 and 3 or 4 molecules of H_2, see Figure 1.7 b) & c), a highly undesirable situation. The methane may be burned for process heat or steam reformed back to H_2 and CO, but the latter is costly and alone the separation of the gases may be tedious.

Deoxygenation over noble-metal catalysts of real feedstocks like vegetable oils or waste fats has

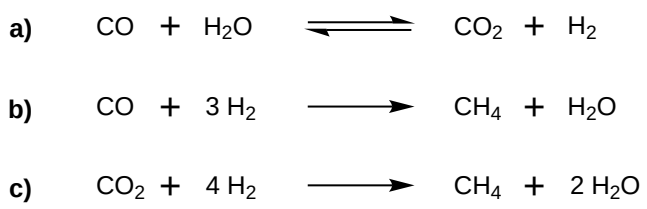

Figure 1.7: Side reactions taking place over a) Water-Gas Shift (WGS), b) & c) CO & CO_2 methanation, respectively.

not been studied extensively and could be challenging. First of all they contain impurities like salts, sterols, phospholipids etc., and secondly the triglycerides in real fatty feedstock are always more or less unsaturated. Deactivation is suspected to form especially from unsaturated fatty acids, for instance from cyclisation, dehydrogenations and Diels-Alder reactions [20, 208, 214]. This means that hydrogen saturation of double-bonds in the fatty acids is also a necessary step in the deoxygenation.

1.4.3 Cracking-type catalysis

The deoxygenation of methyl octanoate over H-ZSM-5 at 500°C resulted lighter hydrocarbon gases and aromatisation, the latter of which proceeded through self-condensation products like tetradecane, 8-pentadecanone and octyl octanoate. The aromatisation selectivity as well as the conversion were much lower at 400°C [215], Interestingly, in the cationic form of zeolite X, methyl octanoate was converted to longer hydrocarbons (C_{14}–C_{16}) over basic CsNaX, without forming any aromatics, while the weakly acidic NaX resulted marked amounts of aromatic production before deactivating the condensation pathways [216].

H-ZSM-5 [217], rare-earth-modified Y-zeolite [26], MCM-41, and mesoporous silica [25] were used to crack palm oil at 400-500°C. Under these circumstances, the reaction mainly yielded gasoline-range hydrocarbons, and the diesel yield was at best moderate. The selectivity to diesel-range hydrocarbons rose with decreasing cracking temperature, however the conversion dropped as well.

Na et al. studied the decomposition of oleic acid in an autoclave at 400°C over basic hydrotalcites, yielding both the decarboxylation products heptadecane and heptadecene as well as cracking products like alkanes and minor carboxylic acids [27]. Quirino et al. studied soybeen oil pyrolytic vapour decomposition over Al_2O_3-supported tin- and zincoxides between 350 and 400°C, which yielded decarboxylation and cracking products of similar composition as Na et al. [218].

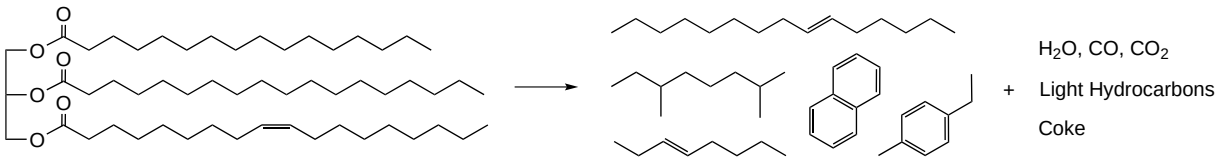

Figure 1.8: The deoxygenation and cracking-type products (alkanes and olefins, light gases, aromatics) formed during conversion of glycerides and fatty acids over acidic porous materials.

Generally the reported yields of hydrocarbons are low in most cases. The liquid yields are mostly in the gasoline range and with less diesel and varying amounts of gases produced, as sketched in Figure 1.8. The aromatisation inside and on the catalysts leads to deactivation by coking, however this problem could be solved if the cracking reactions are performed in a fluid catalytic cracking

system where burning the coke in a regeneration zone is possible (provided that the catalyst can endure this treatment). The aromatics in the product diesel pool are problematic as well and should be minimised for environmental reasons and due to lowering of the cetane number of the diesel [198]. The vapors of uncatalysed pyrolysis of palm, soybean, and castor oil at 350 to 400°C led to a catalytic H-ZSM-5 bed was reported to yield hydrocarbon condensates at over 98% yield without aromatics, but containing shorter-chain fatty acids as a result of C-C scission [219].

1.5 Alternative diesel fuels from biomass

The potential supply of fats and oils with present technology is only sufficient to cover a minor fraction of the present global diesel demand. Utilisation of more abundant biomass resources, namely lignocelluloses, such as straw, wood, fibers etc. is therefore imperative. With regards to diesel three overall strategies exists for this purpose, for instance as sketched by Lange [220]:

1. Upgrading of bio-oils or bio-tars from flash pyrolysis
2. Aqueous-phase reforming of carbohydrates
3. Gasification and Fischer-Tropsch-Synthesis (FTS)

1.5.1 Upgrading of bio-oils

One auspicious way of dealing with lignocelluloses relevant for diesel production is to convert the biomass via so-called *flash pyrolysis*, i.e. fast heating of finely ground biomass to 400-650°C at short residence times, often under inert gas and with sand or other ceramics as a heat carrier. This protocol produces a gas fraction containing various carbonaceous gases, a residual char fraction and various amounts of condensable tars, which are called bio-oils or flash pyrolysis oils. Depending on the pyrolysis conditions the yield of bio-oil may be over half of the biomass input mass.

Another way of producing bio-oils is by hydrothermal upgrading (HTU), for instance the proprietary technology CatLiq, which takes place in aqueous solutions or suspensions at near-critical conditions of water (T_{Cr} = 374°C, P_{Cr} = 221 bar). This treatment leads to dehydration, cyclisations and rearrangements of for instance carbohydrates [221]. Lignocellulose networks are furthermore degraded and the products as well undergo rearrangements, decarbonylations, and decarboxylations [222, 223]. Catalysts, for instance acids, bases or metals can enhance the reactions [223–226]. This may also be applied to aqueous sludge or organic waste streams for instance from food processing plants [227].

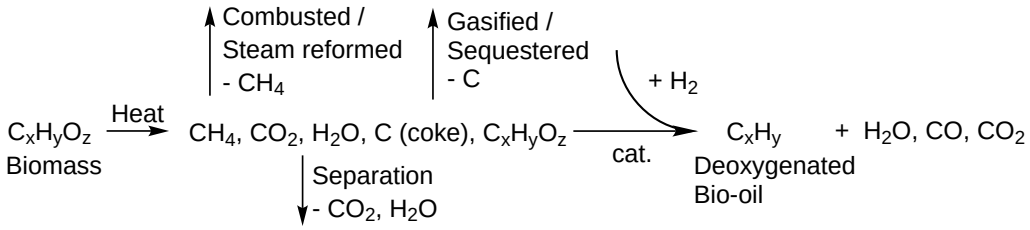

Figure 1.9: Principle behind production and upgrading of bio-oils via flash pyrolysis.

Such bio-oils are comprised of hundreds of different chemical compounds, spanning ketones, aldehydes, carboxylic acids, aromatic ethers, phenols, and alcohols, as well as poly-functional molecules. The oils often contain an emulgated amount of water. They are therefore unsuited for direct use as engine fuels, but they may be catalytically hydrodeoxygenated to various types of fuels: Petrol, jetfuel or diesel - this depends on the distillation properties of the final hydrocarbons. This is sketched in Figure 1.9

Upgrading of bio-oils from flash pyrolysis bears some resemblance to HDO of fatty feedstocks, and the catalysts can also be divided into the same categories, namely cracking-type, sulphided metals and transition metals, with the notable inclusion that bio-oils may also be treated over a catalyst during the pyrolysis itself - so-called catalytic pyrolysis. Necessary H_2 for the reactions should be obtained cheaply, possibly by reforming other biomass, natural gas, or the resulting light gases in the pyrolysis in connection with the HDO upgrading. However the consumption of H_2 is potentially much higher than that for deoxygenation of triglycerides due to a much higher content of both oxygen (high O/C-ratio) and aromatics as can be rationalised from Figure 1.10 [19, 228, 229].

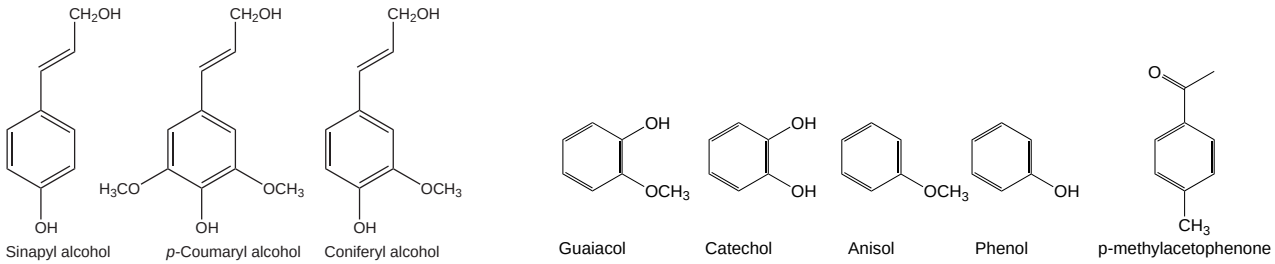

Figure 1.10: *Left-hand side:* Monolignols, the primary monomers that constitute the lignin network in biomass; *Right-hand side:* Different phenolic compounds used for studying upgrading of bio-oil [230].

Upgrading should remove part or all of the oxygenates (decrease O/C-ratio) and saturate aromatics, at least partly (increase H/C-ratio). The presence of aromatics in diesel fuels is limited by fuel standards to some extent [45, 198]. The difference from the well-defined triglyceride molecules largely complicates HDO of bio-oils. Removal of much of the oxygen in the bio-oils as well as water can be a pretreatment to hydrocracking in conventional refinery operation, for instance together with normal petroleum gas-oil feeds, justifying two-stage processes [231, 232]. Small amounts of oxygen in alcohols or ethers may be tolerated in the fuel - in petrol this may enhance the fuel quality in terms of octane number [229].

The conditions for maximal yield of respectively coke, tar, or bio-oils can be tuned via the reaction conditions and retention time for the pyrolysis: Low temperature and long residence time optimises the yield of char, high temperatures and long residence times optimise the yield of smaller gases, while moderate temperature and short residence time is most optimal for bio-oil production - see for instance Bridgwater, Huber or Lange [19, 47, 220, 233].

1.5.1.1 Cracking & catalytic pyrolysis

Aho and co-workers studied the pyrolysis of pine sawdust at 400°C followed by upgrading at 450°C over H-Y, H-BEA and ferrierite as their Fe-modified counterparts, yielding between 43 and 53 wt% liquid [234]. The catalytic pyrolysis over quartz sand, zeolites H-BEA, H-Y, H-ZSM-5 and H-MOR at 450°C gave maximal liquid yield of 27 wt% over quartz sand but highest removal of oxygen over H-ZSM-5 [235]. All materials could be regenerated by oxidation of formed coke [234, 235].

Valle et al. studied valorisation of bio-oil by heating to 400°C for deposition of pyrolytic lignin before cracking the bio-oil at 500°C on H- and Ni-modified Y-zeolites, maintaining low liquid yields and high yield of C_2–C_4 and C_{5+} gases in the catalytic reaction - however CH_4 formation is almost completely avoided [236]. Co-treating of the residue from atmospheric petroleum distillation with

10 wt% pretreated bio-oil containing up to 28 wt% oxygen at 520°C over a standard FCC catalyst was found feasible and yielded normal ranges of light hydrocarbon gases, petrol and coke, likely due to the preceding removal of the most reactive oxygen functionalites in the bio-oil [237].

H-ZSM-5 was more effective than CoO/MoO_3 for the catalytic pyrolysis of lignin at 650°C due to its ability to crack the aliphatic lignin linkers to small hydrocarbon gases [238], while catalytic pyrolysis of glucose at 400-600°C over H-ZSM-5 yielded mostly aromatics and coke - low coke formation and high mono-aromatics formation was optimal at short residence time and high temperature [37]. For glucose and over sugars at 600°C, the type of zeolite catalyst is greatly affecting the yields of aromatics, coke and gases [239].

1.5.1.2 Supported sulphided catalysts

Generally, the deoxygenation over sulphided metal catalysts has been studied at 200-400°C and 10-200 bar of H_2. Delmon et al. investigated sulphided CoMo/C as a catalyst for the HDO of p-methylphenol, p-methylacetophenone, guaiacol and di-ethyldecandioate. Presence and higher concentrations of H_2S in the feed was found to enhance most of the deoxygenation reactions, however not the esters. Diaminopropane was found to inhibit some of the deoxygenation reactions, especially acid sites, which were involved in the ester conversion. It was furthermore found that increasing the loading of active phase on the support did not correlate linearly with an increase in the activity due to larger size of CoMo particles [240–243]. It was found that carbonyl compounds exhibited 1. order rate in reduction behaviour at 200-300°C [244], while in a batch-reactor between at 350-390°C the HDO experimental reaction rate order was found to 2.3 with respect to the total oxygen content, while it was not very dependent on hydrogen pressure.

I batch systems it has been found that the hydrogen pressure only had minor influence on the reaction rate over sulphided CoMo Deoxygenation of various oxygen-containing functionalities showed different reaction orders [245]. This was also observed over sulphided $NiMo/Al_2O_3$, where French and co-authors found that temperature controlled the reaction rate at up to 360°C , high H_2 pressures and. At higher temperatures the loss of carbon by formation of carbonaceous gases (CO, CO_2, CH_4) was considerable. A moderate to high degree of deoxygenation may be attractive, such as leaving a few wt% of the bio-oil as oxygen in the form of ketones or ethers [232].

Sulphided $CoMo/Al_2O_3$ was less active than sulphided $NiMo/Al_2O_3$ for the HDO of guaiacol in batch mode at 200-350°C, but the CoMo was more selective to HDO products [246]. Different phenolic and aliphatic oxygenates were converted over supported sulphided CoMo and NiMo catalyst, and reaction behaviour related to different mechanistic deoxygenation pathways of either phenolic or aliphatic alcohol [247]. Dilchio Rocha and co-authors suggested using pressurised hydrogen over FeS at 520°C in the first stage of single- or two-stage so-called hydropyrolysis of biomass, with supported sulphided NiMo as catalyst in the potential second bed. This procedure reduced the formation of coke and gas and enhanced bio-oil formation with less oxygen functionalities compared to zeolite catalysts [248].

1.5.1.3 Supported metal catalysts

The upgrading of bio-oils by supported metal catalysts is sparsely studied compared to sulphided catalysts - maybe due to suspected deactivation by aromatics and coking - the former largely present in the bio-oils and the latter likely formed herefrom during the HDO process. Elliot et al. studied HDO over Pd/C followed by hydrocracking in a flow system and optimal HDO behaviour was found to be 340°C at 136 bar H_2 [231]. Heeres and co-workers also contributed to the field: At 250 or 350°C and pressures of H_2 at 100 or 200 bar Ru/C was found to be superior to Pt/C and Pd/C as well as Ru supported on SiO_2 or Al_2O_3 and more active than alumina-supported sulphided NiMo and CoMo. The highest oil yield was 60 wt% corresponding to removal of 90% oxygen, with the formed liquid being much less acidic, containing less water, and having a HHV of about 40 MJ/kg [38].

By employing a two-stage hydrodeoxygenation strategy also using Ru/C as a catalyst, the intermediate and produced oils were characterised by a range of analytical techniques to elucidate content of different chemical functionalities. During 3-stage hydrodeoxygenation it was observed that especially carboxylic acids, aldehydes, diols, phenolic groups were removed from the bio-oils from hydrodeoxygenation [249]. By upgrading of bio-oil (O/C = 0.53, H/C = 1.55) in an autoclave it was found that the recovery of carbon in the oil phase increased from 55% at 230°C to 70% at 340°C, the overall H/C ratio decreased from 1.71 to 1.6, and the O/C ratio decreased from 0.33 to 0.18 over a 5 wt% Ru/C catalyst [237]. A number of different commercial and laboratory Ru/C catalysts have been tested, and deactivation observed to take place by coke formation in the pore system. The deactivation was dependent on fabrication procedure, possibly yielding different reactivities depending on particle size of ruthenium on the surface [250].

1.5.2 Aqueous-phase reforming

An different approach to fuels and chemicals production has been pursued especially by the group of James Dumesic and co-workers, who have studied the upgrading of sugars and polyols to hydrocarbons by reforming biomass in water - aqueous-phase reforming (APR). As can ben seen in Figure 1.11, the principle behind this scheme is the simultaneous catalytic reduction and reforming of sugars and sugar derivatives. Polyols are very soluble in water, usually fully soluble, but once they get sufficiently reduced for instance to monofunctional hydrocarbons, at the same time lowering their density, they spontaneously separate to an upper, non-polar hydrocarbon-phase low in oxygen content. A sweep-stream of hydrocarbons may be used to enhance this separation [30].

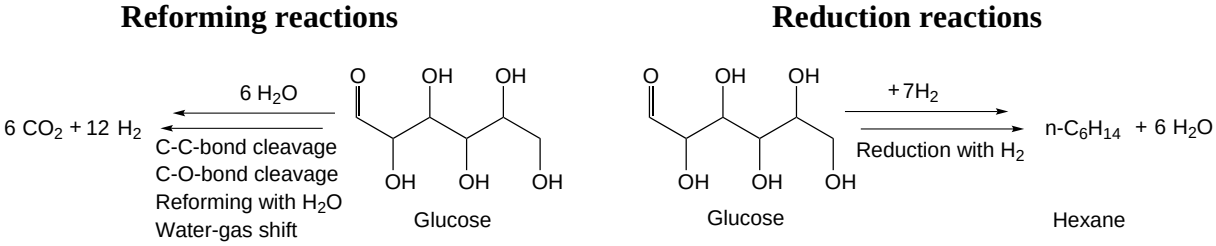

Figure 1.11: Principle behind aqueous-phase reforming of glucose.

1.5.2.1 Aqueous reforming of polyols

A range of catalysts have been suggested for the APR of sorbitol to optimise the hydrocarbon yields, but Pt/SiO_2–Al_2O_3, Pt/ZrO_2 or Pt-Re/C have been found advantageous [251, 252], and it is suggested that a bifunctional catalyst containing a metal and an acid functionality is needed to facilitate all reactions [251, 253]. Pt or Pt-Re alloys facilitate the dehydrogenation and C-C-scissions to liberate CO species, which are then water-gas-shifted to CO_2 and H_2 [252]. Pt has a high activation barrier for breaking the C-O bond meaning that methanation is supressed.

The APR is usually performed around 200-250°C and at pressures of 18-40 bar. Due to the fact that the initial reaction takes place in aqueous environment and at very mild conditions, many known problems of reforming are strongly minimised. Aromatisation reactions are suppressed in the aqueous environment. The water pushes the water-gas-shift equilibrium towards CO_2 and H_2, so deactivation by CO does not take place. The resulting organic liquid contains a mixture of different monofunctional hydrocarbons such as ketones, carboxylic acids, alcohol, and more or less saturated heterocycles in the range of C_4-C_6, while gas-phase-products constitute CO_2 and minor amounts of C_1-C_6 alkanes - some of these can be further upgraded [252, 254].

1.5.2.2 Condensationens prior to reduction

Carbohydrates are built up from units of maximally 6 carbon atoms, meaning that longer hydrocarbons with more than six atoms cannot be obtained without C-C-coupling-reactions. This may be done prior to APR or reduction, as carbohydrates, being polyols with a carbonyl group, may undergo crossed aldol condensation to couple carbonylic compounds, ketones and aldehydes, to other carbonyls. 5-(hydroxymethyl)furfural (HMF), which can be made via dehydrations and isomerisations from fructose, glucose or cellulose [255], is suggested as a sugar derivative that may undergo such reaction. For instance either one or two molecules of HMF may be reacted with acetone over bi-metallic solid oxides, as seen in Figure 1.12, yielding either a C_9 or C_{15} building block that can be reduced with hydrogen [29, 256].

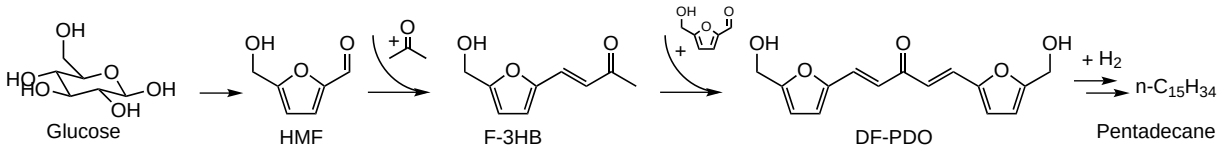

Figure 1.12: Aldol crossed-condensations and reductions from carbohydrate and acetone. Dehydrations in all the reactions are not shown. HMF: 5-(hydroxymethyl)furfural; D-3HB (furfurylalcohol)-3-hydroxybutene; DF-PDO: 1,5-(di-furfurylalcohol)-1,4-penta-dien-3-one.

1.5.2.3 Product condensation & reduction

A final step in the biomass conversion is the reduction of remaining monofunctional hydrocarbons and unsaturated carbon-carbon-bonds. Further processing can then employ various types of catalytic reactions. Cracking can be done over zeolites (eg. H-ZSM-5) to yield a mixture of light hydrocarbon gases, iso-alkanes and aromatics. Light olefins or alcohols via dehydration could be upgraded to larger olefins by oligomerisation, which is proposed as a route to yield diesel-length hydrocarbons

[252]. γ-valerolactone upgrading was investigated in two catalytic reactors in series first by aqueous phase ring-opening and decarboxylation over SiO_2/Al_2O_3 at 375°C to butene, followed by oligomerisation at 170-225°C over for instance H-ZSM-5, while operating up to 36 bars. This gave up to over 75% total yields of C_{8+} hydrocarbons [257].

Ketonisation followed by reduction with hydrogen is proposed as a way to upgrade carboxylic acids migrating to the hydrocarbon phase during the APR. The ketonisation merges two carboxylic acids together, as seen in Figure 1.13. A temperature range of 175-350°C at 5 bar over $CeZrO_x$ catalysts has been investigated, and higher temperatures and low pressures of H_2O and CO_2 were found advantageous for pushing the reaction towards the ketone, as well as suppressing stepwise ester ketonisation [258, 259]. Also acids in flash pyrolysis oils could be ketonised with reasonable success [260].

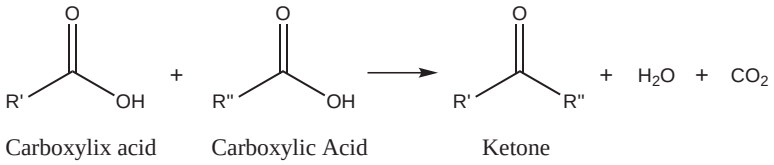

Figure 1.13: Ketonisation of carboxylic acids and hydrogenation.

Two ketone molecules, directly from APR or from subsequent ketonisation may be reacted under acidic conditions to form an enone as condensate (an unsaturated ketone) by splitting off water. Saturation/reduction with hydrogen must be performed immediately of the resulting enone during reaction to pull the equilibrium towards condensation products, as has been proposed over $Pd/Ce_xZr_{1-x}O_y$ at 325-350°C [259, 261].

The mild temperatures, advantageous phase-separation behaviour, and internal production of hydrogen are the main assets of this method. Sugars and polyols are however not as cheap nor abundant as waste lignocellulosic biomass, so a greater feedstock tolerance would make this process extremely viable, for instance such as the cascade-proces recently proposed by Serrano-Ruiz et al. from cellulose via γ-valerolactone and ketonisation to 5-nonanone [262]. Larger water-soluble biomass-derived molecules may pose problems to APR if reacted directly, as they can result heavy coking [29].

1.5.3 Gasification and Fischer-Tropsch-synthesis

The Fischer-Tropsch-synthesis (FTS) was initially developed by German scientists Franz Fischer and Hans Tropsch in the 1920s. By steam gasification of coal, steam reforming of natural gas or gasification of biomass, a synthesis gas (syn-gas) consisting of CO and H_2 can be obtained after some workup, which is used for the FTS yielding primarily straight-chained alkanes. At the time of Fischer and Tropsch coal was the relevant raw material for producing syn-gas, providing a means of turning inexpensive coal into liquid fuels - so-called coal-to-liquids (CTL). This has been employed by Germany during World War II, and South African company Sasol has been using it for over 50 years - the plant in Sasolburg is the biggest point CO_2-emitter in the world [263]. The principle behind this concept based on biomass is shown in Figure 1.14.

Today, the process is based on natural gas in other areas in the world - so-called gas-to-liquids (GTL) - especially near large oil fields with a huge excess of cheap natural gas. However, biomass may also be gasified with sufficient heat and converted to a syn-gas suitable for FTS (H_2/CO-ratio of 2.1), and co-gasification-reforming schemes employing both biomass, natural gas and coal may be advantageous to employ in the future [264]. Gasification may open up to production of other liquids fuels than alkanes from FTS, including methanol, ethanol, DME, and hydrogen [35].

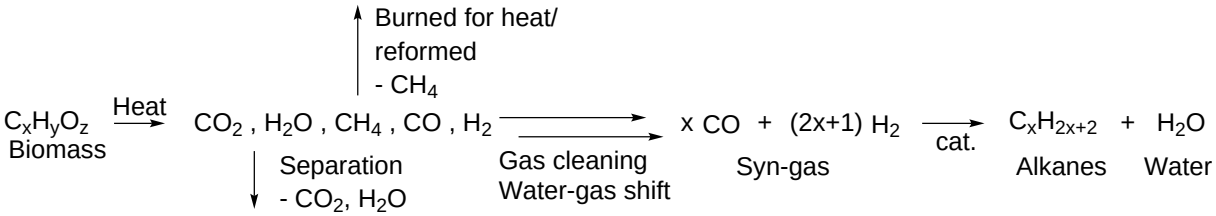

Figure 1.14: Principle behind the biomass gasification and Fischer-Tropsch-synthesis pathway to diesel.

As illustrated in Figure 1.14 also steam and CO_2 as well as small hydrocarbon gases result from gasification. The WGS reaction (Figure 1.7 a) at page 25) can be used to get the desirable H_2/CO-ratio of the syn-gas. Afterwards CO_2 and H_2O is separated from the mixture.

A large part of the carbon from gasification ends up as CO_2. In terms of carbon capture and sequestration (CCS) this procedure has the advantage of producing the CO_2 concentrated and maybe at elevated pressure. Thus having a net negative CO_2-emission from BTL-processes is possible, because "burying" CO_2 underground from biomass, being renewable, removes CO_2 from the atmosphere, if biomass is replanted to substitute the consumed amount [263].

Gasifiers are economy-of-scale equipment - the bigger, the cheaper and thus better [265]. Biomass residues especially from agriculture on the other hand have a low energy density and then needs to be transported over major distances, consuming fuel or energy, to centralised plants. Upgrading the low carbon- and energy density of certain biomasses, especially straw, for instance via decentralised small pyrolysis plants, may therefore be advantageous as described by Dinjus et al. [266].

1.5.3.1 Gasification

The gasification of biomass has been extensively studied, yet a range of technical challenges remain. All types of biomass may in principle be gasificed and then converted, but different reactivity of various raw materials will naturally determine the ease of gasification processing.
Usually, the biomass is heated to 700-1100°C for instance in a simple fixed bed or more advanced fluidised bed system [267], either in inert gas or with minor amounts of oxygen (resulting in some combustion reactions to heat the reactions) and usually at low pressures, with steam and/or other recycled process gases. The pyrolysis and gasification, however, are gradual processes in which the biomass particles degas and volatilise step-wise [267]. Temperatures of at least 1000°C may be necessary for total carbon conversion to gas, depending on the biomass and conditions used, also due to varying ash content, as alkali and earth-alkali ions affect the reactivity during gasification [268]. Ash may pose problems in terms of both disposal and operation, but can be reused as a heat carrier in the gasification to ensure optimal regeneration of process heat and sufficient burnout of coke and

soot [269].

Catalytic pyrolysis at lower temperatures is a suggestion for reduction of gasification temperature, for instance of carbohydrates [192, 270]. Also catalytic gasification of biomass in super-critical water has been proposed [271]. Catalytic techniques often lead to more complete gasification and may even give the possibility of lowering the process temperature. Through careful optimisation it was however found that at only 400°C the non-catalytic gasification efficiency in air-steam mixtures in a bubbling fluidised-bed could be as high as 60% [272].

1.5.3.2 Gas cleaning

Cooling of the gasification products must be performed to stop gas-phase reactions downstream. However, some amounts of tar is produced while gasifying biomass [273], which can clog up pipes downstream upon cooling and/or form coke on surfaces [274, 275]. Sulphur, phosphorous and nitrogen contained in the biomass form compounds that may poison the catalysts downstream - especially the level of sulphurous gases must be brought down to ppm-level, as the active metals in FTS catalysts iron or cobalt will otherwise form sulphides. Catalytic removal of tars, ammonia and sulphides has been proposed for solving this problem [274, 276]. For instance nickel catalysts have been tested in high-temperature cleaning of gas streams containing containing tars, NH_3, CH_4, and H_2S. Reduced nickel worked well for tar cracking at 700°C, however, 900°C was necessary to crack NH_3 and CH_4, and H_2S inhibited reaction, especially at 700°C [277].

1.5.3.3 Fischer-Tropsch-synthesis

An enormous body of literature is available within research on FTS catalysis [278], which is usually performed by metal-oxide-supported metals at 150-330°C and 50-200 bar. While supported ruthenium has been shown to be the most active metal for FTS [197], iron and cobalt are normally used industriallty, since the platinum group metals are usually too expensive to allow for commercial use at this scale. The Co or Fe may then be doped with smaller amounts of other metals as promotors, for instance Mn, Ni, Pt, Ru, K, or Ce. The formal reaction scheme is shown in Figure 1.14.

Apart from water (see Figure 1.14), straight-chain alkanes are achieved from FTS due to the reaction mechanism of chain propagation, which is ideal for diesel fuels if they have the right carbon number. Another important feature of the reaction is that for a certain carbon chain length i, the weight fraction in the product mixture is given from the statistical probablility of chain growth, α, by:

$$W_i = i \cdot (1-\alpha)^2 \cdot \alpha^{i-1}$$

This equation is called the Anderson-Schultz-Flory-distribution (ASF) [279, 280]. The product distribution as a function of the chain growth probability, α, is shown in Figure 1.15 for certain groups of alkanes. Often the selectivity is expressed for instance as the yield of hydrocarbons with a chain-length of at least 5 carbon atoms, C_{5+}. This is the group of hydrocarbons most relevant in terms of refinery processing and fuel production. FTS-catalysts always form methane to some degree, and a low selectivity to methane and as well the lighter hydrocarbon gases is usually desired

(mathematically this means a higher value of α in the ASF) [279, 280]. It follows mathematically from the ASF that methane is always the product produced in the highest amount on a molar basis; however the weight fraction is small due to the large molar weight of the heavier paraffins formed at high values of α [279].

The primary catalysts for FTS Co and Fe usually have $\alpha \approx 0.7-0.9$, which can be optimised by addition of promotors to the primary metal. The largest fraction of diesel pool of C_{12}-C_{18}-hydrocarbons is achieved with $\alpha \approx 0.88$, as is evident from Figure 1.15. Iron has been shown to be the more active metal under the most severe conditions, i.e. at higher temperature, pressure and space velocity, while contrarily cobalt is the more active catalyst in less forcing environments [279, 281].

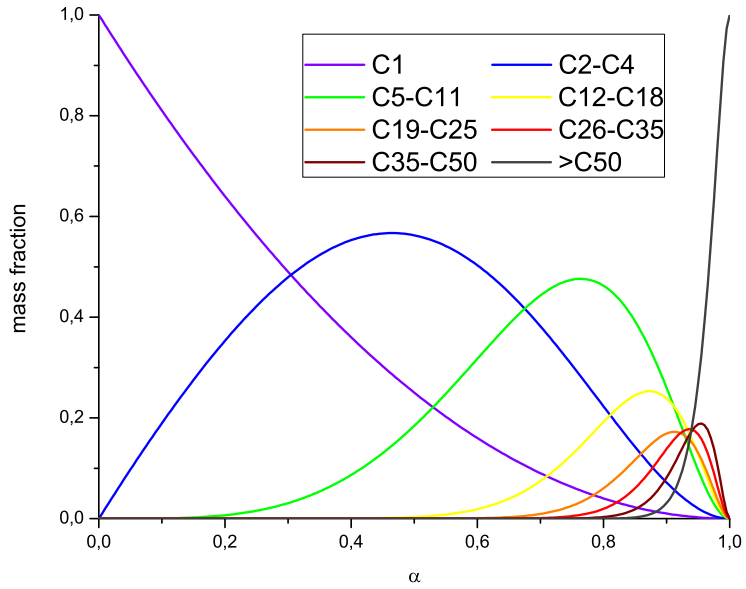

Figure 1.15: The Anderson-Schultz-Flory-distribution: Statistical mass fractions of product groups as a function of the chain growth probability α.

In addition to straight-chain hydrocarbons, impurities of aldehydes, alcohols, and fatty acids are also formed. Such oxygenated by-products should later be reduced by HDO if used for diesel synthesis. Light isomerisation may be necessary to achieve sufficiently good cold properties [282]. The FTS catalysts are sensitive to poisons - especially sulphur, which form sulphides with the catalyst metal if present over ppm-level.

The particle-sizes and structure of the catalyst metal, as well as the microscopic environment in which they are used, affects the overall reaction behaviour. By supporting nanoparticles of Co, Fe and their alloys inside carbon nanotubes showed that activity was enhanced, and the C_{5+}-selectivity could be enhanced as well, which was attributed to a longer contact time with the catalysts particles in the confined environment of the nanotubes [283, 284]. Co had the the highest C_{5+}-selectivity, and Co particles up to the size of the carbon nanotube diameter of 12 nm could be selectively located inside the nanotubes. Reduced sintering (irreversible deactivation) inside the nanotubes due to the confinement and stronger support interaction enhanced the FTS catalyst lifetime [283]. Larger Co particles had higher C_{5+}-selectivity but lower overall activity due to lower surface area of larger particles [283, 284]. The optimal particle size is around 6-8 nm for Co as the C_{5+}-selectivity does not increase above this particle size [285]. Oxidation of the Co crystallites takes place during reaction

and impedes activity, however, the oxidised Co may be reduced to regain activity [283]. The working Co catalyst have been shown to be metallic [285]. The Co-Fe alloys had high selectivities towards C_{2+}-alcohols as up to 26% of the carbon could be converted to alcohol [284]

Confinement of active sites inside micro- or mesoporous materials, such as zeolites, can dramatically alter the behaviour of the FTS catalysts and thereby change the product distribution away from ASF and towards a more selective range of products, for instance due to shape and size selectivity [286]. Support acidity and microporosity may be used to directly isomerise products as well [287].

The pressure has a profound influence on the value of α as higher pressures usually resulting higher chain-growth probabilities [279]. Promotion by alloying with transition metals and doping with alkalis have also been investigted. For example, small amounts of K in a Co catalyst increased the reduction temperature and decreased the activity, but enhanced C_{5+}-selectivity and the selectivity towards olefins instead of paraffins. Potassium may, however, also enhance the activity, which is dependent on temperature [279]. Ru decreased the reduction temperature on Co and increased activity and C_{5+}-selectivity [288]. Mo addition to Fe reduced the deactivation by sintering of the active iron particles and enhanced the formation of iron carbides [289] - part of the mechanism for FTS over Fe involves formation of carbides [290, 291]. Ce and Mn promotors enhance the formation of active carbide species for the chain growth over the Fe catalyst, while Ce is also a structural promotor for Fe [290]. Iron catalysts, depending on promotion, can also catalyse the water-gas-shift equilibrium during FTS [290].

Several researchers have tried to optimise the production of alcohols, aldehyde, or ketones [284, 292, 293]. The production of longer-chain alcohols or aldehydes may be another prospective development within FTS, since upgrading and drop-in blend for either petrol, jet fuel or diesel can now be tailored, or even be steered towards the production of bulk chemicals via FTS. As was shown by Mentzel and co-authors, higher alcohols may even be a preferable feedstock for producing petrol-range fuel from the methanol-to-hydrocarbons reaction over acidic zeolites [294].

1.6 Diesel fuel properties

Diesel may be defined as anything that can be used as fuel in an unmodified diesel engine and has fuel properties as a middle distillate (or middle-cut) from petroleum oil refining. The most important properties for diesel oils are cetane number, heating value and filter blocking point, and these are used to characterise and compare fuels - especially alternative fuels relative to the norm for diesel fuel. Diesel oil constitutes the middle distillate (or middle-cut) from raw petroleum distillation, and part of it is also produced via hydrocracking of vacuum gas oil. The number of carbon atoms in the fuel ranges from 12 to 18 and primarily consists of alkanes.

The cetane number indicates the ease of ignition of the diesel oil in the engine. Since the diesel is injected in a compression-ignition engine when the piston is approaching the cylinder top dead center (near full compression) it must ignite immediately, contrary to petrol engines [295]. European diesel must have a cetane number over 51 while the North American norm specifies a cetane number of 47 [42]. Straight alkanes ignite easier than brached ones, and the higher the cetane number, the easier the ignition takes place [296].

The heating value and density describes the energy density in the fuel and therefore also how much work can be performed by the engine per litre of fuel and therefore also mileage. Usually this heating value is 43 MJ/kg or 36 MJ/L for petrodiesel [43], however, it is not specified in European or American diesel fuel standards [42]. The cold filter plugging point (CFPP) specifies the temperature at which a designated test filter is plugged with diesel wax crystals and is the most common way to report the cold properties of diesel. Additives are often used to lower the CFPP, which is necessary during winter time in for instance North America, Russia, Central Europe or the Nordic countries. On the contrary, longer paraffins can be added to summer diesel to enhance the cetane number.

Pour Point (PP) and Cloud Point (CP) are other measures for describing the cold properties. The CP describes the temperature where, upon cooling, visible diesel crystals start to form as a cloud wax, and this is usually a bit higher than CFPP. PP is measured by first cooling a diesel sample to solid and then heating it up. The temperature within regular intervals at which it starts flowing is the PP.

A number of other important features of diesel fuels are viscosity of the fuel, the lubricity as a measure of the wear that is imposed on the engine, the storage and oxidation stability (especially in the case of FAME), the distillation characteristics and the flash point, see Table 1.1. From an environmental point of view especially the aromatics and sulphur contents are important, since sulphurous oxides and aromatic particles emitted from the engine are harmful to biota in the immediate surroundings.

These measures have relevance for the biofuels to be used as diesels as well, as any diesel oil should be within the specification limits; for a more profound list of relevant biofuel properties (specifically FAME) see for instance Knothe [42].

Table 1.1: Property description for diesel oils specifications [42, 43, 45, 198].

Property	*Unit*	*Description*
Density	kg/L	Density of the fuel.
LHV	MJ/kg	Lower Heating Value; energy content in the fuel.
CN	%	Cetane Number; measure of the ease of ignition. Measured in a test engine as the percentage of cetane (n–hexadecane, n–$C_{16}H_{34}$, CN = 100) in a mixture with α-methylnaphthalene (1-methylnaphthalene, $C_{11}H_{10}$, CN = 0) to be used to get the same ignition properties as the test fuel [295]. In the latest decades, however, iso-cetane (iso-hexadecane, 2,2,4,4,6,8,8-heptamethylnonane, i–$C_{16}H_{34}$, CN = 15) has been used instead of α-methylnaphthalene [296].
CFPP	°C	Cold Filter Plugging Point; The lowest temperature, measured in steps on 1°C, where diesel can still flow through a test filter.
PP	°C	Pour Point; The lowest temperature, measured in steps of 3°C, at which diesel in a test jar still flows.
CP	°C	Cloud Point; The temperature at which the fuel gets cloudy by diesel crystals.
Kinematic Viscosity	mm^2/s	Describes the ease of pumping and injecting the fuel.
Lubricity HFRR	μm	High Frequency Rotating Rig; The diameter of the scar made by rubbing a steel ball againts a steel disc submerged in the test fuel. The usual description of the wear that the fuel causes to the engine.
Storage stability	—	Arbritrary evaluation of the difficulties of storing the fuel over a longer time - relevant with storage tanks containing impurities, especially water.
Aromatics	wt%	Content of aromatics in the fuel (can be split in mono- and polyaromates).
Sulphur	wt%	Sulphur content in the fuel.
Distillation range	°C -°C	Specifies distillation characteristics; the temperature where 10 wt% respectively 90 wt% of the diesel is distilled of. Relevant for vaporisation and ignition in the engine.
Flash Point	°C	Safety measure; the temperature of the diesel fuel at which a spark can ignite the vapors over it.

1.7 Comparison of diesel fuels

Much depend upon the processing and reaction conditions of each process, the feedstock used and mechanistic details of the catalytic processes, especially from upgraded bio-oils or hydrocarbons from aqueous-phase reformed biomass. However both the production of FAME, renewable diesel from HDO of fats and BTL/GTL have reached such maturity that an actual comparison of the produced fuels is possible. Relevant properties have been compared in the literature with respect to diesel fuels derived from biomass [43, 45, 198].

Table 1.2: Comparison of diesel fuels from biomass with EN 590 Summer petrodiesel. GTL is "gas-to-liquids" from gasified natural gas and Fischer-Tropsch-synthesis; the FAME is from rapeseed oil. Table adapted from S. Mikkonen of Neste Oil Oy [45].

	unit	EN 590 diesel	Fat HDO Diesel	GTL	FAME (rape)
Density at 15°C	g/L	835	775 - 785	770 - 785	885
Viscosity at 40°C	mm^2/s	3.5	2.9 - 3.5	3.2 - 4.5	4.5
Cetane number		53	80 - 99	73 - 81	51
Distillation range	°C	180 - 360	190 - 320	190 - 330	350 - 370
Cloud point	°C	-5	-5 to -25[1]	0 to -25	-5
LHV	MJ/kg	42.7	44	43	< 37.5
LHV	MJ/L	35.7	34.4	34	< 33.2
Aromates, total	wt%	< 30	0	0	0
Polyaromates	wt%	< 4	0	0	0
Oxygen content	wt%	0	0	0	11
Sulphur content	mg/kg	< 10	< 10	< 10	< 10
Lubricity HFRR +60°C	μm	< 460[2]	< 460[2]	< 460[2]	< 460
Storage stability		Good	Good	Good	Challenging

[1] This requires a light isomerisation of the n-alkanes produced by the hydrotreatment.
[2] By using normal additives. FAME blended with petrodiesel lubricate the engine and may not require further additivation

Both the fat HDO and the Fischer-Tropsch-synthesised diesel oils have the advantage of producing long-chain alkanes as primary product with a cetane number nearing 100, depending on chain length. Thus they may be used as cetane boosters/additives to diesels fuels not falling within the specification on cetane number.

The cold properties of n-alkanes by HDO of oils and fats are problematic if they are not isomerised afterwards. Isomerisation betters cold properties but lowers the cetane number due to branching. But also FAME can have troublesome cold properties, especially more saturated types like those from animal waste fats. Saturated FAME, on the other hand, have higher cetane numbers than unsaturated ones [15, 198]. The production of renewable diesel is usually not inhibited by FFA, which deoxygenates more readily than ester compounds [16] - contrary to FAME where FFA usually leads to addition of an esterification step in the production chain.

Removing sulphur from petrodiesel via hydrodesulphurisation has the negative effect that the resulting fuel does not lubricate the engine sufficiently. Additivation of the fuel is therefore needed (these additives may often derive from fats and oils). FAME fuels have excellent lubrication properties, and in mixtures down to as low as 2 wt% FAME no further lubrication additives in the fuel are needed to lubricate the engine [15, 198]. On the other hand FAME is more prone to degradation by microorganisms if the storage system contains water - this may be an issue with old, remote or

sparcely serviced tanks. The alkanes from HDO of fats and oil or FTS have, due to their chemical resemblence with diesel fuel, neither of these properties.

Production of FAME from fats uses the mildest reaction conditions, the cheapest plant design and may be decentralised, for instance in connection with abbatoir waste treatment or food production. More forcing conditions are used for hydrodeoxygenation of fats and oils, and it is more suited for traditional refinery infrastructure with possibilities of heat recovery and easy access to hydrogen and isomerisation units. Gasification and Fischer-Tropsch-synthesis may in principle be applied for all types of biomass, but the method requires the most forcing reaction conditions and the most extensive plant design. Gasifiers are economy-of-scale plants and usually pose the biggest investment in a BTL/GTL plant, so this procedure is only viable for very big plants and thus huge amounts of available biomass [266].

At present and in the near future the diesel biofuels are being mixed in with petrodiesel in low blends (no more than 5 or 10 wt% on a larger scale) and here most of the blend properties are not very different from those of pure petrodiesel. Various diesel oils from biomass may thus be expected to be blended into the diesel mix. In the EU, 5.75% of the energy in the fuel should come from biomass sources by the end of 2010 [5], but for many present-day fuel systems only 5 wt% FAME in the fuel is warrantied for the engine. Blending with alkanes from HDO of oils and fats or FTS thus makes it possible to reach this without compromising engine warranty [45].

1.8 Summary of the literature and outlook

Currently both transesterification and hydrodeoxygenation of fats and oils have achieved industrial maturity as methods for production of diesel from biomass. Feedstock price of the oil or fat remain the largest cost in the production. In Europe, rapeseed oil is often used as a feedstock for FAME while soy beans is more normal in North America and palm oil in the tropical regions of the world, for instance in South-East Asia or Latin America.

The transesterification of fats and oils, and esterification of FFA, is the most widespread methods. Benign production at ambient pressure at the boiling-point of co-reactant methanol yields FAME. Industrially the reaction is based on homogeneous mineral acids and bases as catalysts which are used batch-wise and discarded after use, and heterogeneous analogues have been vastly investigated. This includes solid oxides of basic or acidic character, meso- or microporous materials, organic functionalised resins or other solids. The application of reusable catalysts would cut costs and produce less waste, and allow for a simpler and more economical process design.

The deoxygenation of fats and oils can be performed over three types of catalysts, namely supported sulphided transistion metals, supported transition metals in metallic form, and porous acidic or basic materials for cracking. The sulphided metals requires sulphur and hydrogen in the feed to remain active, so co-treating with hydrodesulphurisation feedstock in refineries is an option. The metallic catalysts may formally run without hydrogen, but require it to avoid deactivating side-reactions. Hydrodeoxygenation of fats and oils is still in need of unsulphided catalysts to avoid adding sulphur to the feedstock, and of metal catalysts with a longer lifetime than those previously reported. Deactivation phenomena needs to be studied and understood better to avoid them. Cracking of fats and oils generally still gives too poor yields of primary fuels like gasoline, jet fuel, and diesel due to high production of lighter gases and coke.

Fats and oils are sparse resources: The amount of waste oils from eg. abattoirs or restaurants is limited compared to the global diesel consumption, and the land use associated with the growth of vegetable oil resources cannot cope with demand for fuels either - only a minor percentage of the global diesel demand can be covered with the current two technologies based on fats and oils with the available resources in the near- and medium-term future [198]. The advent algae-based triglycerides on a large scale could help to solve this feedstock issue and make it possible to produce triglycerides for biofuels on an industrial scale in an environmentally acceptable manner; however this is yet to be industrially demonstrated [297, 298].

The growing of crops for biofuel production on productive soil have several drawbacks from an environmental point of view: Switching to growing agricultural crops for biofuels means that productivity of the remaining agricultural production must either be increased or forest or wilderness must be cleared to make room for new agricultural production with severe ecological implications for the invaded ecosystems [298]. Emissions of nitrous oxide (N_2O, a greenhouse gas several orders of magnitude stronger than CO_2 [2]) from fertilisation is one effect of intensive agriculture, and fertiliser production also emits CO_2. Farming in itself also requires fueling for tractors etc [2, 299, 300].

Thus, only lignocellulosic resources like straw, wood and waste appear to be sustainable feed-

stocks that are available in sufficient amount to cover a large fraction of the global fuel demand. Until now, three catalytic strategies for conversion to fuels have been formulated for these feedstocks:

Flash pyrolysis of biomass or near-critical hydrothermal ugrading of biomass can yield a type of bio-crude commonly referred to as bio-oil, containing up to 40 wt% oxygen. This oxygen may removed by deoxygenation, which generally can use the same three types of catalysts that are used when upgrading fats and oils, namely supported metals, sulphided metals or porous materials. The hydrogen consumption and deactivation phenomena may, however, be even more severe and complex than for HDO of fats and oils. The cracking-type catalysts like zeolites appear to be most practical for bio-oils, requiring no hydrogen and allowing for regeneration of zeolites or metal oxides by oxidation by burning away coke formed as by-products.

Carbohydrates and hydrolysed cellulose can be converted by condensations, reductions and reforming reactions in the aqueous-phase as advocated first by the group of Dumesic [29]. The reforming reactions can take place at quite moderate temperatures and usually over supported Pt or Pt-Re catalysts, and up to 95% energy efficiency to be contained in the fuel can be achieved for the integrated process. Furthermore hydrogen is supplied internally by the reforming. Bio-oils may as well be processed once condensation reactions and ketonisations possible from the multifunctional bio-oil mixtures can be controlled.

The research into bio-oils production and upgrading and the aqueous phase reforming may therefore play an increasingly prominent role in the future, despite their more challenging nature. The potential ability to use more parts of for instance wood or straw residues would make the aqueous-phase upgrading even more promising, especially due to its high energy efficiency and carbon containment in the product.

A final method, in principle possible with all types of biomass, is the complete gasification of the biomass into a producer gas, which can be cleaned into syn-gas (CO and H_2) and then liquified as alkanes via FTS. Gasification requires high temperatures and expensive process equipment. The gasification products contains tars and impurities of sulphur and nitrogen from the biomass, which must be removed prior to FTS. This gas cleaning is complex to integrate. The consecutive FTS is usually catalysed by Co and Fe metals, however, the activities and selectivities can be vastly modified by varying, promoting, and confining the active sites.

Major logistic challenges need to be resolved as well: Biomass is a local resource [301], while gasifiers are usually huge equipment placed centrally. Dinjus et al. described the logistics around a gasification fuel economy, and suggested that residues like straw or wood could be upgraded by flash pyrolysis first in small decentralised plants [266]. Then the bio-oil and char fraction, now with a much higher carbon- and energy density can be transported to and upgraded at central gasification-FTS plants.

Primary and easy-to-upgrade feedstocks like plant oils are not and cannot be avaible in quantities sufficient to replace the entire diesel oil demand, so waste products from food production, agriculture and forestry hold greater perspective for use in the future. It is necessary that the processes for future biofuel production have sufficient tolerance to use diverse raw materials, primarily in the form of waste, as feedstocks.

Chapter 2

2

Catalytic Production of Fatty Acid Methyl Ester

The esterification and transesterification of fats and oils with methanol to yield fatty acid methyl esters (FAME), according to Figure 1.2 and Figure 1.3 in section 1.3, are generally produced in industrial scale in a two-stage batch proces employing a strong mineral acid and a ditto base as homogeneous catalysts, respectively. The homogeneous catalysts are responsible for high yields with low amount of catalyst used per batch, but they are not recovered during the production of the FAME and end up as neutral salts that have to be disposed of.

Heterogeneous catalysts would, on the other hand, not be lost during inter-stage neutralisation, workup and separation of the products. Furthermore, process simplification in terms of continuous operation for instance in packed-bed reactors yielding a more even product quality would be possible, and the expenses for obtaining catalysts could be lowered. Therefore the substitution of the homogeneous catalysts in FAME production represent an important goal for catalytic science and techonology.

2.1 Heterogeneous catalysts for production of FAME: Introduction

A wide range of solid inorganic acids have been suggested as heterogeneous catalysts for respectively esterification and, to a certain degree, transesterification. Tungstated or sulphated oxides like WO_3/ZrO_2, SO_4^{2-}/ZrO_2, SO_4^{2-}/ZrO_2–TiO_2, SO_4^{2-}/SnO_2, SO_4^{2-}/SnO_2–SiO_2, SO_4^{2-}/SnO_2–AlO_2, heteropolyacids like the protonated or partly protonated forms of $PMo_{12}O_{40}^{3-}$, $SiMo_{12}O_{40}^{4-}$, $PW_{12}O_{40}^{3-}$, $SiW_{12}O_{40}^{4-}$, niobic or tantalic acid have been reported and recently reviewed by Sharma, Singh and Korstad as potential catalysts for esterification [302].

Basic catalysts suggested for the transesterification include basic oxides like MgO, CaO, SrO, BaO, ZnO, La_2O_3, either unsupported or supported on other oxides, mixed oxides like $MgO \cdot CaO$, $MgO \cdot Al_2O_3$, $MgO \cdot La_2O_3$, $CaO \cdot La_2O_3$, $Ca_2Fe_2O_5$, $CaMnO_3$, $CaCeO_3$, $CaTiO_3$, and $CaZrO_3$, or supported bases like KF, Li_2O, K_2O or Na_2O [62, 303], or Mg-Al-hydrotalcites for instance substituted or doped with other ions [73–75].

In some instances the inorganic acids or bases may, however, dissolve in the polar alcohol phase (which due to esterification can also contain water, see Figure 1.3) over time resulting in leaching of the catalyst. The flexibility of shaping the inorganic materials to the desired technical application is not great. Often the porosities and solubilities are non-tunable. Many of the inorganic catalysts are powder, which are unwanted for instance in for instance packed-bed reactors due to very high pressure drops observed. Extrudating the powders, for instance with other ceramic binders and carriers, may help shape powders to more suitable sizes and shapes for flow reactors.

Organic acids and bases, however, offer different and often better possibilities for tailoring the catalysts for the liquid-liquid-phase reactions. Supporting the catalysts for instance polymers, resins, or porous inorganic materials leave options for synthetic chemistry. This allows pairing of strong acidity or basicity with a suitable porous support material and a desirable macroscopic appearance and making organic-inorganic hydrid catalysts.

Ionic liquids (ILs) have been suggested as an alternative reaction medium for the ester reactions and it has been shown that a neutral IL can be mixed with a given mineral acid or base, for instance H_2SO_4, K_2CO_3, or NaOMe, as catalyst to obtain an active and monophasic reaction medium [137, 304]. However, it may be much more prosperous to functionalise the ILs themselves as strong acids or bases. Lewis-acidic ILs with metal chlorides as anions have proven to be active in transesterification between 80 and 180°C in a number of studies [139, 305, 306]. Sulphonic acid-functionalised ILs have been used as strong acids for FFA esterification [307, 308]. Recently it has also appeared that at mild temperatures around the boiling point of methanol, strong sulphonic acid-functionalised ILs did even catalyse the transesterification at reasonable rates [141, 142, 309].

Other types of sulphonic acids are, however, available as well for formation of FAME. Okayasu and co-workers polymerised vinyl-sulphonic acid and nested it to mesoporous silica or polystyrene and achieved high loading of sulphonic acid and high activities for esterifications of smaller fatty acids with ethanol at 50°C [125, 310]. Grossi and co-authors prepared a sulphonic acid super-absorbant based on polystyrene (PS) and demontrated higher activity for oleic acid esterification than commercial acidic resins and even p-toluenesulphonic acid [123]. A hydrophilic polymer like sulphonated polyvinylalcohol was reported to be more active for esterification than a sulphonated PS at 60°C by Caetano and co-workers [122]. Soldi et al. reported high yields even for transesterification over a sulphonated PS at 60°C [124]. On SBA-15 linked with arene-sulphonic acids, Melero et al. achieved 90% yield of FAME from crude palm oil after 2 h at 160°C [126].

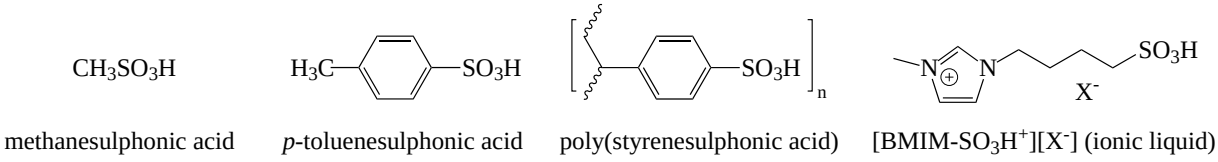

methanesulphonic acid | *p*-toluenesulphonic acid | poly(styrenesulphonic acid) | [BMIM-SO_3H^+][X^-] (ionic liquid)

Figure 2.1: A few different strong sulphonic acids. X^- denotes a counter-anion.

Commercial sulphonic acid resins and ion-exchange resins are often available, however, no studies so far have reported yields comparable to those achieved by laboratory catalysts for transesterification with acidic resins [311]. At around 60°C, however, esterification of FFA around 90% yield within an hour have been achieved on various sulphonic acid-resins [118–121]. Shibasaki-Kitakawa et al. reported the continuous esterification of FFA over a sulphonic acid-resin followed by transesterification of glycerides over a basic resin in two packed-bed reactors in series [117].

Another starting material for solid sulphonic acids has been reported as catalyst for the esterification in FAME production in the recent years. By carbonatisation (slow pyrolysis) of carbohydrates and subsequent sulphonation by sulphuric acid, a layered graphene-like material can be obtained with strong sulphonic acid functionalities connected to the graphene layers (sulphonated pyrolysed

sugars, SPS) [128, 132, 312, 313]. The suggested structure of SPS is shown in Figure 2.2.

Both esterification of oleic acid with ethanol at 80°C and transesterification of triolein with ethanol at 100°C are catalysed with activities comparable to those of sulphuric acid, and up to 98% yield from transesterification of triolein with methanol after 5 h at 130°C has been achieved [312]. The high activities reported for the SPS are likely connected to the swelling of SPS on contact with hydrophilic solvents like methanol because the dry catalyst has a surface area of just 1-2 m^2/g [128, 130, 312, 313]. Ideally, most of the the oxygen should be removed to avoid interference and side-reactions with the hot sulphuric acid during the sulphonation. However, some oxygen remaining in the carbon material and moderate pyrolysis temperature of 400-450°C has been found optimal in terms of incorporation of a high amount of sulphonic acid functionalities and esterification activity [313].

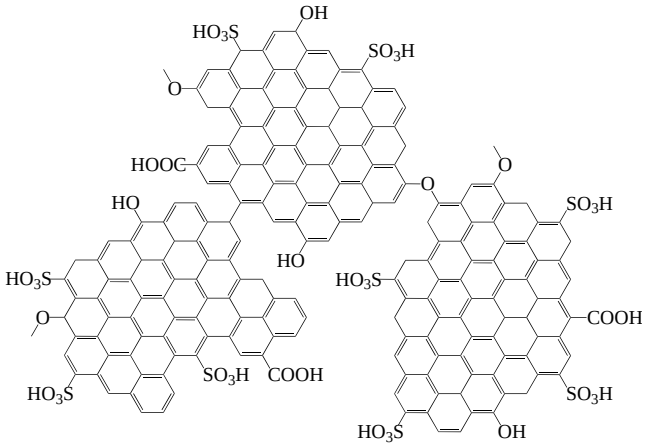

Figure 2.2: Structure of the sulphonated pyrolysis carbohydrates as suggested in literature [130, 132, 312, 313].

Also wood pyrolysis char has been sulphonated for esterification catalysis, and the resulting material can have higher surface area by yielding microchannels in the resulting catalyst [131] - by impregnating wood with $ZnCl_2$ prior to pyrolysis, a surface area of the final sulphonated catalyst up to 1560 m^2/g was achieved, which was several times more active in esterification reactions at 70 and 100°C compared to the sulphonated pyrolysed wood not impregnated with $ZnCl_2$ [314]. Lien and co-workers observed over 90% transesterification of soybean oil after 2 h at 150°C over 3 wt% sulphonated pyrolysed glucose, but leaching of sulphonic acids was reported at this temperature [133].

Peng et al. recently described the use of SBA-15 as rod-structure-directing agent for the SPS synthesis, and the removal of SBA-15 by HF after sulphonation was highly advantageous in the esterification of oleic acid with ethanol at 80°C [135]. The surface area of the resulting carbon material was over 800 m^2/g, in stark contrast to the 2 m^2/g achieved for the "naked" carbohydrate carbonatisation and sulphonation [135, 313]. Mo and co-workers impregnated a polymer with carbohydrate template followed by pyrolysis and sulphonation and achieved 20% esterification of palmitic acid with metrhanol at 60°C after 1 h, however gradual deactivation was also observed. Interestingly, the polymer matrix swelled upon immersion in the methanol reactant [54].

In general, the SPS-approach has the advantage that water-soluble carbohydrates can be impreg-

nated in other supports prior to pyrolysis and sulphonation. However, most SPS catalysts developed in literature are powders, which are not desirable when to use when scaling up to technical-scale synthesis, although extrudation may be a possibility.

Based on the literature reports, the goal of the present work have therefore been to develop macrostructured, heterogeneous catalysts for FAME production. This was pursued by using a model mixture of methanol, lauric acid and trioctanoate to investigate and optimise the synthesis conditions for the sulphonated pyrolysed carbohydrates by esterification experiments and characterisation of acidic and porous properties. The active SPS-phase has been supported by nesting it on various support materials, either by impregnation of sucrose on either open-cell ceramics or mesoporous ceramic pellets prior to pyrolysis and sulphonation, or by suspension of the active SPS in a polyurethane (PUR) matrix. Two of the resulting SPS impregnated on ceramics have been tested in the continuous esterification of lauric acid with methanol.

Transesterification catalysis have been pursued by investigating and relating a number of organic amidine and guanidine bases as well as amine-functionalised ionic liquids and carbonates. Also, a combination of transesterification and esterification in one pot has been attempted over sulphonic acid-functionalised ionic liquids.

Due to ease of comparison and uniformity of the performed reactions, the same model feed has been employed for studying catalytic behaviour during esterification and transesterification - a mixture of methanol, trioctanoate and lauric acid. Unlike FAME synthesis from methanol and oils and fats the three reactants formed a single phase, making sampling during the course of the reaction easier. The expected esterification and transesterification reactions are given in Figure 2.3. Thus, esterification of lauric acid leads to formation methyl laurate, while transesterification of trioctanoate leads to formation of methyl octanoate. Therefore the esterification and transesterification activity or potential hydrolysis reactions can be directly related to either reactant.

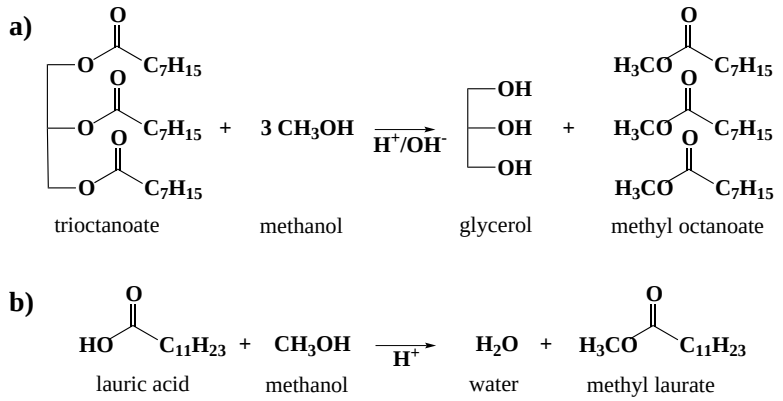

Figure 2.3: Reactions of the model feed of methanol, trioctanoate and lauric acid: Transesterification (**a**)) and esterification (**b**)).

Theoretically, in the presence of water, the acidic and basic catalysts may hydrolyse the ester bonds to form FFA - in the case of the basic catalyst, the hydrolysis leads to soap formation (the salt of the base and FFA). However, it is possible that the acidic transesterification may take place via hydrolysis of the fat and consecutive esterification of the FFA as is shown in Figure 2.4.

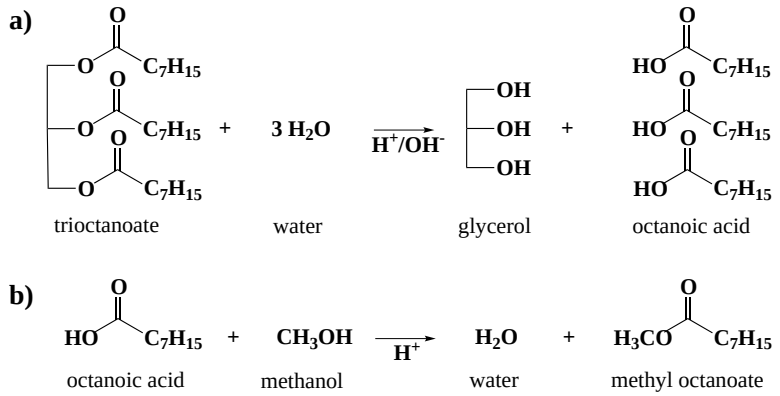

Figure 2.4: Potential hydrolysis (**a**)) and esterification (**b**)) of trioctanoate in the presence of water and methanol.

2.2 Heterogeneous catalysts for production of FAME: Experimental

2.2.1 Activity measurement of catalysts

The reaction mixture was composed of the reactants methanol (>99.9%, Bie & Berntsen), lauric acid (dodecanoic acid, >99%, Fluka), and trioctanoate (tricaprylin, >99%, Sigma), while dodecane (>99%, Sigma-Aldrich) was used as an internal standard. Pyridine (>99.8%, Fluka) and N-methyl-N-(trimethylsilyl)-trifluoroacetamide (MSTFA, >98.5%, Fluka) were used for sample preparation for GC analysis. Methyl laurate (methyl dodecanoate, >99.5%, Aldrich), methyl caprylate (methyl octanoate, >99% (GC), Fluka), octanoic acid (caprylic acid, >99%, Sigma), and glycerol (>99.0%, Sigma-Aldrich) were used as reference standards for the GC analysis along with the reactants used.

The investigated catalysts were weighed and added each to a 25 ml two-necked round-bottomed flask, placed in a heated oil bath with a magnatic stirring, and glass plugs were mounted in the flask necks. The oil bath temperature was adjusted to a temperature of ca. 65°C, effectively giving a temperature in the glass flasks of 60°C, which was measured by a thermometer. Typically 0.2 g of catalyst (ionic liquid: 0.5 g) was added to each flask.

For testing the acidic catalysts, a monophasic reaction solution consisting of 0.724 g lauric acid, 1.700 g trioctanoate and 1.167 ml methanol (0.926 g) was mixed prior to reaction, giving an effective molar ratio between methanol, trioctanoate and lauric acid of 8:1:1. Furthermore, 0.0703 g of n-dodecane was added to the mixture as an internal standard. For the experimentation with basic catalysts, a monophasic reaction mixture consisting of 2.023 g tripalmitin and 1.566 ml methanol (1.240 g), yielding a molar ratio of methanol and trioctanoate of 9:1, while 0.0733 g of n-dodecane was added as an internal standard.

Typically, 6 acidic or basic catalysts were tested in parallel using the same preparation of reaction mixture. When the catalysts were heated, 4.00 ml (3.35 g) of the reactant solution was added to the heated flasks containing the catalysts with stirring running at ca. 500 rev/min. All reactions were performed as time series experiments by sampling over time between 0 and 96 h: 10.0 μL of each flask were taken out as sample with a precision pipette after 0.25, 0.5, 1, 3, 7, 24, 48, and 96 h and added to a GC glass vial, while a sample from the untreated reaction mixture was also taken out as the 0 h sample. Each of the samples taken out were treated with 1.00 ml of pyridine and 100 μL of MSTFA and silylated for at least 30 min at 60°C and analysed on GC.

After the reaction was completed, the reaction solution from each flask with a solid catalyst was filtered to remove the catalyst, and the filtrate was diluted with water and a concentrated solution of barium nitrate ($Ba(NO_3)_2$) was added to test the mixture for presence of sulphate species by precipitation of any SO_4^{2-} as $BaSO_4$.

2.2.2 Liquid product GC analysis

The liquid samples obtained from reaction solutions with SPS as catalysts were quantified by an Agilent Technologies 6890N gas chromatograph (GC) equipped with flame ionization detector (FID), split/splitless injection system and a HP-5 capillary column (J&W Scientific, 30 m × 0.32 mm × 0.25

μm (5 mol% phenyl)-methylpolysiloxane). The liquid samples taken from reaction solutions with ionic liquids, the supported and impregnated SPS in polyurethane or on ceramics, and the basic catalysts tested were quantified by an Agilent Technologies 7890A GC equipped with FID, cool-on-column injector and a high-temperature DB-5HT capillary column (J&W Scientific, 15 m × 0.32 mm × 0.25 μm (5 mol% phenyl)-methylpolysiloxane) joined with a precolumn (or guard-column, J&W Scientific, 1 m × 0.53 mm, of fused deactivated silica).

For the GC analysis He (>99.999%, AGA) was used as column, septum purge and make-up gas, H_2 (>99.999% or technical quality, AGA) was used as FID ionisation fuel, and dehumidified pressurised atmospheric air was used as oxidant for the FID. All the reference standards applied were run on both of the GCs.

2.2.3 Sulphonic acid-functionalised ionic liquids

Four sulphonic acid-functionalised ionic liquids were tested as acidic catalysts for esterification and transesterificatoin with the reaction model mixture described in section 2.2.1. Butyl(methylimidazolium)sulphonate was used as cation with either mesylate ([BMIM–SO_3H^+][$MeSO_3^-$]), bis(triflamide) ([BMIM–SO_3H^+][NTf_2^-]), or hydrogen sulphate ([BMIM–SO_3H^+][HSO_4^-]) as anion, and butyl(pyridinium)sulphonate hydrogensulphate ([BP–SO_3H^+][HSO_4^-]) was investigated as well. All ionic liquids were in-house synthesised chemicals (>95% purity by NMR) by Olivier Nguyen van Buu.

2.2.4 Sulphonic acid-functionalised pyrolysed carbohydrates

The sulphonated were prepared on the basis of the method first proposed by Toda and co-authors [128, 313]:

1. Initially, either sucrose (>99.5%, Sigma), starch (analytical grade, Riedel-de-Haën), glucose (>99.5%, Sigma), or cellulose (powder, ca. 20μm, Aldrich) were weighed and about 2-15 g carbohydrate per batch were pyrolysed for 1-15 h at 300-450°C and a heating rate of 100°C/h in Ar (>99.99%, AGA) flow. A glass tube or a tubular steel reactor was placed and isolated with vermiculite in a programmed tubular furnace and connected with argon flow on the inlet side. The carbohydrates were loaded into in a glass boat (1-1.5 g carbohydrate in each boat) in the glass tube or loaded directly into the tubular steel reactor (up to 15 g), and the whole system was tightened. After the pyrolysis the resulting carbon materials were weighed again.

2. The subsequent sulphonation was performed by immersing up to 5 g of carbon materials in a 500 ml round flask with 250 ml of H_2SO_4, either concentrated (96 wt%, Sigma-Aldrich) or fuming sulphuric acid of 15 or 30% oleum (based on 30% SO_3/H_2SO_4, Merck). The solution was heated in an oil bath to 150°C, where it was left for 15 h with a flow of Ar of 5 ml/min to renew the gas atmosphere.

3. After sulphonation the sulphuric acid solution and the carbon material was carefully diluted a factor of 10 in demineralised water. The resulting black powder was filteted and washed extensively with H_2O at 80°C until no trace of SO_4^{2-}-ions could be found in the filtrate by

testing for $BaSO_4$ with concentrated aqueous $Ba(NO_3)_2$. Afterwards the powder was dried in a muffle oven for several hours at 110°C.

2.2.5 Immobilisation of SPS and continuous esterification

For the preparation of the SPS supported in polyurethane (PUR) foam, SPS powder was prepared according to the procedure mentioned in section 2.2.4. The foaming was performed by the Danish Technological Institute (TI) by Jesper Bøgelund. The powder was nested in the PUR foam matrix by being mixed with the reactant during the synthesis of PUR foam, however, the conditions and reactants of the foaming process are not known as the synthesis was proprietary information of TI. The appearance of the resulting was as a soft, open-celled, dark foam. Before reaction, the foam catalysts were cut in pieces of about 3 mm on each side.

For preparation of impregnated SPS supported on ceramics, two types of ceramic structures were used: Open-celled ceramic were obtained from Drache GmbH in the form of 2 cm thick ceramic plates of an open-cell ceramic foam of Al_2O_3 and ZrO_2 (cell diameter ca. 3-4 mm). Four different types of ceramic pellets were delivered by Saint-Gobain Norpro in the form of SiO_2 (surface area 251 m^2/g, average pore diameter 11.1 nm, pore volume of 0.93 mL/g), two types of TiO_2 (#1: Surface area 150 m^2/g, average pore diameter 15 nm; #2: Surface area 40 m^2/g, average pore diameter 28 nm), and ZrO_2 (surface area 186 m^2/g, containing 4.6% SiO_2 as a binder). The SiO_2-, TiO_2-, and ZrO_2-pellets were used as received after drying.

Al_2O_3-cylinders were cut in sizes of 9.5, 15 and 20 mm diameter and lengths of 20 mm by Jakob Engbæk at TI. The received Al_2O_3 open-cell foam cylinders were fragile after pyrolysis & sulphonation so they were re-calcined at 1200°C for 24 h in air with a heating ramp of 100°C/h, yielding a much harder ceramic not degraded by the sulphonation solution. The pelletised ceramics were used as is after vaporisation of any water present in the mesopores at 110°C. All ceramics were weighed and impregnated with a sucrose solution. The sucrose-impregnated ceramics were afterwards pyrolysed at 400°C for 15 h with a 100°C/h heating ramp, sulphonated with sulphuric acid for 15 h at 150°C, washed with 80°C hot water and dried according to the procedure given in section 2.2.4.

The activity of the impregnated SPS (ISPS) was assessed by batch-mode esterification and transesterification as described in section 2.2.1. Furthermore, the pelletised ISPS/SiO_2 were tested as catalysts for continuous esterification of lauric acid and methanol in 1:30 molar ratio, while the open-cell ceramic ISPS/Al_2O_3 was exposed to a 1:1:8 molar mixture of trioctanoate, lauric acid and methanol. n-Dodecane was used as internal standard in both cases.

The reactor setup was a tube of 9.75 mm in inner diameter and 18 cm length, insulated within a tubular furnace, which was connected with fittings to a setup with steel and rubber tubing and a peristaltic feed pump on the inlet side, while a condensing tube with an open-close sampling valve situated on the outlet side. A thermocouple attached to the outlet side of the reactor tube was used to monitor the reaction temperature. The flow rate of feed solution was varied between 0.010 ml/min and 0.200 ml/min and the reactor temperature was varied between 25 and 72°C. Upon loading of the catalyst, the ends of the bed were plugged with quartz wool and connected to the pump. The reactor was placed in a horizontal furnace, a thermocouple was connected and tightened to the outer

part of the reactor inside the furnace, followed by insulation by aluminium foil. A flow of methanol was pumped to the reactor to empty it of air before starting the experimentation.

The open-cell ceramic ISPS/Al_2O_3 was also tested as catalyst for the esterification and transesterification of rapeseed oil (obtained from supermarket) and waste animal fat (supplied by Daka Biodiesel) with methanol in a pilot reactor setup. The reactor was a steel tube of 75 cm and 2.0 cm inner diameter, which was connected with with a pump, an emulsifier with feed inlets and product outlet, as well as a recycle loop. The same ISPS/Al_2O_3 open-cell cylinders were used as catalysts for both feedstocks (rapeseed oil treatment first). The reactor could be run without recycling of the product or with a desired recycle ratio - and the feeding of reactants and the extraction of product can be shut off to operate the reactor like a packed-bed batch reactor. Thus, the reaction mixture can in principle be recycled in the loop infinitely until a desired conversion is reached. This means that the kinetic behaviour of the reaction will be like a batch-reactor, while the hydrodynamic behaviour will be like a packed-bed reactor. The experimentation with industrial feedstocks have been performed by Lene Fjerbæk at the University of Southern Denmark (SDU). Analysis of these samples were made by an HPLC-method, however, details are not available about the apparatus and eluents used.

2.2.6 Characterisation of SPS and ISPS

The BET surface areas of SPS and of SPS-impregnated and unimpregnated SiO_2-pellets and SPS-Al_2O_3 open-cell cylinders were determined by N_2 physisorption. The samples were degassed prior to measurement at 150 °C for 4 h under vacuum. Adsorption- and desorption isotherms were measured with liquid N_2 at 77 K on a Micromeritics ASAP 2020 pore analyser.

Elemental CHNS-analysis of the PS, SPS, ISPS/SiO_2-pellets and ISPS/Al_2O_3 open-cell cylinders was performed by Theis Brock-Nannestad at the University of Copenhagen with a Flash EA 1112 NC Analyser from CE Instruments, ThermoFisher Scientific equipped with a TCD detector. The content of carbon, hydrogen, nitrogen, and sulphur can be detected by CHNS-analysis, however, the oxygen content cannot.

Aqueous titrations of the PS, SPS, SPS/SiO_2-pellets and ISPS/Al_2O_3 open-cell cylinders were carried out with a Metrohm autotitrator with a pH working-electrode. The titration of ca 0.2 g of the suspended catalysts was performed at 600 rev/min magnetic stirring in a beaker using a KOH (>85%, Fluka, <1% Na, <0.5% other impurities, Fluka) solution of 0.0359 M as titrant, which had been adjusted by a tripled manual titration with 0.1000 M solution of aqueous hydrochloric acid (Titrisol, Merck). Prior to titration, ca. 5 g of KCl (>99,5%, Merck) was added to the beaker containing the catalyst to make sure that the sulphonic acid functionalities were ion-exchanged with potassium to minimise the delay in pH on addition of base.

2.2.7 Basic catalysts for transesterification

A number of different catalysts were tested for their transesterification activity as suspected bases. The activity of the catalysts were tested according to the basic procedure mentioned in section 2.2.1.

Butyl(methylimidazolium)amine was used as a cation in three different ionic liquids, with either

bromide ([BMIM–NH_2^+][Br^-]), boron tetraflourate ([BMIM–NH_2^+][BF_4^-]) or bis(triflamide) ([BMIM–NH_2^+][NTf_2^-]) as anion. All the ionic liquids were in-house synthesised chemicals (>98% purity on NMR) by Olivier Nguyen van Buu.

Cesium carbonate (Cs_2CO_3, >99%, Aldrich), guanidinium carbonate (Gua_2CO_3, 99%, Aldrich), guanidinium chloride (GuaCl, 99%, Sigma) were obtained and employed as catalysts, while magnesium lanthanum mixed-oxide ($MgO \cdot La_2O_3$) was synthesised in-house by Yury Gorbanev according to a procedure given in the literature [315, 316] and used as well.

Tetramethylguanidine (TMG, >99%, Aldrich), 1,8-Diazabicyclo[5.4.0]undec-7-ene (DBU, >99.0%, Fluka), 1,5-Diazabicyclo[4.3.0]non-5-ene (DBN, >98.0% (GC), Aldrich), 1,5,7-triazabicyclo[4.4.0]dec-5-ene (TBD, >99.0%, Fluka) were applied as guanidine and amidine strongly basic catalysts.

1,8-Bis(tetramethylguanidino)naphtalene (Bis-TMG-Naphthalene, >98.0% (NT), Fluka) was a commercial chemical, while Merrifield's peptide resin (70-90 mesh, 1.0-1.5 mmol/g Cl- loading, 1 % PVB/PS, Aldrich) linked with TMG in-house (ca. 0.7 mmol/g TMG), Benzyl-TMG, Hexyl-TMG, and Propyl-TMG were in-house synthesised chemicals (>99% purity by NMR after synthesis) by Olivier Nguyen van Buu and used as catalysts as well.

2.3 Sulphonic acid-functionalised ionic liquids

The sulphonated cation [BMIM–SO_3H^+] with [NTf_2^-] or [$MeSO_3^-$] as anions were applied as catalytic reaction media for conversion of the model mixture of methanol, lauric acid and trioctanoate in 8:1:1 molar ratio to methyl laurate and methyl octanoate.

Apparently, at 60°C and 0.5 g of IL, the conversion of lauric acid amounted to 98% with both liquids after 0.5 h and the conversion of trioctanoate was respectively 98% and 99% using the IL with [$MeSO_3^-$]- and [NTf_2^-]-anions after 24 h. The latter observation was surprising, as it was not suspected that the acidic catalyst would be very active for transesterification. This prompted the repetition of the two time series and the addition of two other time series experiments with different ionic liquids as catalysts.

Thus, The ILs of [BMIM–SO_3H^+] with [NTf_2^-], [$MeSO_3^-$], and [HSO_4^-] and the IL of [BP–SO_3H^+] with [HSO_4^-] were tested in the latter set of experiments. The values for the conversions and yields of the four ILs are shown in Figure 2.5. From the experiments performed twice, the average values from the two experients are used, as they were within ca. 2% deviation.

All the ILs showed complete turnover of the lauric acid within 3 h. The fastest conversion after 0.5 and 1 h was reached by [BMIM–SO_3H^+][$MeSO_3^-$], barely ahead of [BMIM–SO_3H^+][NTf_2^-], whereas the turnover of the lauric acid over the ILs with [HSO_4^-]-anions were somewhat slower. Some minor deviation in the conversion of lauric acid can be observed in the time series over [BMIM–SO_3H^+]-[HSO_4^-] and [BP–SO_3H^+][HSO_4^-] in the first samples.

However, the analysis of the resulting methyl laurate presented in Figure 2.5 appeared somewhat peculiar, since some concentrations reached over 100% during the first hours, followed by levelling off at about 80% yield. No other products containing the lauric acid chain have been observed. It may be suspected that the missing methyl laurate has been hydrolysed during the sample preparation before the GC analysis due to trace amounts of water in the chemicals.

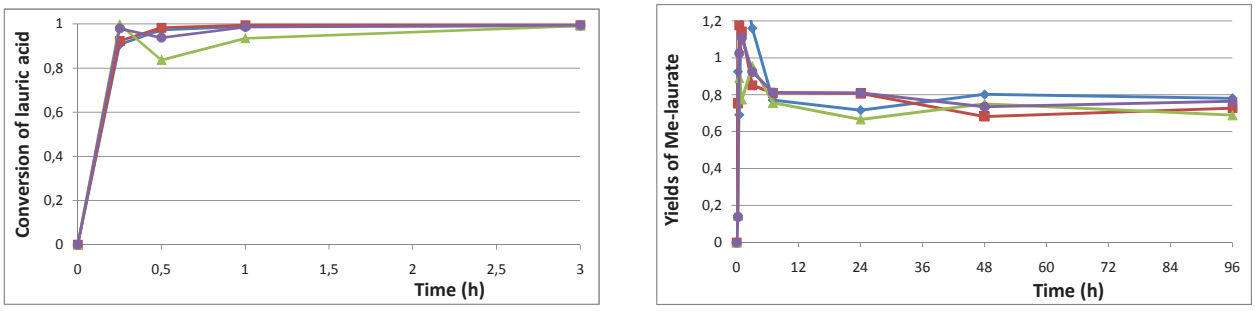

Figure 2.5: Conversion of lauric acid *(left-hand side)* and yield of methyl laurate *(right-hand side)* with sulphonic acid-functionalised ionic liquids as catalysing reaction medium. Legend: [BMIM–SO_3H^+][-NTf_2^-] (—♦—), [BMIN–SO_3H^+][$MeSO_3^-$] (—■—), [BMIM–SO_3H^+][HSO_4^-] (—▲—), and [BP–SO_3H^+][HSO_4^-] (—●—). Conditions: 60°C, 4.3 mmol trioctanoate, 4.3 mmol lauric acid, 34.6 mmol methanol, dodecane as internal standard.

It should also be noted that the ionic liquids and the reactant solution formed two separate phases, ionic liquid on the bottom and the organic reaction mixture on the top, however, it is not known how much of the reactants and products are absorbed in the IL-phase and have not measured. No visible expansion of the ionic liquid phase could not be observed. The stirring rate was sufficiently

fast to emulsify the ionic liquid-phase into small droplets suspended in the organic phase, so samples were taken out from the upper phase after a short period without stirring. Esters or acids may have been absorbed .

The conversions of trioctanoate and the yields of methyl octanoate from the analyses of the samples, as shown in Figure 2.6, reveals that the ionic liquids were also active for the conversion of the triglycerides at 60°C. The more active catalysts for esterification of lauric acid were also more active in the transesterification of trictanoate, in all probability due to higher acidity. In fact, after 24 h, over 95% conversion of trioctanoate was observed with the [BMIN–SO_3H^+][NTf_2^-], [BMIN–SO_3H^+][$MeSO_3^-$], and [BMIN–SO_3H^+][HSO_4^-].

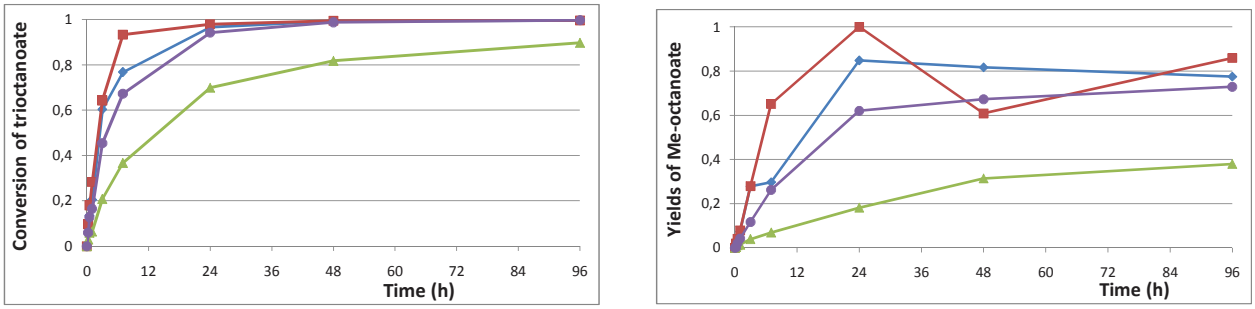

Figure 2.6: Conversion of trioctanoate *(left-hand side)* and yield of methyl octanoate *(right-hand side)* with sulphonic acid-functionalised ionic liquids as catalysing reaction medium. Legend: [BMIM–SO_3H^+]-[NTf_2–] (—♦—), BMIN–SO_3H^+-$MeSO_3^-$ (—■—), BMIM–SO_3H^+-HSO_4^- (—▲—), and BP–SO_3H^+-HSO_4^- (—●—). Conditions: 60°C, 5 mmol trioctanoate, 45 mmol methanol, dodecane as internal standard.

The high conversion of >95% and the somewhat lower yields achieved at 60°C are comparable to the FAME yield of 83% and 88% achieved by Li et al. by using [BP–SO_3H^+][$CF_3SO_3^-$] at 80°C after 6 and 8 h [141], respectively. This is furthermore comparable to the yields achieved by Liang and Yang around 98% after 7 h at 70°C using a tetra-(butyl-sulphonic acid) ionic liquid based on hexamethylenetetramine, or Ghiaci and co-authors achieving 75, 77, and 82% yields after 6 h at 60°C over various polysulphonic polyaromatic ionic liquids, considering the multifunctional nature of the ionic liquids applied in both literature reports [142, 309].

The yields of methyl octanoate were somewhat lower than the conversion of trioctanoate would predict. The gaps observed between the amounts of trioctanoate and methyl octanoate was found not to be due to hydrolysis of octanoate esters to octanoic acid, as octanoic acid was found at maximally 1-2% of the samples of the reaction mixtures throughout the time series. The missing compounds were, however, found to be larger amounts of the intermediates of glyceryl mono- and di-octanoate from the trioctanoate, which had not been converted to the methyl octanoate. Some of the ester or the corresponding acid may as well be absorbed in the ionic liquid-phase, which has not been analysed.

The production of methyl octanoate stagnated after 24 h, so it is suspected that the reaction rates of the mono- and di-octanoates were slower than that of the trioctanoate. It is known that mono- and di-glycerides act as emulsifiers, and during the end of the time series, a thickening of the reaction mixtures could be observed (the solutions became "cloudy"). The increased viscosity of the mixture could therefore have led to lower rates of reaction to to decrease of diffusion rate and poorer mixing.

Strong acids usually need higher temperatures to function as catalyst for the direct transesterification, as the conversion is normally unacceptably slow around 60°C [86, 93, 317, 318]. Therefore

it may be speculated that the reaction have taken place due to the formation of octanoic acid intermediate through acidic hydrolysis of the glycerides to free fatty acid, which was then converted to methyl octanoate, as given in Figure 2.4. However, very little octanoic acid was observed during the reaction, possibly also deriving from the fact that esterification of the free fatty acids proceeded very fast (as was the case of the esterification of lauric acid) in the ionic liquids.

Water could be added to the reaction mixture in varying amounts to investigate the role of water in the mechanism and possibly elucidate this hypothesis. Liang and Yang found a slight depression of the FAME yields with addition of up to 2 wt% water to the reaction mixture [142]. This indicates that the reaction from trioctanoate taking place in the acidic medium was, as claimed, direct acidic transesterification - although this property may well be dependent on the hydrophilicity of the ionic liquid applied.

2.4 Sulphonic acid-functionalised pyrolysed carbohydrates

From the previous works in literature it is evident that SPS can have high sulphonic acid loading and acidity, resulting in a high esterification rate at benign temperatures, but the preparation conditions have a profound influence on the properties of the final catalyst [313].

It has been reported that the structure of the resulting material is an amorphous graphene layer structure with its very few oxygen functionalities situated on the edges of the graphene layers (cf. Figure 2.2) [312]. However, the removal of oxygen functionalities is not complete during the pyrolysis of the carbohydrates, especially at lower temperature, as given by Okamura et al. [313]. It may be expected that the concentrated sulphuric acid at 150°C during sulphonation will also react with any phenolic groups present, creating water and a phenylic hydrogen sulfate group (this may later hydrolyse during washing with hot H_2O).

The sulphonic acid-functionalities are as strong as sulphuric acid [132], so the loading and position of the sulphonic acid groups determines the capacity for and the possible rate of esterification. An investigation of the dependency of the carbohydrate source, the pyrolysis conditions and the sulphonation medium have therefore been performed in the present work. A model mixture of lauric acid, trioctanoate and methanol in a molar ratio of 1:1:8 has been used as reaction medium for the activity tests. The yields reported are obtained by relating the obtained GC areas with those of reference solutions.

A photograph of sucrose and starch before and after the pyrolysis at 400°C for 15 h is depicted in Figure 2.7. After sulphonation, washing and drying, a batch of the grainy black SPS powder appeared as depicted on the photograph in Figure 2.8.

Figure 2.7: Photograph showing pyrolysed *(upper left)* and unpyrolysed *(lower left)* starch and pyrolysed *(upper right)* and unpyrolysed *(lower right)* sucrose.

Figure 2.8: SPS, washed and dried.

2.4.1 Variation of the carbohydrate source

The influence of the carbohydrate source on the SPS catalyst activity was investigated by synthesising the SPS from sucrose, glucose, starch, and cellulose as carbohydrate precursors. The results of the SPS-catalysed time series from 0 to 96 h are shown in Figure 2.9. It is clear that all of the tested SPS feedstocks provided suitable catalysts for esterification as lauric acid and methanol yielded more than 95% methyl laurate over the tested materials. It can be seen that the sucrose-based SPS show a slightly higher than the cellulose- and glucose-based SPS. It is furthermore observed that some percent of methyl octanoate resulted from the acidic transesterification of trioctanoate, at least with the sulphonated pyrolysed cellulose and glucose. Initially it was observed that methyl octanoate is

also produced over the glucose-based SPS, albeit this is not found in the reaction mixture at later instances in the experimentation. The tiny amounts observed are, however, almost in the range of experimental inaccuracy.

From these results it may be suspected that the pyrolysis of the materials produce a material that is not very dependent on the type of carbohydrate used for the SPS. It was expected that the cellulose was more thermally stable and therefore a more difficult molecule to use to achieve sufficient pyrolysis, but its activity was nonetheless on the same scale as the glucose- and sucrose-based SPS.

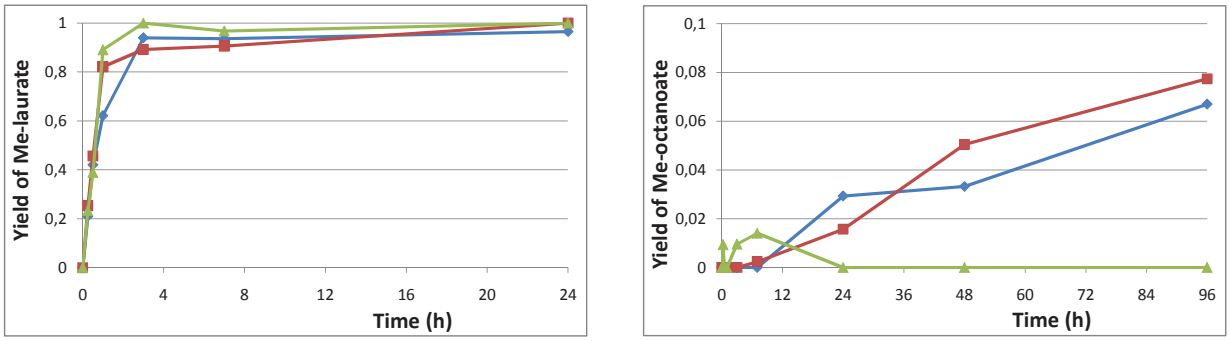

Figure 2.9: Yield of methyl laurate *(left-hand side)* and methyl octanoate *(right-hand side)* over sulphonated, pyrolysed carbohydrates as a function of time by variation of the catalyst carbon source (pyrolysis: 400°C for 15 h, sulphonation 150°C for 15 h with conc. H_2SO_4). Legend: Glucose (—◆—), Cellulose (—■—), Sucrose (—▲—), Conditions: 60°C, 4.3 mmol trioctanoate, 4.3 mmol lauric acid, 34.6 mmol methanol, dodecane as internal standard.

2.4.2 Variation of the pyrolysis conditions

The conditions for the slow pyrolysis to achieve the carbonaceous catalyst material was varied while the subsequent sulphonation, washing and drying conditions were kept constant. Thus, a pyrolysis time of 1, 4, and 15 h at 400°C and a pyrolysis temperature of 300, 350, 400, and 450°C at 15 h of pyrolysis were evaluated. The produced SPS catalysts were applied to react the model mixture of methanol, lauric acid and trioctanoate at 60°C with the results for esterification and transesterification given in Figure 2.10.

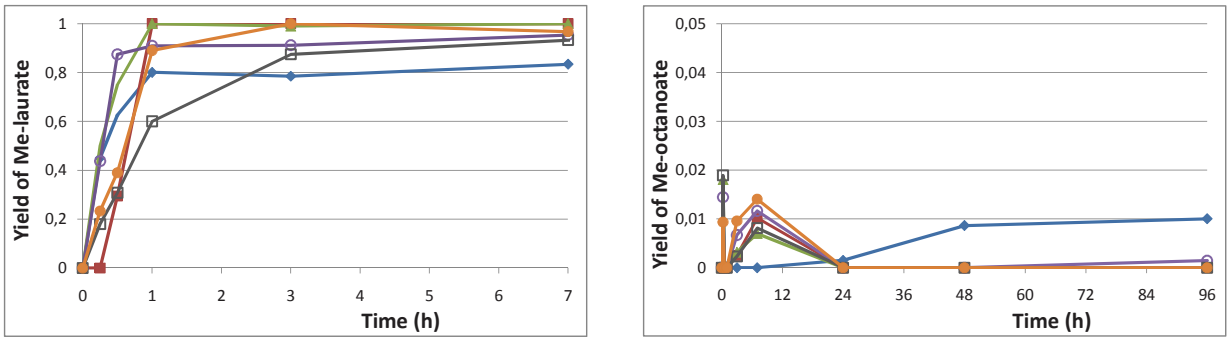

Figure 2.10: Yield of methyl laurate *(left-hand side)* and methyl octanoate *(right-hand side)* over sulphonated, pyrolysed sucrose (SPS) as a function of time by variation of the carbonatisation temperature and time for the SPS. Legend: 300°C for 15 h (—◆—), 350°C for 15 h (—■—), 450°C for 15 h (—▲—), 400°C for 1 h (—○—), 400°C for 4 h (—□—), 400°C for 15 h (—●—). Reaction conditions: 60°C, 4.3 mmol trioctanoate, 4.3 mmol lauric acid, 34.6 mmol methanol, dodecane as internal standard.

In all cases the sulphonated pyrolysed carbohydrates worked quite efficiently for the esterification to methyl laurate and tended towards full conversion within a few hours, albeit at somewhat

different rates. Only vague variation tendencies as a function of the pyrolysis conditions during SPS synthesis may be observed. After 3 h of reaction 100% yield of methyl laurate is observed in the samples of SPS that have been pyrolysed for 15 h at 350, 400, and 450°C. This could indicate that sufficient pyrolysis time is an advantage for this catalyst type. This is possibly due to the fact that as much water as possible should be removed from the carbohydrates to avoid high dilution of the sulphuric acid during sulphonation, thus yielding a higher amount of sulphonic acid functionalities. 15 h at 300°C was not sufficient to achieve the same yield in 3 h achieved at higher pyrolysis temperatures. This tendence is, however, only clear from the 3 h samples. This observation does not explain why there was not a bigger difference between the various pyrolysis temperatures; neither does it explain why the SPS from 1 h pyrolysis at 400°C was more active than that from 4 h pyrolysis.

It can safely be concluded that no significant transesterification activity was observed, as the yield never climbed above 2% and no methyl octanoate were observed in the most samples taken after 7 h. The low amounts observed also lie on the border of GC noise and experimental uncertainty.

No systematic influence of the pyrolysis temperature of the SPS on the yield of methyl ester can be conluded, although the pyrolysis time and temperature should at least be sufficient to remove as much water as possible from the carbohydrates. 400°C have been reported to be the optimal pyrolysis temperature of glucose, while lower and higher temperatures yielded slightly lower conversion - interestingly SPS from pyrolysis at temperatures of 550 and 600°C were almost inactive and non-acidic in methanol and water due to absence of swelling of the catalysts [313].

It may be speculated that the synthesis of the SPS could be simplified by performing the initial dehydration of the carbohydrate in sulphuric acid instead of by pyrolysis, but it would most likely require using bigger amounts of sulphuric acid for the same batch to gain the same sulphonation degree. This has therefore not been attempted.

2.4.3 Variation of the sulphonation medium

The sulphonation medium of pyrolysed sucrose and starch were varied to evaluate if this influenced the activity of the SPS catalyst during esterification and transesterification of lauric acid and trioctanoate, respectively, with methanol. Respectively 30% and 15% fuming as well as concentrated sulphuric acid (96 wt%) were used for the sulphonation, and the SPS catalysts obtained were compared also with the activity of unsulphonated pyrolysed sucrose in Figure 2.11. 30% fuming sulphuric acid was on stock while 15% fuming sulphuric acid was made in-situ by mixing concentrated sulphuric acid with the 30% fuming sulphuric acid.

The standard catalyst based on pyrolysed sucrose sulphonation with concentrated sulphuric was more efficient compared with those based on the fuming sulphuric acid, as the yield of methyl laurate grew most steeply with the standard catalyst. The catalysts based on fuming sulphuric acid were not as efficient, however, some of the masses of catalysts used of these materials were also not as high as 0.21 g.

It was found that the fuming sulphuric acid, especially the 30% SO_3/H_2SO_4 partly degraded the macrostruture of the pyrolysed material. The sulphonation at 150°C in 96% H_2SO_4 resulted a more grainy SPS consisting of coarse particles (as depicted in Figure 2.8). This meant that much of

the carbonaceous material was washed away during the filtration, and not enough catalyst could be recoved to allow ca. 0.21 g of catalyst to be used in all the 4.00 ml reaction mixture. The yields of methyl laurate after 0.25, 0.5, and 1 h have therefore been related to the catalyst mass via the apparent catalyic reaction rates, which are given in Table 2.1. The reaction rates calculated over a given catalyst should be equal at low conversions, but they should lower over time as the reaction approaches equilibrium, which was also the case for most of the catalysts in the table. Some deviation is found to this rule.

Interestingly, the yields of methyl octanoate grew over 10% after 96 h with some of the SPS catalysts based on fuming H_2SO_4. Thus it is probable that the more severe sulphonation conditions yield SPS with higher acidity, in turn leading to a more facile transesterification catalyst. Transesterification have been reported with SPS based on glucose recently, albeit at higher temperatures and thus much higher rates - 96–98% yield of methyl oleate was achieved from triolein after 5 h at 130°C [130].

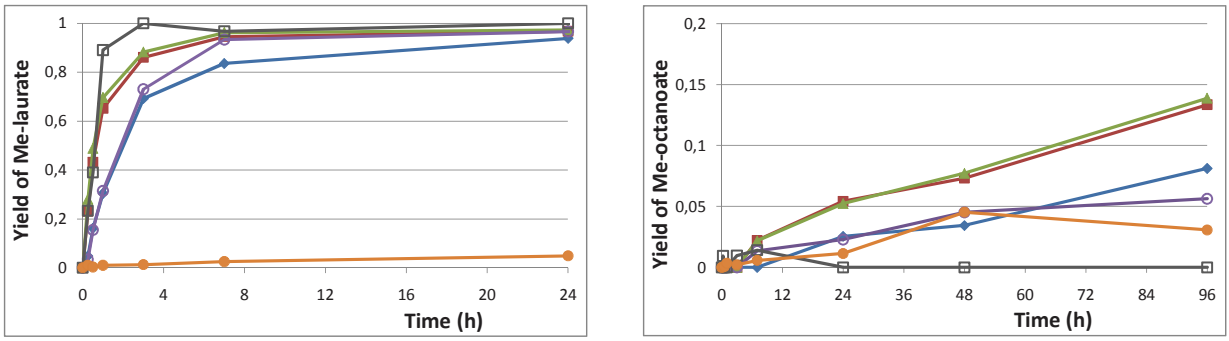

Figure 2.11: Yield of methyl laurate *(left-hand side)* and methyl octanoate *(right-hand side)* over sulphonated, pyrolysed sucrose as a function of time and variation of carbohydrate and percentage of SO_3 in H_2SO_4 during sulphonation. Legend: Sucrose, 30% SO_3/H_2SO_4 (—◆—), Starch, 30% SO_3/H_2SO_4 (—■—), Sucrose, 15% SO_3/H_2SO_4 (—▲—), Starch, 15% SO_3/H_2SO_4 (—○—), Sucrose, 0% SO_3/H_2SO_4 (—□—), Pyrolysed sucrose (not sulphonated) (—●—). Reaction conditions: 60°C, 4.3 mmol trioctanoate, 4.3 mmol lauric acid, 34.6 mmol methanol, dodecane as internal standard.

Table 2.1: Reaction rates based on the yield of methyl laurate after 0.25, 0.5, and 1 h of reaction. Conditions: 60°C, 4.3 mmol trioctanoate, 4.3 mmol lauric acid, 34.6 mmol methanol, dodecane as internal standard.

Catalyst	Catalyst mass [g]	Rate [mmol/g/h)]		
		0.25 h	0.5 h	1 h
S.P. sucrose, 30% SO_3/H_2SO_4	0.0760	8.92	15.2	14.3
S.P. starch, 30% SO_3/H_2SO_4	0.1709	19.3	18.1	13.6
S.P. sucrose, 15% SO_3/H_2SO_4	0.2032	19.7	17.2	12.30
S.P. starch, 15% SO_3/H_2SO_4	0.1606	3.01	6.85	7.00
S.P. sucrose, 96 wt% H_2SO_4	0.2120	15.7	13.2	15.0
Pyrolysed sucrose	0.2800	0.52	0.068	0.13

It can be observed that the esterification rate over PS was very low, as about 5% and 7% yield of methyl laurate was obtained after respectively 24 h and 96 h of reaction at 60°C. The rate was so low that it may be speculated if the observed yield was due to self-catalysed esterification by the lauric acid in the model reaction mixture. It can be stated that the pyrolysed sucrose (PS) was practically inactive even though it may contain minor amounts of weak carboxylic acids linked to the graphene sheets of the carbonised material [132, 312]. Some transesterification was indicated with this catalyst

as well, which should not be expected from weak acids.

Using fuming sulphuric acid for the catalyst sulphonation mostly enhanced the esterification of lauric acid with methanol, but with the 15% SO_3/H_2SO_4 the rate was only 40% of that of the sucrose equivalent in Table 2.1, using the data after 0.5 h reaction. It is not clear why this material was much less active than the other SPS catalysts having been exposed to fuming sulphuric acid. An enhancement of the esterification rate of 60-95% by using 15% fuming sulphuric acid has previously been found in literature by sulphonation of glucose pyrolysed at 400°C [128, 313].

It can be speculated that the sulphonation in fuming sulphuric acid allowed removal of more remaining oxygen in the form of water from the carbonaceous material, possibly also some binders connecting the graphene layers. On the other hand the stronger sulphonation conditions also yielded more sulphonic acid-functionalities on the resulting material. This has for instance been found by Takagaki and co-authors [132].

Thus it can be concluded that using fuming sulphuric acid for the sulphonation enhanced the formation of methyl ester during fatty acid esterification. However, the retention of the sulphonated catalyst during filtration was much poorer with the sulphonated materials.

Reuse of the investigated catalysts has not been attempted so it cannot be established if any trend in the activity as a function of the pyrolysis conditions would establish after several cycles of re-use. However, the spent reaction mixtures were tested with an aqueous solution of $Ba(NO_3)_2$ and no precipitate of $BaSO_4$ were oserved in any solution, thus it can be suspected that leaching of sulphate did not take place and the observed differences in activity would be persistent over time.

2.5 Immobilisation of SPS and continuous esterification

The application of a strong sulphonic acid based on pyrolysed carbohydrates for esterification, as mentioned in 2.4, could hold advantages to use in the esterification step of FAME production. However, the use of powders in liquid-phase large-scale chemical operation is usually not desirable, even though forming powders into extrudates would be a suggestion with inorganic powders. Therefore immobilisation of the active SPS phase (ISPS) on more suitable supports is necessary.

Impregnation of sucrose has been performed on various ceramic support materials followed by pyrolysis, sulphonation, washing and drying. Furthermore, the acidic SPS powder has been suspended in polyurethane foam. These two different types of immobilised or supported SPS catalysts have been tested for esterification and transesterification of lauric acid and trioctanoate, respectively, with methanol, analogously to the unsupported SPS described in section 2.4.

In addition, a pelletised ISPS/SiO_2 and an open-cell ISPS/Al_2O_3 catalyst have been tested for the continuous esterification of a model feed containing methanol and lauric acid in a tubular packed-bed reactor, and an open-cell ISPS/Al_2O_3have moreover been tested in transesterification and esterification of respectively rapeseed oil and abattoir waste fat with methanol.

2.5.1 Impregnation on ceramics and properties of SPS

The ceramic support materials were impregnated with varying amounts of sucrose via aqueous solutions prior to pyrolysis at 400°C/15 h and sulphonation at 150°C/15 h. Table 2.2 shows the applied catalysts and the data of their impregnation properties. The pelletised ceramics could be loaded with up to 10% of their own mass as sucrose, however, the open-cell ceramic cylinders had a much bigger hold-up of free volume in the cells and could potentially absorb many times more sugar than the pellets. However, it is evident that the loosely bound pyrolysed and sulphonated impregnated sucrose on the open-cell alumina is also more easily washed away during the sulphonation, and a larger part of this organic matter is removed during pyrolysis as well.

During the sulphonation, the TiO_2 and the ZrO_2 pellets were somewhat degraded - the TiO_2 crumbled into smaller black pieces while the ZrO_2 degraded into small black flakes and black powder. It was thus evident that the pellets could not endure the treatment with sulphuric acid at 150°C. Titania and zirconia are known to be resistant even to strong acids, so it is suspected that the pellets could have contained a basic binding matrix, for instance CaO. This has, however, not been reported by the manufacturer. Nonetheless, the ISPS degraded pellet materials were applied as catalysts after washing and drying, using 0.5 g of each.

The blackened SiO_2-pellets and the open-cell Al_2O_3 materials formed by impregnation, pyrolysis and sulphonation - ISPS - are depicted in the photographs of Figure 2.12. Characterisation of the powder have been performed by BET area estimation by N_2 physisorption at 77 K, by CHNS elemental analysis, and by wet titration of the solids. This is given in Table 2.3. It can be observed that the SPS had an almost negligible surface area. The BET technique is not that precise, and two repetitive measurements showed no surface area at all for the SPS - however, this magnitude of SPS surface area have been reported previously, and it is known that the surface area increasis by swelling in

liquid solvent [132, 313]. The surface areas of the impregnated ceramics are apparantly very dependent on the original ceramic material. ISPS/alumina lost most of its interior surface area while the ISPS/silica pellets did not and the alumina absorbed more sugar during impregnation, even though the net gain in weight was smaller of the ISPS/alumina.

Table 2.2: Impregnation, carbonatisation and sulphonation.
Ø: Diameter, L: Length; OCC: Open-cell ceramic; IS: Impregnated sucrose; IPS: Impregnated pyrolysed sucrose-impregnated; ISPS Impregnated sulphonated pyrolysed sucrose.

Batch	Material	Dimensions (Ø × L) [mm × mm]	weight gain of support IS [wt%]	IPS [wt%]	ISPS [wt%]
# 1	ZrO_2-pellets	3 × 3-8 [a]	9.47%	3.8%	4.5%
# 2	SiO_2-pellets	3 × 3-8 [a,b]	9.48%	3.8%	4.5%
# 3	TiO_2-pellets	3 × 3-8 [a]	7.95%	3.19%	3.78%
# 4	TiO_2-pellets	3 × 3-8 [a]	7.37%	2.96%	
# 5	Al_2O_3-OCC	14.5 × 20 [a]	39.59%	10.75%	1.12%
# 6	Al_2O_3-OCC	20 × 20 [a]	19.08%	5.53%	3.87%
# 7	Al_2O_3-OCC	9.5 × 20 [b]	7.36%	2.00%	1.40%
# 8	Al_2O_3-OCC	20 × 20 [c]	32.74%	8.48%	5.73%

[a] tested in batch esterification of model feed
[b] tested in continuous esterification of model feed
[c] tested in continuous esterification and transesterification of industrial feedstocks

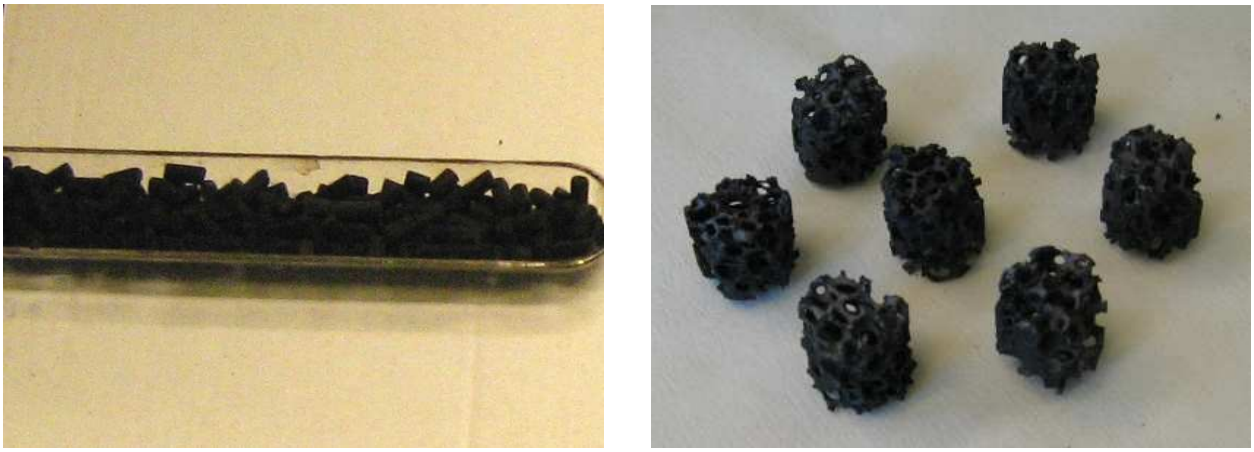

Figure 2.12: Impregnated sulphonated pyrolysed sucrose on SiO_2-pellets (*left-hand side*) and Al_2O_3-open-cell ceramic foam *right-hand side*.

From the gross formula proposed from the CHNS-analysis it appears that the original ratio of H:O in the sucrose is more or less intact after pyrolysis. This means that one of the most important processes of the pyrolysis is the formal removal of water, maybe some CO and CO_2, along with some tar oils (which were observed as condensating products in the pyrolysis reactor outlet). However, this H:O-ratio changed during sulphonation, where the amount of hydrogen was severely lowered (about 60 % compared to the PS), while the amount of oxygen removed is only (28%) - it should be expected that the sulphuric acid, being highly hygroscopic, would lead primarily to dehydration and sulphonation of the pyrolysed sucrose.

The oxygen amount of the biomass cannot be estimated on the impregnated from the CHNS-

analysis and can only be estimated by a mole balance in PS and SPS. Importantly, the loading of organic matter is higher on the ISPS open-cell alumina compared to the pelletised silica, and the amount of sulphate functionalities in the organic matter itself is apparantly 65% percent higher for the ISPS/alumina. It may therefore be expected that the ISPS/alumina is much more active *per mass* than the ISPS/silica. It is also obvious that the content of hydrogen is much higher in the ISPS/alumina than the ISPS/silica. Possibly the ISPS/alumina could have contained a lot of water, whereby the analysis of H is affected, since the high amount of H in ISPS/alumina would otherwise correspond almost to alkene hydrocarbons. This is also indicated by the weight gain of the ISPS/alumina after synthesis, which was only 3.87% (while 10.3% of the sample during CHNS-analysis was measurable compounds).

By titration of the PS, SPS and the ISPS/alumina it can be seen that a loading of almost 3 mmol H^+/g can be achieved in the SPS powder, however, the open-cell ISPS/alumina did not contain as many acidic sites when compared to the loading of organic matter impregnated on the ceramic, thus the sulphonation degree cannot be directly transferred to the supported catalyst. The PS contained very little acidity, possibly in the form of a few carboxylic acids. It was also attempted to titrate the ISPS/silica, however, it did not show a lowering of pH by addition of a KCl-solution, and the titration yielded negligible concentrations of H^+. This is not currently understood.

Table 2.3: Areas, composition and acidity of investigated PS, SPS, ISPS and support materials.

Batch	Material	BET area [m^2/g]	Acidity[a] [mmol H^+/g]	Organic matter[b] [wt%]	Gross formula[c] [mol/mol]
	PS		0.053	100%	$CH_{1.20}O_{0.58}$
	SPS	0.03	2.94	100%	$CH_{0.48}O_{0.42}(SO_3)_{0.016}$
# 2	SiO_2 pellets	233		0%	
# 2	ISPS/SiO_2 pellets	177	0.00	6.1%	$CH_{0.61}O_x(SO_3)_{0.0096}$
# 6	open-cell Al_2O_3	39.2		0%	
# 6	open-cell ISPS/Al_2O_3	3.5	0.174	10.3%	$CH_{1.89}O_x(SO_3)_{0.016}$

[a] Based on ion-exchanged titration.
[b] Known organic matter calculated from the CHNS-analysis, which means that non-sulphonate-oxygen (eg. water) cannot be accounted for on the ISPS.
[c] Suggested from the CHNS-analysis on basis of the known organic matter.

2.5.2 Activity of impregnated SPS on ceramics

A series of batch experiments were conducted to compare the ceramic ISPS catalysts with the unsupported SPS batch experiments. Figure 2.13 shows the yields of methyl laurate and methyl octanoate during sampling from the catalysed esterification and transesterification over the ISPS on ceramic pellets and open-cell ceramic foam. 0.5 g of each of the pelletised materials were used (batch # 1-4), while respectively 7.0 g and 4.2 g were used of batch # 5 and 6. Batch # 1-5 were with 4.00 ml (3.35 g) of reactant mixture (1:1:8 molar ratio of trioctanoate, lauric acid and methanol), while 16 ml was used for batch # 6.

The most active catalysts were the (partly crumbled) pelletised cylinders of TiO_2-cylinders. However, batch # 5 of ISPS/alumina was almost as active (not all of the catalysts could be covered with reactant solution, so comparisons should be made with caution). Batch # 6, having a 6.7 times lower

catalyst-to-reactant ratio than batch # 5, was also less active than batch # 5, but not as much as the difference in should imply due to the lack of reactant solution to completely cover the batch # ISPS/Al_2O_3. The least active catalyst for the esterification was the ISPS/silica, reaching just over 80% yield of methyl laurate after 96 h.

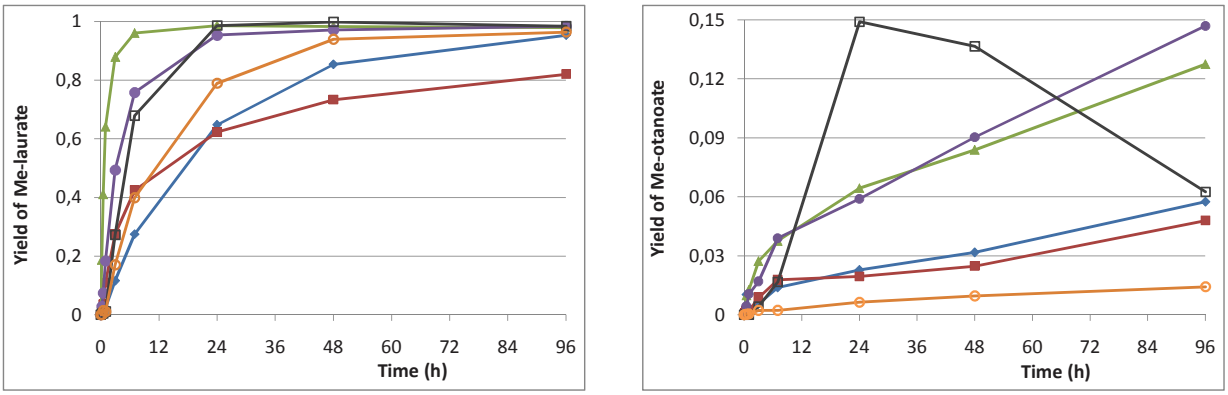

Figure 2.13: Activity measurements of the impregnated sulphonated pyrolysed sucrose in batch-mode. Legend: ISPS/ZrO_2-pellets, batch # 1 (—◆—), ISPS/SiO_2-pellets, batch # 2 (—■—), ISPS/TiO_2-pellets, batch # 3 (—▲—), ISPS/TiO_2-pellets, batch # 4 (—●—), ISPS/Al_2O_3-open-cell, batch # 5 (—□—), ISPS/Al_2O_3-open-cell, batch # 6 (—○—). Reaction conditions: 60°C, 4.3 mmol trioctanoate, 4.3 mmol lauric acid, 34.6 mmol methanol, dodecane as internal standard.

In all of the samples with pelletised catalyst supports, the yield of methyl octanoate grew at the highest rate for the first 7 h whereupon the formation settled on a somewhat slower pace for all the tested ISPS ceramic pellets. The highest activity for transesterification to yield methyl octanoate were found with the two ISPS/TiO_2-catalysts. The ISPS on SiO_2 and ZrO_2 only yielded about 35-40% of the yields obtained for ISPS/TiO_2 during the entire time series. The two open-cell ISPS/Al_2O_3 catalysts showed different activity, and batch # 5 was also the most active during transesterification after 96 h. The yields after 24 h and 48 h of batch # 5 were, however, too high compared to the remaining samples taken out and should be disregarded in terms of activity comparison.

Compared with the SPS, the ISPS show over an order of magnitude lower activity, however, the loading of active phase is only a fraction of that present in the unsupported SPS (merely 3 - 7%, according to Table 2.3), which in fact make the supported and unsupported catalysts comparable.

2.5.3 Immobilisation and activity of SPS in polymer foam

Another strategy for supporting the SPS catalyst on a suitable carrier was building the SPS into a polymer matrix with suitable porosity. 6 different PUR foam catalysts are employed with SPS-loadings of either 16 wt% (3 different), 17 wt%, and 20 wt% loading of SPS and a blank sample of 0% SPS in the PUR foam matrix. However, no further information is available about the foaming proces, apart form the fact that the method and chemicals used should produce an internal open network of pores to allow reactants and products to diffuse in and out of the polymer matrix. It is, however, not known if the polymers foamed together with SPS obtain this open-porous internal network during foaming. The physical appearance of the SPS foam matrix samples was as a hard, slightly plastic and visibly porous material, in which also the SPS powder particles were visible as can be seen in Figure 2.14. Compared to the SPS-free PUR having a light yellowish colour, the PUR

Figure 2.14: Appearance of the polyurethane polymer matrices containing respectively 0% (*left*), 16% (*middle*), and 20% (*right*) SPS.

matrices containing SPS had a greyish colour due to the addition of the black powder.

Ca. 0.56 g of all the catalysts were exposed to 3.35 g of a 1:1:8 molar mixture of lauric acid, trioctanoate and methanol. The yields of methyl laurate and methyl octanoate in the SPS-containing PUR polymer matrices (SPS-PUR) as a function of time are shown in Figure 2.15. All the SPS-containing foams show a rise in the methyl laurate concentration over the first hours, but the rises in the yields started to stagnate after 7 or 24 h for all the SPS-PUR samples. After 96 h, only about 55% yield is obtained in the best case, using the PUR foam containing 17 wt% SPS. The 20 wt% SPS-PUR yielded about 40% methyl laurate, while the three 16 wt% SPS-PUR samples showed even lower yields between 15% and 35% after 96 h. For comparison, the concentration of methyl laurate over the blank PUR foam containing no SPS rose steadily and yielded about 10% methyl laurate after 96 h.

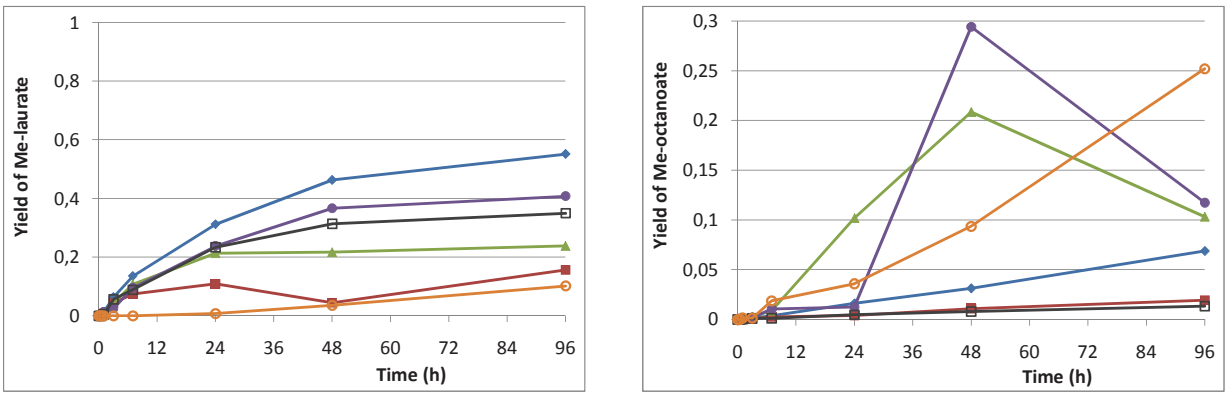

Figure 2.15: Activity measurements of the impregnated sulphonated pyrolysed sucrose in batch-mode. Legend: 17% SPS-PUR (—♦—), 16% SPS-PUR # 1 (—■—), 16% SPS-PUR # 2 (—▲—), 20% SPS-PUR (—●—), 16% SPS-PUR # 3 (—□—), Blank PUR # 6 (—○—). Reaction conditions: 60°C, 4.3 mmol trioctanoate, 4.3 mmol lauric acid, 34.6 mmol methanol, dodecane as internal standard.

Minor amounts of methyl octanoate were also seen to be formed during the course of the experimentation. A few of the values of methyl octanoate yield in the 24 h and 48 h samples are over 10%, but show a drop towards the 96 h sample. Generally these outlying sample concentrations must be considered erroneous outliers compared to the reaction progress observed in all of the other samples. From Figure 2.15 it is observed that the yield of methyl octanoate over the blank sample rose faster than any of the the SPS-PUR indicated a yield of 25% after 96 h, higher than in any of the other samples. This is peculiar and cannot be explained from acidic or basic properties of the PUR material, as the polymer linkage in PUR is a neutral carbamate functionality. The chromatogram areas of the samples were quite small in all of the reactants and products, so some systematic inaccuracy during

sampling and noise signals during GC-FID analysis may have led to this error.

It can be concluded that the SPS-PUR did not show high esterification activities, at least not comparable to the pure SPS powder mentioned in section 2.4, which yielded up to around 90% methyl laurate after 1 h reaction. This could be due addition of the solid acid to the PUR foaming mixture, which was likely affected by acid. The foaming of PUR from isocyanate and alcohol is catalysed by nucleophiles (usually bases like DABCO (1,4-diazabicyclo[2.2.2]octane) are used). Also it is uncertain whether or not the pore structure of the claimed blank sample has resulted during foaming of the SPS-PUR catalysts as well. The sulphonic acid functionalities of the SPS may be completely covered in the polymer and not be accessible. Characterisation and investigation of the foaming would be necessary and highly desirable to give an explanation for the low activity observed.

2.5.4 Continuous esterification of model feed

Two of the SPS-impregnated ceramics were loaded into a tubular steel reactor of 9,5 mm in inner diameter × 15 cm in length and tested in the continuous esterification, namely the ISPS/SiO_2-pellets and the open-cell ISPS/Al_2O_3. The reactor dimensions corresponded to a loading of 7 open-cell ISPS/Al_2O_3 cylinders of 4.354 g (batch # 7) and 4.582 g of ISPS/SiO2-pellets (batch # 2).

The ISPS/SiO_2-pellets were tested as catalysts in the esterification of a 30:1:0.2 mixture of the molar ratios of respectively methanol, lauric acid, and dodecane as an internal standard. 3 samples were taken at each steady-state condition and the average mole fraction calculated at each condition. However, the sum of the GC yields of methyl laurate and remaining lauric acid varied between 80% and 120%. To even out these fluctuations, the yield of methyl laurate and remaining lauric acid was calculated by using the two GC areas with respect to their response-factors obtained from GC reference standards of the pure compounds in methanol. This was justified as no side-reactions take place during the esterification-hydrolysis equilibrium around 60°C in dilute solutions of carboxylic acid in alcohol. When doing this, the yields of methyl laurate and unconverted lauric acid obtained were within 3-4% at each condition, but the internal standard was at the same time disregarded.

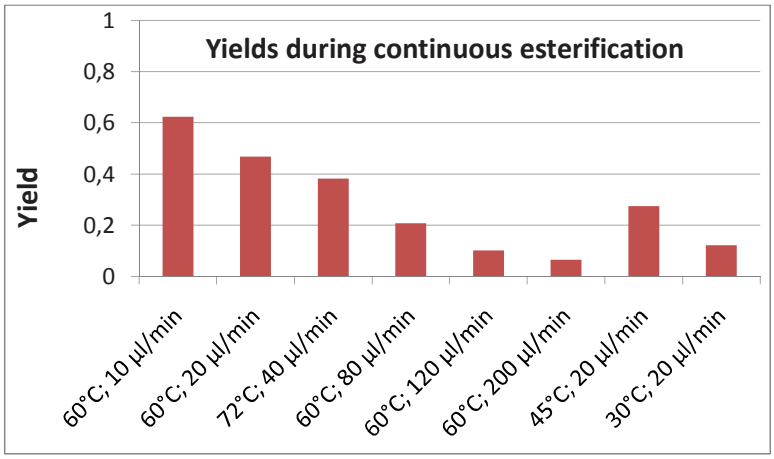

Figure 2.16: Activity for continuous esterification of lauric acid with methanol at 1:30 molar ratio by variation of temperature and flow rate over 4.582 g ISPS/SiO_2.

When the flow rate was increased from 10 to 200 μL/min (WHSV = 1.8-36 · 10^{-3} h^{-1}) the amount

of converted lauric acid (yield of methyl laurate) goes down from 62% to 6.5%, as given in Figure 2.16. This is expected, as increased flow rate lowers the space time and therefore the contact time of the feed with the catalyst, effectively lowering the yield. The sample at 40 μL/min was taken at 72°C, however, the yield of methyl laurate seem to fit well in the row of samples with different flow rates taken at 60°C. When using 45 and 30°C at 20 μL/min for the esterification of lauric acid it is evident that the conversion of lauric acid drops to 27% and 12%, respectively, compared to 47% conversion at 60°C.

The open-cell ISPS/Al_2O_3 of 9,5 mm × 20 mm (batch 7 #) were tested in a mixture with the molar ratios 8:1:1:0.2 of respectively methanol, lauric acid, trioctanoin, and dodecane as an internal standard (similar mixture to that mentioned in section 2.4). Unfortunately, stable operation was only achieved at 3 different conditions (of 2 samples each) because the pump flow was unstable during part of the experimentation. The yields obtained during stable operation are plotted in Table 2.4.

Table 2.4: Esterification yields in 1:8 molar ratio of lauric acid to methanol over 4.354 g open-cell ISPS/Al_2O_3 ceramic cylinders.

Temperature	Flow rate	Yield methyl laurate	Lauric acid remaining
25°C	0.01 ml/min	0.022	0.978
60°C	0.03 ml/min	0.140	0.860
60°C	0.02 ml/min	0.207	0.793

At 25°C and 10 μL/min liquid flow rate (WHSV = $1.9 \cdot 10^{-3}$ h^{-1}) a mere 2% conversion was observed of the lauric acid. At 20 and 30 μL/min of liquid flow rate (WHSV = 3.8 and $5.8 \cdot 10^{-3}$ h^{-1}) and 60°C, the yields were respectively 21% and 14% of methyl laurate. Shorter residence times (higher space velocities) led to lower conversion, while lower temperatures (room temperature) also led to lower conversion.

When comparing the ISPS/SiO_2-pellets with the open-cell ISPS/Al_2O_3, the yield of methyl laurate over the latter at 20 μL/min is 44% lower than over the former. This could be due to the difference in the loading of active phase of the ceramics and the intrinsic properties of the two different catalysts. It may be suspected that higher intrinsic surface area of the SiO_2-pellets allowed a higher deposition of active material and a higher degree of exposure to the alcohol-fatty acid solution. It is also evident that the former catalysts had a much higher molar ratio of methanol to lauric acid in the feed solution. From Table 2.2 it is evident that the SiO_2-pellets contained more than 3 times active SPS phase compared to open-cell ISPS/Al_2O_3 on a mass basis, and it can be concluded that the active phase in open-cell ISPS/Al_2O_3 was more active in the esterification than the ISPS/SiO_2 when considering the differences in active phase loading.

The open-cell ISPS/Al_2O_3 probably has very advantageous flow properties for viscous oil emulsions which can only penetrate small pores slowly. Also, it could be visibly observed that some of the SPS impregnated on the open-cell Al_2O_3 was situated on the exterior surface of Al_2O_3 as small lumps and was thus exposed directly to the liquid flow, at least immediately after the sulphonation. This is an advantage in terms of the low pore diffusivities of larger fat molecules. The viscosity of dilute lauric acid in methanol is probably a few orders of magnitude lower than that of typical fats and oils, thus the hydrodynamic properties of the feed have not been problematic during these experiments. ISPS/SiO_2-pellets, despite having a reasonable bed porosity upon reactor loading and

therefore minimal pressure drop during reactant pumping, owe their high loading of active phase to their micro- and mesoporosity. However, this may not be an advantage when using bigger molecules like triglycerides and FFAs.

However, during these experiments it has been clearly demonstrated that continuous esterification of the model feed was possible over both ISPS/SiO_2-pellets and ISPS/Al_2O_3-open-cell cylinders.

2.5.5 Continuous esterification of industrial fatty feedstocks

The SPS impregnated on open-cell Al_2O_3 was subjected to further investigation in a larger flow-reactor to evaluate the possibility of using the catalyst for esterification or transesterification on real feeds and in a larger scale. 25 ISPSAl_2O_3-cylinders based on open-cell ceramic cylinders (batch # 8) were stacked uniaxially after each other the reactor. The cylinders were 2.0 cm in diameter and 2.0 cm in length with an average cell diameter of 3 mm of the connected cavities in the open-cell Al_2O_3. Cylindric static mixers were placed as spacers between each stack of 5 catalyst cylinders, effectively dividing the bed in 5 equal-sized beds of 5 ISPS/Al_2O_3 cylinders. The reactor was operated without the continuous addition of reactants and extraction of products, i.e. as a batch reactor. A sketch of the packed-bed reactor is given in Figure 2.17.

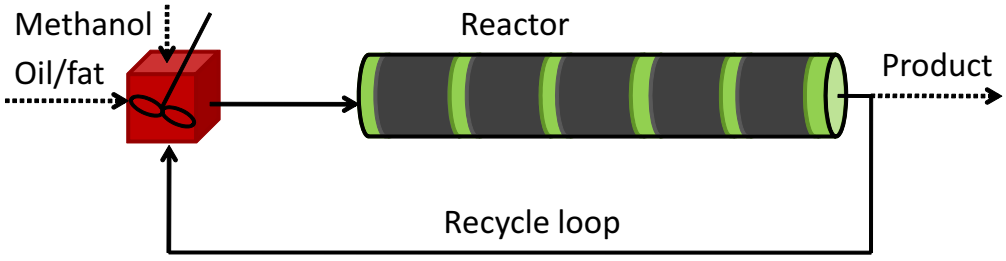

Figure 2.17: A schematic of the tubular packed-bed loop reactor. The red box is a mixer (emulsifier), the green short cylinders constitute the static mixers between the black cylindrical catalysts of ISPS supported on open-cell-Al_2O_3. The addition of reactants and the product stream (dotted lines) was shut off for an "infinite recycle ratio", thus converting the reactor into a packed-bed batch reactor.

0.5 kg of methanol and 2.0 kg of rapeseed oil were added as reactants to the continuous loop. Then the extraction of product and the reactant inlets were closed and the emulsification by the stirring mixer ensured maintenance of the emulsion of methanol and oil. The flow speed is unimportant in this context, as the average contact time across the bed is independent of the pumping speed in a closed loop. After 3 days of reaction at 60°C the yield of FAME was at a marginal level of about 2%, which must stem from transesterification reaction as the rapeseed oil did not contain any FFA.

As the produced amount of FAME from the rapeseed oil is low it may be speculated that the formed FAME is simply produced due to the thermal transesterification effect at 60°C. However, the amount of active catalytic sites is not high compared to the reactant amount. On the other hand, the open-cell ceramic had excellent flow properties as the pressure drop across the entire catalyst bed during pumping was minimal.

After the experimentation with rapeseed oil, 0.5 kg methanol and 2.0 kg abattoir waste fat from Daka Biodiesel was tested according to the same procedure and using the same catalyst. Waste fats usually contain anywhere between 5% and 30% fats, depending on the season, so it was expected

that the acidic catalyst would work efficiently in the esterification of the FFA to FAME. However, after 22 h of reaction running no traces of FAME were observed during analysis.

Abattoir waste fats contain some amounts of alkali salts and these react with the Brønsted-acidic catalyst and ion-exchanges it to the polar methanol phase. Also the waste fat was likely sufficiently buffered by the minor presence of various salts (sulphates, phosphates, carbonates) to absorb the proton to the liquid. Therefore it is easily suspected that the activity of the catalyst has been lost due to the ion-exchange. This explains the absence of any FAME in the analysis of the organic products. The ion-exchange was confirmed upon titration of some of the spent cylinders, which contained 0.00 mmol H^+/g compared to 0.174 mmol H^+/g of the fresh ISPS/Al_2O_3 (batch # 6) and 2.94 mmol H^+/g of the fresh SPS. Thus, it can be concluded that the catalyst deactivated by ion-exchange with alkali ions in the abattoir waste fat.

2.6 Basic catalysts for transesterification

A number of bases of different types have been screened as candidates for transesterification catalysts that may be immobilised on a solid support for FAME synthesis. Despite the fact that sulphonic acid-functionalised ionic liquids may be used for the transesterification as described in section 2.3, strong bases usually work several orders of magnitude faster than strong acids. The role of the base in the transesterification with methanol is to facilitate the formation of methoxide ions as the active species, as transesterification takes place by attack of the alkoxide on the carbonyl C-atom [85]. For instance, if the NaOH or KOH are added, they will form water and methoxide ion as showed in Figure 2.4 a), however, the water formed is undesired as it can lead to basic hydrolysis of the esters. More generally any base added will react with the methanol to form methoxide ion and correponding acid according to the equilibrium in Figure 2.18 b).

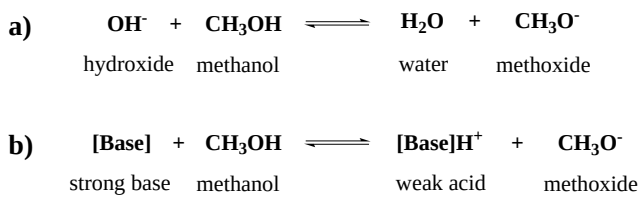

Figure 2.18: a) formation of methoxide ions and water by methanol and hydroxide during the industrial production of FAME aided by KOH or NaOH, and **b)** the general role of any strong base added to the methanol-containing solution to catalyse transesterification.

2.6.1 Amine-functionalised ionic liquids

Ionic liquids have advantageous phase properties for ester reactions, and the possibility of fine-tuning hydrophilic and lipophilic properties can enhance the separation properties after reaction. Thus, three amine-functionalised ionic liquids were therefore tested for transesterification, namely the bromide ($[Br^-]$), boron flourate ($[BF_4^-]$), and bis(triflamide) ($[NTf_2^-]$) of amine-functionalised butylmethylimidazolium ($[BMIM–NH_2^+]$). It was suspected that the amine functionality or the anion of the ionic liquid could add basicity and take up protons to form methoxide from methanol, thus facilitating transesterification. The yield of methyl octanoate and remaining trioctanoate observed from the time series with these three ionic liquids are shown in Figure 2.19.

It is clear that only around 0.1% yield of methyl octanoate was obtained, possibly due to an impurity in the trioctanoate or formed in the glass vials after sampling, as the amount of methyl octanoate was not increasing with time. The amount of trioctanoate is generally around 100%, but vary somewhat between some 90% and 125%. It is therefore evident that some inaccuracy during the sampling, workup and analysis of the samples contributed to the variation. The inaccuracy contributed more than what would usually be expected from GC analysis.

To conclude, the ionic liquids are completely inactive. Furthermore no octanoic acid is observed in any of the samples, thus excluding loss of the reactant or product as FFA. This proved that despite the suitable phase properties of ionic liquids a strong base (or strongly acidic ionic liquid, see section 2.3) is necessary to facilitate the transesterification reaction.

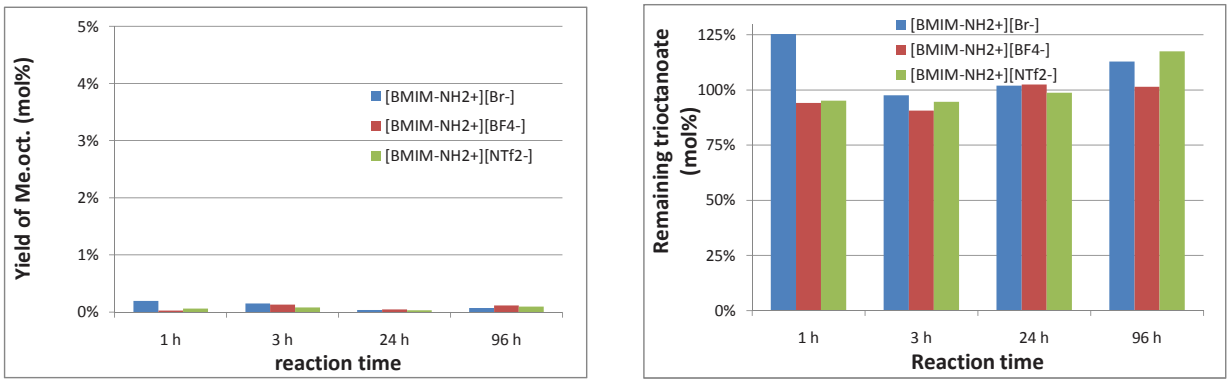

Figure 2.19: Yield of methyl octanoate *(left-hand side)* and remaining trioctanoate *(right-hand side)* with amine-functionalised ionic liquids as catalysing medium. The amine-functional cation was [BMIM–NH_2^+] using either bromide ([Br−], ■), borofluorate ([BF_4−], ■), or bis(triflamide) ([NTf_2−], ■) as cation. Conditions: 60°C, 5 mmol trioctanoate, 45 mmol methanol, dodecane as internal standard.

2.6.2 Basic inorganic salts

Four organic and inorganic salts have been tested as catalysts for transesterification of the model mixture of methanol and trioctanote. Guanidinium chloride (GuaCl), guanidinium carbonate (Gua_2CO_3), and cesium carbonate (Cs_2CO_3) represented compounds that are all soluble in water and small alcohols. They were compared with the mixed oxide of $MgO{\cdot}La_2O_3$, which was expected to be insoluble.

The role of guanidinium carbonate in the transesterification have previously been debated. It has been claimed that carbonate vaporised from the solution as CO_2 and that the remaining guanidine acted as a strong base [319]. However, the carbonate could also be suspected to act as the base according to Figure 2.18 when the salt dissolves into the carbonate and guanidinium ions in methanol. It is at least not clarified by Peter & Weidner why the acidic CO_2 vaporised from a basic solution of methanol [319].

The results of the experimentation are given in Figure 2.20. It can be observed that Gua_2CO_3 and Cs_2CO_3 showed formation of methyl octanoate at comparable rates, albeit the inorganic Cs-salt at a slightly higher rate. Over 90% yield is established after 3 h of reaction. The guanidinium chloride was completely inactive, being weakly acidic.

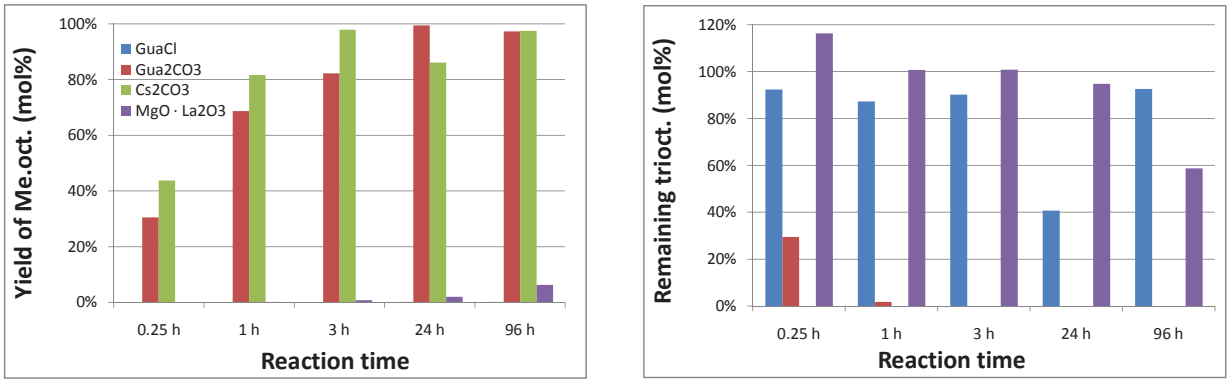

Figure 2.20: Yield of methyl octanoate *(left-hand side)* and remaining trioctanoate *(right-hand side)* with various salts used as catalysing medium. Legend: Guanidinium chloride (GuaCl, ■, 4 mmol), guanidinium carbonate (Gua_2CO_3, ■, 1.8 mmol), cesium carbonate (Cs_2CO_3, ■, 1.8 mmol), Magnesium lanthanum mixed oxide ($MgO{\cdot}La_2O_3$, ■, 0.22 mmol). Conditions: 60°C, 5 mmol trioctanoate, 45 mmol methanol, dodecane as internal standard.

This clearly demonstrated that the guanidinium cation facilitated the carbonate dissolution in the methanol. Guanidine is a strong base ($pK_a = 13.6$), thus the corresponding acid, the guanidinium ion, is weak and was most likely stable in the methanol solution. Therefore the dissolved carbonate ion (CO_3^{2-}) acted as the base forming methoxide ions according to Figure 2.18. However, the rates of reaction measured over CO_3^{2-}-base were not as high as those reported (ref. [319]) and monitoring of the CO_2-pressure over the solutions have not been performed in the present work, so any dependency of the pressure on the turnover rate of methanolysis cannot be established [319].

The $MgO \cdot La_2O_3$ proved to be almost inactive compared with the carbonate, however, only 0.22 mmol $MgO \cdot La_2O_3$ was added compared to 1.8 mmol of the carbonates, and a mere 7% yield of methyl octanoate is observed after 96 h.

Again it was found that the remaining trioctanoates amount were sometimes too low to complete the mass balance due to inaccuracy of the trioctanoate analysis, albeit the remaining trioctanoate in most samples of GuaCl and $MgO \cdot La_2O_3$ were between 90% and 100%. No or only minor traces of octanoic acid were found during the experimentation with these catalysts, so the hydrolysis cannot account for the missing reactant.

2.6.3 Amidines and guanidines

The posibility of using strong organic basis for the transesterification have been investigated. Organic molecules often allow for the linkage to a polymeric support or a ceramic with functional groups through organic synthesis, and this would make anchoring of the base to a given support easier and possibly prevent leaching of the active basic sites over time.

Transesterifications over amines of varying basicity have previously been investigated. Villa and co-workers nested various amines to carbon nanotubes and achieved up to 80% conversion of tributyrate with methanol at 60°C after 8 h. Differences in activity were ascribed to basicity, which were higher for more substituted amines [79]. Conversions of tributyrate of equal magnitudes were achieved at 115°C using various di-amines [80]. Quarternary amine with OH^--counterions linked to silica or a polymeric resin for transesterification of triacetin with methanol achieved up to 65% yield in 4 h at 60°C [85]. This model reaction was also studied over a number of simple amines, but relatively high temperatures were necessary due to low basicity of the amines used [320]. Other transesterification reactions have been studied as well. For instance, methyl esters have succesfully been transtesterified with higher alcohols over MCM-41 functionalised with NH_2-linkers at 110°C [83].

Initially, cyclic and uncyclic guanidine (TMG respectively TBD) and cyclic amidines (DBU and DBN) have therefore been tested for transesterification of trioctanoate with methanol at 60°C and ambient pressure. The yields are given from Figure 2.21.

It is obvious that the reaction has run to completion almost instantaneously under the applied conditions. 2 mmol catalyst was added to the solution in the case of DBU, DBN and TMG, compared to 45 mmol MeOH and 5 mmol trioctanoate in the reaction mixture. The amounts of base used per mass are ca. half those of the masses of the acidic ionic liquids used in section 2.3, but nonetheless reaction was complete within minutes, not hours.

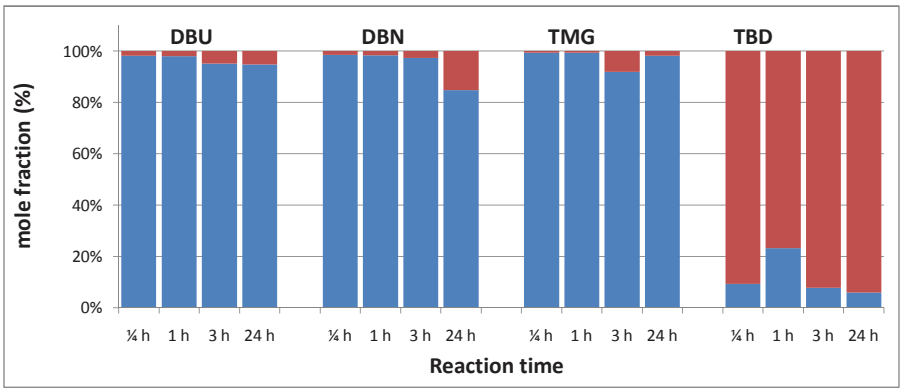

Figure 2.21: Yield of methyl octanoate (■) and by-product octanoic acid (■) during transesterification experiments using DBU (1,8-Diazabicyclo[5.4.0]undec-7-ene, 2.01 mmol), DBN (1,5-Diazabicyclo[4.3.0]non-5-ene, 2.06 mmol), TMG (1,1,3,3-tetramethylguanidine, 2.01 mmol), and TBD (1,5,7-triazabicyclo[4.4.0]dec-5-ene, 0.39 mmol) as catalysts. Conditions in each experiment: 60°C, 5 mmol trioctanoate, 45 mmol methanol, dodecane as internal standard.

It is clear that over time - and in the case of TBD from the very beginning of the experimentation - irreversible basic hydrolysis of trioctanoate or methyl octanoate have taken place. The TBD chemical may possibly have been impure and contained some water. Amidines and guanidines are very hygroscopic and should generally be stored with a desiccant. Water may also have been present as an impurity in the methanol and in the reactant solution (although anhydrous methanol was used).

Interestingly, only one fifth of TBD was added to the reaction solution compared to DBU, DBN and TMG, however, TBD still led to full conversion of trioctanoate within 15 min (albeit to the fatty acid and not the ester). It may be speculated that the lower amount of catalyst was the reason for the high yield of the fatty acid instead of the methyl ester - impurities of water could be bound by the hygroscopic organic bases, but only in the case that sufficient base was present in the reactant solution. It has previously been stated that the strongly basic organic amines are hygroscopic and that loss of activity may take place over time during transesterification [319].

To study the effect of substituting TMG with various linkers, a handful of substituted tetramethylguanidines were tested with the same model mixture. The results are given in Figure 2.22. The substituted guanidines used were propyl-, hexyl-, and benzyl- tetramethylguanidines. 0.35 mol was used for the propyl-TMG, while 0.26 mol was used for the latter two (compared with 5 mmol trioctanoate and 45 mmol methanol in each reaction mixture).

From the left-hand side of Figure 2.22 it is observed that the conversion is completed within 1 h and the with saturated substituents (propyl- and hexyl-TMG) within 15 min. The difference in is not clear, but the benzylic substituent attached to the TMG may contribute to a slight destabilisation of the resonance structure of the benzyltetramethylguanidinium ion making the Benzyl-TMG less basic.

However, compared with the experiments with the unsubstituted guanidines and amidines in Figure 2.21, the hydrolysis was much more prominent, and methyl octanoate was the primary product only in the 15 min sample. Hereafter about 80-100% octanoic acid is observed in the samples. It is suspected that the hygroscopic guanidines were contaminated with large amounts of water (a prerequisite of hydrolysis), that moisture was absorbed from the air, or that the reaction mixture

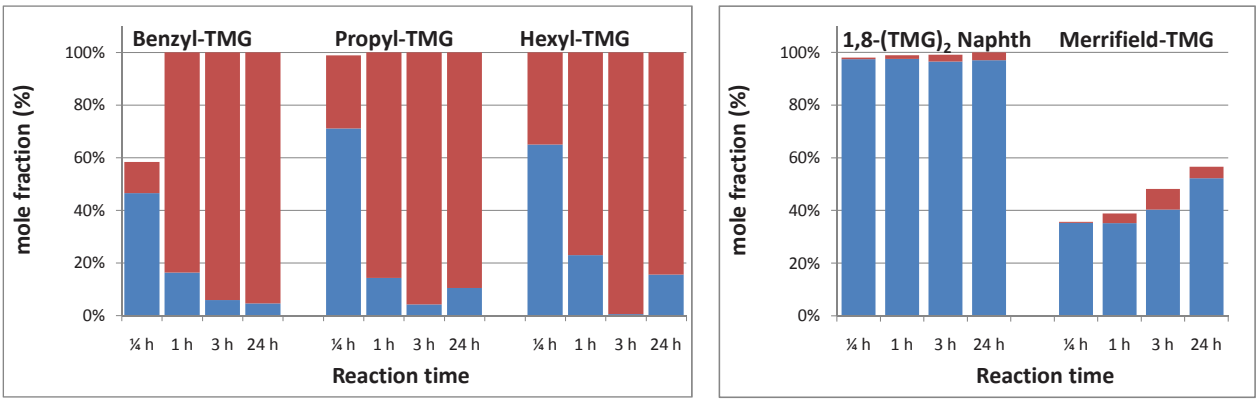

Figure 2.22: Yield of methyl octanoate (■) and by-product octanoic acid (■) during transesterification experiments over substituted and nested guanidines. *left-hand side:* 2 mmol each of alkyl-substituted tetramethylguanidines (TMGs); *right-hand side:* 1.99 mmol of 1,8-Bis(TMG)-Naphthalene and 0.51 mmol TMG on Merrifield resin. Conditions in each experiment: 60°C, 5 mmol trioctanoate, 45 mmol methanol, dodecane as internal standard.

contained water.

For comparison with the unsubstituted guanidine and amidines ca. 2 mmol was used of the 1,8-bis(TMG)-napthalene "proton sponge" while a TMG-amount corresponding to ca. 0.5 mmol was available with the TMG-functionalised Merrifield-resin. The results are shown in the right-hand side of Figure 2.22. Full conversion was achieved with 1,8-bis(TMG)-napthalene within minutes. In comparison with the substituted guanidines it is interesting, though, that very little hydrolysis of the octanoate esters took place. The activity of the Merrifield-TMG seem to have stalled somewhat, since over 30% methyl octanoate was observed at 15 min, but below 60% conversion was observed after 24 h. Contamination or deactivation cannot be excluded, perhaps due to a collapse of the TMG during or after the linking to the support, by incomplete linkage or by a deactivation mechanism connected to the support in parallel with that described by for instance by Liu and co-authors [85].

Schuchardt and co-workers studied substituted and polystyrene-linked guanidines, including cyclic guanidines (R-TBD) and achieved up to 75% conversion during transesterification of triglycerides using 5 mol% of various substituted guanidines nested on PS, but pentamethylguanidine (PMG, the simplest completely substituted guanidine-analogue) yielded above 90% FAME within 1 h [78]. Using 1 mol% of various substituted guanidines, TBD and Methyl-TBD appeared to be even more active than PMG [77]. Thus, the non-polymeric guanidines were always more active than their nested counterparts [78]. However, leaching of the TMG was as well observed, and the nested guanidines gradually lost activity for each reuse in the transesterification. Also the creation of a "double-linkage" to TMG from the support will result an inactive alkyl-guanidinium cation [78].

2.7 Heterogeneous catalysts for production of FAME: Conclusion

The most widespread method of producing biomass-based diesel is the formation of FAME from fats and oils and methanol. Esterification of FFAs in fats with methanol is catalysed by acids, while the consecutive transesterification of the fatty acid glyceride esters are catalysed by bases - even though very strong acids can be introduced, for instance as sulphonic acid-functionalised ionic liquids. Industrially the reactions are usually performed with mineral acids and bases mixed in the methanol phase, making the practical reuse of the homogeneous catalyst cumbersome.

Acid-functionalised ionic liquids as catalysts and reaction medium for both esterification and transesterification may be another promising way to catalyse the production of FAME in a batch-wise production process. The most acidic sulphonic acid-functionalised ILs investigated converted the lauric acid with methanol to methyl laurate within an hour and catalysed the transesterification of trioctanoate with methanol at about 99% conversion in 24 h. Interestingly, however, the mono- or di-glycerides were not converted as fast as the triglycerides, possibly due to emulgation properties. The optimisation of catalytic activity, separation of products and reaction medium as well as the leaching of the ionic liquid need thorough investigations before this method reaches sufficient technical maturity.

It has been shown that a highly acidic sulphonic acid based on pyrolysed carbohydrates (SPS) could be applied for the esterification of FFA for the production of FAME. Both starch, cellulose, glucose, and sucrose have been applied as starting materials for SPS synthesis, however, the latter was found to be slightly more active than cellulose and glucose for the esterification over SPS. No specific influence of the pyrolysis temperature on the activity of the final SPS catalysts could be established, however, sufficient pyrolysis time was necessary to ensure the efficiency of the sulphonation. Sulphonation in 15% or 30% fuming sulphuric acid led to the degradation of the material into a very fine powder and partial dissolution of the material in the wash water. The remaining sulphonated material, however, was more active than the SPS obtained in concentrated sulphuric acid sulphonation. Tests for sulphate leaching was performed with $Ba(NO_3)_2$, however no sulphate species were found in the reaction solution. Thus, it is established that the sulphonated functionalities are stable at 60°C reaction temperature.

The solid catalysts being reported to this date are usually based on small pellets or powders, however, in this work immobilisation of the active phase on an open-cell ceramic support has been carried out, which is more suitable for continuous tubular reactors due to low pressure drop. The SPS catalyst has been scaled up by supporting a suspension of SPS in polyerethane polymer, and impregnated on porous or open-cell ceramics by impregnation prior to catalyst synthesis. The supported SPS catalysts were less active than their unsupported analogues, due to over an order of magnitude lower amount of active sites per unit mass.

The supported catalysts may be easier to integrate with continuous reactors for production of FAME, for instance as tubular packed-bed reactors. The supported SPS catalysts was tested for continuous esterification of model compounds with methanol. The esterification activity was tested in a tubular backed-bed flow reactor with ISPS/SiO_2-pellets and open-cell-ISPS/Al_2O_3. Both catalysts

were active albeit at low flow-rates of reactant solution. Furthermore, the open-cell-ISPS/Al_2O_3 yielded a marginal conversion due to transesterification of an emulsion of rapeseed oil and methanol at 60°C after 72 h of reaction in a packed-bed batch reactor loop. However, no esterification or transesterification at all was observed during the treatment of waste abattoir fats with methanol over the same catalyst during 22 h batch loop reaction. This was due to ion-exchange of Brønsted-acidic sulphonic functionalities with alkali ions in the feedstock, which remains an overall challenge when employing waste feedstocks, especially abattoir waste. The catalyst deactivates on the uptake of the alkali ions and a regeneration strategy must be developed.

It was proven that easily soluble carbonates catalysed the transesterification, while the guanidinium ion from soluble salt, being a weak acid, in itself did not catalyse the transesterification. Basic amine-functionalised ionic liquids were completely inactive. However, a number of homogeneous organic guanidines and amidines were tested and achieved full conversion within 0.25 - 1 h, thus the reaction rate was at the same order of magnitude as the industrially used hydroxides or methoxides.

The alkyl- and aryl-substituted and nested guanidines tested had somewhat lower activities for the transesterification due to a lower loading of the active phase, but also a slightly lower basicity. Thus, the strong organic bases investigated for transesterification can be linked to porous solids, for instance ceramics or polymers, to obtain solid basic catalysts. This will make a continuous flow packed-bed reactor system for production of FAME easier to realise. However, some of the investigated guanidines were sensitive to water, which was possibly absorbed and resulted hydrolysis of the esters. This can make the guanidines difficult to apply with waste feedstock, for instance abattoir wastes, which may contain several percent of water.

Chapter 3

Catalytic Hydrodeoxygenation of Fats and Oils

3.1 Hydrodeoxygenation of fats and oils: Introduction

As mentioned in section 1.4 three types of catalysts exists for upgrading of oils and fats to hydrocarbons. Cracking reactions over porous acidic or basic materials at elevated temperatures provides a neat catalyst regeneration strategy (burning the coke formed), but the yields of diesel-range products have not been impressive to date and the cracking often lead to petrol-range hydrocarbons instead. The supported sulphided catalysts appear attractive from the point of view that they are already used in refineries for removal of for instance sulphur from the crude, and oxygen may potentially be removed as well with hydrogen. However, the use of supported transition-metal particles represents an attrative alternative. First and foremost support metallic particles do not contain noxious elements like sulphur that may potentially end up in the product or should be added continuously. Secondly the reported selectivities of for instance Pt and Pd towards decarboxylation and decarbonylation to alkanes are unrivaled [17], thus they may principally lower the consumption of H_2 compared to their sulphided equivalents according to Figure 1.6.

Naturally occuring oils and fats represents quite chemically varied fatty acid profiles, which changes between plants, animals, and it varies considerably within a species. Normally rough fatty acid ditributions are known [12, 214]. Simakova et al. showed, however, that the reaction rate was independent of the fatty acid chain length (from C_{17}-C_{22}) during deoxygenation of dilute dissolved fatty acids over Pd/Sibunit at 300°C [23]. This result is important, as fats and oils contain a distribution of various fatty acids, and as 3 fatty acids are bound to glycerol as a triester, the possible number of different molecules found in oils and fats is huge. For this reason most authors have worked with model compounds to ensure that the reactants under study were chemically well-defined.

A number of catalyst metals and supports have been tested by Snåre et al. who found Pd and Pt to be the most active catalysts metals for deoxygenation, as well as the most selective towards decarboxylation and decarbonylation. The gas phase composition was addressed as well and contained mixtures of CO and CO_2 i varying ratios, and it was established that methanation is thermodynamically favored and thus may be an unwanted side reaction [17] (Figure 1.7). In fact both the reduction, decarbonylation and decarboxylation (Figure 1.5 and Figure 1.6) are thermodynamically favored [17], so the properties of the catalyst are clearly important for the product distribution. Do et al. reported formation primarily of CO over Pt/Al_2O_3 during deoxygenation of methyl esters, but almost no methane was formed during the experimentation even in H_2 atmosphere. Immer and co-authors claimed that solely CO_2 was formed from decarboxylation of stearic acid and suspected that H_2 was in fact inhibiting the reaction [321].

Clearly, when the gas atmosphere over the catalysts contain both H_2 and formed CO and CO_2,

the methanation reaction and WGS-equilibrium cannot be excluded. To date, however, no reports in the literature have appeared which directly quantify the extent of methanation and water-gas shift reactions, although these gas-phase side-reactions are of importance during deoxygenation and their quantification would help to reveal mechanistic information. Berenblyum and co-workers recently proposed that the deoxygenation could take place via a formic acid intermediate on the adsorbed surface of palladium [322]. This can be difficult to assess as formic acid would decompose once formed around 300-350°C, especially in the presence of a Pd catalyst [323], however, the decomposition may either yield CO_2 and H_2 via dehydrogenation or CO and H_2O via dehydration, and the degree of either reaction may as well be influenced by the catalytic properties of the surface. This is illustrated in Figure 3.1. Thus, the influence of WGS equilibrium on the gas-phase composition and the amount of CO and CO_2 measured may in theory be minimal.

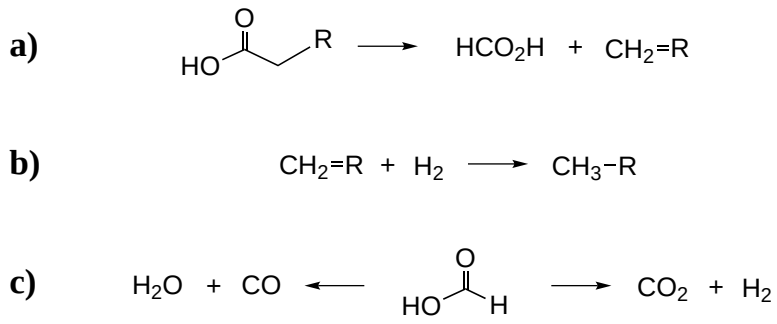

Figure 3.1: Decarboxylation via formic acid mechanism proposed by Berenblyum [322]. a) Catalytic formation of 1-alkene and formic acid from fatty acid, b) saturation of the fatty acid by hydrogen, c) decomposition of the formic acid via dehydration (left-hand side) or dehydrogenation (right-hand side).

Snåre and co-authors investigated the deoxygenation of unsaturated fatty acids and their methyl esters and confirmed the rapid isomerisation and hydrogen-transfer reactions taking place on the Pd/C active surface at 300°C [324]. Rozmysłowicz and co-workers also studied conversion of unsaturated fatty acids via saturation/desaturation reactions and deoxygenation and found that extensive amounts of coke and catalyst deactivation resulted in H_2-sparse conditions, especially with more concentrated solutions of the unsaturated fatty acids. Likewise, stearic acid was the main product from unsaturated fatty acids using little or no hydrogen, also confirming the saturation/desaturation transfer of hydrogen between molecules [20]. Immer et al. confirmed the hydrogenation transfer between feedstock and solvent and also found that saturation was necessary for obtaining a high reaction rate [321].

As sketched, the formed products in both gas and liquid phase gives the impression of great complexity in the network of reactions and the yields of products obtained. Usually the investigations have been performed in batch- or semibatch mode and in diluted systems, but industrially more concentrated reactant streams and continuous reactors are preferred.

The catalyst studies so far have concentrated on shorter reaction runs and the longest reaction have been within a few days. It is necessary to demonstrate more extensive reaction times and investigate catalyst stability and/or deactivation during more the deoxygenation. Also, most authors have worked with fatty acids and their methyl or ethyl esters, possibly due to the often cumbersome chemical analysis for the direct quantification of triglycerides. From the point of view of studying

chemical reactivity and selectivity this may probably be too simplistic, however, as triglycerides are usually the main component of the fats and oils.

Therefore, in the present work, the conversion over alumina-supported noble-metal catalysts of model mixtures of tripalmitin and oleic acid resembling waste fats have been studied in batch mode. The effect of pressure, temperature and active catalyst metal have been investigated. Stearic acid, ethyl stearate, and tristearin have been deoxygenated over Pd/C catalysts in continuous mode to relate the reactivities of different molecules. Furthermore deoxygenation of stearic acid over Pd/C has been performed for 2 weeks time-on-stream for logging step-changes and steady-state behaviour.

3.2 Batch hydrodeoxygenation: Experimental

3.2.1 Chemicals

The reactants n-tetradecane, oleic acid (>99.0%), n-docosane (>98.0%), tripalmitin (>99.0%), and N-methyl-N-trimethylsilyl-trifluoroacetamide (MSTFA) (>97.0%) were obtained from Fluka. The catalyst precursor salts $H_2PtCl_6 \cdot 6\ H_2O$ (>99.0%) and $Pd(NO_3)_2 \cdot 2\ H_2O$ (>99.8%) were obtained from Fluka, while $Ni(NO_3)_2 \cdot 6\ H_2O$ (>99.0%), $HAuCl_4 \cdot 3\ H_2O$ (>99.9%), $RuCl_3 \cdot 2\ H_2O$ (>99.9%), and $Rh(NO_3)_3 \cdot H_2O$ (>99.0%) were purchased from Sigma-Aldrich

The support material γ-Al_2O_3 was on stock in the laboratory. The gases H_2 (>99.999%), 5% CO/He (>99.999%), N_2 (>99.999%), and Formier gas (10% H_2 in N_2, >99.99%) were all purchased from AGA. All chemicals were used as received.

3.2.2 Catalyst preparation

All applied catalysts were prepared with a metal loading of 5 wt% metal on the support. The supported metal catalysts were prepared by the incipient-wetness impregnation method described in literature [325]: The active metal precursor salt was dissolved in demineralised water and added to dry, fractionated (<180 μm) γ-alumina powder. The impregnated catalyst was dried in an oven at 110°C in 2 h and afterwards calcined in atmospheric air by ramping with a 100°C/h to 400°C where the temperature was kept for 8 h. Any remaining chloride ions on the

3.2.3 Catalyst characterisation

The BET surface areas of the calcined catalysts and the γ-alumina support were determined by N_2 physisorption. Before measurement the samples were degassed at 200°C for 4 h under vacuum. Adsorption- and desorption isotherm were measured with liquid N_2 at 77K on a Micromeritics ASAP 2020 pore analyzer.

CO pulse-chemisorption was performed to determine the active metal dispersion and mean particle size. This was done on a Micromeritics Autochem II 2920 with a pulse loop size of 0.366 ml. 0.1 g catalyst sample was weighed, flushed with He, heated and reduced in 10% H_2/N_2 at 150°C for 2 h. The sample was then flushed with He and cooled, and CO pulse-chemisorption was performed at 25°C with 5 % CO/He in He carrier gas. CO-concentration in the effluent was continuously measured by a thermal conductivity detector (TCD) against reference carrier gas. For the Ni catalyst, the reduction was attempted under mere severe conditions at up to 400°C for 12 h, which was needed to entirely reduce the NiO. The stoichiometries for area calculation were Pt:CO = Ni:CO = 1:1 and Pd:CO = 2:1, based on literature reports [326]

3.2.4 Hydrodeoxygenation reaction

Hydrodeoxygenation was performed in a 50 ml stainless steel autoclave (MicroClave from Autoclave Engineers). A reaction mixture of totally ca. 9 g (taking up 11 ml of volume) was added to the auto-

clave, consisting of 0.806 g tripalmitin, 0.094 g oleic acid, 0.03 g of n-docosane as internal standard and about 8.1 g n-tetradecane as solvent. Thus, the mixture consisted of 10 wt% reactant molecules fat mixture - consisting of 75 mol% tripalmitin (90 mol% of the fatty acid chains present) and 25 mol% oleic acid (10 mol% of the fatty acid chains present). The remaining 90 wt% of the feed consist of unreactive alkanes. A 0.15 ml reference sample was taken out and 0.20 g catalyst added to the remaining liquid.

The autoclave was then sealed at room temperature, flushed several times first with pressurised argon and then hydrogen, the relevant pressure of H_2 was added and the autoclave was heated to the desired reaction temperature and stirred at 900 rpm.

Samples of 0.15 ml were taken out from the reactor after quenching the reactor to 0°C and depressurising. After sampling, the reactor was tightened and the gas atmosphere filled and purges at least 3 times first with pressurised Ar, then with pressurised H_2 according to desired start pressure. Then the reactor was re-heated to reaction temperature.

A standard hydrodeoxygenation experiment was performed at 325°C over 5 wt% Pt/γ-alumina as a catalyst under 20 bars of H_2, by sampling after 1, 2, 5, and 20 h. The amount of hydrogen in the reactor after each filling corresponded to about 5 times the necessary amount of hydrogen compared to complete reduction of the liquid reactants to alkanes.

By sampling in this manner after 1, 2, 5 and 20 h, temperature and hydrogen pressure variation was performed to investigated dependency on the conversion of the reactants and the preference for decarboxylation, decarbonylation or full reduction. The same was done to study a number of different transition-metals as active catalyst phase. Control experiments were furthermore performed by reacting solely oleic acid or tripalmitin, by omitting respectively active metal, hydrogen or catalyst.

3.2.5 Product analysis

0.15 ml of the samples taken out from the liquid-phase was mixed with 20 μL of MSTFA, the vial capped and silylation was completed at 60°C for 30 min. After silylation, the samples were analysed on GC. Silylation converts FFAs to trimethylsilyl esters to make them sufficiently volatile to allow analysis with reduced peak tailing in gas chromatography [211].

The products were quantified with an Agilent Technologies 6890N split/splitless-injection gas chromatograph with equipped with flame ionisation detector (GC-FID). Furthermore, qualitative analysis of certain samples were performed by an Agilent Technologies 6850 split/splitless GC equipped with a mass spectrometer (GC-MS).

A GC with split/splitless injector is not suitable to quantify the amount of tripalmitin in the samples due to the low volatility of the large triglyceride moleculs. The yield of pentadecane and hexadecane were therefore used to assess tripalmitin conversion according to Figure 3.2 in section 3.3, as alkanes of this size are measured quantitatively with good precision by split/splitless GC-FID. This assumption was justified from the observation that n-pentadecane and n-hexadecane were the only products of tripalmitin conversion.

3.3 Batch hydrodeoxygenation: Results and discussion

A number of parameters were varied to study the hydrodeoxygenation over supported transition-metal catalysts in batch reactor: The temperature was varied between 250-375°C over Pt/γ-Al_2O_3 while keeping the start pressure of H_2 constant at 20 bar. In another series of experiments, the pressure of H_2 was varied between 0 to 40 bar in various experiments over Pt/γ-Al_2O_3 at a constant reaction temperature of 325°C. Ni, Ru, Rh, Pd, Pt, and Au were tested as supported metal catalysts on γ-Al_2O_3 in the autoclave at 325°C at 20 bar H_2. Furthermore, a number of control experiments were conducted to elucidate the role of the support material, the reactor, the presence of hydrogen, and the composition of the reaction mixture. All deoxygenation experiments were conducted by making time series of the conversions and yields after 1, 2, 5, and 20 h of reaction. The gas atmosphere was renewed according to the initial reaction conditions after extracting the liquid samples of 1, 2, and 5 h reaction time.

The reactant molecules, oleic acid and tripalmitin, are respectively a C_{18} fatty acid and a 3 × C_{16} fatty acid glyceryl triester (triglyceride). Thus, the reaction products from both reactants can be distinguished from each other: Oleic acid is suspected to form heptadecane from saturation and decarbonylation or decarboxylation and form octadecane from the full reduction of the fatty acid with hydrogen. Tripalmitin may form pentadecane via decarboxylation or decarbonylation and form hexadecane from full reduction. This is depicted in Figure 3.2.

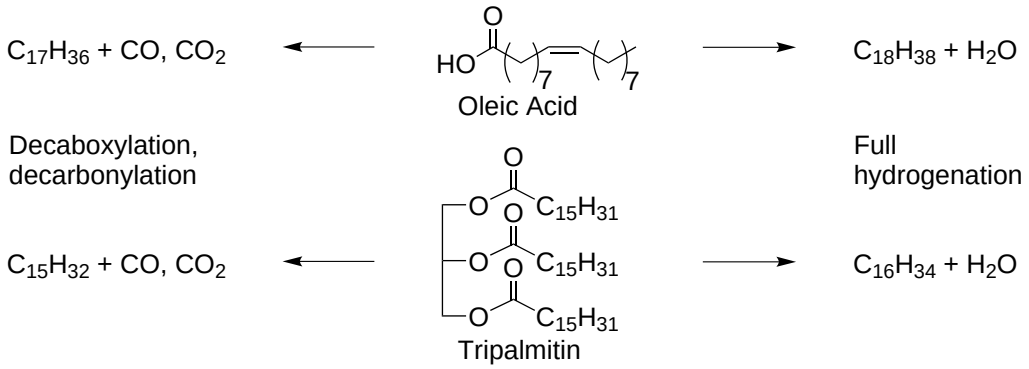

Figure 3.2: Deoxygenation products from decarbonylation and decarboxylation *(left-hand side)* and full reduction *(right-hand side)*. The resulting C_3-product from glycerol is omitted.

3.3.1 Deoxygenation time series over Pt/alumina

The yields and conversions of the deoxygenation of oleic acid and tripalmitin over 5 wt% Pt/γ-Al_2O_3 at 325°C and 20 bar H_2 can be seen in Figure 3.3 as a function of reaction time.

From the time series it is evident that oleic acid was converted to alkanes at over twice the rate than that of tripalmitin. 100% conversion of oleic acid was achieved after 5 h, but over 30% tripalmitin remained after 20 h reaction. This may be due to the larger size of the tripalmitin molecule and a more hindered access to the ester functionalities compared to the carboxylic acid.

It is also evident that despite a moderate pressure of H_2 in the gas atmosphere, the amounts of heptadecane (C_{17}) and pentadecane (C_{15}), i.e. products obtained from loss of CO_2 or CO, were both

more than an order of magnitude higher than those of octadecane (C_{18}) and hexadecane (C_{16}). This result is in accordance with the observations made previously by Murzin et al. [17, 207, 208].

The saturation of the C-C-double-bond of oleic acid was observed to take place very fast and no oleic acid was in fact observed after 1 h of the above-mentioned reaction - the remaining acid was stearic acid. Saturation of the oleic acid double bond occured in all experiments involving hydrogen, as it proceeded at much lower temperatures and at much faster rates than the deoxygenation of the acid or ester functionalities. For the sake of clarity, the unconverted acid reactant is considered to be the sum of stearic and oleic acids (termed "C_{18} acid") and conversion is considered to be complete conversion to alkanes.

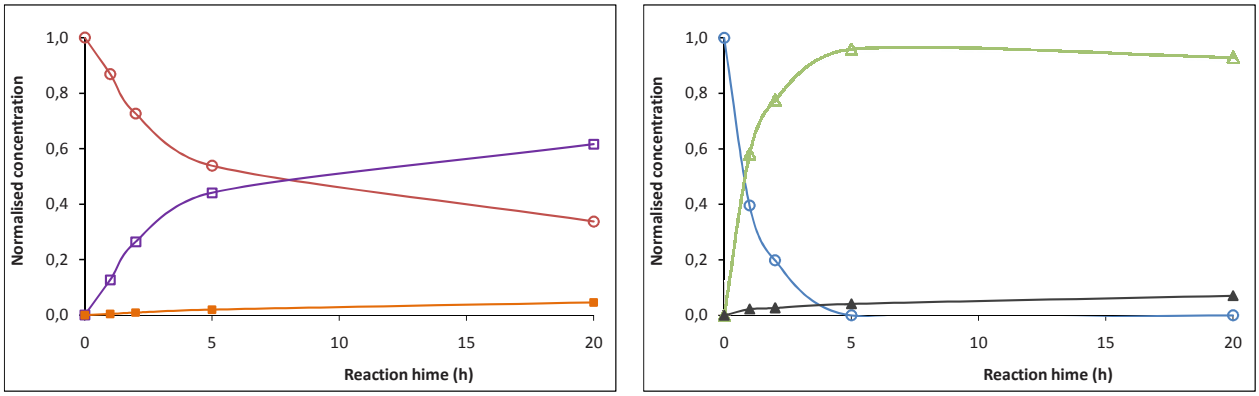

Figure 3.3: Hydrodeoxygenation time series at 325°C and 20 bar H_2 over 0.2 g of 5 wt% Pt/γ-Al_2O_3. Legend: Tripalmitin (○) and its products pentadecane (□ C_{15}) and hexadecane (■ C_{16}) *(left-hand side)*, and C_{18} acid (○) and its products heptadecane (△ C_{17}) and octadecane (▲ C_{18}) *(right-hand side)*.

It has been shown in literature that both CO_2 and CO can be formed during deoxygenation, by respectively decarboxylation and decarbonylation, and both were during the conversion of ethyl stearate and stearic acid to alkanes [44, 207]. As Pt is likely active for the WGS equilibrium (Figure 1.7, page 25), the direct products from deoxygenation cannot necessarily be observed if the reactions yield CO or CO_2 exclusively since a mixture of CO, CO_2, H_2O, and H_2 will always form. In fact it was found by for instance Resasco et al. that methyl octanoate and methyl stearate decarbonylated over 1 wt% Pt/γ-Al_2O_3 to yield CO, C_7- or C_{17}-alkene and, presumably, methanol, which was however not observed [210].

Gas-phase analyses were performed as part of the experimentation before extracting the liquid samples after 1, 2, and 5 h. A gas-valve was carefully opened to fill a gas bag with the gaseous content of the cooled reactor, and via a septum the gas in the bag was transferred to a gas syringe and injected into a split/splitless-injection GC equipped with TCD and FID. In all cases, the content of CH_4 constituted about 60% of the carbonaceous gases found and about 40% was a mixture of CO and CO_2. Hydrogen could not be detected with the present GC setup, however. Pt is known not to be very active in methanation reactions due to the high dissociation energy of CO [327], but clearly methanation has taken place. At around 300°C the methanation is thermodynamically favored [44]. However, also the reactor interior made of stainless stell could have contributed, as Fe is known to be a good Fischer-Tropsch catalyst [327]. Clearly, the formation of methane is problematic as it is a 20 times more potent greenhouse gas than CO_2 [2] and it consumes the hydrogen otherwise needed

to reduce the oxygen functionalities or prevent formation of unsaturated compounds.

No C_3-compounds like e.g. propane were found in the gas samples, which would be indicative of the tripalmitin conversion. It may have been dissolved mostly in the tetradecane solvent, though.

3.3.2 Effect of reaction temperature

To test the dependence of the deoxygenation on temperature, a number of reaction runs were conducted at temperatures between 250 and 375°C. 0.2 g of 5 wt% Pt/γ-Al_2O_3 was used as catalyst to deoxygenate a reaction mixture of 10 wt% fatty feedstock in tetradecane as solvent. The autoclave was charged with H_2 so that the pressure at the reaction temperature was 20 bar. The conversions after 5 h are plotted for various temperatures in the left-hand side of Figure 3.4.

At 250 and 275°C the conversions were below 10% after 5 h reaction. However, half of the C_{18} acid was converted at 300°C while only 10% Tripalmitin were observed to be converted to alkanes. At the investigated temperatures above 300°C the C_{18} acid was fully converted to alkanes, while the total yield of C_{15} and C_{16} alkanes rose in steps of 40, 55 and finally 100% at increasing temperature. It is evident that the C_{18} acid reacted faster than the tripalmitin (except at the lowest temperatures with very low conversions observed) as was also observed in section 3.3.1.

In the right-hand side of Figure 3.4 the towards full reduction to hexadecane and octadecane. In all cases the selectivity is below 7% for producing even-carbon-numbered alkanes via reduction compared to the odd-carbon-numbered alkanes of both C_{18} acid and tripalmitin over the Pt catalyst. The preference of the Pt catalyst to split off the carboxylate functionality as CO_2 or CO, however, increased with temperature, making the selectivity for hydrogenation drop ca. 2-3%. It could also be speculated that thermal decomposition was more pronounced at the higher temperatures.

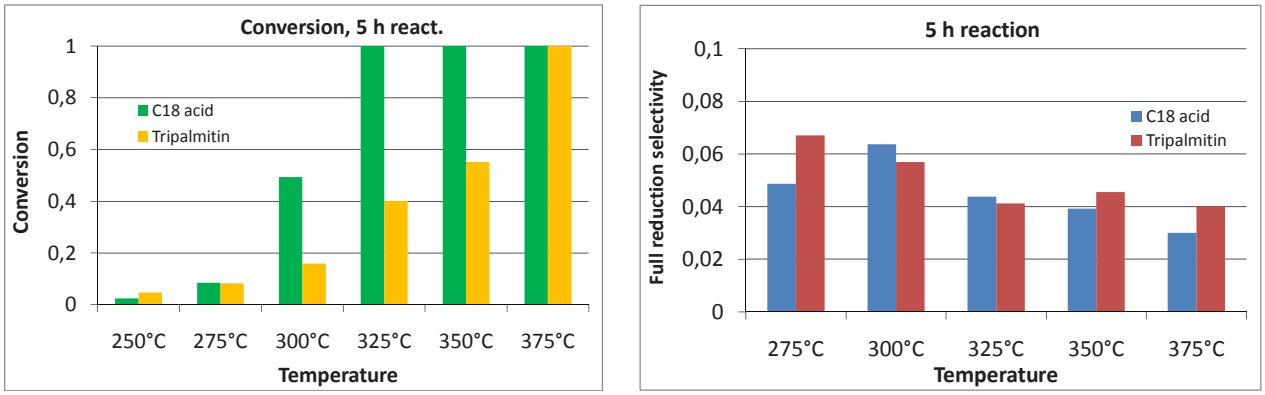

Figure 3.4: Temperature variation over 5 wt% Pt/γ-Al_2O_3 at 20 bar H_2 pressure after 5 h. *Left-hand side*: Conversion of respectively C_{18} acid (■) and tripalmitin (■). *Right-hand side*: Ratio of decarboxylation/decarbonylation to full reduction of respectively C_{18} acid (■ C_{17}/C_{18}) and tripalmitin (■ C_{15}/C_{16}).

3.3.3 Effect of hydrogen pressure

The effect of hydrogen pressure variation was investigated to assess if this had an influence on the activity and selectivity of the Pt catalyst. Thus, hydrogen pressures of 0 to 40 bar were investigated in a series of reaction performed at 325°C using tripalmitin and oleic acid as reactants. From Figure 3.5 and Figure 3.7 the yield of C_{15}-C_{18} alkanes at increasing pressure can be seen.

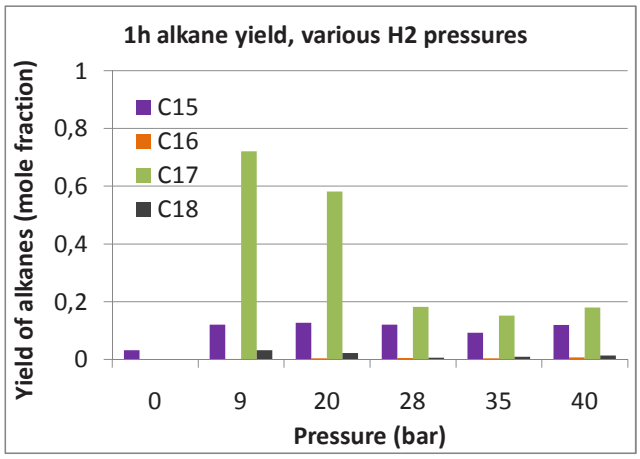

Figure 3.5: Yields of alkanes from C_{18} acid and tripalmitin at different pressures of H_2 after 1 h reaction over Pt/γ-Al_2O_3 at 325°C. Legend: Pentadecane (C_{15}), hexadecane (C_{16}), heptadecane (C_{17}), octadecane (C_{18})

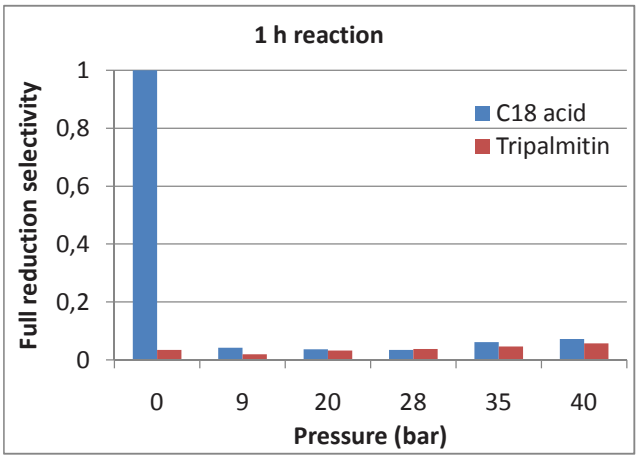

Figure 3.6: RSelectivity towards full reduction at different deoxygenation pressures of H_2 over 5 wt% Pt/γ-Al_2O_3 at 325°C after 1 h of respectively C_{18} acid (C_{17}/C_{18}) and tripalmitin (C_{15}/C_{16}).

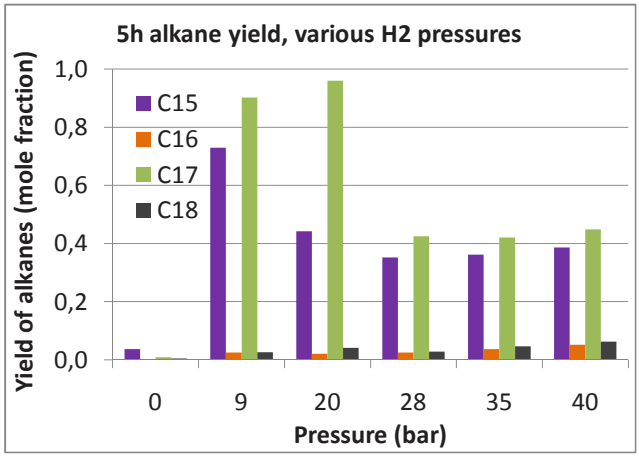

Figure 3.7: Yields of alkanes from C_{18} acid and tripalmitin at different pressures of H_2 after 5 h reaction over Pt/γ-Al_2O_3 at 325°C. Legend: Pentadecane (C_{15}), hexadecane (C_{16}), heptadecane (C_{17}), octadecane (C_{18})

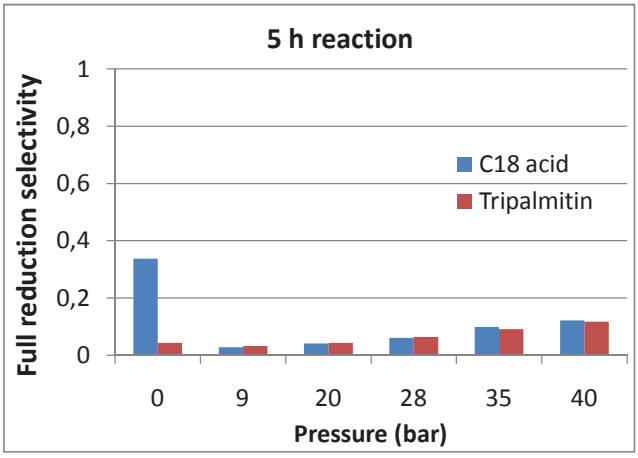

Figure 3.8: Selectivity towards full reduction at different deoxygenation pressures of H_2 over 5 wt% Pt/γ-Al_2O_3 at 325°C after 5 h of respectively C_{18} acid (C_{17}/C_{18}) and tripalmitin (C_{15}/C_{16}).

The highest turnover after 1 h is observed at the pressure of 9 bar H_2, yielding as high as 72% heptadecane after 1 h reaction, while under 20 bar H_2 the yield of heptadecane is only 58%. Interestingly, after 5 h, the yield of heptadecane was higher under 20 bar than under 9 bar H_2. It may be speculated that the catalyst may have deactivated more with only 9 bar H_2, likely due to coking - perhaps by insufficient addition of hydrogen to keep the catalyst active. The yield of pentadecane under 9 bar of H_2 compared to 20 bar showed comparable yields of about 13%, as well comparable with the higher pressures of H_2, however, after 5 h about 72% yield is obtained under 9 bar H_2 compared to 44% under 20 bar. This may indicate that the deoxygenation of the ester is inhibited by hydrogen and proceeds via a pathway were competitive adsorption or by-production can hinder the reaction. The deoxygenation under 28, 35 and 40 bar hydrogen pressure more or less had the same product yields, but were not as high as with the lower pressures. After 1 h about 15%, 10% pentadecane and very small amounts of hexadecane and octadecane had been formed. After 5 h reaction a little

above 40% heptadecane and about 35% pentadecane had been formed and the products of complete reduction of the ester and fatty acid were between 3% and 6%.

When the pressure of H_2 is increased, it is found that the selectivity for the full reduction increased after 1 and 5 h, as can be observed from Figure 3.6 and Figure 3.8, respectively. Interestingly, during the course of the reaction, the selectivity to even-carbon-numbered alkanes increased (i.e., when more feedstock was converted). At the highest pressures of 35 and 40 bar H_2 the reduction selectivity almost doubled from 1 to 5 h.

Thus it can be stated that the preference for either complete reduction or decarboxylation and decarbonylation is to some degree dependent on the pressure og hydrogen, but it was not the most important feature for the selectivity under the pressures investigated here.

The experiment without added H_2 show no alkane products. A small impurity of pentadecane is visible, but otherwise no product alkanes are found. The catalysts were reduced by the addition of H_2, stirring and heating before the reaction temperature was reached, and as no H_2 was present the catalyst have most likely not been activated.

3.3.4 Other alumina-supported transition metal catalysts

To assess the effect of other transition metals as catalysts, experiments were conducted with various other γ-Al_2O_3-supported transitions metals for the deoxygenation reactions. Thus, 5 wt% of respectively Pd, Ni, Ru, Rh, and Au were prepared supported on the γ-Al_2O_3 by impregnation. The reactions were conduted at 20 bar H_2 and 325°C with a mixture of tripalmitin and oleic acid in tetradecane solvent.

As can be seen in from the plots of the alkane yields after 1 and 5 h in Figure 3.9 and Figure 3.11, respectively, platinum was the most active catalyst metal followed by palladium in terms of C_{18} acid conversion. However, palladium was much more active than platinum to convert tripalmitin to alkanes. This peculiar difference between Pd and Pt could further point to more fundamental differences between the reaction pathways of respectively triglycerides and FFAs, but has not been addressed in the present study.

From Figure 3.9 and Figure 3.11 the selectivities for full reduction tripalmitin and C_{18} acid after 1 and 5 h are given. Ru, Pd, and Pt had the lowest selectivities towards hexadecane and octadecane after 1 h, however, Ru was almost inactive but showed a remarkable selectivity towards heptadecane - it is possible that the metal is well suited just for the scission of the carboxylic acid functionality from the free fatty acids. For Pd and Pt the selectivity towards even-carbon-number alkanes increase slightly with increasing reaction time. Rhodium showed moderate activity, but also higher selectivity to even-carbon-number alkanes than Pt and Pd. The Rh catalyst, however, mediated the formation of the same amounts of even-carbon-number alkanes as Pt after both 1 and 5 h.

Ni had a rather high selectivity for the complete reduction of C_{18} acid, but it also appears to be deactivated since the yields do not grow very much from 1 to 5 h of reaction (meaning that the reduction selectivity is high, compared to the other catalysts). The gold catalyst was completely inactive after 1 h, but minor yields below 10% of C_{15}, C_{17} and C_{18} were observed after 5 h reaction. Care should be taken when comparing selectivities at very low yields, as impurities can give rise to

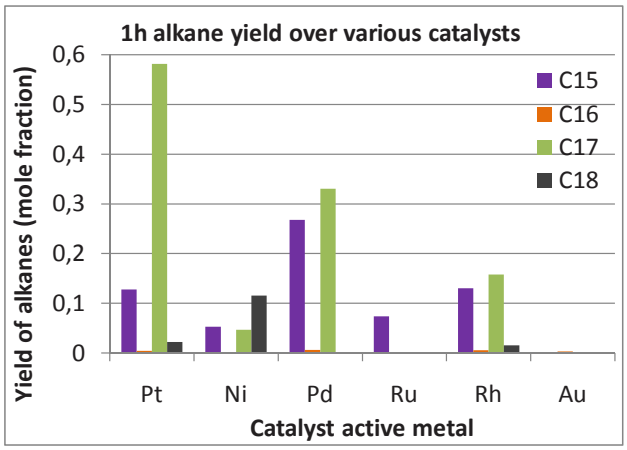

Figure 3.9: Yields of alkanes from C_{18} acid and tripalmitin over various 5 wt% transition metals on γ-Al_2O_3 at 325°C and 20 bar H_2 after 1 h reaction. Legend: Pentadecane (C_{15}), hexadecane (C_{16}), heptadecane (C_{17}), octadecane (C_{18})

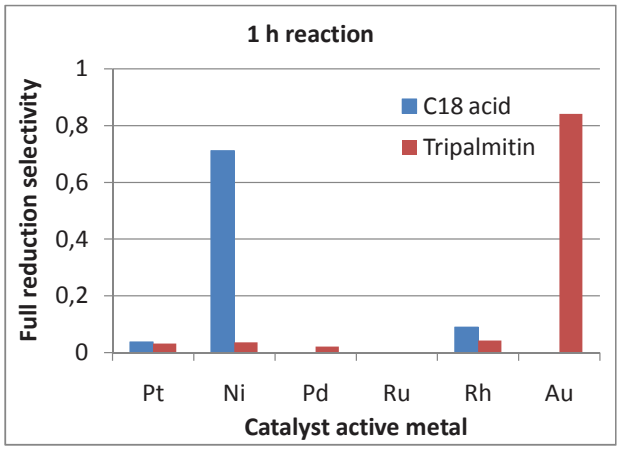

Figure 3.10: Selectivity towards full reduction over various 5 wt% transition metals on γ-Al_2O_3 of respectively C_{18} acid (C_{17}/C_{18}) and tripalmitin (C_{15}/C_{16}). 325°C and 20 bar H_2 after 1 h reaction.

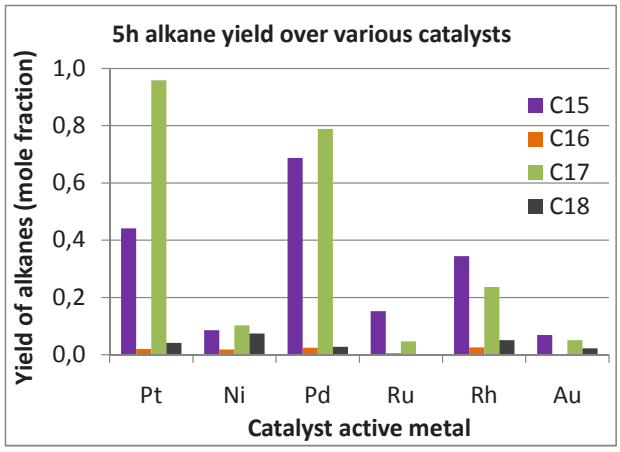

Figure 3.11: Yields of alkanes from C_{18} acid and tripalmitin over various 5 wt% transition metals on γ-Al_2O_3 at 325°C and 20 bar H_2 after 5 h reaction. Legend: Pentadecane (C_{15}), hexadecane (C_{16}), heptadecane (C_{17}), octadecane (C_{18})

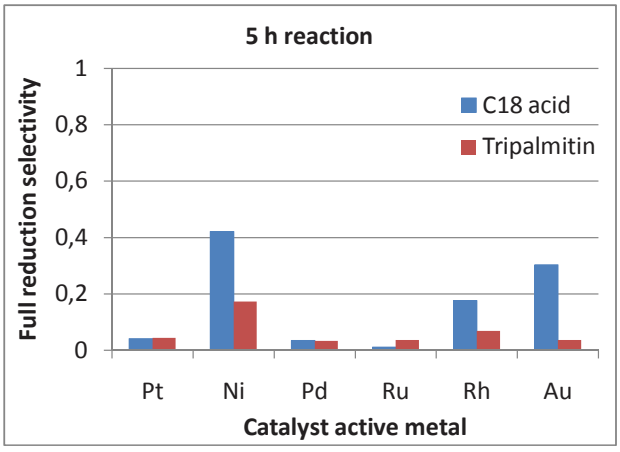

Figure 3.12: Selectivity towards full reduction over various 5 wt% transition metals on γ-Al_2O_3 of respectively C_{18} acid (C_{17}/C_{18}) and tripalmitin (C_{15}/C_{16}). 325°C and 20 bar H_2 after 5 h reaction.

significant errors.

The Ni, Pd, and Pt were subjected to further characterisation study to elucidate if their difference in activity could be related to their intrinsic physical properties. The microscopic properties of the catalysts used are shown in Table 3.1. It is evident that the higher the molar loading of the active metal on the support, the more of the original surface areas of the γ-Al_2O_3 of 255 m^2/g is lost (by plugging and shrinking of pores by the active phase, as indicated by the shrinking pore volumes of Table 3.1).

The Pt and Pd particles are of about the same size according to the CO pulse chemisorption experiments in Table 3.1, but the lower atomic weight of Pd (and therefore higher molar metal loading on the support) means that the active surface areas of the Pd is twice as big as that of Pt. Despite this fact the Pt was still more active that Pd for deoxygenation of C_{18} acid. The nickel catalyst was much less active compared to Pd and Pt - the slightly bigger size of the particles may have played a role in its lower activity for deoxygenation reactions.

Table 3.1: 5 wt% Ni, Pd, and Pt on γ-Al_2O_3 characterisation

Material	mol% metal[1]	BET-area m^2/g	Pore volume ml/g	Mean metal particle size nm	Metal surf. area m^2/g
γ-Al_2O_3	—	255	0.607	—	—
5 wt% Pt/γ-Al_2O_3	2.68	251	0.575	5.4	2.82
5 wt% Pd/γ-Al_2O_3	4.80	236	0.539	4.6	5.69
5 wt% Ni/γ-Al_2O_3	8.38	217	0.523	8.2	4.81

[1] Calculated molar percentage of active metal on the γ-Al_2O_3 support

3.3.5 Feed variation and diffusion effect

It was suspected that the application of bulky fatty acid and triglyceride molecules may have led to diffusion limitations in the catalyst interior. Furthermore, some authors have reported that cracking-type reactions may take place at elevated temperatures with various acidic catalysts [27, 218]. A closer investigation of the diffusion properties and overall reaction pathways was necessary. Therefore, control experiments using 5 wt% Pt/γ-Al_2O_3 catalyst of 125<X<180 μm in size) at 20 bar H_2 and 325°C was performed and samples taken out after 1, 2, 5, and 20 h, exactly as the time series experimentation mentioned in section 3.3.1.

A Mason-Boudart-test was conducted to assess if diffusion would be limiting the catalytic reaction. Thus, the 5 wt% Pt/γ-Al_2O_3 at the standard size of 125<X<180 μm was crushed down to <50 μm size by crushing in a mortar and sieving. Then a time series with 0.2 g of the finely crushed catalyst with reaction sampling after 1, 2, 5, and 20 h were conducted. Within a few percent, this produced the same yields of alkanes as those obtained with the larger catalyst particles.

It was then investigated if the C_{18} acid or tripalmitin underwent C-C-scission other places than at the carboxylic acid/ester functionalities. This is in fact a prerequisite for using this type of model feed to elucidate reactivities of each compound. First, a reaction only employing oleic acid as reactant was conducted. Heptadecane was observed as the major product and octadecane as the minor one, while no pentadecane nor hexadecane were observed as products in any of the extracted samples. It is thus confirmed that no C_{16} or C_{15} products were formed from the C_{18} acid via cracking-type reactions, just as in the time series experiment of section 3.3.1. Secondly, a deoxygenation experiment employing solely tripalmitin as a reactant was conducted. Here again it was observed that primarily pentadecane and minor amounts of hexadecane were seen in agreement with the observations reported in section 3.3.1.

Interestingly, a few percent of palmitic acid were observed after 1, 2 and 5 h of reaction. This indicated that the tripalmitin may have reacted at least partly via a mechanism involving hydrolysis or partial hydrogenation to split off a fatty acid, which then further reacted in the same manner as C_{18} acid. This is supported by the selectivities of full reduction for Pd and Pt, which are almost identical for C_{18} acid and tripalmitin after 5 h, as seen in 3.12. However, the pressure variation experiments mentioned in section 3.3.3 indicated that another reaction pathway may have existed for the tripalmitin deoxygenation which was inhibited by too high pressures of H_2. Further investigation of this phenomenon would be highly interesting, both in terms of finding the optimum reaction conditions and for product selectivity.

A reference experiment solely with the solvent n-tetradecane and no oleic acid or tripalmitin at

325°C and 20 bar H_2 over 5 wt% Pt/γ-Al_2O_3 was conducted. After 20 h about 1% of the tetradecane had been converted to branched C14-alkane isomers (only methyltridecanes were observed). Thus it is evident that minor isomerisation can take place, but this has not been observed with the reaction products.

3.3.6 Control experiments and gas variation

One central step in the batch experimentation was to assess the influence of added H_2 in the gas and establish the necessity of the use of a catalyst- i.e. to exclude the influence of the reactor interior, thermal reactions etc. Therefore experiments were made with this purpose at 325°C and 20 bar gas atmosphere (H_2 or N_2) either over no catalyst, over pure γ-Al_2O_3, or 5 wt% Pt/γ-Al_2O_3, and the obtained results are summarised in Table 3.2.

Without the aid of added catalyst in 20 bar H_2 at 325°C atmosphere, the yields of alkanes were only 3% from C_{18} acid and 4% from tripalmitin after 5 h. Thus the reactor interior or the thermal degradation had minor influence on the deoxygenation activity. Then the support material γ-Al_2O_3 was employed as catalytic material with either H_2 or N_2 in the gas atmosphere. The deoxygenation yielded 7% and 6% under H_2 from respectively C_{18} acid and tripalmitin, while only 2% and 5% were found when using N_2 in the gas atmosphere. It can therefore be stated that also the γ-Al_2O_3 could not function as a catalyst by itself, as it did not have a notable catalytic effect alone.

Finally it was investigated whether or not H_2 would be necessary for the deoxygenation over the Pt catalyst by performing the reaction in 20 bar N_2 atmosphere at 325°C. The conversion of C_{18} acid reached as high as 99% after 5 h reaction, however, only unsaturated compounds of C_{17} size were observed under these reaction conditions. For comparison, 100% conversion to saturated products were obtained in H_2-containing gas. It is however important to acknowledge that the conversion of tripalmitin under N_2 was only about 4%. This confirmed that triglycerides must have H_2 present in the feed to react.

Table 3.2: Conversion of C_{18} acid with supported catalyst, with support and without any catalyst in control experiments. Conditions: 20 bar gas, 325°C, 5 h reaction, 0.2 g catalyst

Catalyst	Gas atmosphere	Oleic acid conversion (%)	Tripalmitin conversion (%)
5 wt% Pt/γ-Al_2O_3	H_2	100	46
5 wt% Pt/γ-Al_2O_3	N_2	99	4
γ-Al_2O_3	H_2	7	6
γ-Al_2O_3	N_2	2	5
-none-	H_2	3	4

3.4 Continuous hydrodeoxygenation: Experimental

In recent years a number of reports have appeared on the noble-metal catalysed deoxygenation of fatty acids, fatty esters or triglycerides. Most of these have focused on batch or semi-batch reactors, i.e. autoclaves, where the semibatch-type system allow for renewal of the gas atmosphere while maintaining the liquid phase in the reactor.

The continuous systems are more relevant in industrial chemistry on the scale of fuel production. Therefore continuous deoxygenation experiments have been performed, primarily over 2 wt% palladium supported on beads of a synthetic disordered mesoporous carbon type "Sibunit".

Sibunit is a carbon matrix produced by reacting carbon black in a flow of light hydrocarbon gases around 1000°C. This causes deposition of graphite-like carbonaceous material from the gases as a binding material between the carbon black particles, so-called pyrolytic carbon. The resulting material is then reacted and activated in a flow of hot steam, leaving mesopores in the resulting material mostly by removal of the original carbon black in gaseous form [328]. The resulting porous carbon material is then shaped to beads. The mesoporosity of the Sibunit beads makes them suitable as catalyst supports, especially for larger reactant molecules like fatty acids and derivatives.

In the few studies that have appeared in literature on continuous deoxygenation over supported noble-metal catalysts, the long-term reaction performance has not been investigated, although this is a parameter of utmost interest from an industrial perspective, along with the deactivation mechanisms and the operation limits for avoiding or minimising deactivation. This is therefore investigated with deoxygenation of stearic acid in a ca. 300 h time-on-stream (TOS) experiment over 2 wt% Pd on Sibunit.

To study the influence of the type of functional group in the feedstock, experiments have also been made to compare the deoxygenation behaviour of stearic acid, ethyl stearate and tristearin over Pd/Sibunit, with and without hydrogen present in the gas atmosphere.

3.4.1 Chemicals and materials

Sibunit beads of ca. 1.6 mm in diameter were obtained from Boreskov Institute of Catalysis, Novosibirk, Russia. $PdCl_2$ (>99.9%), Stearic acid (>99%), myristic acid (>99%) and eicosane (>99%) were supplied by Sigma-Aldrich. The silylation agent N,O-bis(trimethylsilyl)-trifluoroacetamide (BSTFA, >99% purity) was delivered from Acros Organics, while n-dodecane (>99%) and pyridine (>99%) were obtained from Fluka. Ar (>99.99%) and 5% H_2/Ar gases were delivered from AGA. All chemicals were used as received.

3.4.2 Synthesis of Pd/C

The 2 wt% palladium on Sibunit (Pd/C) catalyst was prepared by the following method [329]:

Sibunit beads of about 1.6 mm in diameter were treated with 5 wt% HNO_3 overnight at 25°C and dried for several hours at 80°C. An aqueous solution of H_2PdCl_4 was regulated to pH = 9 with Na_2CO_3, and the dried Sibunit beads were added to this solution for deposition of the Pd(II)-hydro-

complexes. The deposition was continued for 6 h at 25°C; then, the beads were filtered and washed with H_2O until no chloride ions could be detected in the filtrate. Then the catalyst was dried at 80°C and calcined at 200°C for 2 h.

3.4.3 Reactor configuration, loading and sampling

On the inlet side of the reactor the setup consisted of a specially designed heated liquid piston pump, heated feed vessel and solvent vessel, as well as gas flow controllers and gas lines for Ar and H_2. The liquid vessels were continuously flushed by bubbling N_2 at 20 ml/min through the liquid and out of the system to evacuate dissolved oxygen in the feed. On the outlet side of the reactor the setup was equipped with heated lines, liquid sampling valve and collector for the remaining liquid effluent, as well as gas flow controllers for regulating pressure and blending the effluent with carrier gas before online analysis of CO and CO_2. The temperature, pressure and CO/CO_2 could be logged via a computer. During experimentation, the tubes, fittings, pump and vessel exposed to liquid fatty feed were heated to 100°C as the saturated fatty compounds used as reactants had melting points between 45 and 90°C. Also, stearic acid in dodecane was not sufficiently soluble at ambient temperature. The configuration of the continuous setup is shown in Figure 3.14. The reactor itself was a tube of 18 cm height and 1.58 cm inner diameter for a total volume of 35.1 ml. Before each run, the reactor was loaded in the bottom in three steps:

- In the bottom a layer of quartz wool, then 6 ml of quartz sand 0.2-0.8 mm i diamter, and then a layer of quartz wool;
- In the middle a catalyst bed of 10 g Sibunit or 10 g of 2 wt% Pd supported on Sibunit
- In the top a layer of quartz wool, then 4 ml of quartz sand 0.2-0.8 mm i diamter, and then a layer of quartz wool.

Figure 3.13 shows the loading of the reactor. A thermocouple was inserted through the reactor outlet to measure the temperature from the interior of the reactor.

During experimentation, liquid samples were taken out from the outlet of the reactor by two valves. 2 minutes prior to sampling, the content of the sampling nozzle was purged. Samples were collected in glas vials and weighed, followed by addition of external standard. This was diluted in 4 ml of dodecane and heated in an oven at 70°C until the dodecane had dissolved the sample. Then, 10 μL of the dodecane-diluted sanple was added to a GC vial, along with 100 μL pyridine, 100 μL BSTFA (silylation reagent) and 40 μL 0.013 M myristic acid in dodecane (silylation control compound). The vial was capped and allowed to silylate in an oven at 70°C for at least 30 min. before being analysed by a gas chromatograph (GC).

The samples from the long-term experiments with stearic acid, the comparison experiments with ethyl stearate and stearic acid and the step change experiments were analysed on a 5890N HP Agilent split/splitless-injection GC with a flame-ionisation detector (FID). The gas-phase was analysed with a Siemens Ultramat 6 IR-analyser, which was set up to measure the CO and CO_2 content. The gas was diluted before measurement on the Ultramat.

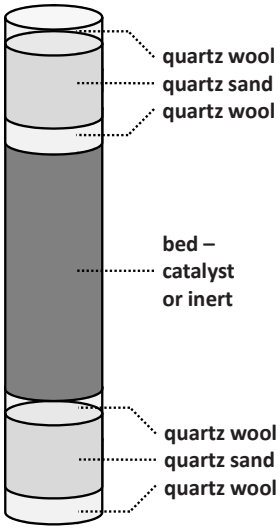

Figure 3.13: The packing of the flow reactor before each experiment.

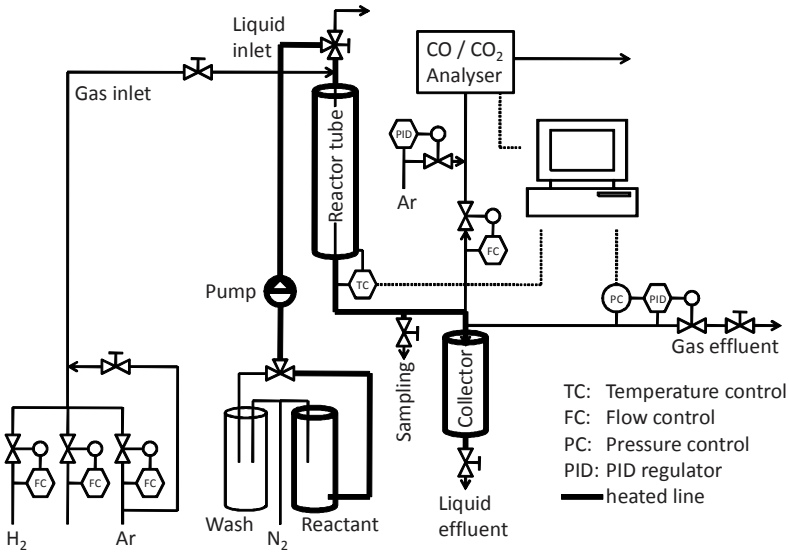

Figure 3.14: Schematic representation of the continuous flow reactor used in the experimentation, produced on the basis of Bernas et al. [330].

After reaction, the Sibunit beads (with or without Pd) were taken out of the reactor sequentially and sorted into batches depending on their position in the catalyst bed.

3.4.4 Long-term performance of catalyst

The performance of deoxygenation has been evaluated over the same catalyst in both pure Ar and 5% H_2/Ar, and in both dilute and concentrated stearic acid liquid feed. During the entire course of the experimentation, a liquid flow of 0.075 ml/min and a gas flow of 42 Nml/min was employed, and the deoxygenation conditions were 300°C and 20 bar. Liquid samples have been analysed by GC and CO/CO_2 in the gas phase have been measured by online NDIR-analysis.

Stearic acid, pure and in solution with dodecane, was used as a model reactant for the long-term experiments at a liquid flow rate of 0.075 ml/min. The reactor was loaded with 10 g 2 wt% Pd/Sibunit beads of 1.4-1.8 mm diameter, according to the procedure in Section 3.4.3. Prior to reaction the catalyst was reduced for 0.5 h in 1 bar H_2 at ambient temperature, then ramped at 10°C/min to 150°C, and then kept at this temperature for 1 h. Afterwards the reactor was ramped at 10°C/min to 300°C and the reaction started.

The entire experimentation programme is seen in Table 3.3. First, experiments with dilute stearic acid in dodecane were performed for the first 3016 min TOS, first 300 min in 42 Nml/min Ar, then with 42 Nml/min 5 wt% H_2/Ar at 20 bar until TOS = 1575 min, then Ar gas until the flow was switched to dodecane at TOS = 3016 min. The reactor was quenched to 150°C at TOS = 3300 min (in 15 min), while dodecane wash was continued until TOS = 4356 min. After the experimentation with dilute stearic acid the reactor was quenched to 150°C, washed first with dodecane and then flushed in pure Ar at 20 bar. The reactor was reheated to 300°C for the next experimentation with pure stearic acid. First, the deoxygenation was continued without H_2 in the feed until TOS = 7056 min, where the reactor was quenched to 150°C and washed with dodecane and Ar overnight. Following this the reactor was reheated to 300°C and pure stearic acid was reacted with 5 wt% H_2/Ar until a

Table 3.3: Overview of the step changes applied during long-term deoxygenation.

Step change #	TOS (min)	Condition	Changes applied
			Diluted stearic acid in 5% H_2/Ar
	-55	liquid	Flow of dodecane started at 300°C
Step I)	0	liquid	10 mol% stearic acid in dodecane at 300°C
Step II)	300	Gas	5% H_2/Ar
			Diluted stearic acid in Ar
Step III)	1575	Gas	Pure Ar.
Step IV)	1816	Liquid	6.55 mol% stearic acid in dodecane
Step V)	3016	Liquid	Dodecane
	3300	Temperature	Quenching to 150°C in 15 min
	4359	Temperature	Cooling to 25°C in 15 min
			100% stearic acid in Ar experiment
	4359	Temperature	Heating startup from 25°C to 300°C
	4389		Reactor heated
Step VI)	4481	Liquid	100% stearic acid
Step VII)	7056	Liquid	Dodecane
	7056	Temperature	Quenching from 300°C to 150°C
			100% stearic acid in 5% H_2/Ar
	7056	Temperature	Heating from 150°C to 300°C at 15°C /min
	7056	Gas	5% H_2/Ar
Step VIII)	7066	Liquid	100% stearic acid
Step IX)	18506	Liquid	Dodecane
	20021	Temperature	Cooling reactor to 25°C

complete TOS of 19000 min (13.2 days).

3.4.5 Comparison of fatty acid functional groups

Stearic acid, ethyl stearate and tristearin were used as model compounds for these 3 experiments. Prior to each experiment, a total of 10 g of 2 wt% Pd/Sibunit beads of 1.4-1.8 mm diameter were loaded by the procedure mentioned in Section 3.4.3; however, a little quartz wool was used as spacers to divide the catalyst bed into 5 equally large zones for easier separation afterwards. The reactant was added to the heated reactant vessel. The catalyst was reduced for in 1 bar of H_2 (i.e. 20 bar of 5 % H_2/Ar at 42 Nml/min) for 0.5 h at ambient temperature, heated 10°C/min to 150°C which was kept for 1 h. Afterwards the reactor was heated 10°C/min to the reaction temperature at 300°C where the reaction was started by switching on the feed pumping.

The gas atmosphere used in all cases was 20 bar 5% H_2/Ar at 42 Nml/min, however after 75 h (stearic acid: 96 h) TOS the gas flows were switched to pure Ar and the reaction continued for another 75 h.

3.4.6 Catalyst characterisation

The distributions of particle diameter and the mean diameters of the catalysts used were calculated based on the frequency of particles counted from images obtained by operating with acceleration voltage of 120 kV on a LEO 912 OMEGA energy-filtered transmission electron microscope (TEM).

More than 100 particles were counted to obtain the average particle diameter of Pd. Spent and fresh catalyst beads were crushed to a powder which was carefully mixed. Then each powder was glued to an epoxy plate before obtaining the TEM micrographs.

The X-ray Diffraction (XRD) mean particle diameter based on volume of the particles were calculated with the Scherrer formula from powder diffractograms obtained with a Siemens D5000 X-ray Powder Diffractometer.

Specific surface area and pore size distributions were obtained for all the catalysts tested. Fresh and spent catalyst batches from the long-term experimentation with stearic acid deoxygenation were analysed with a physisorption / chemisorption Sorptometer 1900 from Carlo Erba instruments with liquid N_2 at 77 K. The fresh and spent catalysts from the deoxygenation experiments with different feedstocks were analysed with a Micromeritics ASAP 2020 Physisportion apparatus also using liquid N_2 at 77K. In both cases, specific surface areas were calculated using the Brunauer-Emmett-Teller (BET) equation from the N_2 adsorption-desorption isotherms. The pore size distributions were obtained from the Dollimore-Heal correlation.

The distribution of active metal in fresh catalyst beads was investigated by laser ablation connected to an inductively-coupled plasma mass-spectrometer (LA-ICP-MS), with laser ablation system of New Wave UP-213 and Perkin-Elmer ICP-MS Sciex Elan 6100 DRC Plus. A number of catalyst beads were cut in half and fixed in epoxy glue for the measurements.

Reactor effluent contents of Pd were measured by ICP-EOS with a Perkin-Elmer 5300 DV optical emission spectrometer. 0.2 g of effluent was added to 5 ml of concentrated (65 wt%) HNO_3 (aq) and 1 ml of 30 wt% H_2O_2 (aq), heated in a microwave oven and then diluted to 100 ml (aq) before ICP-OES analysis.

3.5 Continuous hydrodeoxygenation: Long-term test & step changes

3.5.1 Long-term deoxygenation of stearic acid

3.5.1.1 Dilute stearic acid in 5% hydrogen in Ar - step changes II)-III)

Steady-state decarboxylation of 10 mol% stearic acid diluted in dodecane was performed at 300°C and 20 bar of 5% H_2/Ar, taking place at 450-1575 min TOS. The results from the online CO/CO_2 analysis and the liquid samples taken after the reactor are shown in Figure 3.15.

The conversion of stearic acid to heptadecane was between 91 to 99% at 100% selectivity, however, in most samples the stearic acid molar fractions were about 2%. At TOS = 300-500 min about 1% monoaromatic C_{17}-products were observed. This was however a residual from the conversion in pure Ar at TOS = 0-300 min, and after TOS = 500 min no unsaturated compounds were observed in the liquid samples.

The CO_2 and CO concentrations were also stable corresponding to about 40% and 20% conversion of stearic acid compared to the feed rate, respectively. Thus, about 35-40% of the carbonaceous gases were missing, most likely due to the thermodynamically favored methanation that consumed hydrogen to form methane and water (see Figure 1.7 on page 25). However, it was not possible to measure the methane by online analysis due to the present configuration of the Ultramat NDIR-analyser, so this assumption could not be directly confirmed.

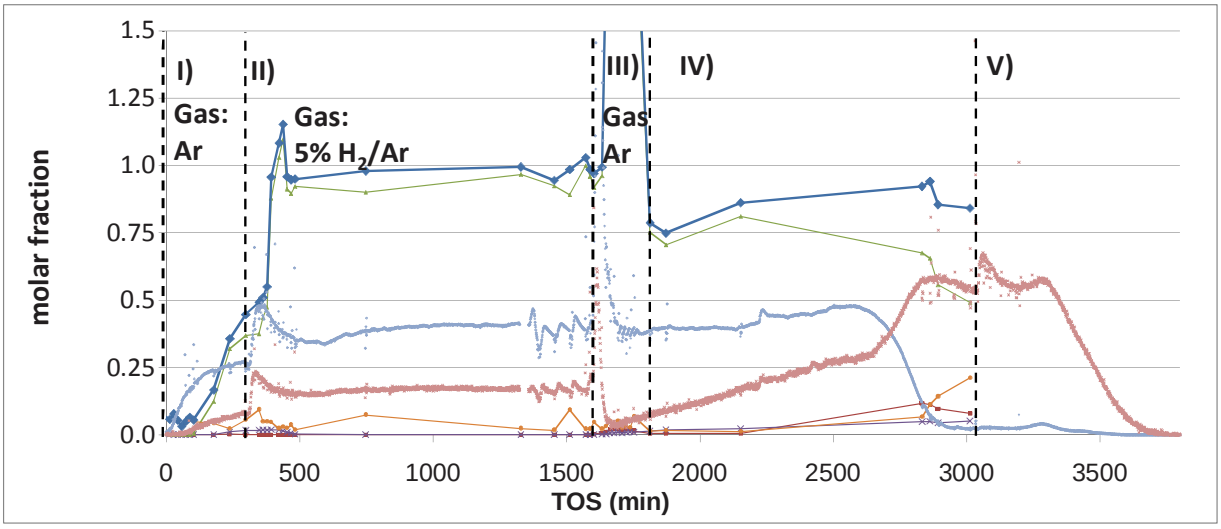

Figure 3.15: Continuous deoxygenation of dilute stearic acid over 2 wt% Pd/Sibunit. Legend: Liquid molar sum (—◆—), Stearic acid (—●—), heptadecane (—▲—), heptadecene (—■—), undecylbenzene (—×—), CO (·), CO_2 (·).

3.5.1.2 Dilute stearic acid in Ar - step changes IV)-V)

To investigate the effect of pure Ar on the deoxygenation during stable operation in dilute liquid feed, the sweeping gas was switched to Ar at TOS = 1575 min.

However an unintended blocking of the Ar gas feed line had to be removed first, which gave rise to the increased gas- and liquid concentrations seen after step change III) at TOS = 1575-1800 min in Figure 3.15. At TOS = 1800 the liquid samples reached a stable level. The liquid feed was renewed

with a dilute solution of 6.55 mol% stearic acid in dodecane - the molar fractions in Figure 3.15 are calculated on basis of this number at TOS = 1816-4359 min.

Initially, at step change IV) (TOS = 1816 min), heptadecane is almost the exclusive product corresponding to a conversion of stearic acid at 75%. Neither stearic acid nor unsaturated side products are detected at this position, but during the course of the experimental interval between step change IV) and V) both unconverted stearic acid and unsaturated products were formed. Around TOS = 2800 min about 8-12% yield of 1-heptadecene and 4-5% yield of C_{17}-monoaromatics were obtained, while the yield of heptadecane fell below 70% and declined afterwards. The mass balance only reached 75% and increased to about 95% at TOS = 2800 min. This is an indication that products or reactant were held up in the catalyst beads or that heavy condensation products were formed that could not be detected by the GC analysis method applied. Thus it can be expected that some of the unsaturated compounds have actually condensed to heavier products or simply started to form coke by cyclisation and liberation of H_2.

The CO_2-level corresponded to 40% conversion in the start of step change IV) at TOS = 1816 min, which rose slightly to 48% at TOS = 2600 min. Interestingly, almost no CO was present in the gas atmosphere at TOS = 1650, i.e. 1 h after the step change III) to Ar gas. At this point the CO concentration rose steadily to around 28% at TOS = 2600 min. Surprisingly, at TOS = 2600-2800 the gas atmosphere reversed in composition, as the CO-level rose to above 50% while the CO_2-level decreased to just 3%.

The heptadecene and C_{17}-monoaromatics formed strongly points to deactivation of the catalyst by coking. A possible explanation of the gas-phase behaviour is that the unsaturation of the products formed have led to the liberation of more and more hydrogen used to partly methanate, partly water-gas-shift the CO_2 to CO (see Figure 1.7 on page 25). However, the unsaturated hydrocarbons formed by the catalytic liberation of H_2 result in C-C-coupling and build-up of carbonaceous by-products in the pore system of the catalyst. The switch-over of resulting gas from CO_2 to CO over time has very recently been reported also by Immer and co-authors [331] who suspected that too long experimentation in H_2-deficient atmosphere led to the shift in gas production.

Unsaturated compounds are often formed under conditions leading to deactivation [20, 211]. The liquid flow was switched from dilute stearic acid to dodecane flow at TOS = 3016 min (step change V)), while the Ar gas flow of 42 Nml/min was maintained. Surprisingly, the CO-concentration remained on levels corresponding to a conversion of about 55-65% for several hours, and it did not start to decline until the reactor was cooled to 150°C at TOS = 3300 min. The sum of all CO and CO_2 measured after this point amounted to 4.21 mmol, and it may be hypothesised that the CO was covering the surface of the Pd parcticles. However, if applying a mean particle diameter of 12 nm (measured by XRD, see section 3.5.3.2), asuming that Pd particles are spheres and that the Pd:CO adsorption ratio is 2:1 [326], maximally 0.250 mmol can be adsorbed on the Pd particles. Thus, CO and CO_2 produced after the flow was switched to dodecane must primarily have come from reactant still present in the reactor. It is suspected that a large amount of stearic acid was still situated in the pore structure of the catalyst beads, as a large part of the catalysts beads were inert - namely all but the outermost layer where the Pd particles are supported. The stearic acid continued to slowly

diffuse inside the catalyst beads and deoxygenates over time.

It has been suggested that the deoxygenation takes place via formic acid formation on the catalyst surface, as depicted in Figure 3.1. Fatty acid decarbonylates to directly yield a 1-alkene and formic acid. The alkene would be saturated by H_2 in the gas feed, while the formic acid would disintegrate to yield either CO_2 and H_2 (by dehydrogenation) or CO and H_2O (by dehydration) [322, 332]. As formic acid would decompose over the Pd catalyst it was not possible to confirm this mechanism in the present work. The measured liquid yield of up to 15% unsaturated products can be explained by the decarbonylation pathway or by formic acid formation and dehydration. Lack of H_2 means that saturation of formed alkenes was slow and dependent on release of H_2 by dehydrogenation.

3.5.1.3 Concentrated stearic acid in pure Ar - step changes VI)-VII)

After the reaction with diluted stearic acid the reactor was flushed in Ar at 150°C, then in dodecane and then again in Ar overnight. Then the reactor was reheated to to 300°C at 10°C/min, and once the temperature of the reactor was stable the flow of pure stearic was started. Liquid samples and online gas analysis were monitored during two days, at TOS = 4359-7056 min as shown in Figure 3.16.

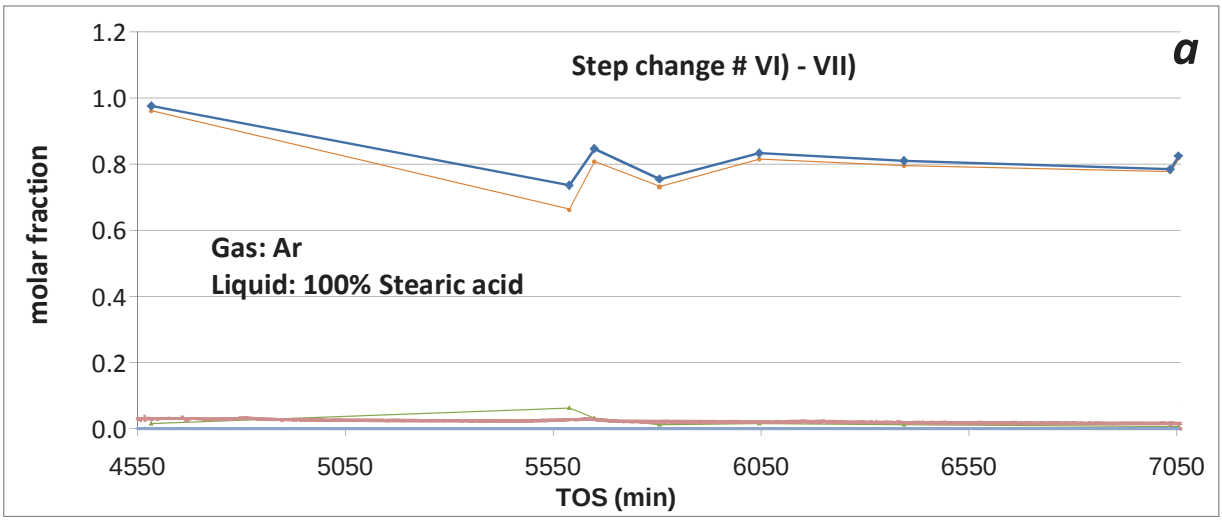

Figure 3.16: Deoxygenation of concentrated stearic acid in pure Ar flow over 2 wt% Pd/Sibunit. Legend: Liquid mole balance (—◆—), Stearic acid (—●—), heptadecane (—▲—), heptadecene (—■—), undecylbenzene (—×—), CO (x), CO_2 (•).

The first sample taken out had a mole fraction of stearic of almost 100%, but this declined in the following samples to around 80%. Heptadecane yield declined gradually from 2% to 1% with the exception of one sample. Likewise, the concentration of CO in the gas phase gradually declined from about 3% to 1.5 % in the end of the experimentation interval. There was, however, no trace of CO_2. Thus, there is a slightly better correspondance between the gas and liquid analysis offhand, and it seems likely that the lack of H_2 in the feed have minimised the extent of methanation.

However, about 20% of the stearic acid is missing in the liquid product analysis. It is suspected that undetectable heavy condensation products have been formed. No 1-heptadecene is observed, but two heptadecene molecules may undergo coupling-reaction to form tetratriacontene (a C_{34}-alkene). Ketonisation from two molecules of stearic acid to form 18-oxopentatriacontane (a C_{35}-

ketone) is however not likely as ketonisations usually require a basic or acidic co-catalyst in addition to a transition metal for reaction to take place [17, 228, 260]. If heavy condensation product are formed it is likely that they cannot be detected by the current GC method. Heavy hydrocarbons would be difficult to vaporise in the split/splitless injector and the column may not have been heated sufficiently in the applied GC method to allow vaporisation of the species.

3.5.1.4 Pure stearic acid under 5% hydrogen in Ar - step changes VIII)-IX)

Following the experimentation the final assessment of steady-state catalytic behaviour was deoxygenation of neat stearic acid in hydrogen-containing atmosphere. After flushing the reactor with dodecane followed by Ar at 150°C, the reactor was reheated in 5% H_2/Ar and stearic acid was led to the reactor to obtain the steady-state deoxygenation as seen in Figure 3.17. Liquid samples confirming the stable behaviour were obtained at TOS = 8300-18500 min between step changes VIII) and IX) in Table 3.3.

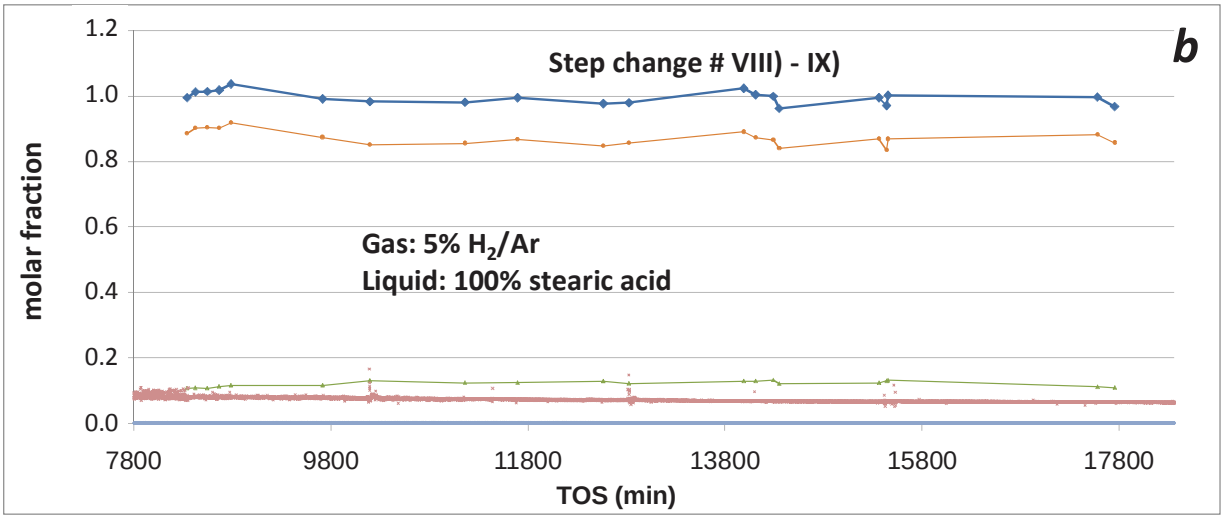

Figure 3.17: Deoxygenation of concentrated stearic acid in 5% H_2/Ar over 2 wt% Pd/Sibunit. Legend: Liquid mole balance (—◆—), Stearic acid (—●—), heptadecane (—▲—), heptadecene (—■—), undecylbenzene (—×—), CO (x), CO_2 (•).

During this experimentation interval a constant yield of 12% heptadecane at 100% selectivity was obtained, while the remaining liquid was unconverted stearic acid. The gas-phase yielded a level of CO corresponding to ca. 7% conversion, steadily decreasing from 8% to 6% over the course of the entire 10200 min TOS. No CO_2 was observed, but the lack of part of the CO_x was again observed, most likely due to methane formation with hydrogen.

The lack of CO_2 could originate from the WGS equilibrium by consumption of H_2 (Figure 1.7) to yield H_2O and CO. This would, on the other hand, result in some CO_2 left in the gas atmosphere, but this is not the case. Immer and co-workers suggested that the deoxygenation proceedes via decarbonylation over a catalyst already aged [331]. In this mechanism, as is suggested in Figure 1.6, a fatty acid decarbonylates to yield a 1-alkene while CO and H_2O are liberated, for instance via formic acid as previously stated [321, 322, 332] (see Figure 3.1). The alkene is then quickly saturated to an alkane by H_2 in the gas. This would explain the complete absence of CO_2 during the deoxygenation of concentrated stearic acid, suggesting that WGS does not take place. Whether or not

decarboxylation and WGS or decarbonylation dominated, the net result was the same: One molecule of heptadecane, of CO and of H_2O have been formed during the deoxygenation.

3.5.1.5 Overview of longterm experimentation

Table 3.4 shows the overview of the steady-state behaviour of deoxygenation at 300°C and 42 Nml/min sweeping gas at 20 bar of 0.075 ml/min solutions of stearic acid.

It is evident that the experimentation in pure Ar atmosphere both led to deactivation while resulting molar balances of reactants and products were somewhat below 1. This point suggests that deactivation took place by dehydrogenation and coking reactions in the pore system, and that the products were either trapped in the pores or too heavy to be analysed in the GC-FID used to analyse the samples. It should be noted that the experiments have been performed with the same catalyst bed exposed to each condition consecutively, so deactivation is naturally cumulative of the previous conditions applied.

Table 3.4: Yield of heptadecane on basis of stearic acid in the feed under stable conditions. 300°C, 20 bar sweeping gas at 42 Nml/min, liquid feed 0.075 ml/min. Dilution is in dodecane

	Sweeping gas atmosphere	
Liquid Feed:	5 % H2 in Ar	Pure Ar
Diluted stearic acid (mol% stearic acid in dodecane)	95% (15 mol%)	75% decreasing to 55%; formation of unsaturated and aromatic C17 compounds (10 mol%)
Pure stearic acid	12 %	2% decreasing to 1%; Possible formation of heavier products

Lestari et al. observed initial deactivation in 20 bar pure Ar at 360°C over 5 wt% Pd/Sibunit during the continuous stearic acid deoxygenation [211]. However, at this temperature it was not possible to regain the initial catalyst activity by switching gas flow to 5% H_2/Ar, but a stable conversion of 15% was reached. This is comparable to the 12% obtained in the present work, albeit the degree of deactivation of the catalysts may be different.

Importantly, part of the lost activity from deoxygenation in Ar could be regenerated as 12% heptadecane yield was obtained steadily in over a week of experimentation. This further suggests that the use of 5% H_2/Ar is sufficient to sustain the catalyst activity for an extended period of reaction. However, as is evident from Figure 3.17, part of the CO_x formed will still be converted to methane by methanation. It is not completely certain why decarbonylation and unsaturated products are not seen during the experimentation with concentrated stearic acid under pure Ar gas flow.

3.5.2 Transients during deoxygenation step-changes

In industrial practice not only the steady-state behaviour is relevant for the performance of a catalytic reactor, but also the behaviour when changing conditions and flows, starting and stopping the reactor. In terms of catalyst evaluation in lab scale it is likewise relevant to investigate the start-up,

shut-down and step changes and the responses of the reactor setup taking place between the steady states. This may reveal details about the flow behaviour and some of the pathways of the catalytic reactions taking place in the catalyst bed. Thus, four step changes are treated here, namely:

- Startup in Ar and dilute stearic acid - step change I)
- Switch to 5% H_2/Ar in dilute stearic acid - step change II)
- Start-up of 100 stearic acid in 5% H_2/Ar - step change VIII)
- Shut-down of 100 stearic acid in 5% H_2/Ar - step change IX)

The step changes are shown in Figure 3.18 (I) and II)), Figure 3.19 (VIII)), and Figure 3.20 (IX)), respectively.

3.5.2.1 Startup in Ar and dilute stearic acid - step change I)

After the activation of the catalyst by reduction in H_2 the gas was changed to Ar at 42 ml/min to flush the reactor overnight. Then, liquid flow of 0.075 ml/min dodecane was started to the reactor at TOS = -55 min. At TOS = 0 min the liquid flow was switched to 0.075 ml/min of 10 mol% stearic acid diluted in dodecane - step change I). The propagation of the reactant and products of deoxygenation were monitored during the step change as seen in Figure 3.18.

The CO_2 started to rise after about a 15 min lag. Then, it gradually rose and stabilised at a level corresponding to 26% conversion in the course of the next 4-5 h. The CO concentration started to rise at TOS = 90 min, and gradually stabilised at a level corresponding to 8 % at TOS = 300 min.

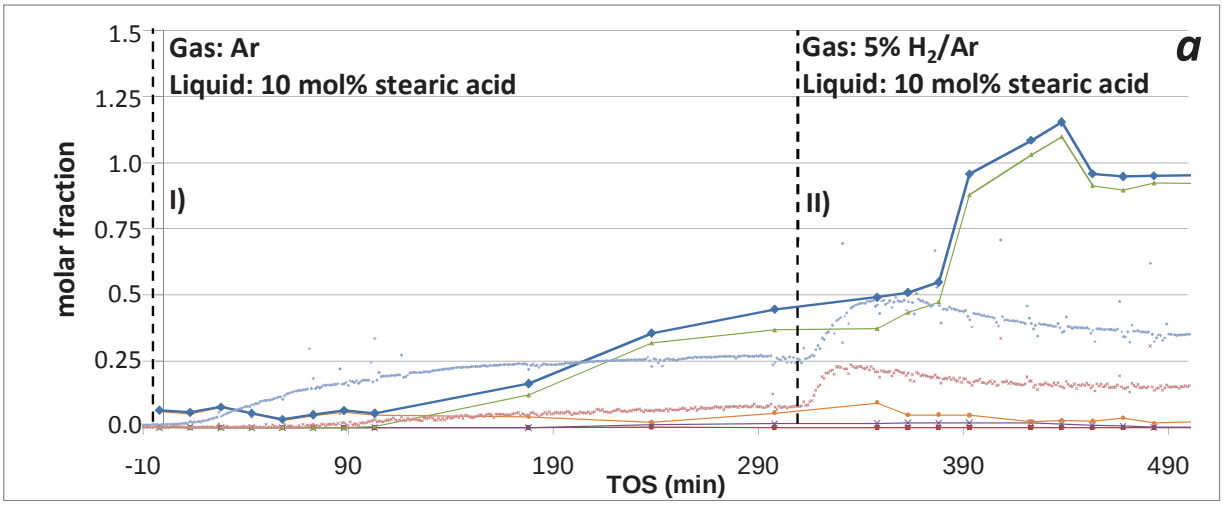

Figure 3.18: Step changes of dodecane to dilute stearic acid under Ar (step change I)) and change to 5% H_2/Ar (Step change II)), performed over 2 wt% Pd/Sibunit. Legend: Liquid mole balance (—◆—), Stearic acid (—●—), heptadecane (—▲—), heptadecene (—■—), undecylbenzene (—×—), CO (x), CO_2 (•).

Minor amounts of stearic acid were found in the liquid samples taken out between 0 and 120 min, which were probably due to impurities located in the sampling system from previous runs. However, ca. 1½ -2 h after the step change, the concentration of heptadecane started to rise and developed into a stable concentration corresponding to 37% conversion of stearic acid 5 h after step change I). A few

percent of unconverted stearic acid is still observed in this time interval. At TOS = 300 min, 1% yield of a monoaromatic C_{17}-product was obtained. As previously stated this behaviour is connected with deactivation of catalyst.

Importantly, the content of CO_2 and CO in the gas phase accurately corresponded to the amount of liquid products observed at TOS = 300 min. This indicates that no major side-reactions have taken place in this time interval.

3.5.2.2 Switch to 5% hydrogen in Ar - step change II)

At 300 min TOS the gas flow was switched to 5% H_2/Ar while keeping the liquid flow constant. The concentrations of CO_2 and CO from the online gas analysis started to respond and rise after 15 min, forming maxima of concentrations corresponding to 49% and 23% conversion after 1 h and 1/2 h respectively, after which the concentrations of both CO_2 and CO slowly declined and settled around 35% and 17% at steady-state. The liquid concentration started to respond to the step change after 1 h (at TOS = 360 min). Then the concentration of heptadecane increased and peaked at a molar concentration around 110%, after which the concentration declined and settled at 90% after totally 2.5 h (TOS = 450 min). This is shown in Figure 3.18 after the dashed line marking step change II).

Naturally the molar balance should complete around 100% in steady-state behaviour, but the step changes the concentration response may temporarily reach values over 100% due to the changed reaction conditions. It is suspected that stearic acid absorbed in the porous catalyst beads from 0-300 min TOS is converted at a faster rate when H_2 is present in the gas atmosphere and thus released as heptadecane, giving a temporary mole balance of over 100%.

The low net flow of stearic acid to the reactor is responsible for the response-time of 1 h of the reactant and products in the liquid feed. The liquid feedstock likely built up a trickling film that wetted the catalyst bed. Stearic acid has a normal boiling point of 383°C and thus passes the reactor in the liquid phase. Heptadecane and 1-heptadecene have normal boiling points of 302°C and could thus be present in the gas phase at 1 bar, but due to the long response time of these molecules after the step change they are expected also to propagate through the reactor in the liquid phase.

The normal boiling point of dodecane is 216°C, while the pressure of the saturated vapors at 300°C is 6 bar. Although the reactor pressure was 20 bar, the gas flow was so high and the amount of the dodecane solvent supplied so low that only about 4 bar of dodecane vapor could have been formed if all the dodecane vaporised. Thus, it must be assumed that dodecane vaporised and passed through the reactor in the gas-phase at 300°C. When the temperature cooled after the reactor outlet, most of the dodecane condensed again.

Contrary to the case of deoxygenation in pure Ar at TOS = 300 min, the content of CO_2 and CO in the gas phase only corresponded to about 60% of the products formed with the amount of product observed. This is likely due to the formation of methane from both CO and CO_2 in the hydrogen-containing atmosphere.

3.5.2.3 Start-up of 100% stearic acid in 5% hydrogen in Ar - step change VIII)

Following the deoxygenation of concentrated stearic acid under pure Ar gas (TOS = 4481-7056 min, see Table 3.3), the reactor was flushed for several hours with pure dodecane at 150°C and left at this temperature overnight solely with Ar gas flow. Then the reactor was reheated to 300°C and the gas was switched to 42 ml/min of 5% H_2/Ar. Flow of concentrated stearic acid was started at TOS = 7066 min. This is seen in Figure 3.19.

The CO signal started to increase slowly after 5 minutes, but 3 h after step change IX) a concentration corresponding to only 4-5% conversion was seen. Only insignificant amounts of CO_2 were observed at the same time. The concentration of both stearic acid and heptadecane started to increase 1 h after step change IX) and 2-2½ h after the step change a relatively stable yield of 12% heptadecane started to result.

The difference between the calculated conversion in respectively liquid and gas phase points to side reactions in the gas phase, possibly methanation. Almost two thirds of the CO formed by deoxygenation have reacted further to form methane.

Compared to the start-up step change I) in dilute stearic acid, the liquid product composition from start-up in concentrated liquid feed respond faster to the step change. The higher net flow of liquid simply reached the outlet of the reactor much faster, and the film pattern of trickling liquid flow is established faster as well.

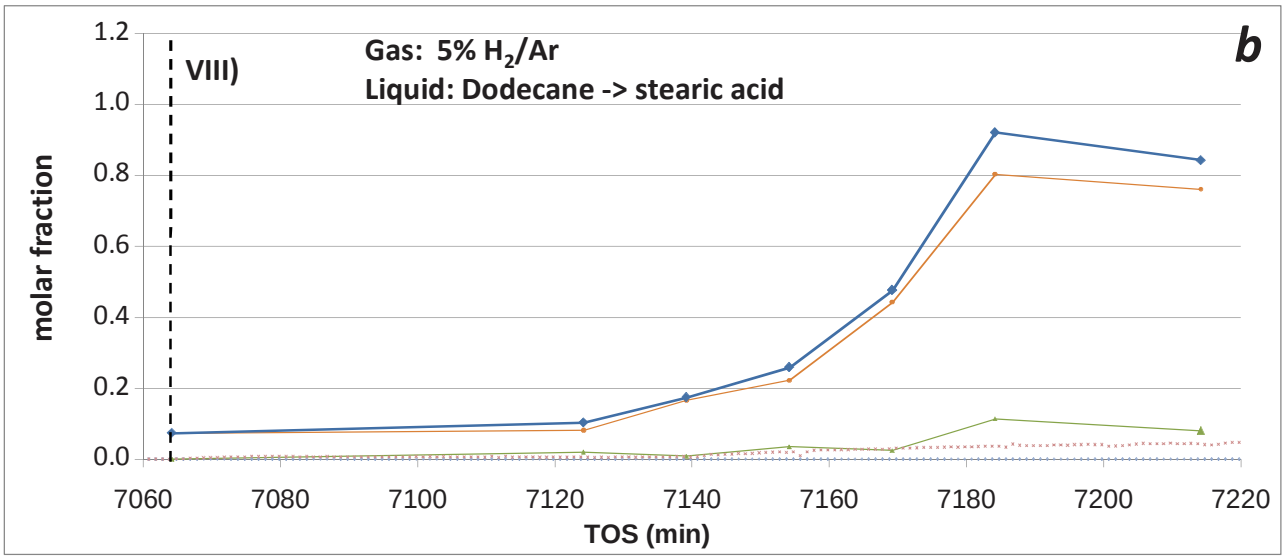

Figure 3.19: Step change of dodecane to concentrated stearic acid flow over 2 wt% Pd/Sibunit - step change VIII). Legend: Liquid mole balance (—♦—), Stearic acid (—●—), heptadecane (—▲—), heptadecene (—■—), undecylbenzene (—×—), CO (x), CO_2 (•).

3.5.2.4 Shut-down of 100% stearic acid in 5% hydrogen in Ar - step change IX)

The shutdown of the reactor after more than 10000 min steady-state deoxygenation of concentrated stearic acid was monitored. The flow was switched to pure dodecane at TOS = 18506 min (step change IX)) and the response after this step change is shown in Figure 3.20.

The CO/CO_2 online gas analysis revealed that the CO produced decreased steadily from a level corresponding to 6-7% conversion at the start of the step change to about 2% after 6 h. The rapid

responses observed when starting up the reactor in dilute stearic acid were not seen from the gas analysis. Initially, the amount of CO present in the gas phase corresponded to 55% of the heptadecane present - thus, 45% of the CO have probably reacted to methane. No CO_2 was observed.

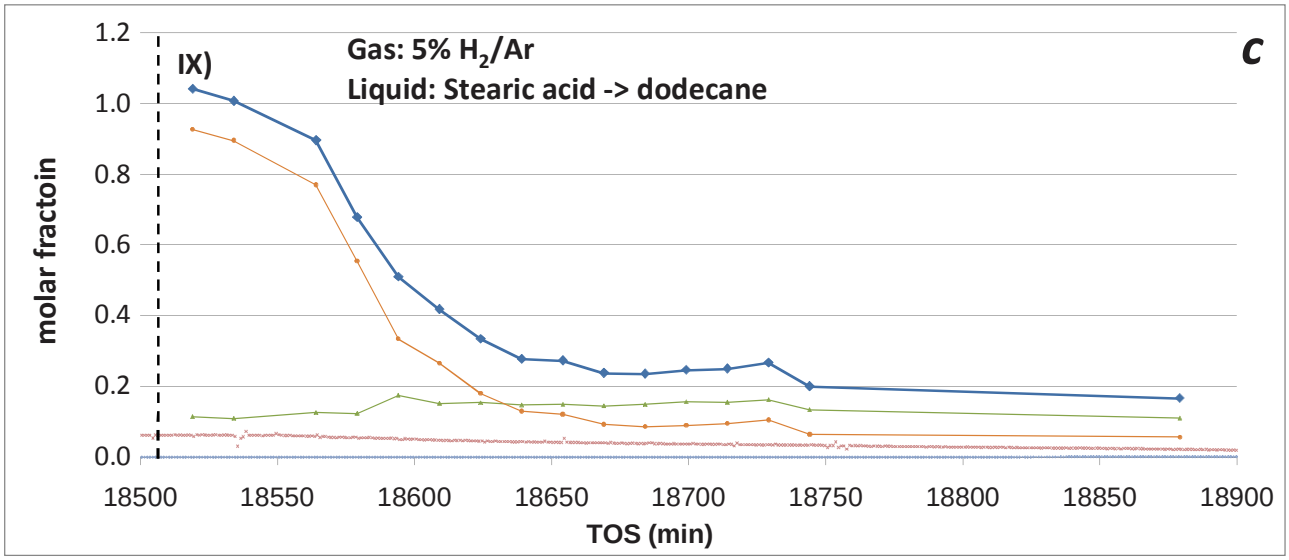

Figure 3.20: Step change of concentrated stearic acid flow to dodecane over 2 wt% Pd/Sibunit - step change IX). Legend: Liquid mole balance (—◆—), Stearic acid (—●—), heptadecane (—▲—), heptadecene (—■—), undecylbenzene (—×—), CO (x), CO_2 (•).

The response in stearic acid from the step change occured after about 1 h. The stearic acid molar fraction did, however not drop to a molar concentration of 0. Instead, a molar fraction of 10% stearic acid is obtained, after 2½ h (TOS = 18660 min), which was then constant for about an hour, after which it decreased only slowly. The heptadecane production was about 12% initially, and the liquid sample analysis showed a response after 1 h to the step change also from heptadecane. However, instead of declining the molar fraction of heptadecane increased slightly to about 17%, which persisted for over 2 h. After this the heptadecane molar fraction decreased slowly for the next few hours.

A plausible interpretation of this step change result is that stearic acid was situated throughout the pore system of the catalyst and was only released very slowly to the exterior to leave the reactor - in fact most of the stearic acid were only released after having reacted to heptadecane, likewise releasing CO or CO_2. The interior pore volume was considerable (0.35 ml/g) and worked as a reactant holdup, and most of the catalyst interior was inert due to the eggshell-impregnation of Pd in the outer rim of the beads. Possibly the exterior liquid film on the catalyst beads of stearic acid was gradually eliminated when the flow of stearic acid was changed to dodecane. This explanation further supports the fact that CO concentration only diminished very slowly despite constant flow of 42 Nml/min of Ar as observed from Figure 3.20.

In all cases the gas phase responsed to the step changes have taken place within a few minutes (5-15 min), but steady-state gas-phase compositions took 2-4 h to develop, which was somewhat slower that the change in liquid sample composition, which delevoped steady-states in 1-2 h.

3.5.3 Characterisation of catalysts

To investigate the causes of the observed deactivation during the long-term experimentation with concentrated and diluted stearic acid, the catalyst beads were sorted in batches depending on their axial location in the tubular reactor and analysed via BET, TEM, and XRD. Before unloading the catalyst bed it was flushed in dodecane and Ar at 150°C, followed by flushing solely in Ar.

Catalyst deactivation may take place by a number of mechanisms. For instance, if the temperature is high enough, the surface area of the metal particles may decrease due to agglomeration or sintering of the metal particles - the particles grow together via migration on the support. Impurities in the feed or side products of the reaction may poison the catalysts, for instance species binding too strongly to the active metal surface to desorp so that the active site is blocked. Furthermore the active catalyst phase may also leach to the solvent or reactant passing the catalysts bed, thus washing the active phase out of reactor.

To investigate the location of active Pd particles in the sibunit carbon beads, the fresh catalyst was subjected to laser ablation (LA-ICP-MS) analysis (Figure 3.21). 2 particles cut in half were used for the measurements. These confirmed that all of the palladium is impregnated in the outer rim of the sibunit beads in an eggshell-like layer corresponding to about the outer fifth of the catalyst beads, while the centre of the sibunit particle is completely free of Pd. This impregnation type minimises the diffusion pathway for the otherwise bulky fat molecules.

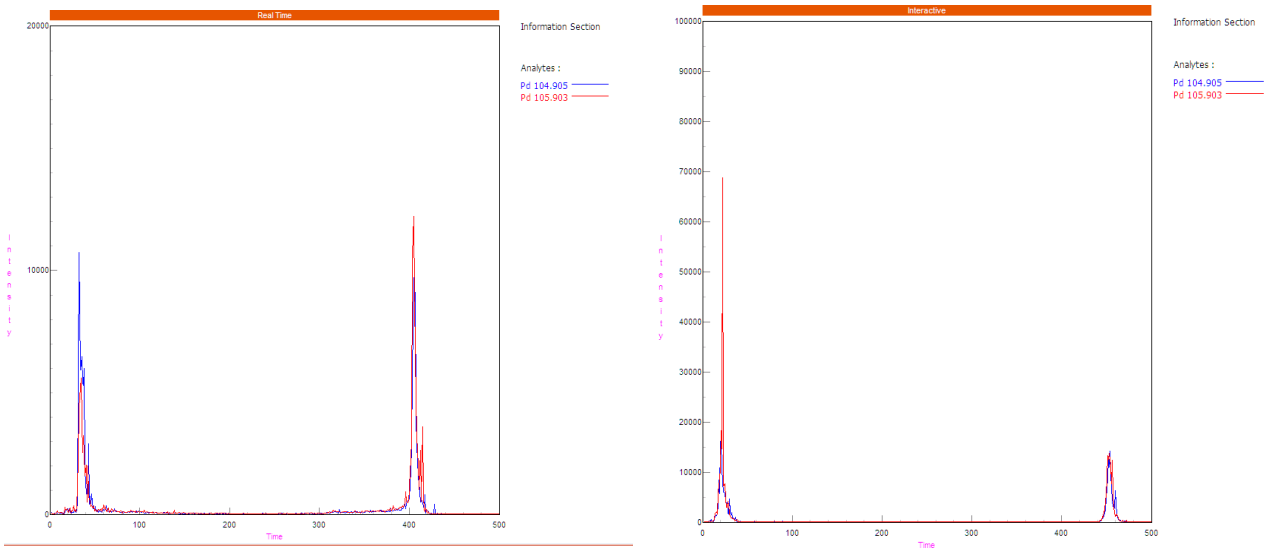

Figure 3.21: Laser ablation of the catalyst beads coupled with ICP-MS to detect ions of palladium. The laser moved at a constant rate over the catalyst diameter, blasting any species to the plasma phase to be detected by the MS.

The surface area, pore size distributions, free volume, and mean particle sizes of the fresh catalyst beads and some of the the spent catalyst batches 3.5 were investigated via XRD and TEM. TEM micrographs, the particle size distributions, and the XRD pattern for the fresh and spent catalyst samples # 1, 4, and 6 (from Table 3.5) are shown in Figures 3.22, 3.23, 3.24, and 3.25, respectively.

Table 3.5: Characterisation of the spent catalyst depending on position in the catalyst bed

Sample # (flow direction: ↓)	Sample mass	Total Surface area (BET)	Pore volume (BET)	Tot. vol. adsorb.	Pore size distribution based on pore diameter in nm				TEM Pd diameter (XRD in parenthesis)
	[g][1]	[m^2/g]	[ml/g]	[ml/g][2]	>10 %	5-10 %	2-5 %	<2 %	[nm][3]
1	1.22	101	0.321	327	1.3	7.4	76.2	15.2	7.7±3.5 (11.9)
2	1.17	118	0.430	395	1.3	8.5	77.8	12.3	—
3	1.13	130	0.377	361	1.1	8.7	71.4	18.8	—
4	2.69	137	0.383	345	1.5	9.1	76.3	13.2	7.1±4.5 (12.4)
5	2.65	157	0.502	410	1.4	10.5	70.4	17.7	—
6	3.87	166	0.474	383	1.3	10.0	67.0	21.8	6.0±4.5 (11.4)
Fresh cat.	—	361	0.873	623	2.0	15.5	73.2	9.3	6.7±2.8 (12.8)

[1] Masses of the spent catalysts samples taken out and sorted consecutively.
[2] N_2 at 298 K and 1 atm.
[3] XRD mean Pd particle is based on volume calculated from the Scherrer equation; TEM is based on the number of particles.

3.5.3.1 Coking in the catalyst pores

The summed mass of the spent catalyst beads was 12.72, however only 10 g of catalyst beads were loaded into the reactor. It is suspected that this weight gain is due to the formation of carbon in the pore system, although it could also be due to the presence of remaining fatty acids in the pores. The weight gain corresponds to 0.227 mol of C, assuming 100% carbon. For comparison, the total amount of stearic acid fed to the reactor amounts to 3.43 mol or 61.7 mol of carbon atoms.

The results from BET analysis of spent and fresh catalyst beads are shown in Table 3.5 as a function of their axial position in the tubular reactor.

Importantly, the catalyst beads near the inlet in the reactor (sample #1) had the lowest BET surface area of 101 m^2/g, which increased monotonously to 166 m^2/g near the outlet (sample # 6). However, the fresh catalyst has a surface area of 361 m^2/g. Thus, surface area decreased from 72% near the inlet to 54% near the outlet. As the catalyst bed was left with dodecane and 5% H_2/Ar flow for 19 h at 300°C and stearic acid is assumed to be washed out of the catalysts beads, it is therefore concluded that deactivation is caused by coking reactions, which have been reported in the literature [214, 330].

The development of this deactivation profile is not fully understood. Possibly the catalyst was more exposed to reactants and side reactions near the reactor inlet, thus forming coke and heavier compounds leading to deactivation. If a temperature gradient had been built up downdraft in the reactor, the reaction rates would likely have been different from each other, which could easily also apply to side reactions leading to carbon build-up.

Compared to the fresh catalyst beads, the deactivated beads had a higher percentage of small pores below 2 nm in diameter and a lower percentage of large pores above 5 nm in diameter. This suggests that coking caused narrowing of the pores and that partial or complete occlusion of some of the smaller pores have taken place. Previously it has been reported that deactivation during deoxygenation of stearic acid over 1% wt Pd/C takes place via dehydrogenation in hydrogen-deficient atmosphere, leading to formation of alkenes and monoaromatics via cyclisations [20, 23, 331]. It can

therefore be concluded that the unsaturated liquid products observed when using pure Ar atmosphere were indicative of the deactivation taking place.

Deactivation and coke formed in the pores did not hinder conversion completely as 12% heptadecane was formed selectively from stearic acid in the final 10500 min TOS (see Figure 3.17) under 5% H_2/Ar.

3.5.3.2 Pd particle sizes

From the X-ray diffractograms the mean particle diameter, <d>, can be calculated via the Scherrer equation based on diffraction pattern intensity, which correlates with the mean volume of the Pd particles:

$< d >= \frac{K\lambda}{\beta \cos\theta}$

K is a shape factor usually around 0.9, λ is the wavelength of the X-ray source, β is the full width at half maximum peak intensity, and θ is the Bragg angle. The surface area from the TEM micrographs are however based on the frequency (i.e. the number) of particles. Thus, the bigger particles contribute much more to the mean particle size in the X-ray diffractograms as compared to the TEM micrographs, which is the reason behind the lower surface areas measured by TEM compared to XRD.

The mean Pd particle diameters based on TEM micrographs varies from 7.7 nm in the top (near the inlet) to 6.1 in the bottom. The fresh catalyst is however 6.7 nm. TEM only counts from the small fraction of the sample that is exposed to the electron beam, thus it is somewhat dependent on the specific sample part which is being analysed. From the figures 3.22, 3.23, 3.24, and 3.25 it is evident that the TEM particle size distributions are quite similar, and that the variation may be within experimental uncertainty.

The diffraction patterns of all of the spent catalysts as well as the fresh catalyst showed mean diameters ranging from 11.4 nm to 12.8 nm (volume-based), as shown in Table 3.5. The variation was not systemtic, and a slightly larger mean particle size of Pd was found on the fresh catalyst compared to the spent ones, while the XRD mean particle sizes did not change monotonically as a function of bed location.

It is concluded that the variations between the mean particle sizes of the catalysts are too small to be significant. Furthermore it is excluded that sintering or agglomeration took place or contributed to the deactivation of the Pd/C catalyst. This is in accordance with other reports in the literature on deoxygenation over 1 wt% or 5 wt% Pd supported on carbon [23, 214, 330, 331].

3.5.3.3 Leaching of Pd

During the entire two-week experimentation, two consecutive batches of effluent from the collector vessel were collected, each of ca. 0.5 kg. The two batches were melted and each of them thoroughly homogenised by stirring, and samples of a few mg were analysed by ICP-EOS to assess the amount of Pd. In the first batch the content of Pd was 1.67 mg/kg effluent, while in the second only 0.59 mg/kg effluent was found. This corresponded to 0.43% and 0.15%, respectively, of the total carbon-supported Pd present in the catalyst bed. Thus, the degree of leaching over the two weeks was

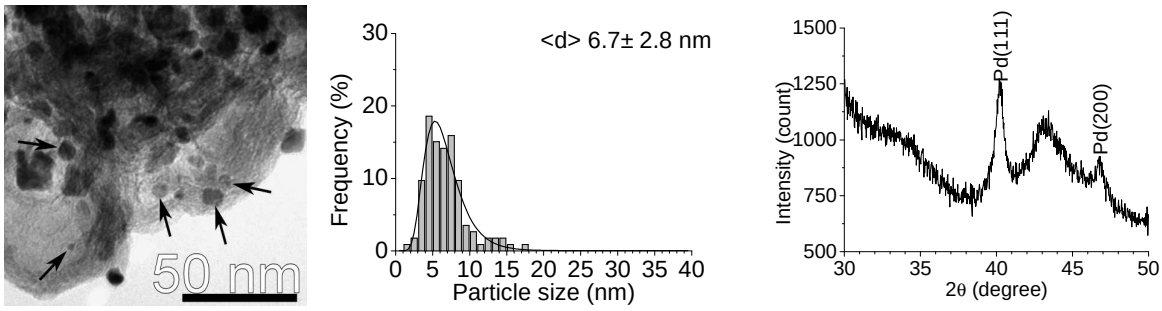

Figure 3.22: TEM micrograph (left-hand side), particle size distribution (middle), and XRD-pattern (right-hand side) of the **fresh catalyst**.

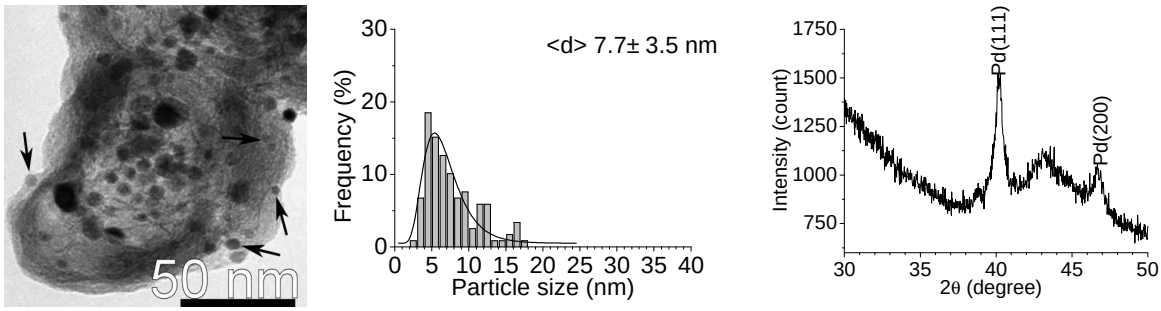

Figure 3.23: TEM micrograph (left-hand side), particle size distribution (middle), and XRD-pattern (right-hand side) of **spent catalyst sample # 1** (from the top of the catalyst bed).

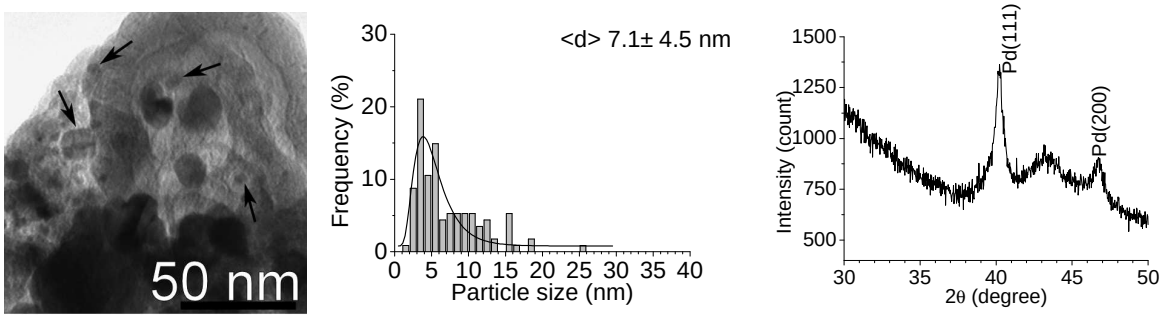

Figure 3.24: TEM micrograph (left-hand side), particle size distribution (middle), and XRD-pattern (right-hand side) of **spent catalyst sample # 5** (from the middle of the catalyst bed).

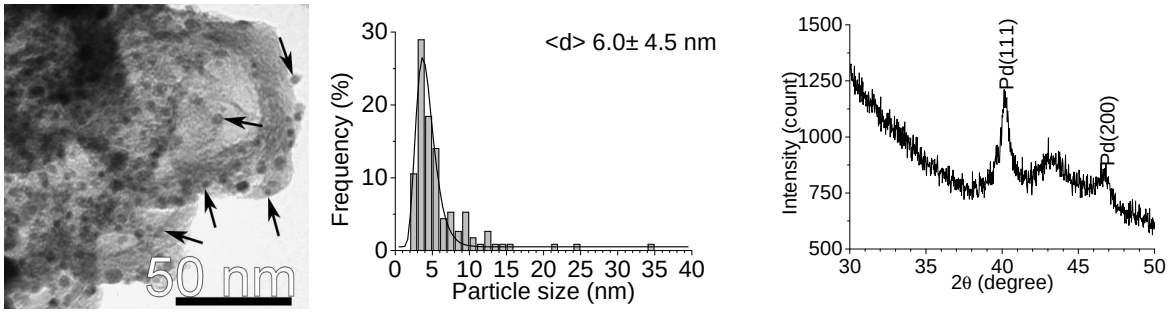

Figure 3.25: TEM micrograph (left-hand side), particle size distribution (middle), and XRD-pattern (right-hand side) of **spent catalyst sample # 9** (from the bottom of the catalyst bed).

minimal, corresponding to 0.58% of the Pd. It is also evident that the leaching degree lowered over time. The leached palladium probably constituted a minimal fraction of loosely bound Pd particles which were slowly washed out by the feed. Deactivation was therefore not due to leaching of the active metal. Minimal leaching of Pd during deoxygenation over Pd/Sibunit have recently been reported [23, 330].

3.5.4 Effect of Sibunit support and temperature

The step change experiments in Section 3.5.1 prompted the investigation of hydrodynamic properties of the reactor without a catalyst to determine evaluate the flow behaviour of the stearic acid in the reactor. The thermal influence as well as the influence of the reactor and the support material of Sibunit beads. Thus, 10 g of Sibunit beads of the same sizes interval as the ones used in Section 3.5.1 catalyst was loaded into the reactor following the description in Section 3.4.3 and in Figure 3.13.

The reactor was flushed for 6 h in Ar at a flow of 42 Nml/min at 20 bar. Then dodecane flow at 0.075 ml/min was started and the reactor was left at these conditions overnight to reach steady-state. At TOS = 0 min the liquid flow of stearic acid was started, and this was left for the next 480 min TOS where the flow was switched back to dodecane. The results are shown in Figure 3.26.

Two samples at TOS = 0 min and 60 min with stearic acid content below 10% of were observed during the first hour of the step change, however the response from the reactor to the liquid flow change cannot have propagated so fast through the reactor, meaning that these constitute impurities of stearic acid in the liquid sampling system. Two consecutive valves constituted the sampling system and could not be dismantled, by which cleaning of the connecting fittings was difficult. At TOS = 90-210 min the CO-level increased from a level corresponding to 0% to 5 % conversion. CO_2 was however only observed at levels corresponding to under 0.5% conversion during the entire treatment.

The stearic acid concentration started to increase at TOS = 90 min - most steeply after 165 min TOS. At TOS = 150 min the production of heptadecane increased from 0 to about 5% yield, thus reaching the same level as the CO produced. When the production of heptadecanestarted to increase also about 1% of monoaromatic C_{17}-compounds were found, but this only persisted for about an hour. Between 0 and 1% of 1-heptadecene was also formed alongside with the heptadecane. At TOS = 240 the molar balance of the liquid samples level reached a steady-state level of about 97%, 90% hereof being unconverted stearic acid, thus 1.5 h was necessary for the liquid profile to develop in the reactor. Thus, it took 4 h to reach stable operation after the step-change.

The step change back to dodecane liquid flow was initiated by switching the liquid feed at TOS = 480 min. 1 h after the change, the concentration of stearic acid in the reactor started to drop quite steeply for the next hour, but after TOS = 600 min the drop in stearic acid concentration flattened off towards a molar fraction of stearic acid of 8% at TOS = 840 min. It is furthermore seen that the heptadecane yield dropped to about 3% 2 h after the step change, but it increased to 4-5% towards TOS = 840 min. Also, the CO-level remains quite stable corresponding to 5% conversion for the first 6 h after the step change (until TOS = 840 min), but after this point the CO-level decreased steadily until TOS = 1100 min.

This behaviour of switching from stearic acid to dodecane is similar to that observed during

switch to dodecane in diluted stearic acid flow in Figure 3.15, section 3.5.1.2 or in concentrated stearic acid flow in Figure 3.20, section 3.5.2.4. It is thus confirmed that stearic acid is simply still present in the pore system of the Sibunit and continued to partly react and partly diffuse to the exterior of the Sibunit to be removed by the flow of Ar and dodecane. This can explain why about 3-4% of the liquid compounds were "missing" in the mole balance at TOS = 240-480 min: The stearic acid was absorbed in the pores of the Sibunit beads as soon as it reached the Sibunit beads, and this is naturally missing in the mole balance. It may be argued that as accumulation of reactant is taking place in the reactor, the stable behaviour of TOS = 240-480 min cannot stricly be called "steady-state".

Apparantly, with the lack of catalyst and added H_2 there is a good correspondance between the liquid sample analysis and the CO-concentration in the gas atmosphere, especially at the conditions approaching steady-state from TOS = 195 min until the step change started to affect the liquid profile in the reactor at TOS = 540 min.

It may be speculated that the production of CO during the deoxygenation of stearic acid, as observed during the entire run of section 3.5.1, were produced as the thermal effect and due to a catalytic effect of the support while the Pd catalyst may have been deactivated completely. Further investigations of these phenomena would be necessary to further elucidate the different reaction routes from the fatty acids to alkanes.

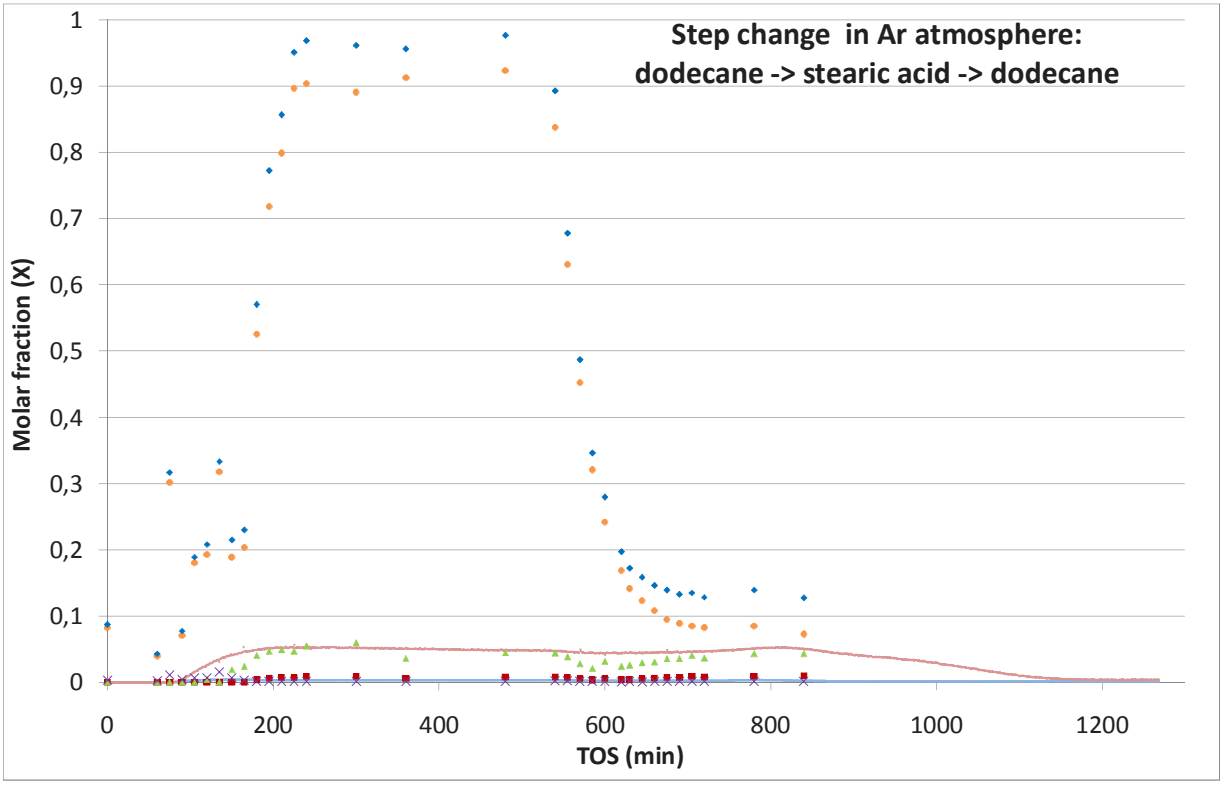

Figure 3.26: Step change behaviour of dodecane -> stearic acid -> dodecane. Pumping speed 0.075 ml/min. 300°C and 20 bar Ar at 42 Nml/min. Legend: Liquid mole balance (♦), Stearic acid (●), heptadecane (▲), heptadecene (■), undecylbenzene (×), CO (x), CO_2 (•)

3.6 Continuous hydrodeoxygenation: Stearic acid and derivatives

Both fatty acids, fatty acid alkyl esters and triglycerides have been suggested as feedstocks for deoxygenation [16, 208, 210, 324]. Both free fatty acids and glycerides are present in fats and oils, and the former is especially present in waste feedstocks. It is therefore interesting to relate these feedstocks in terms of deoxygenation reactivity and reaction pathways. The aim of the present study is therefore to compare the deoxygenation activity during reaction in both H_2-containing and inert gas flow and by using a fresh catalyst for each feedstock. For comparison, stearic acid, ethyl stearate, and tristearin (glyceryl-tristearate) have been used as model compounds. The treatment was performed at 300°C and at 20 bar pressure. During the first 4500 min TOS (stearic acid: 5760 min) a gas flow of 42 Nml/min of 5% H_2/Ar was fed to the reactor. Then the gas atmosphere was changed to pure Ar at 42 Nml/min.

The packing of the reactor was performed almost as shown in Figure 3.13, with the notable exception that the catalyst bed for each feed was loaded into the reactor by separating the catalyst beads into five equally big beds of 2 g each, separated each by a layer of quartz wool. This made it much easier to sort the spent beads into 5 equally sized batches after reaction for characterisation of the spent catalysts.

After flushing with Ar, the catalysts were reduced prior to reaction in 5% H_2/Ar: The reactor was heated at ca. 10°C/min to 150°C where it was kept for 1 h. Then the temperature was increased to the reaction temperature of 300°C at 10°C/min where the reactor was kept for 0.5 h before the flow of stearic acid was started. The CO/CO_2 online analysis was unfortunately switched off during part of the experimentation.

3.6.1 Stearic acid

Pumping of stearic acid feed to the reactor was started TOS = 0 min, and the liquid samples responded to the reactant flow after 180 min as visualised in Figure 3.27. Initially almost 100% heptadecane was formed and only traces of stearic acid were observed. However, the yield of stearic acid had decreased to 80% at TOS = 1560 min and 72% at TOS = 5760 min, thus showing a slow and gradual deactivation during the deoxygenation in 5% H_2/Ar. Correspondingly, the amount of unconverted stearic acid of 17-23% were observed at TOS = 1560-5760 min. These results clearly show that the 12% yield of heptadecane obtained in section 3.5.1.4 was the product of an already deactivated catalyst.

The CO and CO_2-levels started to increased 60 min after the pumping of stearic acid was started. The online analyser was offline during the period of TOS = 360-2280 min. However, the online gas analysis of the gas-phase clearly shows that CO_2 corresponding to 30 % and CO corresponding to 5% conversion was formed initially at TOS = 135 min, but the two gas concentrations steadily aproached each other and met at a level correponding to 16% conversion of feedstock for each gas at TOS = 5760 min.

At TOS = 5760 the gas atmosphere was changed to pure Ar. This led to a drop in the CO-level to 2% conversion and a peak increase in the CO_2-level in the gas; however, the CO_2-level dropped

again to a level of 0% conversion at TOS = 6040, while the CO-concentration rose to a peak of 5% an declined thereafter.

After the change to Ar gas step change the heptadecane-concentration remained constant at a yield of ca. 75% for 2 h, but then the concentration dropped steeply to 8% at 5 h after the change to Ar gas. The heptadecane yield further decreased and leveled off at ca. 2%, following the concentration of CO. The steep drop in heptadecane concentration is followed by an equally steep rise in stearic acid concentration a few hours after the pure Ar-flow was started. The peak CO-concentration around TOS = 6040 min is accompanied by a peak of 1-heptadecene of 2% yield and undecylbenzene of 1% yield. Thus, catalyst deactivation in hydrogen-deficient gas flow was also in this case accompanied by formation of unsaturated C_{17}-products. The remaining duration of the experiment, until TOS = 9000 min, 3% decreasing to 2% heptadecane yield was obtained, in accordance with behaviour of the the deactivated catalyst described in Section 3.5.1.3

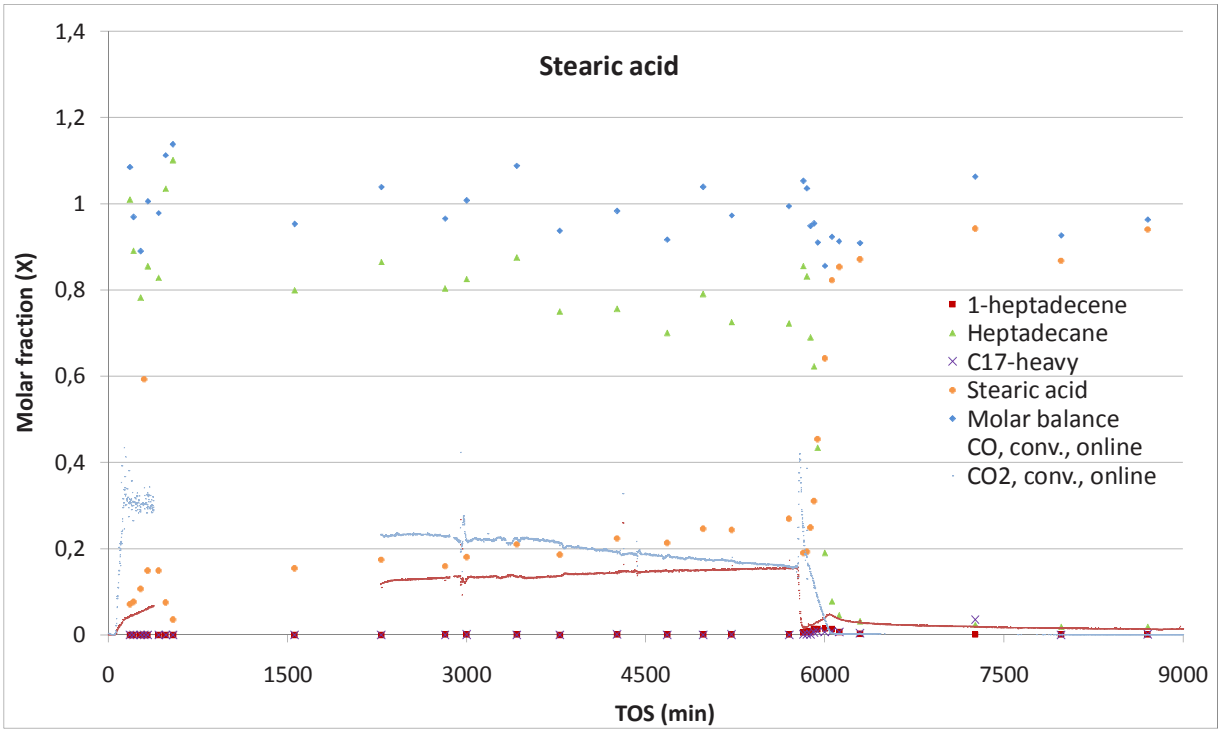

Figure 3.27: Conversion of concentrated stearic acid flow at 0.075 ml/min over 2 wt% Pd/Sibunit at 300°C and 20 bar. TOS = 0-5760 min: 5% H_2/Ar; TOS = 5760-9000 min: Ar. Legend: Liquid mole balance (♦), (●), Stearic acid (●), heptadecane (▲), heptadecene (■), undecylbenzene (×), CO (•), CO_2 (•).

3.6.2 Ethyl stearate

The ethyl stearate liquid pumping was started at TOS = 0 min. The response in terms of heptadecane was an initial yield of 90% after 3 h, decreasing quickly to 75% in the next few hours, as is shown in Figure 3.28. In the beginning of the run about 2-3% unsaturated compounds in the form of 1-heptadecene and undecylbenzene were formed from the ethyl stearate, although these decreased to 1% during the reaction in 5% H_2/Ar. The heptadecane formation stabilised at ca. 62% yield from TOS = 800 min while the analysis of the ethyl stearate showed between 25% and 40% unconverted ester - this varied considerably, as did the amount of stearic acid observed in 2% to 12% yield. This

led to a fluctuating mass balance between ca. 90% and 115%.

Initially, the gas analyser was offline for the first 2500 min TOS, so no information of gas composition is found for the first time interval. However, the gas analysis from TOS = 2500 min showed a remarkably constant level of CO corresponding to 1.5% conversion, while it appeared that the CO_2-concentration in the gas-phase leveled off at around 18-19% conversion level before TOS = 4500 min.

The gas atmosphere was changed from 5% H_2/Ar to pure Ar at TOS = 4500 min. and the gas atmosphere was affected after about 20 min. A steep drop in CO_2 concentration took place for about an hour to a CO_2-level corresponding to practically 0% conversion. The CO-level fell more moderately over a number of hours.

60 min after the change to Ar gas flow the heptadecane yield started to drop steeply as well, and after another 60 min the yield reached 7% and after 120 min only 2%. 6 h after the gas change the yield of heptadecane was below 1% and remained so for the remaining experimentation period. The ethyl stearate responded to the change by increasing to a level over 100% within a few hours, and between 110% and 130% was during the rest of the experiment. Mole balances over 100% are not possible at steady-state, so this is clearly an inaccuracy in the sampling method, most likely from using a too high response factor for the liquid concentrations from the GC-FID liquid analysis.

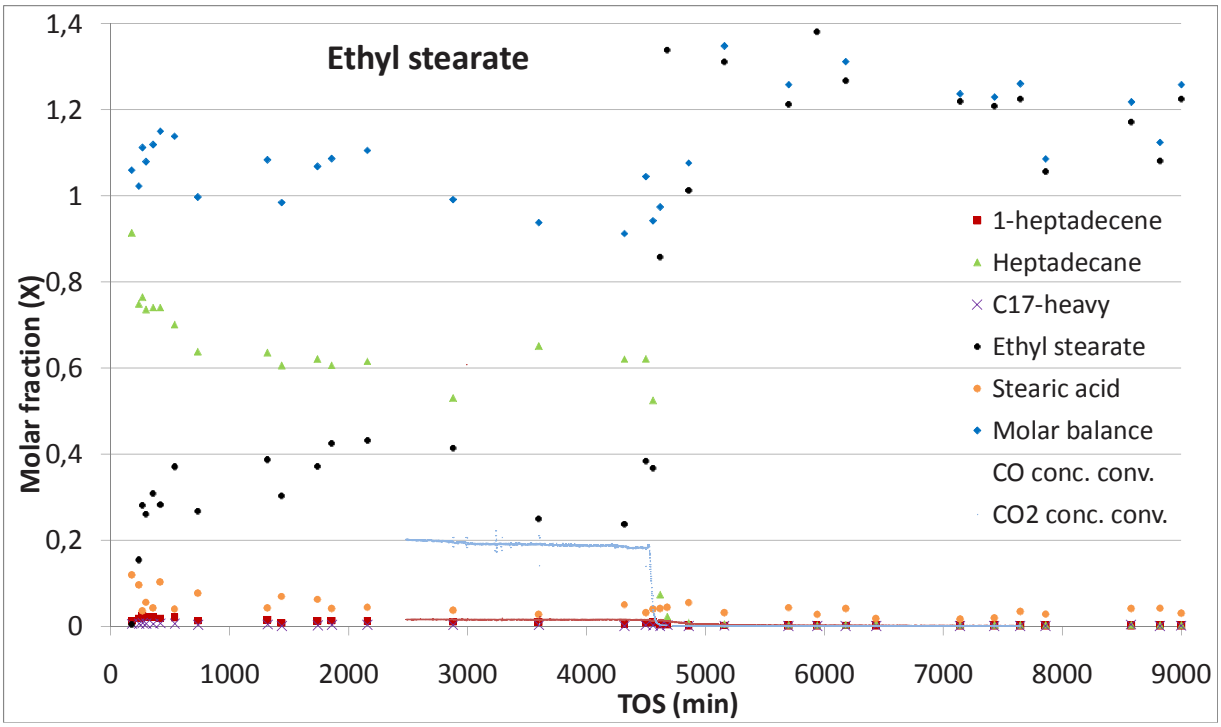

Figure 3.28: Conversion of concentrated ethyl stearate flow at 0.075 ml/min over 2 wt% Pd/Sibunit at 300°C and 20 bar. TOS = 0-4500 min: 5% H_2/Ar; TOS = 4500-9000 min: Ar. Legend: Liquid mole balance (♦), Ethyl stearate (●), Stearic acid (●), heptadecane (▲), heptadecene (■), undecylbenzene (×), CO (•), CO_2 (•).

Stearic acid was observed throughout the entire experimentation between 12% and 2% yield, possibly as an intermediate of the conversion of ethyl stearate. Despite the catalyst being completely inactive in the Ar atmosphere, about 4-5% stearic acid were still observed in the liquid samples from the ractor. One explanation could be that the deoxygenation via stearic acid is faster than a potential

direct deoxygenation cleavage of the ester bond. This could happen through hydrolysis of the ester with water vapor. However, there may be several reaction routes for the deoxygenation since stearic acid was still formed (and not consumed to form C_{17}-hydrocarbons) during the period of pure Ar atmosphere at TOS = 4500 - 9000 min.

3.6.3 Tristearin

Triglycerides are the major constituent of most fats and oils, however the analysis of the triglycerides can be somewhat troublesome. Not many reports have appeared where an actual quantification of the triglycerides themselves are performed. In the analysis performed here, the amounts from the triglycerides calculated from the chromatograms by the cool-on-column GC-FID analysis were too small to check to a molar balance of 100% and has therefore been omitted in the graphics of Figure 3.29. Technical tristearin was used in the experimentation, which upon fatty acid analysis by transesterification appeared to contain about 35% palmitic acid and 65% stearic acid as fatty acid chains in the glycerides. Therefore, the products pentadecane (C_{15}) and heptadecane (C_{17}) can be expected from decarbonylation and decarboxylation and hexadecane (C_{16}) and octadecane (C_{18}) via complete reduction with H_2.

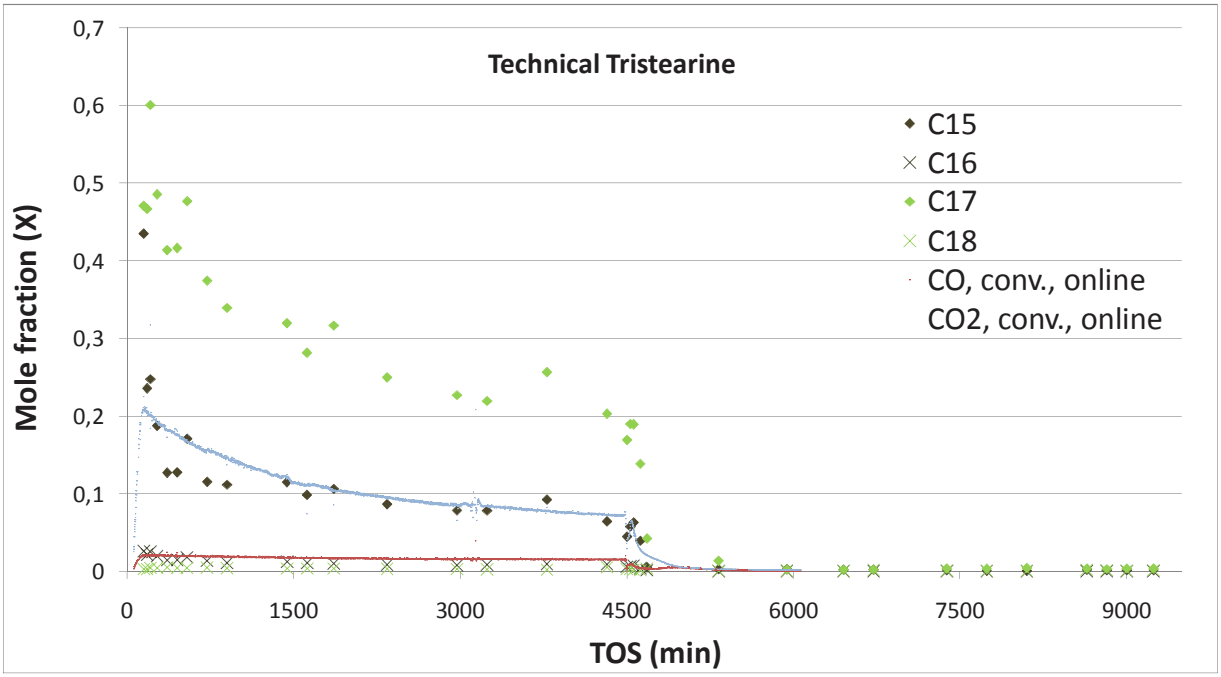

Figure 3.29: Conversion of concentrated tristearin flow at 0.075 ml/min over 2 wt% Pd/Sibunit at 300°C and 20 bar. TOS = 0-4500 min: 5% H_2/Ar; TOS = 4500-9240 min: Ar. Legend: Pentadecane (♦), hexadecane (×), heptadecane (♦), octadecane (×), CO (•), CO_2 (•).

After start-up of the flow to the reactor, the gas signal responded after 60 min TOS where the CO_2-concentration peaked corresponding to ca. 21% yield and CO peaked at ca. 2.5%. The CO level was almost constant for the remaining reaction i 5% H_2/Ar, while the CO_2-level dropped to 7% conversion in the same time interval. The yields of heptadecane and pentadecane reached respectively 60% and 25% after 150 min TOS, but both declined towards respectively 21% and 7% when nearing TOS = 4500 min. Thus, the turnover rate of the catalyst bed had been reduced to 33% of the

immediate initial activity.

The gas flow was changed to pure Ar at TOS = 4500, and the CO/CO_2 concentration responded to this change immediately by dropping to 0, followed by a concentration peak after 40 min, and a gradual decline over the next hours to a level below 1% conversion. The liquid production of heptadecane and pentadecane declined after 120 min, leveling off and nearing zero in the following hours. During the remaining experimentation until shutdown at TOS = 9240 min no further conversion to alkanes was detected.

3.6.4 Comparison of reactants

It is evident that the shift to pure Ar atmosphere swiftly led to deactivation in all of the liquid feeds applied. Also, in all of the deoxygenation reactions in hydrogen-containing atmosphere, the yields of liquid hydrocarbons produced did not corresponnde to the CO- and CO_2-levels in the gas effluent - methanation most likely consumed a large part of the CO_x formed. It appears that the reactor still produced a few percent of heptadecane in the pure Ar gas flow with stearic acid as a reactant, perhaps due to a thermal mechanism or catalysis by the support as described in section 3.5.4. This behaviour is not seen with the ester compounds.

Interestingly, the gas atmosphere during the stearic acid experiment showed a gradual rise of CO and decline of CO_2 formation in H_2-containing gas flow. Ethyl stearate and tristearin yielded primarily CO_2 and a constant level of CO during reaction in H_2/Ar atmosphere, which is in contrast to the results reported by Resasco et al. [210], who reacted methyl stearate over Pt/γ-Al_2O_3 in a semibatch reactor and primarily detected CO formation in the gas atmosphere during heptadecane formation in both H_2 and He atmosphere at 325°C [210]. This difference may have to do with the difference in catalyst metal or support or the fact that different reactor- and catalyst types were used.

The deoxygenation of stearic acid and tripalmitin have minor peaks of CO and CO_2 after changing the gas atmosphere pure Ar gas, and a few hours "extra" catalyst lifetime with formation of mostly saturated, but also unsatuated hydrocarbon products can be observed. It could be suspected that part of the mechanism requires removal of H_2 to the sweeping gas - such as the formic acid formation/decomposition mechanism proposed by Berenblyum and co-authors [322], where the formic acid must decompose to H_2 and CO_2. Thus, H_2 is both needed as a reactant to avoid formation of unsaturated compounds and deactivation, but also inhibiting part of the mechanism or leading to formation of CO, as observed by Immer et al. [321].

Ethyl stearate and tristearin yielded identical production levels of CO (despite different conversions of the reactants), and it may be speculated that the same gas-producing reactions takes place. Interestingly, varying minor amounts of stearic acid were obtained during the entire experimentation with ethyl stearate as a possible part of the deoxygenation reaction mechanism, but during the run in technical tristearin no palmitic or stearic acid were observed. Further careful studies to define the reactions of the gases during deoxygenation would be highly desirable. The influence of gas pressure and content is far from understood, as is the influence of methanation, water-gas-shift reactions and the role of CO as a possible poison for the catalyst. This could for instance be tracked by measuring methane, by mass spectroscopy using isotopic labeling of gases and reactants, or by dosing various

gases to the reactor with and without reactants to measure the influence on the liquid and gas phases.

Neither stearic acid nor ethyl stearate yielded any products from full reduction of the fatty acid chain (i.e. octadecane). However, technical tristearin yielded 2-3% even-carbon-numbered alkanes during the reaction in hydrogen-containing atmosphere, decreasing to about 1% during the period of reaction with 5% H_2/Ar gas. It may be speculated that these derived impurities of C_{19} and C_{17} fatty acids, but they were not found during analysis by transesterification, thus the octadecane and hexadecane observed must derive from stearic and palmitic acid. This is somewhat contrary to the assumption that ethyl stearate and tristearin should have reacted via identical reaction routes, thus the reaction network was more complex. No unsaturated compounds were observed during the entire treatment of tristearin, but minor amounts of 1-heptadecene and monoaromatic C_{17}-compounds were observed for both stearic acid and ethyl stearate, especially during start-up and gas atmosphere change.

Both the stearic acid and ethyl stearate experimentation initially had a yield of around 100% of formed alkanes, but the yield of the former was 75% at TOS = 4500 min in contrast to 62% of the latter. However the tristearin initially yielded about 85% alkanes, which dropped to as low as 28% at 4500 min. All the molecules were supplied at the same liquid volume feeding rate, 0.075 ml/min at a pump and tubing temperature of 100°C, and as they have about the same densities the feeding of carbon is also more of less the same. Thus it can be stated that the catalyst deactivated faster during tristearin than ethyl stearate deoxygenation, which again deactivated faster than during stearic acid deoxygenation. This supports a "the simpler, the better"-approach regarding the feedstock molecules during the deoxygenation - the more complicated and hindered the molecule, the faster the deactivation of the catalyst.

An assessment of the degree of deactivation was made by BET measurements of the batches of the spent catalyst beads from the three different feeds by comparison with the fresh catalyst as seen in Figure 3.30. Here it is evident that the catalyst beads used for ethyl stearate deoxygenation have endured the least deactivation by loss of surface area compared to the fresh catalyst (36% surface area lost on average), tristearin somewhat more (44% surface area lost) and stearic acid the most (46% surface area lost). This order is different from the order of the degree of deactivation of the catalysts mentioned above. The picture of deactivation must therefore be refined to include that various feedstocks may be more or less tolerant to coking of the catalyst during deoxygenation - or other deactivation phenomena may have taken place at the same time, which have not been investigated. This possibly had to do with different accessibility on active Pd sites for the two esters and the fatty acid, especially on the partly deactivated catalysts. Coking or buildup of reactants or products is the reason behind the shrinking of the internal pore surface area.

The surface area distribution of the spent catalyst beads in Figure 3.30 was also surprising and somewhat different compared to the clear deactivation profile described in section 3.5.3 and Table 3.5. However, the variation of surface areas was bigger during long-term experimentation of stearic acid compared to the areas given in Figure 3.30, which are also bigger. The stearic acid and tristearin surface areas were biggest in the middle of the catalysts beds, so that deactivation by pore clogging primarily took place in the top and bottom of the catalyst bed. The ethyl stearate conversion resulted

a deactivation profile where the areas decreased downwards in the bed, completely contrary to the deactivation mentioned in Table 3.5. Generally this behaviour was unexpected, but possibly small temperature differences depending on axial bed position have led to these surface area distributions.

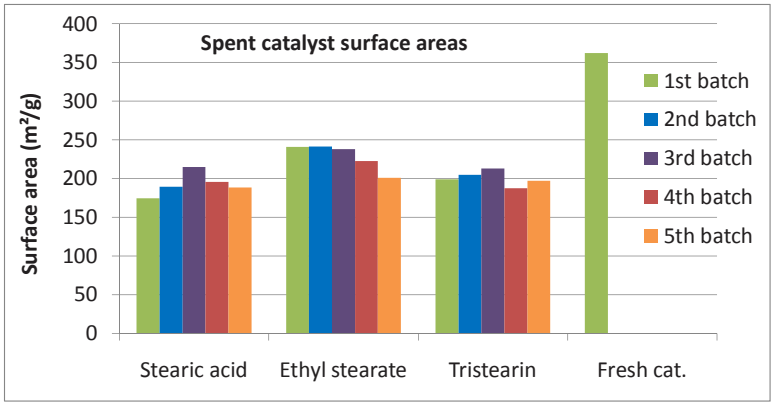

Figure 3.30: Surface area of the catalyst for stearic acid, ethyl stearate and tristearin deoxygenation. Measured by N_2 physisorption and calculated with the BET method. The batches are numbered by position downwards in the bed, i.e. ascending order away from the inlet.

3.7 Hydrodeoxygenation of fats and oils: Conclusion

The supported transition-metal catalysed deoxygenation of fatty compounds have been investigated in both batch and continuous reactor.

Tripalmitin and oleic acid dissolved in n-tetradecane were investigated for hydrodeoxygenation over noble-metal catalysts in an autoclave as a batch reactor. Hydrogen pressure and temperature was varied between 0 and 40 bar H_2 and 250-375°C over 5 wt% Pt/γ-Al_2O_3. Furthermore a number of metals were tested as active materials for the deoxygenation. Part of the triglycerides are split to FFA before deoxygeation.

Oleic acid was converted to alkanes faster than tripalmitin over 5 wt% Pt/γ-Al_2O_3, possibly due to less sterical hindrance. The deoxygenation activity below 300°C was low and resulted in yields below 10% after 5 h reaction at 20 bar H_2, but all of the oleic was converted to alkane at 325°C after 5 h - this was only reached for tripalmitin at 375°C. The optimum pressure of both tripalmitin and oleic acid at 325°C was around 10-20 bar of H_2 - higher pressures of H_2 resulted lower yields of alkanes while no H_2 in the gas atmosphere led to the formation of unsaturated hydrocarbons. Higher H_2-pressures as well yielded more even-carbon-numbered alkanes by complete reduction of the fatty acid chains.

The best catalysts amongst Ni, Rh, Ru, Pd, Pt, and Au supported on γ-Al_2O_3 was found to be Pt and Pd, as the others tested were not as active and usually not as selective towards decarboxylation and decarbonylation as Pd and Pt. Pt was more active for the oleic acid conversion than Pd, but the opposite was the case for tripalmitin. The surface area Pt on γ-Al_2O_3 were only half of that of the corresponding Pd. γ-Al_2O_3 was not active for the deoxygenation alone. Catalytic methanation result from the carbonaceous gases formed in the H_2-rich gas, and this reaction should be avoided in an industrial system.

Stearic acid was deoxygenated in a continuous packed-bed reactor at 300°C at 20 bar over 2 wt% Pd on Sibunit carbon during a catalytic run of almost 2 weeks, employing various step changes. Almost complete conversion of dilute stearic acid to heptadecane was achieved in 5% H_2/Ar with the fresh catalyst, but switching to Ar led to formation of unsaturated products, decreasing conversion and a switch to formation of CO gas. Concentrated stearic acid was converted almost exclusively to heptadecane in both 5% H_2/Ar, but the conversion was several times higher (12%) with hydrogen in the gas compared to deoxygenation without hydrogen. Thus, H_2 was necessary to avoid the gradual deactivation of the catalyst in diluted stearic acid in dodecane and yielded higher conversion of the fatty acid.

A gradual deactivation profile was observed in the catalyst bed as 72% of the original catalyst surface area was lost near the reactor inlet, while only 54% was lost in the bottom. The deactivation and coking reactions were more pronounced in the inlet zone of the reactor compared to the outlet. Deactivation took place by coking while leaching, sintering and agglomeration could be excluded.

The response behaviour during step changes, especially the liberation of CO and the considerable number of hours necessary before the liquid samples were free from stearic acid revealed that the porous catalyst beads in the bed absorbed the stearic acid and released it over a number of hours in

inert liquid flow. Thus, stearic acid either diffused very slowly in the pores, perhaps due to capillary forces, justifying the use of a catalyst with eggshell-impregnation of the active metal phase. The treatment of stearic acid over Sibunit beads without Pd or added H_2 yielded about 5-6% conversion of the stearic acid primarily to heptadecane in Ar atmosphere. CO was produced as the main gaseous product, while no or very little CO_2 was observed from this experiment. This may hint that CO production during transition-metal-catalysed deoxygenation is caused by a deactivated catalyst where only a thermal or support effect is responsible for the conversion to alkanes.

The reactivities of FFA, ethyl and triester over 2 wt% Pd/Sibunit in continuous deoxygenation were assessed under 5% H_2/Ar, and after 3 days TOS the conversion to alkanes was 75% with stearic acid, 62% with ethyl stearate, and 27% with technical tristearin as the liquid feed molecules. Ethyl stearate and tristearin conversion yielded primarily CO_2 in the gas phase and a low and constant amount of CO, while the gas composition during stearic acid deoxygenation steadily changed from primarily CO_2 as gaseous product to an equimolar mixture of CO and CO_2. When the gas flow was switched to Ar, the catalyst deactivated fast with all of the three feedstocks. The stearic acid sustained the slowest deactivation after switch to pure Ar gas flow compared to ethyl stearate and tristearin. Technical tristearine yielded minor amounts of C_{18}- and C_{16}-alkane through full reduction of the fatty acid chains, which was otherwise not observed with ethyl stearate and stearic acid.

The excellent selectivities of transition metals towards the decarboxylation or decarbonylation pathways during deoxygenation of fatty acids and triglycerides make these catalysts promient for this reaction. However, the hydrogen consumption, methane formation and lifetime of the supported noble-metal catalysts is still below that of sulphided hydrotreatment catalysts, and further investigations and developments are required to increase catalyst lifetime and avoid side reactions and deactivation for the noble-metal catalysts.

Although palladium and platinum have been found active in the present work, alternatives ought to be found as Pt and Pd are scarce metals and expensive. However, rational and sparse use of the metals could be justified for deoxygenation reactions, but this requires a profound comprehension of the reaction involved, including mechanisms and selectivity for various liquid products, gas product selectivities, side reactions, stable behaviour in long-term experimentation, and deactivation. Catalysts used in industrial settings should be thoroughly investigated according to these parameters. The current study may add to this.

Chapter 4

4

Outlook and Concluding Remarks

Although the deposits of easily accessible fossil fuels may last for longer than projected at present, it is important from both an economic and environmental point of view to develop alternative fuel technologies with a lower impact on the environment and less susceptible to fluctuating oil prices. Solar, wind, wave, or geothermal power plants are installed in increasing numbers, but although their usage is projected to rise dramatically in the coming years they are not projected to gain a significantly higher share of the global energy consumption - as the growing global energy demand is also being covered by fossil energy resources. Nuclear power may as well contribute to the production of CO_2-neutral energy, but the nuclear waste problem is at best only partly solved.

Electrical energy cannot be stored economically in large amounts with the current technology. And despite the promising perspective of a hydrogen economy no competitive system for using H_2 as a standard vehicle fuel exists yet, mostly due to the difficulties of storing the gas. Thus, the chemical energy density remains the determining factor for the energy system in the transport sector, and it is difficult to imagine this to change from hydrocarbons in the near future. And hydrocarbons is still the only option for instance for aviation fuels and production of bulk chemicals.

The sinister forecasts of our addiction to oil, gas and coal puts an increasing pressure on us to develop viable alternatives to the fossil resources and turn them into a green, sustainable industry. This puts biomass in a central position in a shift away from fossil feedstocks, as biomass is the sole applicable renewable carbonaceous resource at present. The production of biofuels, bioenergy and biochemicals may help to solve the problems of increasing global resource consumption, warming climate and deterioration of ecosystems around the globe.

The purpose of this thesis has been to contribute to the investigations and development of catalysts for production of diesel fuel from biomass, especially with focus on methods employing waste oils and fats as raw materials. A handful of technologies exist that potentially may yield diesel fuel, however only fatty acid methyl esters (FAME) and alkanes via hydrodeoxygenation (HDO), both from fats and oils, have yet been introduced on the diesel market in a larger scale. Catalysis will most likely play a key role in enabling the conversion of any biomass to sustainable transportation biofuels, and a profound basic and technical understanding of the catalytic reactions will be essential for making the processes economical and efficient.

Biomass-based diesel and biofuels as such may contribute to meet the immense global challenge of finding sustainable energy for the ever-increasing demand from the transportation sector. It is, however, of equally immense importance that this biofuel is produced sustainably, for instance by using waste agricultural and industrial products, and that the production does not foster bigger ecological problems than it solves.

Chapter 5

5

References

[1] International Energy Agency. *World Energy Outlook*. International Energy Agency, Paris, France, (2010).

[2] Forster, P., Ramaswamy, V., Artaxo, P., Berntsen, T., Betts, R., Fahey, D., Haywood, J., Lean, J., Lowe, D., Myhre, G., Nganga, J., Prinn, R., Raga, G., Schulz, M., and Van Dorland, R. *Changes in Atmospheric Constituents and in Radiative Forcing*, chapter 2, 131–234. Cambridge University Press, Cambridge, United Kingdom, 1 edition (2007).

[3] International Energy Agency (IEA). *Key World Energy Statistics*. International Energy Agency, IEA Publications, 9 rue de la Fédération, 75739 Paris Cedex 15, France, (2006).

[4] Thomas, J. M., Hernandez-Garrido, J. C., and Bell, R. G. *Top. Catal.* **52**, 1630–1639 (2009).

[5] The European Union. *J. Eur. Union* **12**, 1–20 (2003).

[6] Commission of the European Communities. *Communication: "Renewable Energy Road Map. Renewable energies in the 21st century: building a more sustainable future"* **COM(2006) 848 final** (2007).

[7] The European Union. *J. Eur. Union* **140**, 1–47 (2009).

[8] Nørskov, J. K., Bligaard, T., Rossmeisl, J., and Christensen, C. H. *Nat. Chem.* **1**, 37–46 (2009).

[9] Thomas, J. M. and Thomas, W. J. *Principles and practice of Heterogeneous Catalysis*. VCH Verlagsgesellschaft mbH, Weinheim, Germany, 1st edition (1997).

[10] Ma, F. and Hanna, M. A. *Bioresour. Technol.* **70**, 1–15 (1999).

[11] Van Gerpen, J. *Fuel Process. Technol.* **86**, 1097–1107 (2005).

[12] Knothe, G., Van Gerpen, J., and Krahl, J. *The Biodiesel Handbook*. AOCS Press, Urbana, Illinois, USA, 1 edition, (2005).

[13] Meher, L., Vidya Sagar, D., and Naik, S. *Renew. Sustain. Energy Rev.* **10**, 248–268 (2006).

[14] Mittelbach, M. and Remschmidt, C. *Biodiesel: The Comprehensive Handbook*. Martin Mittelbach, Graz, Austria, 3 edition, (2006).

[15] Knothe, G. *Top. Catal.* **53**, 714–720 (2010).

[16] Kubičková, I., Snåre, M., Eränen, K., Mäki-Arvela, P., and Murzin, D. Y. *Catal. Today* **106**, 197–200 (2005).

[17] Snåre, M., Kubičková, I., Mäki-Arvela, P., Eränen, K., and Murzin, D. Y. *Ind. Eng. Chem. Res.* **45**, 5708–5715 (2006).

[18] Huber, G. W., O´Connor, P., and Corma, A. *Appl. Catal., A* **329**, 120–129 (2007).

[19] Huber, G. W. and Corma, A. *Angew. Chem., Int. Ed.* **46**, 7184–7201 (2007).

[20] Rozmysłowicz, B., Mäki-Arvela, P., Lestari, S., Simakova, O. A., Eränen, K., Simakova, I., Murzin, D. Y., and Salmi, T. *Top. Catal.* **53**, 1274–1277 (2010).

[21] Guzman, A., Torres, J. E., Prada, L. P., and Nuñez, M. L. *Catal. Today* **156**, 38–43 (2010).

[22] Šimáček, P. and Kubička, D. *Fuel* **89**, 1508–1513 (2010).

[23] Simakova, I., Simakova, O., Mäki-Arvela, P., and Murzin, D. Y. *Catal. Today* **150**, 28–31 (2010).

[24] Kikhtyanin, O. V., Rubanov, A. E., Ayupov, A. B., and Echevsky, G. V. *Fuel* **89**, 3085–3092 (2010).

[25] Twaiq, F. A., Zabidi, N. A. M., Mohameda, A. R., and Bhatia, S. *Fuel Process. Technol.* **84**, 105–120 (2003).

[26] Tamunaidu, P. and Bhatia, S. *Bioresour. Technol.* **98**, 3593–3601 (2007).

[27] Na, J.-G., Yi, B. E., Kim, J. N., Yi, K. B., Park, S.-Y., Park, J.-H., Kim, J.-N., and Ko, C. H. *Catal. Today* **156**,

44–48 (2009).
[28] Simonetti, D. and Dumesic, J. *Catal. Rev. - Sci. Eng.* **51**, 441–484 (2009).
[29] Huber, G. W., Chheda, J. N., Barrett, C. J., and Dumesic, J. A. *Science* **308**, 1446–1450 (2005).
[30] Chheda, J. N., Huber, G. W., and Dumesic, J. A. *Angew. Chem., Int. Ed.* **46**, 7164–7183 (2007).
[31] Serrano-Ruiz, J. C., Wang, D., and Dumesic, J. A. *Green Chem.* **12**, 574–577 (2010).
[32] Rostrup-Nielsen, J. R. *Catal. Rev. - Sci. Eng.* **46**, 247–270 (2004).
[33] Rostrup-Nielsen, J. R. *Science* **308**, 1421–1422 (2005).
[34] Abatzoglou, N., Dalai, A., and Gitzhofer, F. In *3rd IASME/WSEAS international conference on energy, environment, ecosystems and sustainable development, Greece*, 223–232, (2007).
[35] Zhang, W. *Fuel Process. Technol.* **91**, 866–876 (2010).
[36] Stöcker, M. *Angew. Chem., Int. Ed.* **47**, 9200–9211 (2008).
[37] Carlson, T. R., Jae, J., Lin, Y.-C., Tompsett, G. A., and Huber, G. W. *J. Catal.* **270**, 110–124 (2010).
[38] Wildschut, J., Mahfud, F. H., Venderbosch, R. H., and Heeres, H. J. *Ind. Eng. Chem. Res.* **48**, 10324–10334 (2009).
[39] Laurent, E. and Delmon, B. *J. Catal.* **146**, 281–291 (1994).
[40] Zhang, S., Yan, Y., Li, T., and Ren, Z. *Bioresour. Technol.* **96**, 545–550 (2005).
[41] Donnis, B., Egeberg, R. G., Blom, P., and Knudsen, K. G. *Top. Catal.* **52**, 229–240 (2009).
[42] Knothe, G. *J. Am. Oil Chem. Soc.* **83**, 823–833 (2006).
[43] Koskinen, M., Sourander, M., and Nurminen, M. *Hydrocarb. Process.* **85**, 81–86 (2006).
[44] Snåre, M. and Murzin, D. Y. *Ind. Eng. Chem. Res.* **45**, 6875–6875 (2006).
[45] Mikkonen, S. *Hydrocarb. Process.* **87**, 63–66 (2008).
[46] Srivastava, A. and Prasad, R. *Renew. Sustain. Energy Rev.* **4**, 111–133 (2000).
[47] Huber, G. W., Iborra, S., and Corma, A. *Chem. Rev.* **106**, 4044–4098 (2006).
[48] Lotero, E., Liu, Y., Lopez, D. E., Suwannakarn, K., Bruce, D. A., and Goodwin, J. G. *Ind. Eng. Chem. Res.* **44**, 5353–5363 (2005).
[49] Jacobson, K., Gopinath, R., Meher, L. C., and Dalai, A. K. *Appl. Catal., B* **85**, 86–91 (2008).
[50] Casanave, D., Duplan, J.-L., and Freund, E. *Pure Appl. Chem.* **79**, 2071–2081 (2007).
[51] Sivasamy, A., Cheah, K., Fornasiero, P., Kemausuor, F., Zinoviev, S., and Miertus, S. *ChemSusChem* **2**, 278–300 (2009).
[52] Demirbas, A. *Prog. Energ. Combust.* **31**, 466–487 (2005).
[53] Verziu, M., El Haskouri, J., Beltran, D., Amoros, P., Macovei, D., Gheorghe, N. G., Teodorescu, C. M., Coman, S. M., and Parvulescu, V. I. *Top. Catal.* **53**, 763–772 (2010).
[54] Mo, X., Lotero, E., Lu, C., Liu, Y., and Goodwin, J. G. *Catal. Lett.* **123**, 1–6 (2008).
[55] Liu, X., He, H., Wang, Y., and Zhu, S. *Catal. Commun.* **8**, 1107–1111 (2007).
[56] Sree, R., Seshubabu, N., Saiprasad, P., and Lingaiah, N. *Fuel Process. Technol.* **90**, 152–157 (2009).
[57] Kozlowski, J. T., Aronson, M. T., and Davis, R. J. *Appl. Catal., B* **96**, 508–515 (2010).
[58] Caland, L. B., Santos, L. S. S., Moura, C. V. R., and Moura, E. M. *Catal. Lett.* **128**, 392–400 (2008).
[59] Bournay, L., Casanave, D., Delfort, B., Hillion, G., and Chodorge, J. *Catal. Today* **106**, 190–192 (2005).
[60] Pugnet, V., Maury, S., Coupard, V., Dandeu, a., Quoineaud, A.-A., Bonneau, J.-L., and Tichit, D. *Appl. Catal., A* **374**, 71–78 (2010).
[61] Russbueldt, B. M. and Hoelderich, W. F. *J. Catal.* **271**, 290–304 (2010).
[62] Kawashima, A., Matsubara, K., and Honda, K. *Bioresour. Technol.* **99**, 3439–3443 (2008).
[63] Shu, Q., Yang, B., Yuan, H., Qing, S., and Zhu, G. *Catal. Commun.* **8**, 2158–2164 (2007).
[64] Macario, A., Giordano, G., Onida, B., Cocina, D., Tagarelli, A., and Giuffrè, A. M. *Appl. Catal., A* **378**, 160–168 (2010).
[65] Li, E. and Rudolph, V. *Energy Fuels* **22**, 145–149 (2008).

[66] Georgogianni, K. G., Katsoulidis, A. P., Pomonis, P. J., and Kontominas, M. G. *Fuel Process. Technol.* **90**, 671–676 (2009).

[67] Georgogianni, K. G., Katsoulidis, A. K., Pomonis, P. J., Manos, G., and Kontominas, M. G. *Fuel Process. Technol.* **90**, 1016–1022 (2009).

[68] Zeng, H., Feng, Z., Deng, X., and Li, Y. *Fuel* **87**, 3071–3076 (2008).

[69] Cantrell, D., Gillie, L., Lee, A., and Wilson, K. *Appl. Catal., A* **287**, 183–190 (2005).

[70] Liu, Y., Lotero, E., Goodwin Jr, J. G., and Mo, X. *Appl. Catal., A* **331**, 138–148 (2007).

[71] Brito, A., Borges, M. E., Garín, M., and Hernández, A. *Energy Fuels* **23**, 2952–2958 (2009).

[72] Kim, M. J., Park, S. M., Chang, D. R., and Seo, G. *Fuel Processing Technology* **91**, 618–624 (2010).

[73] Chuayplod, P. and Trakarnpruk, W. *Ind. Eng. Chem. Res.* **48**, 4177–4183 (2009).

[74] Macala, G. S., Robertson, A. W., Johnson, C. L., Day, Z. B., Lewis, R. S., White, M. G., Iretskii, A. V., and Ford, P. C. *Catal. Lett.* **122**, 205–209 (2008).

[75] Li, E., Xu, Z. P., and Rudolph, V. *Appl. Catal., B* **88**, 42–49 (2009).

[76] Guerreiro, L., Pereira, P., Fonseca, I., Martin-Aranda, R., Ramos, A., Dias, J., Oliveira, R., and Vital, J. *Catal. Today* **156**, 191–197 (2010).

[77] Schuchardt, U. *J. Mol. Catal. A: Chem.* **99**, 65–70 (1995).

[78] Schuchardt, U. *J. Mol. Catal. A: Chem.* **109**, 37–44 (1996).

[79] Villa, A., Tessonnier, J.-P., Majoulet, O., Su, D. S., and Schlögl, R. *Chem. Commun.* , 4405–4407 (2009).

[80] Cerro-Alarcón, M., Corma, A., Iborra, S., Martínez, C., and Sabater, M. J. *Appl. Catal., A* **382**, 36–42 (2010).

[81] Cerro-Alarcón, M., Corma, A., Iborra, S., and Gómez, J. P. *Appl. Catal., A* **346**, 52–57 (2008).

[82] Kim, M.-Y., Seo, G., Kwon, O. Z., and Chang, D. R. *Chem. Commun.* , 3110–3112 (2009).

[83] Saravanamurugan, S., Han, D., Koo, J., and Park, S. *Catal. Commun.* **9**, 158–163 (2008).

[84] Savonnet, M., Aguado, S., Ravon, U., Bazer-Bachi, D., Lecocq, V., Bats, N., Pinel, C., and Farrusseng, D. *Green Chem.* **11**, 1729–1732 (2009).

[85] Liu, Y., Lotero, E., Goodwin Jr, J. G., and Lu, C. *J. Catal.* **246**, 428–433 (2007).

[86] Sunita, G., Devassy, B. M., Vinu, A., Sawant, D. P., Balasubramanian, V., and Halligudi, S. *Catal. Commun.* **9**, 696–702 (2008).

[87] Park, Y.-M., Lee, J. Y., Chung, S.-H., Park, I. S., Lee, S.-Y., Kim, D.-K., Lee, J.-S., and Lee, K.-Y. *Bioresour. Technol.* **101 Suppl**, S59–61 (2010).

[88] Komintarachat, C. and Chuepeng, S. *Ind. Eng. Chem. Res.* **48**, 9350–9353 (2009).

[89] Rao, K. N., Sridhar, A., Lee, A. F., Tavener, S. J., Young, N. A., and Wilson, K. *Green Chem.* **8**, 790–797 (2006).

[90] Ngaosuwan, K., Mo, X., Goodwin Jr, J. G., and Praserthdam, P. *Appl. Catal., A* **380**, 81–86 (2010).

[91] Kulkarni, M. G., Gopinath, R., Meher, L. C., and Dalai, A. K. *Green Chem.* **8**, 1056 (2006).

[92] Zhang, X., Li, J., Chen, Y., Wang, J., Feng, L., Wang, X., and Cao, F. *Energy Fuels* **23**, 4640–4646 (2009).

[93] Morin, P., Hamad, B., Sapaly, G., Carneiro Rocha, M., Pries de Oliveira, P., Gonzalez, W., Andrade Sales, E., and Essayem, N. *Appl. Catal., A* **330**, 69–76 (2007).

[94] Caetano, C., Fonseca, I., Ramos, A., Vital, J., and Castanheiro, J. *Catal. Commun.* **9**, 1996–1999 (2008).

[95] Oliveira, C. F., Dezaneti, L. M., A.C. Garcia, F., de Macedo, J. L., Dias, J. A., Dias, S. C., and Alvim, K. S. *Appl. Catal., A* **372**, 153–161 (2010).

[96] Cardoso, A. L., Augusti, R., and Silva, M. J. *J. Am. Oil Chem. Soc.* **85**, 555–560 (2008).

[97] Godói Silva, V. W., Laier, L. O., and Silva, M. J. D. *Catal. Lett.* **135**, 207–211 (2010).

[98] Xu, L., Wang, Y., Yang, X., Yu, X., Guo, Y., and Clark, J. H. *Green Chem.* **10**, 746–755 (2008).

[99] Srilatha, K., Lingaiah, N., Devi, B. P., Prasad, R., Venkateswar, S., and Prasad, P. S. *Appl. Catal., A* **365**, 28–33 (2009).

[100] Xu, L., Wang, Y., Yang, X., Hu, J., Li, W., and Guo, Y. *Green Chem.* **11**, 314–317 (2009).
[101] Alsalme, A., Kozhevnikova, E. F., and Kozhevnikov, I. V. *Appl. Catal., A* **349**, 170–176 (2008).
[102] Lam, M. K., Lee, K. T., and Mohamed, A. R. *Appl. Catal., B* **93**, 134–139 (2009).
[103] Suwannakarn, K., Lotero, E., Goodwin Jr, J. G., and Lu, C. *J. Catal.* **255**, 279–286 (2008).
[104] Hu, X., Zhou, Z., Sun, D., Wang, Y., and Zhang, Z. *Catal. Lett.* **133**, 90–96 (2009).
[105] Du, Y., Liu, S., Ji, Y., Zhang, Y., Wei, S., Liu, F., and Xiao, F.-S. *Catal. Lett.* **124**, 133–138 (2008).
[106] López, D. E., Goodwin Jr, J. G., Bruce, D. A., and Furuta, S. *Appl. Catal., A* **339**, 76–83 (2008).
[107] Rattanaphra, D., Harvey, A., and Srinophakun, P. *Top. Catal.* **53**, 773–782 (2010).
[108] Yu, G., Zhou, X., Li, C., Chen, L., and Wang, J. *Catal. Today* **148**, 169–173 (2009).
[109] de Almeida, R. M., Noda, L. K., Gonçalves, N. S., Meneghetti, S. M., and Meneghetti, M. R. *Appl. Catal., A* **347**, 100–105 (2008).
[110] Juan, J. C., Zhang, J., and Yarmo, M. A. *Appl. Catal., A* **332**, 209–215 (2007).
[111] Shi, W., He, B., Ding, J., Li, J., Yan, F., and Liang, X. *Bioresour. Technol.* **101**, 1501–5 (2010).
[112] Chung, K.-H., Chang, D.-R., and Park, B.-G. *Bioresour. Technol.* **99**, 7438–43 (2008).
[113] Carmo Jr, A., Desouza, L., Dacosta, C., Longo, E., Zamian, J., and da Rocha Filho, G. *Fuel* **88**, 461–468 (2009).
[114] Jiménez-Morales, I., Santamaría-González, J., Maireles-Torres, P., and Jiménez-López, A. *Appl. Catal., A* **379**, 61–68 (2010).
[115] Wu, S., Liu, P., Leng, Y., and Wang, J. *Catal. Lett.* **132**, 500–505 (2009).
[116] Dhainaut, J., Dacquin, J.-P., Lee, A. F., and Wilson, K. *Green Chem.* **12**, 296 (2010).
[117] Shibasaki-Kitakawa, N., Tsuji, T., Chida, K., Kubo, M., and Yonemoto, T. *Energy Fuels* **24**, 3634–3638 (2010).
[118] Bianchi, C. L., Boffito, D. C., Pirola, C., and Ragaini, V. *Catal. Lett.* **134**, 179–183 (2009).
[119] Özbay, N., Oktar, N., and Tapan, N. *Fuel* **87**, 1789–1798 (2008).
[120] Park, J.-Y., Kim, D.-K., and Lee, J.-S. *Bioresour. Technol.* **101**, S62–S65 (2010).
[121] Feng, Y., He, B., Cao, Y., Li, J., Liu, M., Yan, F., and Liang, X. *Bioresour. Technol.* **101**, 1518–1521 (2010).
[122] Caetano, C., Guerreiro, L., Fonseca, I., Ramos, A., Vital, J., and Castanheiro, J. *Appl. Catal., A* **359**, 41–46 (2009).
[123] Grossi, C. V., Jardim, E. D. O., Araújo, M. D., Lago, R. M., and Silva, M. J. D. *Fuel* **89**, 257–259 (2010).
[124] Soldi, R. A., Oliveira, A. R., Ramos, L. P., and César-Oliveira, M. A. F. *Appl. Catal., A* **361**, 42–48 (2009).
[125] Okayasu, T., Saito, K., Nishide, H., and Hearn, M. T. W. *Chem. Commun.* , 4708–4710 (2009).
[126] Melero, J. A., Bautista, L. F., Iglesias, J., Morales, G., Sánchez-Vázquez, R., and Suárez-Marcos, I. *Top. Catal.* **53**, 795–804 (2010).
[127] Zieba, A., Drelinkiewicz, A., Konyushenko, E., and Stejskal, J. *Appl. Catal., A* **383**, 169–181 (2010).
[128] Toda, M., Takagaki, A., Okamura, M., Kondo, J. N., Hayashi, S., Domen, K., and Hara, M. *Nature* **438**, 178 (2005).
[129] Suganuma, S., Nakajima, K., Kitano, M., Yamaguchi, D., Kato, H., Hayashi, S., and Hara, M. *J. Am. Chem. Soc.* **130**, 12787–12793 (2008).
[130] Hara, M. *Top. Catal.* **53**, 805–810 (2010).
[131] Dehkhoda, A. M., West, A. H., and Ellis, N. *Appl. Catal., A* **382**, 197–204 (2010).
[132] Takagaki, A., Toda, M., Okamura, M., Kondo, J. N., Hayashi, S., Domen, K., and Hara, M. *Catal. Today* **116**, 157–161 (2006).
[133] Lien, Y.-S., Hsieh, L.-S., and Wu, J. C. S. *Ind. Eng. Chem. Res.* **49**, 2118–2121 (2010).
[134] Nakajima, K., Okamura, M., Kondo, J. N., Domen, K., Tatsumi, T., Hayashi, S., and Hara, M. *Chem. Mater.* **21**, 186–193 (2009).
[135] Peng, L., Philippaerts, A., Ke, X., Van Noyen, J., De Clippel, F., Van Tendeloo, G., Jacobs, P. A., and Sels,

B. F. *Catal. Today* **150**, 140–146 (2010).
[136] Wu, Q., Chen, H., Han, M., Wang, D., and Wang, J. *Ind. Eng. Chem. Res.* **46**, 7955–7960 (2007).
[137] Lapis, A., de Oliveira, L., Neto, B., and Dupont, J. *ChemSusChem* **1**, 759–762 (2008).
[138] Ha, S. H., Lan, M. N., and Koo, Y.-M. *Enzyme Microb. Technol.* **47**, 6–10 (2010).
[139] DaSilveira Neto, B., Alves, M., Lapis, A., Nachtigall, F., Eberlin, M., Dupont, J., and Suarez, P. *J. Catal.* **249**, 154–161 (2007).
[140] Han, M., Yi, W., Wu, Q., Liu, Y., Hong, Y., and Wang, D. *Bioresour. Technol.* **100**, 2308–2310 (2009).
[141] Li, K.-X., Chen, L., Yan, Z.-C., and Wang, H.-L. *Catal. Lett.* **139**, 151–156 (2010).
[142] Liang, X. and Yang, J. *Green Chem.* **12**, 201–204 (2010).
[143] Nassreddine, S., Karout, A., Lorraine Christ, M., and Pierre, A. C. *Appl. Catal., A* **344**, 70–77 (2008).
[144] Sim, J. H., Kamaruddin, A. H., and Bhatia, S. *J. Am. Oil Chem. Soc.* **87**, 1027–1034 (2010).
[145] Shakeri, M. and Kawakami, K. *Catal. Commun.* **10**, 165–168 (2008).
[146] Dizge, N., Aydiner, C., Imer, D. Y., Bayramoglu, M., Tanriseven, A., and Keskinler, B. *Bioresour. Technol.* **100**, 1983–1991 (2009).
[147] Keng, P. S., Basri, M., Ariff, A. B., Abdul Rahman, M. B., Abdul Rahman, R. N. Z., and Salleh, A. B. *Bioresour. Technol.* **99**, 6097–6104 (2008).
[148] Fu, B. and Vasudevan, P. T. *Energy Fuels* **23**, 4105–4111 (2009).
[149] Xiao, M., Mathew, S., and Obbard, J. P. *GCB Bioenergy* **1**, 115–125 (2009).
[150] Hernández-Martín, E. and Otero, C. *Bioresour. Technol.* **99**, 277–286 (2008).
[151] Warabi, Y. *Bioresour. Technol.* **91**, 283–287 (2004).
[152] Yin, J., Xiao, M., and Song, J. *Energy Convers. Manage.* **49**, 908–912 (2008).
[153] Hawash, S., Kamal, N., Zaher, F., Kenawi, O., and Diwani, G. *Fuel* **88**, 579–582 (2009).
[154] Hegel, P., Mabe, G., Pereda, S., and Brignole, E. A. *Ind. Eng. Chem. Res.* **46**, 6360–6365 (2007).
[155] Saka, S., Isayama, Y., Ilham, Z., and Jiayu, X. *Fuel* **89**, 1442–1446 (2010).
[156] Christoph, R., Schmidt, B., Steinberner, U., Dilla, W., and Karinen, R. *"Glycerol". Ullmann's Encyclopedia of Industrial Chemistry*. Wiley-VCH Verlag GmbH & Co, 7th edition (2006).
[157] Zhou, C.-H. C., Beltramini, J. N., Fan, Y.-X., and Lu, G. Q. M. *Chem. Soc. Rev.* **37**, 527–549 (2008).
[158] Pagliaro, M., Ciriminna, R., Kimura, H., Rossi, M., and Della Pina, C. *Angew. Chem., Int. Ed.* **46**, 4434–4440 (2007).
[159] Johnson, D. and Taconi, K. *Environ. Prog.* **26**, 338–348 (2007).
[160] Ohara, T., Sato, T., Shimizu, N., Prescher, G., Schwind, H., Weiberg, O., and Marten, K. *"Acrylic acid and derivatives". Ullmann's Encyclopedia of Industrial Chemistry*. Wiley-CVH Verlag GmbH & Co, 7th edition (2006).
[161] Corma, A., Huber, G. W., Sauvanaud, L., and O'Connor, P. *J. Catal.* **257**, 163–171 (2008).
[162] Kim, Y. T., Jung, K.-D., and Park, E. D. *Microporous Mesoporous Mater.* **131**, 28–36 (2010).
[163] Jia, C.-J., Liu, Y., Schmidt, W., Lu, A.-H., and Schüth, F. *J. Catal.* **269**, 71–79 (2010).
[164] Suprun, W., Lutecki, M., Haber, T., and Papp, H. *J. Mol. Catal. A: Chem.* **309**, 71–78 (2009).
[165] Chai, S., Wang, H., Liang, Y., and Xu, B. *J. Catal.* **250**, 342–349 (2007).
[166] Tsukuda, E., Sato, S., Takahashi, R., and Sodesawa, T. *Catal. Commun.* **8**, 1349–1353 (2007).
[167] Behr, A., Eilting, J., Irawadi, K., Leschinski, J., and Lindner, F. *Green Chem.* **10**, 13–30 (2008).
[168] Chiu, C., Dasari, M., Suppes, G., and Sutterlin, W. *AIChE J.* **52**, 3543–3548 (2006).
[169] Schmidt, S. R., Tanielyan, S. K., Marin, N., Alvez, G., and Augustine, R. L. *Top. Catal.* **53**, 1214–1216 (2010).
[170] Chaminand, J., Djakovitch, L., Gallezot, P., Marion, P., Pinel, C., and Rosier, C. *Green Chem.* **6**, 359–361 (2004).
[171] Kusunoki, Y., Miyazawa, T., Kunimori, K., and Tomishige, K. *Catal. Commun.* **6**, 645–649 (2005).

[172] Miyazawa, T., Kusunoki, Y., Kunimori, K., and Tomishige, K. *J. Catal.* **240**, 213–221 (2006).
[173] Miyazawa, T., Koso, S., Kunimori, K., and Tomishige, K. *Appl. Catal., A* **318**, 244–251 (2007).
[174] Nakagawa, Y., Shinmi, Y., Koso, S., and Tomishige, K. *J. Catal.* **272**, 191–194 (2010).
[175] Qin, L.-Z., Song, M.-J., and Chen, C.-L. *Green Chem.* **12**, 1466–1472 (2010).
[176] Carrettin, S., McMorn, P., Johnston, P., Griffin, K., and Hutchings, G. J. *Chem. Commun.* , 696–697 (2002).
[177] Villa, A., Veith, G. M., and Prati, L. *Angew. Chem., Int. Ed.* **49**, 4499–502 (2010).
[178] Kyriacou, D. and Tougas, T. P. *J. Org. Chem.* **52**, 2318–2319 (1987).
[179] Garcia, R., Besson, M., and Gallezot, P. *Appl. Catal., A* **127**, 165–176 (1995).
[180] Gallezot, P. *Catal. Today* **37**, 405–418 (1997).
[181] Ciriminna, R., Palmisano, G., Pina, C. D., Rossi, M., and Pagliaro, M. *Tetrahedron Lett.* **47**, 6993–6995 (2006).
[182] Taarning, E., Madsen, A. T., Marchetti, J. M., Egeblad, K., and Christensen, C. H. *Green Chem.* **10**, 408–414 (2008).
[183] Ramírez-López, C. and Ochoa-Gómez, J. *Ind. Eng. Chem. Res.* **49**, 6270–6278 (2010).
[184] Lux, S., Stehring, P., and Siebenhofer, M. *Sep. Sci. Technol.* **45**, 1921–1927 (2010).
[185] Taarning, E., Saravanamurugan, S., Spangsberg Holm, M., Xiong, J., West, R. M., and Christensen, C. H. *ChemSusChem* **2**, 625–627 (2009).
[186] West, R. M., Holm, M. S., Saravanamurugan, S., Xiong, J., Beversdorf, Z., Taarning, E., and Christensen, C. H. *J. Catal.* **269**, 122–130 (2010).
[187] Karinen, R. and Krause, A. *Appl. Catal., A* **306**, 128–133 (2006).
[188] Klepácová, K., Mravec, D., Kaszonyi, A., and Bajus, M. *Appl. Catal., A* **328**, 1–13 (2007).
[189] Deutsch, J., Martin, A., and Lieske, H. *J. Catal.* **245**, 428–435 (2007).
[190] Fabbri, D., Bevoni, V., Notari, M., and Rivetti, F. *Fuel* **86**, 690–697 (2007).
[191] Clacens, J. *Appl. Catal., A* **227**, 181–190 (2002).
[192] Kunkes, E., Simonetti, D., Dumesic, J., Pyrz, W., Murillo, L., Chen, J., and Buttrey, D. *J. Catal.* **260**, 164–177 (2008).
[193] Simonetti, D., Kunkes, E., and Dumesic, J. *J. Catal.* **247**, 298–306 (2007).
[194] Dauenhauer, P., Salge, J., and Schmidt, L. *J. Catal.* **244**, 238–247 (2006).
[195] Cheng, C. K., Foo, S. Y., and Adesina, A. A. *Catal. Commun.* **12**, 292–298 (2010).
[196] Sharma, P. O., Swami, S., Goud, S., and Abraham, M. A. *Environ. Prog. Sustainable Energy* **27**, 22–29 (2008).
[197] Simonetti, D. A., Rass-Hansen, J., Kunkes, E. L., Soares, R. R., and Dumesic, J. A. *Green Chem.* **9**, 1073–1083 (2007).
[198] Knothe, G. *Prog. Energ. Combust.* **36**, 364–373 (2010).
[199] Kubička, D. and Kaluža, L. *Appl. Catal., A* **372**, 199–208 (2010).
[200] Šimáček, P., Kubička, D., Šebor, G., and Pospíšil, M. *Fuel* **88**, 456–460 (2009).
[201] Kubička, D., Bejblová, M., and Vlk, J. *Top. Catal.* **53**, 168–178 (2010).
[202] Kubička, D., Šimáček, P., and Žilková, N. *Top. Catal.* **52**, 161–168 (2009).
[203] Kubička, D., Šimáček, P., Kolena, J., Lederer, J., and Šebor, G. In *ICP2007 proceedings - 43rd International Petroleum Conference*, pp. 1–7 (, Bratislava, Slovak Republic, 2007).
[204] Şenol, O., Viljava, T.-R., and Krause, A. O. I. *Appl. Catal., A* **326**, 236–244 (2007).
[205] Ryymin, E.-M., Honkela, M. L., Viljava, T.-R., and Krause, A. O. I. *Appl. Catal., A* **358**, 42–48 (2009).
[206] Şenol, O. I., Ryymin, E. M., Viljava, T.-R., and Krause, A. O. I. *J. Mol. Catal. A: Chem.* **268**, 1–8 (2007).
[207] Snåre, M., Kubičková, I., Mäki-Arvela, P., Eränen, K., Wärnå, J., and Murzin, D. Y. *Chem. Eng. J.* **134**, 29–34 (2007).

[208] Mäki-Arvela, P., Holmbom, B., Salmi, T., and Murzin, D. Y. *Catal. Rev. - Sci. Eng.* **49**, 197–340 (2007).
[209] Morgan, T., Grubb, D., Santillan-Jimenez, E., and Crocker, M. *Top. Catal.* **53**, 820–829 (2010).
[210] Do, P. T., Chiappero, M., Lobban, L. L., and Resasco, D. E. *Catal. Lett.* **130**, 9–18 (2009).
[211] Lestari, S., Mäki-Arvela, P., Eränen, K., Beltramini, J., Max Lu, G. Q., and Murzin, D. Y. *Catal. Lett.* **134**, 250–257 (2009).
[212] Ping, E. W., Wallace, R., Pierson, J., Fuller, T. F., and Jones, C. W. *Microporous Mesoporous Mater.* **132**, 174–180 (2010).
[213] Hancsók, J., Krár, M., Magyar, S., Boda, L., Holló, A., and Kalló, D. *Microporous Mesoporous Mater.* **101**, 148–152 (2007).
[214] Lestari, S., Mäki-Arvela, P., Beltramini, J., Lu, G. Q. M., and Murzin, D. Y. *ChemSusChem* **2**, 1109–19 (2009).
[215] Danuthai, T., Jongpatiwut, S., Rirksomboon, T., Osuwan, S., and Resasco, D. E. *Appl. Catal., A* **361**, 99–105 (2009).
[216] Sooknoi, T., Danuthai, T., Lobban, L. L., Mallinson, R., and Resasco, D. E. *J. Catal.* **258**, 199–209 (2008).
[217] Sang, O. Y. *Energy Sources* **25**, 859–869 (2003).
[218] Quirino, R. L., Tavares, A. P., Peres, A. C., Rubim, J. C., and Suarez, P. A. Z. *J. Am. Oil Chem. Soc.* **86**, 167–172 (2008).
[219] Lima, D. G., Soares, V. C., Riberio, E. B., Carvalho, D. A., Cardoso, E. C. V., Rassi, F. C., Mundim, K. C., Rubim, J. C., and Suarez, P. A. Z. *J. Anal. Appl. Pyrolysis* **71**, 987–996 (2004).
[220] Lange, J.-P. *Biofuels, Bioprod. Biorefin.* **1**, 39–48 (2007).
[221] Srokol, Z. W. and Rothenberg, G. *Top. Catal.* **53**, 1258–1263 (2010).
[222] Hoekman, S. K., Broch, A., and Robbins, C. *Energy Fuels* (2011).
[223] Knežević, D., van Swaaij, W., and Kersten, S. *Ind. Eng. Chem. Res.* **49**, 104–112 (2010).
[224] Karagöz, S., Bhaskar, T., Muto, A., and Sakata, Y. *Bioresour. Technol.* **97**, 90–8 (2006).
[225] Bhaskar, T., Sera, A., Muto, A., and Sakata, Y. *Fuel* **87**, 2236–2242 (2008).
[226] Becker, J., Toft, L. L., Aarup, D. F., Villadsen, S. R., Glasius, M., Iversen, S. B., and Iversen, B. B. *Energy Fuels* **24**, 2737–2746 (2010).
[227] Hammerschmidt, A., Boukis, N., Hauer, E., Galla, U., Dinjus, E., Hitzmann, B., Larsen, T., and Nygaard, S. D. *Fuel* **90**, 555–562 (2011).
[228] Mentzel, U. V. and Holm, M. S. *Appl. Catal., A* **396**, 59–67 (2011).
[229] Barth, T. and Kleinert, M. *Chem. Eng. Technol.* **31**, 773–781 (2008).
[230] Kleinert, M. and Barth, T. *Chem. Eng. Technol.* **31**, 736–745 (2008).
[231] Elliott, D. C., Hart, T. R., Neuenschwander, G. G., Rotness, L. J., and Zacher, A. H. *Environ. Prog. Sustainable Energy* **28**, 441–449 (2009).
[232] French, R. J., Hrdlicka, J., and Baldwin, R. *Environ. Prog. Sustainable Energy* **29**, 142–150 (2010).
[233] Bridgwater, A. V., Czernik, S., and Piskorz, J. *The Status of Biomass Fast Pyrolysis*, chapter 1, 1–22. CPL Press, Birmingham, United Kingdom (2002).
[234] Aho, A., Kumar, N., Lashkul, A., Eränen, K., Ziolek, M., Decyk, P., Salmi, T., Holmbom, B., Hupa, M., and Murzin, D. Y. *Fuel* **89**, 1992–2000 (2010).
[235] Aho, A., Kumar, N., Eränen, K., Salmi, T., Hupa, M., and Murzin, D. Y. *Fuel* **87**, 2493–2501 (2008).
[236] Valle, B., Gayubo, A. G., Alonso, A., Aguayo, A. T., and Bilbao, J. *Appl. Catal., B* **100**, 318–327 (2010).
[237] de Miguel Mercader, F., Groeneveld, M., Kersten, S., Way, N., Schaverien, C., and Hogendoorn, J. *Appl. Catal., B* **96**, 57–66 (2010).
[238] Mullen, C. A. and Boateng, A. A. *Fuel Processing Technology* **91**, 1446–1458 (2010).
[239] Carlson, T. R., Tompsett, G. A., Conner, W. C., and Huber, G. W. *Top. Catal.* **52**, 241–252 (2009).
[240] Ferrari, M., Maggi, R., Delmon, B., and Grange, P. *J. Catal.* **198**, 47–55 (2001).

[241] Ferrari, M., Bosmans, S., Maggi, R., Delmon, B., and Grange, P. *Catal. Today* **65**, 257–264 (2001).
[242] Ferrari, M., Delmon, B., and Grange, P. *Carbon* **40**, 497–511 (2002).
[243] Ferrari, M., Delmon, B., and Grange, P. *Microporous Mesoporous Mater.* **56**, 279–290 (2002).
[244] Laurent, E. and Delmon, B. *Appl. Catal., A* **109**, 77–96 (1994).
[245] Su-Ping, Z. *Energy Sources* **25**, 57–65 (2003).
[246] Gutierrez, A., Domine, M., and Solantausta, Y. In *15th European Biomass Conference & Exhibition*, pp. 1–5 (, Berlin, Germany, 2007).
[247] Şenol, O., Ryymin, E.-M., Viljava, T.-R., and Krause, A. *J. Mol. Catal. A: Chem.* **277**, 107–112 (2007).
[248] Dilcio Rocha, J. *Org. Geochem.* **30**, 1527–1534 (1999).
[249] Oasmaa, A., Kuoppala, E., Ardiyanti, A., Venderbosch, R. H., and Heeres, H. J. *Energy Fuels* **24**, 5264–5272 (2010).
[250] Wildschut, J., Melián-Cabrera, I., and Heeres, H. *Appl. Catal., B* **99**, 298–306 (2010).
[251] Huber, G. W., Cortright, R. D., and Dumesic, J. A. *Angew. Chem., Int. Ed.* **43**, 1549–1551 (2004).
[252] Kunkes, E. L., Simonetti, D. A., West, R. M., Serrano-Ruiz, J. C., Gärtner, C. A., and Dumesic, J. A. *Science* **322**, 417–421 (2008).
[253] Li, N. and Huber, G. W. *J. Catal.* **270**, 48–59 (2010).
[254] West, R. M., Kunkes, E. L., Simonetti, D. A., and Dumesic, J. A. *Catal. Today* **147**, 115–125 (2009).
[255] Román-Leshkov, Y., Barrett, C. J., Liu, Z. Y., and Dumesic, J. A. *Nature* **447**, 982–985 (2007).
[256] Chheda, J. and Dumesic, J. *Catal. Today* **123**, 59–70 (2007).
[257] Bond, J., Alonso, D., Wang, D., West, R., and Dumesic, J. *Science* **327**, 1110–1114 (2010).
[258] Gärtner, C. A., Serrano-Ruiz, J. C., Braden, D. J., and Dumesic, J. A. *J. Catal.* **266**, 71–78 (2009).
[259] Gürbüz, E. I., Kunkes, E. L., and Dumesic, J. A. *Green Chem.* **12**, 223–227 (2010).
[260] Gärtner, C. A., Serrano-Ruiz, J. C., Braden, D. J., and Dumesic, J. A. *ChemSusChem* **2**, 1121–1124 (2009).
[261] Gürbüz, E. I., Kunkes, E. L., and Dumesic, J. A. *Appl. Catal., B* **94**, 134–141 (2010).
[262] Serrano-Ruiz, J. C., Braden, D. J., West, R. M., and Dumesic, J. A. *Appl. Catal., B* **100**, 184–189 (2010).
[263] Kintisch, E. *Science* **320**, 306–308 (2008).
[264] Digman, B., Joo, H., and Kim, D. *Environ. Prog. Sustainable Energy* **28**, 47–51 (2009).
[265] Bridgwater, T. *J. Sci. Food Agric.* **86**, 1755–1768 (2006).
[266] Henrich, E., Dahmen, N., and Dinjus, E. *Biofuels, Bioprod. Biorefin.* **3**, 28–41 (2009).
[267] McKendry, P. *Bioresour. Technol.* **83**, 55–63 (2002).
[268] Moilanen, A., Nasrullah, M., and Kurkela, E. *Environ. Prog. Sustainable Energy* **28**, 355–359 (2009).
[269] Gomez-Barea, A., Vilches, L., Leiva, C., Campoy, M., and Fernandez-Pereira, C. *Chem. Eng. J.* **146**, 227–236 (2009).
[270] Rass-Hansen, J., Christensen, C. H., Sehested, J., Helveg, S., Rostrup-Nielsen, J. R., and Dahl, S. *Green Chem.* **9**, 1016–1021 (2007).
[271] Matsumura, Y., Minowa, T., Potic, B., Kersten, S., Prins, W., Vanswaaij, W., Vandebeld, B., Elliott, D., Neuenschwander, G., and Kruse, A. *Biomass Bioenerg.* **29**, 269–292 (2005).
[272] Campoy, M., Gómez-Barea, A., Villanueva, A. L., and Ollero, P. *Ind. Eng. Chem. Res.* **47**, 5957–5965 (2008).
[273] Wolfesberger, U., Aigner, I., and Hofbauer, H. *Environ. Prog. Sustainable Energy* **28**, 372–379 (2009).
[274] Zwart, R., Van Der Drift, A., Bos, A., Visser, H., Cieplik, M., and Könemann, H. *Environ. Prog. Sustainable Energy* **28**, 324–335 (2009).
[275] Pope, C. J., Marrone, P. A., and Yeh, B. V. *Environ. Prog. Sustainable Energy* **29**, 151–162 (2010).
[276] Torres, W., Pansare, S. S., and Goodwin Jr, J. G. *Catal. Rev. - Sci. Eng.* **49**, 407–456 (2007).
[277] Rönkkönen, H., Klemkaitė, K., Khinsky, A., Baltušnikas, A., Simell, P., Reinikainen, M., Krause, O., and Niemelä, M. *Fuel* **90**, 1076–1089 (2011).

[278] Stranges, A. *Fischer Tropsch Archive (http://www.fischer-tropsch.org). Accessed June 7th, 2011.*
[279] Davis, B. H. *Ind. Eng. Chem. Res.* **46**, 8938–8945 (2007).
[280] Kaneko, T., Derbyshire, F., Makino, E., Gray, D., and Tamura, M. (2005).
[281] Patzlaff, J., Liu, Y., Graffmann, C., and Gaube, J. *Appl. Catal., A* **186**, 109–119 (1999).
[282] Gamba, S., Pellegrini, L. A., Calemma, V., and Gambaro, C. *Catal. Today* **156**, 58–64 (2010).
[283] Tavasoli, A., Trépanier, M., Dalai, A. K., and Abatzoglou, N. *J. Chem. Eng. Data* **55**, 2757–2763 (2010).
[284] Tavasoli, A., Trépanier, M., Malek Abbaslou, R. M., Dalai, A. K., and Abatzoglou, N. *Fuel Process. Technol.* **90**, 1486–1494 (2009).
[285] Bezemer, G. L., Bitter, J. H., Kuipers, H. P. C. E., Oosterbeek, H., Holewijn, J. E., Xu, X., Kapteijn, F., van Dillen, A. J., and de Jong, K. P. *J. Am. Chem. Soc.* **128**, 3956–3964 (2006).
[286] Chen, W., Fan, Z., Pan, X., and Bao, X. *J. Am. Chem. Soc.* **130**, 9414–9419 (2008).
[287] Liu, S., Gujar, A. C., Thomas, P., Toghiani, H., and White, M. G. *Appl. Catal., A* **357**, 18–25 (2009).
[288] Trepanier, M., Tavasoli, A., Dalai, A., and Abatzoglou, N. *Appl. Catal., A* **353**, 193–202 (2009).
[289] Ma, W., Kugler, E. L., Wright, J., and Dadyburjor, D. B. *Energy Fuels* **20**, 2299–2307 (2006).
[290] Herranz, T., Rojas, S., Perezalonso, F., Ojeda, M., Terreros, P., and Fierro, J. *J. Catal.* **243**, 199–211 (2006).
[291] Blanchard, J., Abatzoglou, N., Eslahpazir-Esfandabadi, R., and Gitzhofer, F. *Ind. Eng. Chem. Res.* **49**, 6948–6955 (2010).
[292] Christensen, J. M., Mortensen, P., Trane, R., Jensen, P. A., and Jensen, A. D. *Appl. Catal., A* **366**, 29–43 (2009).
[293] Durham, E., Zhang, S., and Roberts, C. *Appl. Catal., A* **386**, 65–73 (2010).
[294] Mentzel, U. V., Shunmugavel, S., Hruby, S. L., Christensen, C. H., and Holm, M. S. *J. Am. Chem. Soc.* **131**, 17009–17013 (2009).
[295] Dabelstein, W., Reglitzky, A., Schütze, A., and Reders, K. (2007).
[296] Knothe, G., Matheaus, A. C., and Ryan III, T. W. *Fuel* **82**, 971–975 (2003).
[297] Dinh, L., Guo, Y., and Mannan, M. *Environ. Prog. Sustainable Energy* **28**, 38–46 (2009).
[298] Vasudevan, P. and Briggs, M. *J. Ind. Microbiol. Biotechnol.* **35**, 421–430 (2008).
[299] de Paula Gomes, M. S. and Muylaert de Araújo, M. S. *Renew. Sustain. Energy Rev.* **13**, 2201–2204 (2009).
[300] Granda, C. B., Zhu, L., and Holtzapple, M. T. *Environ. Prog. Sustainable Energy* **26**, 233–250 (2007).
[301] Willems, P. A. *Science* **325**, 707–8 (2009).
[302] Sharma, Y. C., Singh, B., and Korstad, J. *Biofuels, Bioprod. Biorefin.* **5**, 69–92 (2011).
[303] Refaat, A. *International Journal of Environment Science and Technology* **8**, 203–221 (2010).
[304] Olivier-Bourbigou, H., Magna, L., and Morvan, D. *Appl. Catal., A* **373**, 1–56 (2010).
[305] Guo, F., Fang, Z., Tian, X.-F., Long, Y.-D., and Jiang, L.-Q. *Bioresour. Technol.* **102**, 6469–6472 (2011).
[306] Liang, X., Gong, G., Wu, H., and Yang, J. *Fuel* **88**, 613–616 (2009).
[307] Zhang, L., Xian, M., He, Y., Li, L., Yang, J., Yu, S., and Xu, X. *Bioresour. Technol.* **100**, 4368–4373 (2009).
[308] Fang, D., Yang, J., and Jiao, C. *ACS Catal.* **1**, 42–47 (2011).
[309] Ghiaci, M., Aghabarari, B., Habibollahi, S., and Gil, A. *Bioresour. Technol.* **102**, 1200–1204 (2011).
[310] Okayasu, T., Saito, K., Nishide, H., and Hearn, M. T. W. *Green Chem.* **12**, 1981–1989 (2010).
[311] Melero, J. A., Iglesias, J., and Morales, G. *Green Chem.* **11**, 1285 (2009).
[312] Hara, M. *ChemSusChem* **2**, 129–135 (2009).
[313] Okamura, M., Takagaki, A., Toda, M., Kondo, J. N., Domen, K., Tatsumi, T., Hara, M., and Hayashi, S. *Chem. Mater.* **18**, 3039–3045 (2006).
[314] Kitano, M., Arai, K., Kodama, A., Kousaka, T., Nakajima, K., Hayashi, S., and Hara, M. *Catal. Lett.* **131**, 242–249 (2009).
[315] Veldurthy, B., Clacens, J. M., and Figueras, F. *Adv. Synth. Catal.* **347**, 767–771 (2005).
[316] Desmartin-Chomel, A., Hamad, B., Palomeque, J., Essayem, N., Bergeret, G., and Figueras, F. *Catal.*

Today **152**, 110–114 (2010).
[317] Baig, A. and Ng, F. T. T. *Energy Fuels* **24**, 4712–4720 (2010).
[318] Garcia, C. M., Teixeira, S., Marciniuk, L. L., and Schuchardt, U. *Bioresour. Technol.* **99**, 6608–6613 (2008).
[319] Peter, S. and Weidner, E. *Eur. J. Lipid Sci. Technol.* **109**, 11–16 (2007).
[320] Zhang, L., Guo, W., Liu, D., Yao, J., Ji, L., Xu, N., and Min, E. *Energy Fuels* **22**, 1353–1357 (2008).
[321] Immer, J. G., Kelly, M. J., and Lamb, H. H. *Appl. Catal., A* **375**, 134–139 (2010).
[322] Berenblyum, A. S., Danyushevsky, V. Y., Katsman, E. A., Podoplelova, T. A., and Flid, V. R. *Pet. Chem.* **50**, 305–311 (2010).
[323] Bulushev, D. A., Beloshapkin, S., and Ross, J. R. *Catal. Today* **154**, 7–12 (2010).
[324] Snåre, M., Kubickova, I., Mäki-Arvela, P., Chichova, D., Eränen, K., and Murzin, D. Y. *Fuel* **87**, 933–945 (2008).
[325] Pinna, F. *Catal. Today* **41**, 129–137 (1998).
[326] Dulaurent, O., Chandes, K., Bouly, C., and Bianchi, D. *J. Catal.* **188**, 237–251 (1999).
[327] Andersson, M., Bligaard, T., Kustov, A., Larsen, K., Greeley, J., Johannessen, T., Christensen, C., and Nørskov, J. K. *J. Catal.* **239**, 501–506 (2006).
[328] Surovikin, V. F., Plaxin, G. V., Semikolenov, V. A., Likholobov, V. A., and Tiunova, I. J. *Porous carbonaceous material*. United States Patent No. US4978649 (1990).
[329] Simonov, P. A., Troitskii, S. Y., and Likholobov, V. A. *Kinet. Catal.* **41**, 255–269 (2000).
[330] Bernas, H., Eränen, K., Simakova, I., Leino, A.-R., Kordás, K., Myllyoja, J., Mäki-Arvela, P., Salmi, T., and Murzin, D. Y. *Fuel* **89**, 2033–2039 (2010).
[331] Immer, J. G. and Lamb, H. H. *Energy Fuels* **24**, 5291–5299 (2010).
[332] Boda, L., Onyestyák, G., Solt, H., Lónyi, F., Valyon, J., and Thernesz, A. *Appl. Catal., A* **374**, 158–169 (2010).

Chapter 6

6

Included Publications

Step changes and deactivation behaviour in the continuous decarboxylation of stearic acid

Anders Theilgaard Madsen[a,b], Bartosz Rozmysłowicz[b], Irina L. Simakova[b,c], Teuvo Kilpiö[b], Anne-Riikka Leino[d], Krisztián Kordás[d], Kari Eränen[b], Päivi Mäki-Arvela[b], Dmitry Yu. Murzin[b,]*

[a]: *Centre for Catalysis and Sustainable Chemistry, Technical University of Denmark, DK-2800 Kgs. Lyngby, Denmark*

[b]: *Process Chemistry Center, Åbo Akademi University, Biskopsgatan 8, FI-20500 Turku/Åbo, Finland*

[c] :*Boreskov Institute of Catalysis. Novosibirsk, Russia*

[d]: *Laboratory of Microelectronics and Materials Physics, University of Oulu, PL 4500, 90014 Oulu*

* To whom correspondence should be addressed: dmurzin@abo.fi

Abstract

Deoxygenation of diluted and concentrated stearic acid over 2% Pd/C beads was performed in a continuous reactor at 300°C and 20 bar pressure of Ar or 5% H_2/Ar. Stable operation was obtained in 5% H_2 atmosphere, with 95% conversion of 10 mol% diluted stearic acid in dodecane and 12% conversion of pure stearic acid. Deactivation took place in H_2-deficient gas atmosphere, probably due to formation of unsaturated products and coking in the pore system. Transient experiments with step changes were performed: 1 h was required for the step change to be visible in liquid sampling, while steady-states were achieved after totally 2.5 - 3 h. Post-reaction analysis of the spent catalyst revealed that a deactivation profile was formed downwards over the catalyst bed.

1. Introduction

The diminishing availability of cheap fossil fuels and their impact on the global environment have led the struggle towards higher fuel efficiency and development of alternative fuels for road vehicles. The EU had mandated that at least 5.75% of the energy content in diesel and petrol should be based on biofuels by the end of 2010, rising to 10% in 2020.[1] Lately, in their 2010 report, the International Energy Agency (IEA) described the urgent need for the swift transition towards more sustainable and environmentally sound energy and fuel production.[2]

Fats and oils are generally the types of biomass resource that, from a chemical point of view, most closely resembles diesel oil and is easiest to upgrade into a diesel fuel.[3,4] Diesel fuel can be made from fats and oils via (trans-)esterification with methanol to form fatty acid methyl esters (FAME), which have previously been extensively investigated. Another way could be through the deoxygenation of fats and oils potentially using hydrogen (so-called HDO, hydrodeoxygenation) to form straight-chain alkanes, which is advantageous under some conditions.[5]

The HDO process was first introduced on an industrial scale in 2007 by Neste Oil in Porvoo, Finland based primarily on palm oil,[6,7] and other companies are following the same route. The reports on understanding the deoxygenation processes have however not been extensive to this date. Generally, three types of catalysts have been described for deoxygenation of fatty feedstocks, namely supported sulphided metals catalysts, supported metallic catalysts, and porous acidic or basic catalysts. Deoxygenation has been described to occur via three different routes: decarboxylation, decarbonylation or full reduction with hydrogen (reactions (1)-(3)), in all cases yielding n-alkanes upon saturation with hydrogen. The primary reaction route and the side reactions taking place are strongly dependent on the catalyst used – especially reactions of hydrogen and product gases may interfere and prompt water-gas-shift (WGS) or methanation (reactions (4)-(6)).

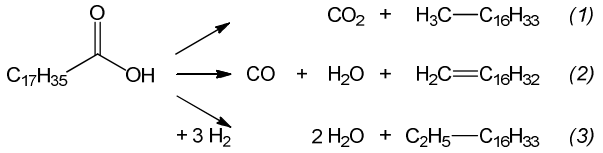

$H_2O + CO \rightleftharpoons CO_2 + H_2$ (4)

$3\,H_2 + CO \rightarrow CH_4 + H_2O$ (5)

$4\,H_2 + CO_2 \rightarrow CH_4 + 2\,H_2O$ (6)

A number of reports have appeared on catalytic cracking-type reactions of various vegetable oils without added hydrogen. These are usually performed at 400-500°C without H_2 in the reaction media.[8-13] FAME have also been used as feedstocks.[14, 15] Porous Brønsted acidic materials tested include H-MCM-41 or zeolites H-ZSM-5 or H-Y.[8-11,15] Porous basic materials tested comprise zeolite (Cs,Na)-X, hydrotalcites or porous SnO-ZnO-Al_2O_3.[12-14] Generally, the procedures result in a mixture of hydrocarbons due to cracking reactions, as well as light gases and coke – petrol can often be the product of the highest yield. Saponification of resulting free fatty acids can also occur over some basic catalysts like MgO.[12, 14]

The sulphided $NiMo/Al_2O_3$ and $CoMo/Al_2O_3$ at 250°C under 15 or 75 bars of H_2 and various sulphidation conditions were studied as HDO catalysts. The

conversion of heptanoic alcohol, acid and esters and the ratio between C_6 and C_7 hydrocarbons varied depending on the catalysts type and added sulphur compounds in the feed. Unsulphided $NiMo/Al_2O_3$ or $CoMo/Al_2O_3$ catalysts were neither very active nor selective towards linear hydrocarbons, however, the sulphided catalysts had high activities and yielded higher ratios of C_6/C_7 hydrocarbon products.[16, 17] The conversion of rapeseed oil over various sulphided $NiMo/Al_2O_3$ have been investigated: employing temperatures in the range of 260-360°C and pressures of 70-150 bar H_2 . The effects of pressure, temperature, sulphidation conditions, and Ni and Mo composition of the catalyst were studied.[18-20] Co-hydrocracking of 5% rapeseed oil in vacuum gas oil over sulphided $NiMo/Al_2O_3$ at higher temperatures (400-420°C) was also investigated.[21] Supporting sulphided CoMo on inorganic mesoporous materials showed that organised mesoporous alumina had better performance than the reference industrial γ-alumina as a support, which in turn exhibited a better performance than MCM-41 mesoporous alumina-silicates. Incorporating more Al into the Si-framework of MCM-41 increased the hydrocarbon yield.[22, 23] The HDO of sunflower and palm oil was also studied over sulphided $NiMo/Al_2O_3$ in mixture with vacuum gas oil or neat.[24, 25] Decarboxylation is generally favoured by higher temperatures and low pressures of H_2 over sulphided catalysts.

Deoxygenation of triglycerides with supported transition-metals has been scarcely studied:[26-31] Typically high-surface-area oxide or carbon materials are used for supporting Pd or Pt metals,[26,27] and isomerisation may be performed simultaneously by using strongly acidic porous materials as support or co-support.[28-30] Also FAME deoxygenation had successfully been performed over Pt-based catalyst at 300-350°C in 6.9 bar of H_2 or He.[31]

Several waste feedstocks such as abattoir waste, used cooking oils or greases contain considerable amounts of free fatty acids (FFAs). It was shown that FFAs are also intermediates in the deoxygenation of corresponding esters.[27,32] The study of FFA can therefore be considered crucial in deoxygenation. Palladium or platinum metals have previously been found to be the most selective and active catalysts for decarboxylation of FFAs.[33] Various decarboxylation parameters have previously been investigated in semibatch-mode (a stirred autoclave with liquid reactants and continuous renewal of only the gas phase), primarily with stearic acid as a feedstock over commercial Pd catalysts, Pd on SBA-15 or Pd on Sibunit carbon (a mesoporous and temperature-stable carbon composite).[34-36] It was found that the deoxygenation rate was independent on the fatty acid chain length in the range C_{18} to C_{23}.[37] Tall Oil Fatty Acids (TOFA) are by-products from the Kraft process (for making cellulose fibres from wood), and their deoxygenation was investigated over Pd/Sibunit.[38] Deactivation was especially pronounced with unsaturated fatty acids, therefore it is suspected to occur via cyclisations from C-C-double-bonds in the feedstock followed by dehydrogenation over Pd catalyst thus forming C_{17}-aromatic hydrocarbons.[35, 38, 39]

Continuous decarboxylation of stearic acid, a typical fatty acid found especially in saturated fats was recently demonstrated in continuous mode over Pd/C catalysts at 300-360°C.[35,40] Continuous reactors are more industrially interesting than batch or semibatch reactors, and it is necessary to obtain information on long-term performance and transients during continuous decarboxylation to describe the catalyst involved. In this work the continuous decarboxylation of stearic acid at 300°C is investigated with the aim of describing step changes during start-up and shutdown, steady-state conversion and deactivation phenomena.

2. Experimental

2.1. Chemicals. Stearic acid (>99% purity) was supplied by Sigma-Aldrich. N,O-bis(trimethylsilyl)-trifluoroacetamide (or BSTFA, of >99% purity) as a silylation agent was delivered from Acros Organics. n-dodecane (>99% purity) and pyridine (>99% purity) were obtained from Fluka. Ar (>99.99%) and 5% H_2/Ar gases were delivered from AGA . All chemicals were used as received.

2.2 Catalyst preparation & characterisation. 2 wt% Pd on Sibunit (synthetic mesoporous carbon) was prepared by the following method as previously published:[41] The Sibunit was treated with 5% HNO_3 overnight at 25°C and dried at 80°C. H_2PdCl_4 was hydrolysed in an aqueous solution, Na_2CO_3 was added until a pH = 9 was reached, and Sibunit was added to this solution for deposition of the Pd(II)-hydro-complexes. The solution was left for 6 h at 25°C, then filtered and washed with H_2O until no chloride ions were detected in the wash water. The catalyst was finally dried and subsequently calcined for 2 h at 200°C.

The particle diameter distributions and mean Pd diameters were calculated based on the frequency of particles from images obtained by a LEO 912 OMEGA energy-filtered transmission electron microscope (TEM) operating with acceleration voltage of 120 kV. At least 100 particles were counted for obtaining average particle diameter of Pd. The fresh and spent catalyst beads were crushed to a powder, mixed thoroughly and glued to an epoxy plate.

The X-ray Diffraction (XRD) mean particle diameter based on volume of the particles were calculated with the Scherrer formula from powder diffractograms

obtained with a Siemens D5000 X-ray Powder Diffractometer

The pore volume and specific surface area measurements were conducted with a physisorption / chemisorption Sorptometer 1900 from Carlo Erba instruments with liquid N_2 at 77 K. Specific surface areas were calculated using the Brunauer-Emmett-Teller (BET) equation from the N_2 adsorption-desorption isotherms. The pore size distribution was obtained from the Dollimore-Heal correlation.

The distribution of active metal in fresh catalyst beads was investigated by laser ablation connected to an inductively-coupled plasma mass-spectrometer (LA-ICP-MS), with laser ablation system of New Wave UP-213 and Perkin-Elmer ICP-MS Sciex Elan 6100 DRC Plus. A number of catalyst beads were cut in half and fixed in epoxy glue for the measurements.

Reactor effluent contents of Pd were measured by ICP-EOS with a Perkin-Elmer 5300 DV optical emission spectrometer. 0.2 g of effluent was added to 5 ml of 65% HNO_3 (aq) and 1 ml of 30 % H_2O_2 (aq), heated in a microwave oven and then diluted to 100 ml (aq) before ICP-OES analysis.

2.3 Reactor loading, catalyst activation and deoxygenation. A tubular reactor of 18 cm height and 1.58 cm inner diameter (volume 35.1 ml) was loaded from the bottom up with a small layer of quartz wool, then 6 ml of quartz sand of 0.2-0.8 mm in diameter and a layer of quartz wool. Afterwards the catalyst bed of 10 g (volume uptake 19.0 ml) of Pd/Sibunit was loaded into the reactor. Thereafter a layer of quartz wool, 4 ml of quartz sand and a layer of quartz wool were introduced. The quartz sand and quartz wool mixed the inlet flow in the reactor as well as the outlet to make liquid flow behaviour and sampling uniform.

A thermocouple was fixed at the centre of the catalyst bed. Then the reactor was mounted and leak-tested with Ar at room temperature and afterwards purged for 16 h at 20 bars with Ar also at room temperature. An aluminium heating element was fitted around the reactor.

The catalyst was then activated in 5% H_2/Ar at 20 bar by heating at 10°C/min to 150°C, kept at 150°C for 1 h, followed by heating at 10°C/min to the reaction temperature of 300°C. Reactions were performed in either pure Ar or 5% H_2/Ar at 42 Nml/min and with a flow of either pure stearic acid or 10 wt% in n-dodecane, both at 0.075 ml/min.

Since stearic acid melts at 70°C, it was kept in a heated storage vessel at 90°C, while the pump and inlet piping were kept at 100°C during experimentation with pure stearic acid. Trace gas impurities (e.g. molecular oxygen) were expelled from the storage vessel by continuous purging of 20 ml/min N_2 gas through the stearic acid. The flow reactor setup is sketched in Figure 1. During experiments liquid samples of ca. 0.1 g were taken out in glass vials downstream the reactor, while remaining liquid effluent was led to a heated collector vessel to be purged at set intervals. Gases were purged continuously by a pressure reduction controller, and part of the gas stream was diluted in He and analysed for CO and CO_2 on a Siemens ULTRAMAT 6 online IR analyser. The glass vials with liquid samples were weighed and 4 ml n-dodecane was added to the glass vial as a solvent. Of this, an aliquot of 10.0 µL of was transferred to a GC vial, followed by addition of 100 µL dodecane, 100 µL pyridine and 50 µL BSTFA for derivatisation and left to stand at 70°C for 60 min. An overview of the reactor changes is given in Table 1.

Table 1: Changes during continuous decarboxylation with diluted and pure stearic acid over 2 wt% Pd/Sibunit

Step change #	TOS (min)	Con-dition	Changes applied
			Diluted stearic acid in 5% H_2/Ar
	-55	liquid	Started flow of dodecane
I)	0	liquid	10 mol% stearic acid in dodecane
II)	300	Gas	5% H_2/Ar
			Diluted stearic acid in 5% H_2/Ar
III)	1575	Gas	pure Ar
IV)	1816	Liquid	6.55 mol% stearic acid in dodecane
V)	3016	Liquid	dodecane
	4389	Temp	Quenching to 150°C started
			100% stearic acid in Ar experiment
	4359	Temp	Heating startup from 150°C to 300°C
	4389		Reactor heated
VI)	4481	Liquid	100% stearic acid
VII)	7056	Liquid	dodecane
	7056	Temp	Quenching from 300°C to 150°C
			100% stearic acid in 5% H_2/Ar
	7056	Temp	Heating from 150°C to 300°C at 15°C/min
	7056	Gas	5% H_2/Ar
VIII)	7066	Liquid	100% stearic acid
IX)	18506	Liquid	Dodecane
	18881	Gas	Pure Ar
	18881	Liquid	Stopped flow
	18881	Temp	Cooling reactor to 25°C

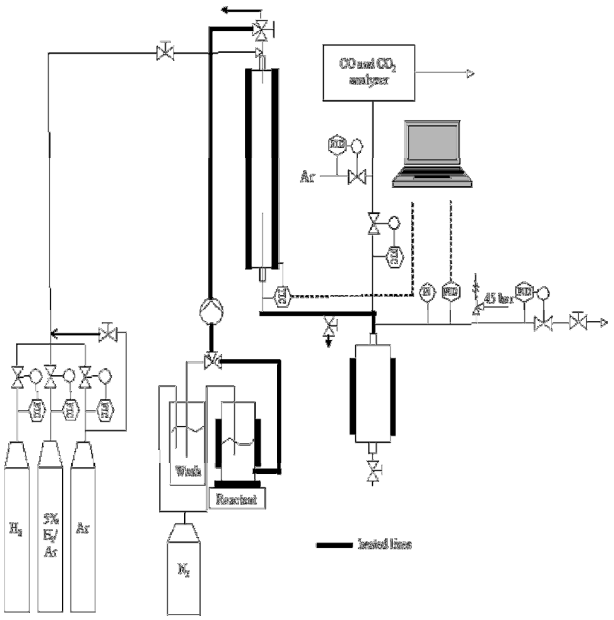

Figure 1: Flow reactor schematic for continuous deoxygenation of stearic acid.

After reaction, the reactor was washed for several hours with dodecane and Ar gas. Thereafter the system was cooled and the pressure carefully reduced. The reactor was disassembled and the spent catalyst beads sorted into sample glasses depending on axial position in the reactor bed.

3. Results & discussion

3.1. Steady state decarboxylation of stearic acid.

3.1.1. Stearic acid diluted in dodecane – step changes II)-III). At 450-1575 min of time-on-stream (TOS) the reaction was performed in 5% H_2/Ar. The reactor was kept at steady state conditions while liquid samples were extracted. The online analysis of CO_2 and CO concentrations showed that a conversion around 60% would have been achieved, however from the liquid samples it is clear that the conversion of stearic acid to heptadecane is close to 95 % at full selectivity. The discrepancy between CO/CO_2 and liquid phase analysis could likely be due to formation of methane via methanation of either CO_2, CO or both due to the hydrogen content in the sweeping gas. Methane formed could not be measured on the Ultramat with the present configuration.

3.1.2. Effect of Ar – step changes IV)-V). To see whether or not this behaviour would persist in hydrogen-free atmosphere the sweeping gas was changed back to Ar at TOS = 1575 min. The concentration in the feed vessel was also lowered from 10 mol% (ca. 15 wt%) to 6.5 mol% (10 wt%) stearic acid.

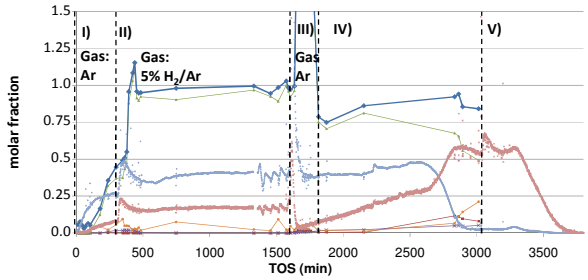

Figure 2: Decarboxylation in liquid flow of stearic acid over Pd/C at 300°C diluted in dodecane at 0.075 ml/min, 5 % H_2/Ar or pure Ar gas at 20 bar at 42 Nml/min. Changes in the operational parameters: I) Gas: Ar, II) Gas: 5% H_2/Ar, III) Erroneous liquid sampling, IV) Gas: Ar, V) Liquid: Dodecane. Legend: Liquid mole balance (-♦-), Stearic acid (-●-), heptadecane (-▲-), heptadecene (-■-), undecylbenzene (-x-), CO (x), CO_2 (♦).The Roman numbers refer to Table 1.

Initially a steep increase in gas and liquid concentrations is seen due to an unintended blocking of the gas feed line (Figure 2, section III), which was then unblocked shortly thereafter. Stable operation was approached and correctly sampled liquid obtained at TOS = 1816 min for pure Ar sweeping gas. Initially only heptadecane and CO_2 were formed and no CO. The CO_2 concentration corresponded to 50 mol% of the concentration of heptadecane. However, the CO concentration exiting the reactor increased over time, and around TOS = 2650-2850 min the CO_2 concentration dropped to practically zero while concentration of CO rose even more before settling at a concentration corresponding to around 55% conversion at 2800 min TOS. The liquid samples also were found to contain high levels of heptadecene (C_{17} alkene) of 8-12% and undecylbenzene (C_{17}-monoaromate) of 4-5%, as well as unconverted stearic acid (20%). The production of heptadecane (C_{17} alkane) started to drop as well. The formation of unsaturated compounds are likely caused by the lack of added H_2, leading to cyclisation and dehydrogenation of the products.

The initial lack of CO may be due to the lack of H_2 affording reverse water-gas-shift (WGS) reaction, however the constant and gradual rise in CO concentration followed (with a delay of 1-2 h) the formation of heptadecane and liberation of H_2 via aromatisation to undecylbenzene. H_2O and H_2 may have been formed via these side reactions.

The formation of linear hydrocarbons from FFAs has been proposed to take place by a mechanism going through formic acid: First, the fatty acid splits into formic acid and 1-alkene. Then formic acid rapidly decomposes, either via dehydrogenation to CO_2 and H_2, or by dehydration to CO and H_2O (overall reaction (1) and (2)). Hydrogen from the gas-phase afterwards saturated the formed alkene.[42,43] This can explain the enhanced formation of unsaturated compounds during reaction in

pure Ar. Formic acid, however, quickly decomposes under the present conditions and therefore cannot be observed in liquid or gas phase.[44]

Heptadecene and aromatic C_{17}-compounds are formed during reaction where catalyst deactivation is often fast.[36,38] Therefore the flow was switched to dodecane at TOS = 3120 min, and the Ar flow was maintained to wash the reactor (Figure 2, step V). The CO and CO_2 concentration did not start to decline until TOS = 3300 min when the reactor was cooled to 150°C. The sum of molar amounts of CO and CO_2 detected in the IR analyser after the liquid flow was switched to dodecane corresponds to 4.21 mmol, while maximally 0.250 mmol of CO can be situated on the surface of the Pd particles (calculated from XRD mean diameter of 12 nm as reported in section 3.3, taking particles as spheres and Pd:CO ratio to 2).[45] Thus, the CO and CO_2 measured in dodecane liquid flow came from reactant holdup in the catalyst bed – the stearic acid situated in the pores of the catalyst particles continued to react.

3.1.3. Effect of concentrated stearic acid under Ar – step change VI)-VII). Following the reaction with 10 wt% stearic acid in dodecane, the reactor was flushed overnight with Ar and cooled to ambient temperature, and reheated to 150°C, flushed for several hours with dodecane and argon and afterwards solely with argon. Then the reactor was reheated to 300°C at 10°C/min, and a flow of pure stearic acid was fed to the reactor to determine the steady-state deoxygenation of concentrated stearic acid in Ar during the following time interval of two days (TOS = 4481 - 7060 min). This is seen in Figure 3a.

The mass balance of the liquid samples performing the deoxygenation of pure stearic acid under Ar was only ca. 80%. At the same time about 2% heptadecane was formed in the start of the period, decreasing with time to about 1% at the end. The online IR-active analysis showed CO corresponding to about 3% conversion, decreasing over time to about 1.5%. No 1-heptadecene is detected, therefore methanation is not supposed to take place. It is suspected that coupling reactions with unsaturated compounds, reactants or both may take place, for instance coupling of formed alkenes to tetratriacontene (C_{34}-alkene). 18-Oxopentatriacontane (C_{35}-ketone) formed via ketonisation is however less likely to have been formed as it usually requires a basic metal oxide as support.[33,46] The heavy components formed would not have vaporised easily in split/splitless injection in GC analysis, and might as well have been too heavy to be seen with the applied GC method. It may be concluded that the lack of added H_2 in the gas feed led to low activity and gradual deactivation of the catalyst during the ca. 2600 min TOS mentioned.

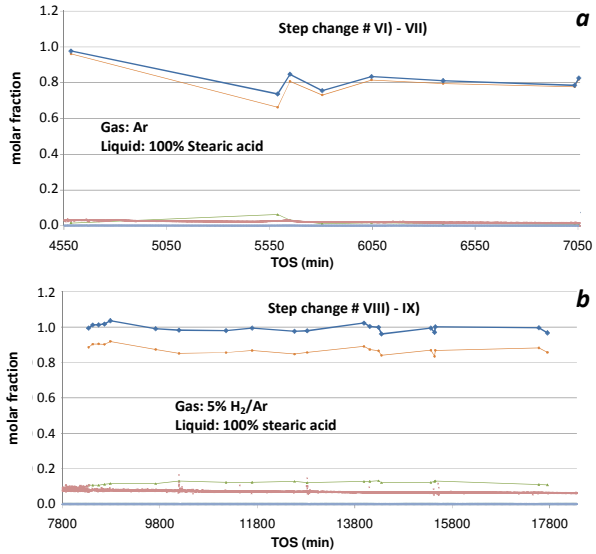

Figure 3: Mole fraction based on stearic acid, steady state decarboxylation of 100 % stearic acid flow. a) Pure Ar gas at 20 bar from step change VI) to VII). b) 5 % H_2/Ar gas at 20 bar from step VIII) to IX). Legend: Liquid mole balance (-♦-), Stearic acid (-●-), heptadecane (-▲-), heptadecene (-■-), undecylbenzene (-x-), CO (x), CO_2 (+).The Roman numbers refer to Table 1.

3.1.4. Effect of concentrated stearic acid under 5% H_2/Ar – step change VIII)-IX). After the above-mentioned Ar-experiment (Section 3.1.3) the next step was to assess the effect of 5% H_2/Ar as gas atmosphere. The reactor was again cooled to 150°C, flushed with dodecane to wash out residual stearic acid and products and reheated to 300°C to make a new attempt to analyse the start-up transient and steady-state conversion in 5% H_2/Ar atmosphere (Figure 3b).

From 8300 to 18500 min TOS the production of heptadecane was constant around 12% (atmosphere 5% H_2/Ar) while no other products were detected in the liquid phase. In the gas-phase only CO was detected, corresponding to a conversion of between 8 % and 6 %, decreasing with time. CO may have been formed from CO_2 due to the WGS equilibrium in the H_2-containing atmosphere or from deoxygenation via formic acid.[42,43] The missing CO or CO_2 was most likely converted to compounds not detectable in the IR-active online analysis – methane being a possible product, or coke via the Boudouard reaction. CO_2 formed from Boudouard reaction can again react with H_2 to CO via WGS or more H_2 to form methane.

3.1.5. Comparison of the catalyst performance in different gas and liquid feeds. The steady-state deoxygenation experiments with stearic acid are compared in Table 2. It is evident that the lack of H_2 in the feed led to deactivation, while stable catalyst activity can be upheld in 5% H_2/Ar. Initial deactivation during the deoxygenation of neat stearic acid was previously

observed using 20 bar Ar instead of 5% H_2/Ar as sweeping gas over 5% Pd/Sibunit at 360°C, but it was not found that the initial catalyst activity could be regained at this temperature - a stable conversion of about 15% neat stearic acid was obtained under 5% H_2/Ar at 360°C,[35] comparable with 12% conversion of neat stearic acid in 5% H_2/Ar at 300°C obtained in the present study.

Table 2: Comparison of the steady state-yields of heptadecane using different stearic acid concentrations in the feed. Conditions: 300°C, 20 bar sweeping gas at 42 Nml/min, liquid feed 0.075 ml/min. Dilution is in dodecane

	Yields of heptadecane (mol%)	
	Sweeping gas atmosphere:	
Liquid Feed:	***5 % H_2 in Ar***	***Pure Ar***
Diluted stearic acid (mol% stearic acid in dodecane)	95% (15 mol%)	75% decreasing to 55 %; formation of unsaturated and aromatic C_{17} compounds (10 mol%)
Pure stearic acid	12 %	2% decreasing to 1%; Possible Formation of heavier products

3.2. ***Transients during step-changes.*** Three transients in the catalytic deoxygenation over Pd/Sibunit are emphasised here, namely the flow pattern during start-up for 10% stearic acid in n-dodecane as well as the start-up and shut-down of 100% stearic acid under 5% H_2/Ar, respectively. The liquid pumping speeds are the same for the three conditions. The transients can be seen in Figure 4 a-c.

There was a considerable hold-up time when switching the flow to or from dodecane until the sampling on the outlet side of the reactor was affected – in all experiments approximately 1 h, as seen from Figure 4a-c. Once the concentration in the liquid samples had started to change, the transient lasted another 1.5 to 2 h before the concentration of the steady-state was reached and the reactor stabilised. During shutdown, the concentration of reactant and products did not fall to zero, as an additional number of hours were needed to completely remove the last compounds probably located in the porous catalyst beads and in cavities connected to the reactor.

3.2.1. *Start-up of stearic acid diluted in dodecane – step change I) and II).* After initial leak-testing of the reactor, the liquid flow was switched to Ar-flushing overnight and the catalyst was reduced in 20 bar of 5% H_2/Ar: First, the reactor was heated at 10°C/min to 150°C, where it was kept for 1 h, and the finally heated at 10°C/min to the reaction temperature of 300°C. Then the flow was switched to pure Ar and the pumping of 10 mol% stearic acid in dodecane begun (at TOS = 0 min), depicted in Figure 4a.

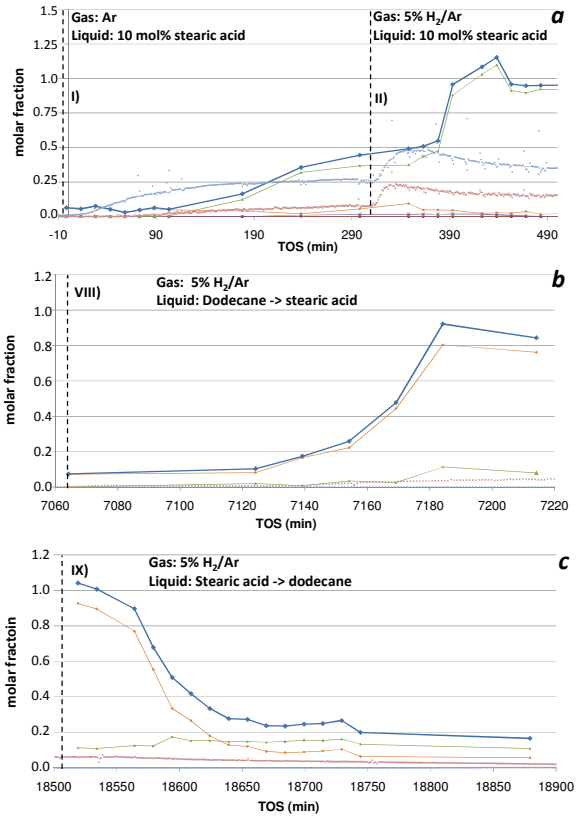

Figure 4: Mole balances based on stearic acid feed content for step change. a) start-up of 10 mol% stearic acid in dodecane flow – step change I)+II). b) start-up of 100 % stearic acid flow – step change VIII). c) shut-down of 100 % stearic acid flow – step change IX). Legend: Liquid mole balance (-♦-), Stearic acid (-●-), heptadecane (-▲-), heptadecene (-■-), undecylbenzene (-x-), CO (x), CO_2 (+).The Roman numbers refer to Table 1.

After about 15 min the CO_2-concentration from the online CO_2/CO analysis started to rise, meaning that decarboxylation of the reactant was taking place. However, the first traces of heptadecane in the liquid phase occur only over 2 h after the step change. The production of CO_2 and CO as well as the heptadecane seems to be stable at TOS = 300 min, with both gas-phase and liquid phase corresponding to 35-40% conversion.

Thereafter, the gas atmosphere was changed to 5% H_2/Ar at TOS = 300 min and the liquid flow kept constant. The CO_2 and CO concentrations as determined by the online CO/CO_2 analysis start to respond to this change after about 15 min, however, the corresponding response in heptadecane concentration is not visible in the liquid phase analysis before 1 h (around TOS = 360 min), and a steady state was only reached 2.5 h after the step change was induced (around TOS = 450 min). At TOS = 475 min the steady state concentration profile had developed, and now the mass balance compute as 90-95% heptadecane compared to theoretical possible value as well as 5 % stearic acid.

It is suspected that the liquid feed built up a trickling film wetting the beads of the catalyst bed and quartz material, and that the slow response in stearic acid concentration was due to the low overall flow of the reactant. The solvent n-dodecane has a normal boiling point of 216°C (vapour pressure is 6 bar at 300°C), the products heptadecane and 1-heptadecene have normal boiling points of ca. 302°C (vapour pressure around 1 bar at 300°C), and as these compounds are not supplied or produced in amounts sufficient to saturate the gas phase they will vaporise and quickly leave the reactor with the sweeping gas once formed. Stearic acid is not suspected to have vaporised (boiling point is 383°C), and will have propagated through the reactor in liquid form. The low feed rate of stearic acid means that a trickling liquid film hereof will propagate through the reactor very slowly.

3.2.2. Start-up of 100 % stearic acid feed in 5% H_2/Ar – step change VIII). Following reaction with liquid feed of 100 % stearic acid under pure Ar atmosphere, the reactor was flushed several hours with liquid dodecane followed by Ar gas at 150°C. Finally the gas atmosphere was switched to 5% H_2/Ar and flow of stearic acid to the reactor was started at TOS = 7060 min. The CO signal increased slightly after 5 minutes (no CO_2 formation was observed), but an increase in the concentration of stearic acid was not seen before 60 to 75 min. The concentration of stearic acid and product heptadecane rose over an additional 1 h period before approaching a steady state concentration with up to 12 % conversion (TOS = 7190 min). This is depicted in Figure 4 b.

3.2.3. Shut-down of 100 % stearic acid feed in 5% H_2/Ar – step change IX). After more than 10000 min on stream in stable behaviour, the flow was switched from pure stearic acid to pure dodecane to initiate reactor shut down (at TOS = 18500 min), see Figure 4 c. The CO signal from the online analysis was affected after a few minutes and started to decline gradually over a period of 8 h. In the liquid sampling the response to this step change is seen after ca. 1 h, and the concentration of stearic acid declined to 10 % at 2.5 h after the step change. Peculiarly, the concentration of heptadecane did not decrease in 3-4 h after the step change. After these few hours the concentrations decreased only very slowly. This is ascribed to the presence of small reservoirs of liquid after the reactor – in the thermocouple fittings or quartz material after the catalyst bed. This also means that the apparatus may not be completely liberated of stearic acid despite the purging with dodecane at 300°C or 150°C through the reactor for several hours prior to switch to stearic acid flow. Therefore minute amounts of stearic acid may appear in the samples already before flow of stearic acid is introduced in the reactor. It is presumed that both stearic acid and products was still situated in the microporous catalysts beads, due to capillary forces, a long time after stopping the liquid flow and from here they are only slowly mixed into the reactor after the switch to dodecane. This could explain the constant production of heptadecane despite the abrupt decrease in stearic acid concentration.

3.3. Post-reaction analyses – catalyst deactivation. A thorough post-reaction analysis of the spent catalyst was performed. The reactor was flushed first in n-dodecane and then flushed extensively in Ar gas at 150°C. The reactor was then dismantled and the catalyst taken out of the reactor in a stepwise manner by sorting the catalyst beads into batches depending on their axial position in the bed.

The total weight of the dried catalyst bed extracted from the reactor summed to 12.72 g versus fresh weight of 10 g, thus the uptake of carbonaceous species is 2.72 g or 0.227 mol of C. In comparison, the total molar amount of stearic acid passing through the reactor is 3.43 mol stearic acid or 61.7 mol of C, giving a ratio of coke-to-stearic acid percentage of 6.6%. The white and transparent quartz wool and quartz sand near the reactor inlet and the outlet were not coloured by the process. This indicates that coking can be attributed to the catalyst itself.

LA-ICP-MS confirmed that palladium is impregnated in an “eggshell-like” layer in the outer rim of the carbon beads, while the centre of the particle is inert, thus minimising the diffusion pathway. It is not expected that the majority of the palladium particles were mobile under the conditions used.

3.3.1. Coking in the pore system: The results from the analysis of the fresh and spent catalyst beads, sorted by position in the catalyst bed are shown in Table 3. The BET area and pore volume decreased downwards in the bed, and a deactivation profile formed downwards in the catalyst bed in a way that the largest amount of coke was formed in the catalyst beads near the reactor feed inlet and it decreased down the catalyst bed. Furthermore it is evident that the catalyst beads near the reactor inlet have a lower percentage of pores in the 5-10 nm range and below 2 nm compared to the beads near the reactor outlet, apparently due to a higher percentage of pores in the 2-5 nm range.

Table 3: Characterisation of the spent catalyst depending on position in the catalyst bed

Sample # (flow direction: ↓)	Catalyst bed position	Total Surface area (BET)	Relative decrease in surf. Area	Pore volume (BET)	Pore size distribution based on pore diameter in nm				TEM Pd diameter (XRD in parenthesis)
					>10	10-5	5-2	<2	
	[mm]	[m^2/g]	%	[ml/g]	%	%	%	%	[nm]*
1	0.0 - 9.6	101	72	0.321	1.3	7.4	76.2	15.2	7.7±3.5 (11.9)
2	9.6 - 19.0	118	67	0.430	1.3	8.5	77.8	12.3	---
3	19.0 - 27.8	130	64	0.377	1.1	8.7	71.4	18.8	---
4	27.8 - 49.2	137	62	0.383	1.5	9.1	76.3	13.2	7.1±4.5 (12.4)
5	49.2 - 69.8	157	57	0.502	1.4	10.5	70.4	17.7	---
6	69.8 - 100	166	54	0.474	1.3	10.0	67.0	21.8	6.0±4.5 (11.4)
Fresh cat.	---	361		0.873	2.0	15.5	73.2	9.3	6.7±2.8 (12.8)
Sibunit***	---	504		1.23	66	10	14	10	---

* XRD mean Pd particle is based on volume calculated from the Scherrer formula; TEM is based on the frequency of particles counted in the micrographs.
** Based on ref.[35]

The coking profile suggests that the larger pores have became narrower due to the gradual coking taking place, and that some of the smaller pores have been occluded partially or completely. The by-products formed in the pores do not completely prevent deoxygenation reaction, since a stable conversion of 12% was obtained constantly in the final 10500 min of TOS with neat stearic acid under 5% H_2/Ar. Further exploration of this catalyst deactivation profile as a function of bed length could be a topic of a subsequent study. It has been reported that deactivation takes place by cyclisation of unsaturated compounds in hydrogen-deficient atmosphere over 1 wt% Pd/Sibunit.[37,38,47] Thus it can be concluded that catalyst deactivation is caused by coking, since the specific BET surface area decreased by 72% to 54% as a function of catalyst bed length 1 cm and 9 cm from the inlet, respectively. This has also been the case in previous studies.[35,40]

3.3.2. Palladium particle sizes. The fresh catalyst beads as well as catalyst samples 1, 4, and 6 in Table 3 were selected for TEM and XRD analysis to obtain average particle sizes of the palladium and particle size distributions. The results are shown in Table 3, and a high-resolution TEM images and calculated particle diameter distribution of the fresh catalyst and sample # 1 are shown in Figure 5.

The differences observed between XRD and TEM mean Pd particle sizes in Table 3 is due to the different way of counting particles – XRD mean particle diameter is based on volume of the particles while TEM mean particle diameter is based on the number of particles in a small area. According to Figure 5, there is a percentage of particles above 10 nm diameter which will contribute much more to the average particle size based on volume (XRD) in contrast to the average Pd diameter based on the frequency of counted particles (TEM). The TEM micrographs indicated an average diameter of palladium on the spent catalyst was 7.7 nm near the inlet, whereas it was 6.1 nm near the outlet of the reactor. Furthermore, the average Pd particle size in the fresh catalyst was 6.7 nm. As TEM only analyses a tiny part of the catalyst bead, these differences are within experimental uncertainty. The mean particle diameters obtained via analysis of scattered X-rays were within a narrower interval around 12 nm. It can be therefore concluded that deactivation is not caused by sintering. This is furthermore in accordance with previous reports on fresh and spent Pd/Sibunit catalysts for decarboxylation, both of 1 wt% or 5 wt% Pd loading. Spent catalysts reported in the literature have active metal dispersions and particle sizes either marginally bigger or of the same sizes as the fresh catalysts.[35,37,40,47]

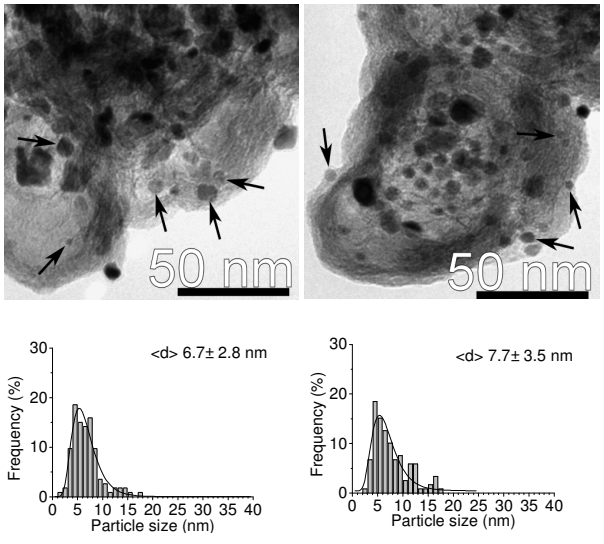

Figure 5: TEM micrographs and particle diameter distribution of a fresh catalyst bead (left-hand side) and a spent catalyst bead from the top of the bed (catalyst sample # 1) (right-hand side)

3.3.3. Leaching. The effluent from the reactor was collected in two batches of about 0.5 kg each and analysed with ICP-EOS. The total mass of Pd in the effluent was 1.15 mg, indicating that 0.58% of the Pd present in the catalyst bed (200 mg) had leached to the effluent during the course of the entire time-on-stream period over 14 days at 300°C. The leaching in the latter 7 days was only about one third of the leaching in the first 7 days of reaction (0.15% versus 0.43%). It is therefore expected that the leaching was due to a few loosely bound palladium particles on the catalyst surface and that leaching ceased with time as these were removed. Deactivation is, therefore, not due to leaching, which is in accordance with results from previous studies concluding that no or below 1% leaching of palladium takes place during deoxygenation over 1 wt% Pd/Sibunit.[37,40]

4. Conclusion

Transient and steady-state behaviour of continuous stearic acid decarboxylation was studied over 2 wt% Pd/Sibunit-carbon at 300°C at 20 bars. Pure Ar or 5% H_2 in Ar were used as sweeping gases, and both pure and dodecane-diluted feeds of stearic acid were employed as reactants.

Diluted stearic acid was almost fully converted to heptadecane in hydrogen-containing gas, while deactivation via formation of unsaturated compounds took place in pure argon gas. Deactivation irreversibly changed the catalyst to produce CO instead of CO_2. Pure stearic acid selectively yielded around 12% heptadecane in hydrogen-containing gas, while only 2% heptadecane and likely formation of heavier compounds resulted from hydrogen-free atmosphere.

The same catalyst was used during all of the experimentation. A deactivation gradient formed during reaction as a function of the distance from the liquid feed inlet – the most deactivated catalyst beads were those closest to the inlet. Deactivation took place mainly by coke formation in the pores and on the surface, but not by agglomeration, leaching or sintering.

Acknowledgements

A. T. Madsen acknowledges support from the Danish Research and Innovation Agency through the consortium “Waste-2-value”, and is furthermore grateful to the Laboratory of Industrial Chemistry and Reaction Engineering at Åbo Akademi University for hosting his stay in the group during 2010. The authors wish to thank Paul Ek from the Process Chemistry Centre, Åbo Akademi University for performing ICP-MS and ICP-EOS measurements.

References

(1) The European Union. Directive 2009/28/EC on the promotion of the use of renewable energy . *Off. J. EU*. **2009**, *140*, 1-47.

(2) International Energy Agency *World Energy Outlook*; International Energy Agency: Paris, France, 2010; p. 700.

(3) Knothe, G.; Van Gerpen, J.; Krahl, J. *The Biodiesel Handbook*; Knothe, G.; Van Gerpen, J.; Krahl, J., Eds.; 1st ed.; AOCS Press: Urbana, Illinois, USA, 2005.

(4) Mittelbach, M.; Remschmidt, C. *Biodiesel: The Comprehensive Handbook*; Mittelbach, M., Ed.; 3rd ed.; Martin Mittelbach: Graz, Austria, 2006.

(5) Kalnes, T. N.; Koers, K. P.; Marker, T.; Shonnard, D. R. A technoeconomic and environmental life cycle comparison of green diesel to biodiesel and syndiesel. *Environ. Prog. Sustainable Energy,* **2009**, *28*, 111-120.

(6) Koskinen, M.; Sourander, M.; Nurminen, M. Apply a comprehensive approach to biofuels. *Hydrocarb. Process*. **2006**, *85*, 81-86.

(7) Mikkonen, S. Second-generation renewable diesel offers advantages. *Hydrocarb. Process*. **2008**, *87*, 63-66.

(8) Sang, O. Y. Biofuel Production from Catalytic Cracking of Palm Oil. *Energy Sources,* **2003**, *25*, 859-869.

(9) Twaiq, F. A.; Zabidi, N. A. M.; Mohameda, A. R.; Bhatia, S. Catalytic conversion of palm oil over mesoporous aluminosilicate MCM-41 for the production of liquid hydrocarbon fuels. *Fuel Process. Technol*. **2003**, *84*, 105-120.

(10) Lima, D. G.; Soares, V. C. D.; Riberio, E. B.; Carvalho, D. A.; Cardoso, É. C. V.; Rassi, F. C.; Mundim, K. C.; Rubim, J. C.; Suarez, P. A. Z. Diesel-like fuel obtained by pyrolysis of vegetable oils. *J. Anal. Appl. Pyrolysis*. **2004**, *71*, 987-996.

(11) Tamunaidu, P.; Bhatia, S. Catalytic cracking of palm oil for the production of biofuels: optimization studies. *Bioresour. technol*. **2007**, *98*, 3593-601.

(12) Na, J.-G.; Yi, B. E.; Kim, J. N.; Yi, K. B.; Park, S.-Y.; Park, J.-H.; Kim, J.-N.; Ko, C. H. Hydrocarbon production from decarboxylation of fatty acid without hydrogen. *Catal. Today,* **2009**, *156*, 44-48.

(13) Quirino, R. L.; Tavares, A. P.; Peres, A. C.; Rubim, J. C.; Suarez, P. A. Z. Studying the Influence of Alumina Catalysts Doped with Tin and Zinc Oxides in the Soybean Oil Pyrolysis Reaction. *J. Am. Oil Chem. Soc.* **2008**, *86*, 167-172.

(14) Sooknoi, T.; Danuthai, T.; Lobban, L. L.; Mallinson, R.; Resasco, D. E. Deoxygenation of methylesters over CsNaX. *J. Catal.* **2008**, *258*, 199-209.

(15) Danuthai, T.; Jongpatiwut, S.; Rirksomboon, T.; Osuwan, S.; Resasco, D. E. Conversion of methylesters to hydrocarbons over an H-ZSM5 zeolite catalyst. *Appl. Catal., A.* **2009**, *361*, 99-105.

(16) Senol, O. I.; Viljava, T.-R.; Krause, A. O. I. Effect of sulphiding agents on the hydrodeoxygenation of aliphatic esters on sulphided catalysts, *Appl. Catal., A*. **2007**, *326*, 236-244.

(17) Ryymin, E.-M.; Honkela, M. L.; Viljava, T.-R.; Krause, A. O. I. Insight to sulfur species in the hydrodeoxygenation of aliphatic esters over sulfided NiMo/γ-Al2O3 catalyst. *Appl. Catal., A.* **2009**, *358*, 42-48.

(18) Šimáček, P.; Kubička, D.; Šebor, G.; Pospíšil, M. Hydroprocessed rapeseed oil as a source of hydrocarbon-based biodiesel. *Fuel,* **2009**, *88*, 456-460.

(19) Šimáček, P.; Kubička, D.; Šebor, G.; Pospíšil, M. Fuel properties of hydroprocessed rapeseed oil. *Fuel,* **2010**, *89*, 611-615.

(20) Kubička, D.; Kaluža, L. Deoxygenation of vegetable oils over sulfided Ni, Mo and NiMo catalysts. *Appl. Catal., A*. **2010**, *372*, 199-208.

(21) Šimáček, P.; Kubička, D. Hydrocracking of petroleum vacuum distillate containing rapeseed oil: Evaluation of diesel fuel. *Fuel,* **2010**, *89*, 1508–1513.

(22) Kubička, D.; Šimáček, P.; Žilková, N. Transformation of Vegetable Oils into Hydrocarbons over Mesoporous-Alumina-Supported CoMo Catalysts. *Top. Catal*. **2009**, *52*, 161-168.

(23) Kubička, D.; Bejblová, M.; Vlk, J. Conversion of Vegetable Oils into Hydrocarbons over CoMo/MCM-41 Catalysts. *Top. Catal.* **2010**, *53*, 168–178.

(24) Huber, G. W.; O'Connor, P.; Corma, A. Processing biomass in conventional oil refineries: Production of high quality diesel by hydrotreating vegetable oils in heavy vacuum oil mixtures. *Appl. Catal., A*. **2007**, *329*, 120–129.

(25) Guzman, A.; Torres, J. E.; Prada, L. P.; Nuñez, M. L. Hydroprocessing of crude palm oil at pilot plant scale. *Catal. Today,* **2010**, *156*, 38-43.

(26) Morgan, T.; Grubb, D.; Santillan-Jimenez, E.; Crocker, M. Conversion of Triglycerides to Hydrocarbons Over Supported Metal Catalysts. *Top. Catal*. **2010**, *53*, 820-829.

(27) Kubičková, I.; Snåre, M.; Eränen, K.; Mäki-Arvela, P.; Murzin, D. Y. Hydrocarbons for diesel fuel via decarboxylation of vegetable oils. *Catal. Today,* **2005**, *106*, 197-200.

(28) Hancsók, J.; Krár, M.; Magyar, S.; Boda, L.; Holló, A.; Kalló, D. Investigation of the production of high cetane number bio gas oil from pre-hydrogenated vegetable oils over Pt/HZSM-22/Al2O3. *Microporous Mesoporous Mater*. **2007**, *101*, 148-152.

(29) Kikhtyanin, O. V.; Rubanov, A. E.; Ayupov, A. B.; Echevsky, G. V. Hydroconversion of sunflower oil on Pd/SAPO-31 catalyst. *Fuel,* **2010**, *89*, 3085-3092.

(30) Ping, E. W.; Wallace, R.; Pierson, J.; Fuller, T. F.; Jones, C. W. Highly dispersed palladium nanoparticles on ultra-porous silica mesocellular foam for the catalytic decarboxylation of stearic acid. *Microporous Mesoporous Mater*. **2010**, *132*, 174-180.

(31) Do, P. T.; Chiappero, M.; Lobban, L. L.; Resasco, D. E. Catalytic Deoxygenation of Methyl-Octanoate and Methyl-Stearate on Pt/Al2O3. *Catal. Lett.* **2009**, *130*, 9-18.

(32) Snåre, M.; Kubičková, I.; Mäki-Arvela, P.; Eränen, K.; Wärnå, J.; Murzin, D. Y. Production of diesel fuel from renewable feeds: Kinetics of ethyl stearate decarboxylation. *Chem. Eng. J.* **2007**, *134*, 29-34.

(33) Snåre, M.; Kubičková, I.; Mäki-Arvela, P.; Eränen, K.; Murzin, D. Y. Heterogeneous Catalytic Deoxygenation of Stearic Acid for Production of Biodiesel. *Ind. Eng. Chem. Res.* **2006**, *45*, 5708-5715.

(34) Lestari, S.; Simakova, I.; Tokarev, A.; Mäki-Arvela, P.; Eränen, K.; Murzin, D. Y. Synthesis of Biodiesel via Deoxygenation of Stearic Acid over Supported Pd/C Catalyst. *Catal. Lett*. **2008**, *122*, 247-251.

(35) Lestari, S.; Mäki-Arvela, P.; Bernas, H.; Simakova, O.; Sjöholm, R.; Beltramini, J.; Lu, G. Q. M.; Myllyoja, J.; Simakova, I.; Murzin, D. Y. Catalytic Deoxygenation of Stearic Acid in a Continuous Reactor over a Mesoporous Carbon-Supported Pd Catalyst. *Energy Fuels,* **2009**, *23*, 3842-3845.

(36) Lestari, S.; Mäki-Arvela, P.; Eränen, K.; Beltramini, J.; Max Lu, G. Q.; Murzin, D. Y. Diesel-like Hydrocarbons from Catalytic Deoxygenation of Stearic Acid over Supported Pd Nanoparticles on SBA-15 Catalysts. *Catal. Lett*. **2009**, *134*, 250-257.

(37) Simakova, I.; Simakova, O.; Mäki-Arvela, P.; Murzin, D. Y. Decarboxylation of fatty acids over Pd supported on mesoporous carbon. *Catal. Today,* **2010**, *150*, 28-31.

(38) Rozmysłowicz, B.; Mäki-Arvela, P.; Lestari, S.; Simakova, O. A.; Eränen, K.; Simakova, I.; Murzin, D. Y.; Salmi, T. Catalytic Deoxygenation of Tall Oil Fatty Acids Over a Palladium-Mesoporous Carbon Catalyst: A New Source of Biofuels. *Top. Catal*. **2010**, *53*, 1274-1277.

(39) Mäki-Arvela, P.; Kubičková, I.; Snåre, M.; Eränen, K.; Murzin, D. Y. Catalytic Deoxygenation of Fatty Acids and Their Derivatives. *Energy Fuels,* **2007**, *21*, 30-41.

(40) Bernas, H.; Eränen, K.; Simakova, I.; Leino, A.-R.; Kordás, K.; Myllyoja, J.; Mäki-Arvela, P.; Salmi, T.; Murzin, D. Y. Deoxygenation of dodecanoic acid under inert atmosphere. *Fuel,* **2010**, *89*, 2033-2039.

(41) Simonov, P. A.; Troitskii, S. Y.; Likholobov, V. A. Preparation of the Pd/C catalysts: A molecular-level study of active site formation. *Kinet. Catal*. **2000**, *41*, 255-269.

(42) Berenblyum, A S.; Danyushevsky, V. Ya.; Katsman, E. A; Podoplelovau, T. A; Flid, V. R. Production of Engine Fuels from Inedible Vegetable Oils and Fats. *Petroleum Chemistry*. **2010**, *50*, 305-311.

(43) Boda, L.; Onyestyák, G.; Solt, H.; Lónyi, F.; Valyon, J.; Thernesz, A. Catalytic hydroconversion of tricaprylin and caprylic acid as model reaction for biofuel production from triglycerides. *Appl. Catal., A*. **2010**, *374*, 158-169.

(44) Bulushev, D. A.; Beloshapkin, S.; Ross, J. R. H. Hydrogen from formic acid decomposition over Pd and Au catalysts. *Catal. Today,* **2010**, *154*, 7-12.

(45) Dulaurent, O.; Chandes, K.; Bouly, C.; Bianchi, D. Heat of Adsorption of Carbon Monoxide on a Pd/Al2O3 Solid Using Infrared Spectroscopy at High Temperatures. *J Catal.* **1999**, *188*, 237-251.

(46) Gärtner, C. A.; Serrano-Ruiz, J. C.; Braden, D. J.; Dumesic, J. A. Catalytic coupling of carboxylic acids by ketonization as a processing step in biomass conversion. *J. Catal*. **2009**, *266*, 71-78.

(47) Immer, J. G.; Lamb, H. H. Fed-Batch Catalytic Deoxygenation of Free Fatty Acids. *Energy Fuels,* **2010**, *24*, 5291-5299.

Fuel xxx (2011) xxx–xxx

Contents lists available at ScienceDirect

Fuel

journal homepage: www.elsevier.com/locate/fuel

Hydrodeoxygenation of waste fat for diesel production: Study on model feed with Pt/alumina catalyst

Anders Theilgaard Madsen, El Hadi Ahmed, Claus Hviid Christensen, Rasmus Fehrmann, Anders Riisager *

Centre for Catalysis and Sustainable Chemistry, Department of Chemistry, Technical University of Denmark, Building 207, DK-2800 Kgs. Lyngby, Denmark

ARTICLE INFO

Article history:
Received 12 April 2011
Received in revised form 31 May 2011
Accepted 1 June 2011
Available online xxxx

Keywords:
Alkanes
Biodiesel
Fats and oils
Hydrogenation
Decarboxylation

ABSTRACT

Hydrodeoxygenation of waste fats and oils is a viable method for producing renewable diesel oil. In this study a model feed consisting of oleic acid and tripalmitin in molar ratio 1:3 was hydrotreated at 325 °C with 20 bars H_2 in a stirred batch autoclave with a 5 wt% Pt/γ-Al_2O_3 catalyst, and samples were extracted periodically and analyzed on GC. Despite the significant hydrogen pressure hydrogenation of both reactants were limited and decarboxylation or decarbonylation of the ester and carboxylic acid functionalities were highly favored, yielding carbon chain lengths of odd numbers. Moreover, Pd/γ-Al_2O_3 was observed to be slightly more active than Pt/γ-Al_2O_3 and had a higher ratio of decarboxylation and decarbonylation to hydrogenation, while Ni/γ-Al_2O_3 was substantially less active than Pt and also showed a markedly lower ratio of decarboxylation and decarbonylation to hydrogenation. Variation of the temperature showed that triglycerides as well as free fatty acids were converted at all investigated temperatures, but the conversion of oleic acid increased significant from 6% to 100% when the temperature was increased from 250 °C to 325 °C. The tripalmitin reacted via a palmitic acid intermediate, and its conversion was limited by formation of this free fatty acid.

1. Introduction

The worldwide production of biofuels is growing. This growth is amongst other factors driven by capital interests, environmental concerns, and the desire to make national fuel supplies more independent of the global petroleum supply and price. The European Union (EU) fuel directive 2009/28/EC stated a target of 5.75% energy content from biofuels in 2010 and a rise to 10% by 2020 [1]. The most developed and widespread industrial method for producing diesel oils from biomass is the base-catalyzed transesterification of oils and fats with alcohol, preferably methanol. The product is referred to as fatty acid methyl ester (FAME). Though most authors specifically refer to FAME as biodiesel, others suggest wider definitions [2,3]. Refined plant oils are usually well suited for transesterification as they have low contents of impurities, especially free fatty acids (FFA) that form soap on addition of base [4]. However, inexpensive feedstocks like used cooking oils, abattoir wastes and trap greases that would be preferable to use contain high amounts of FFA [5,6]; 2–7 wt% for used cooking oils, 5–30 wt% for waste animal fats and trap greases even higher [7,8]. Accordingly, these cheap feedstocks represent some challenges due to more tedious workup. For instance in the USA a production of 5.08 million m^3 of waste fats and greases was reported for 2000, potentially amounting to 4% of the road vehicle diesel demand if converted to an equal amount of diesel [4].

In the past decade another production strategy for diesel oil from fats has been shown possible [9–18]. By reacting fatty feedstock at elevated temperatures over a heterogeneous catalyst in the presence of hydrogen, oxygen functionalities can be split off as H_2O, CO_2 or CO, resulting in long-chain alkanes by hydrodeoxygenation (HDO), as shown in Fig. 1a–d. Compared to transesterification not many studies have appeared on HDO of fats and oils, although it may be especially suited for large scale integration with petroleum refining. The HDO process has first been industrialized by Neste Oil in Porvoo, Finland who are using primarily vegetable oils as feedstock [16,17].

Krause and co-workers studied HDO of sulfided $CoMo/Al_2O_3$ and $NiMo/Al_2O_3$ on heptanoic acid, heptanol and heptanoate methyl and ethyl esters. Sulfidation by addition of H_2S instead of CS_2 shifted the selectivity from C_7 to C_6 hydrocarbons. It was found that NiMo, but not CoMo was very sensitive to the sulfidation conditions and that the unsulfided catalysts were neither very active nor selective to C_6 and C_7 alkane formation [19,20].

Kubička and co-workers evaluated the conversion of rapeseed oil over sulfided catalysts in a number of studies. When the activity and selectivity of sulfided $NiMo/Al_2O_3$ catalyst was compared to that of unsulfided Ni/Al_2O_3 at 270–350 °C, the sulfided catalyst was found to be much more active. However, the unsulfided catalysts primary yielded odd number hydrocarbons (decarboxylation/decarbonylation) while the sulfided yielded primarily even num-

* Corresponding author. Fax: +45 4588 3136.
E-mail address: ar@kemi.dtu.dk (A. Riisager).

0016-2361/$ - see front matter © 2011 Elsevier Ltd. All rights reserved.
doi:10.1016/j.fuel.2011.06.005

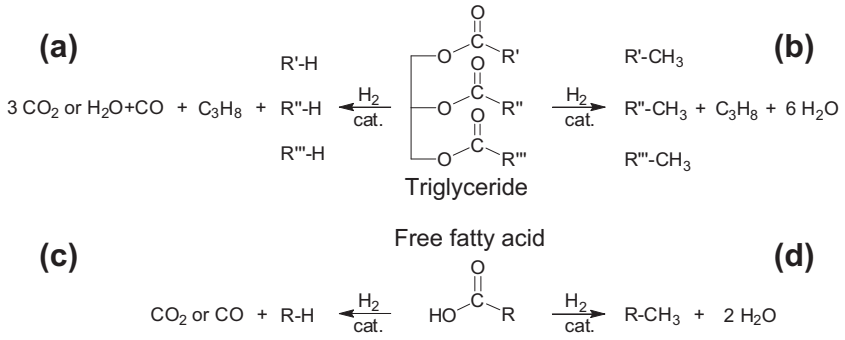

Fig. 1. Decarbonylation, decarboxylation (left) and hydrogenation (right) of triglycerides and free fatty acids.

bered (complete reduction) [21]. The activity of sulfided NiMo/Al_2O_3 superseded that of Mo/Al_2O_3 and Ni/Al_2O_3 separately in liquid phase HDO below 300 °C in H_2 atmosphere [22]. Rapeseed oil HDO over commercial sulfided NiMo/Al_2O_3 at 70 bar H_2 achieved full conversion above 300 °C, while higher temperatures yielded higher selectivity towards odd-number hydrocarbons [23]. Supporting sulfided CoMo on mesoporous Al_2O_3 rather than MCM-41 resulted in higher yields of alkanes, but incorporating of Al into the framework of MCM-41 did improve yields due to support acidity [24,25].

Resasco et al. concluded that HDO of methyl octanoate and methyl stearate over Pt/Al_2O_3 at 330 °C proceeds in inert atmosphere, but addition of H_2 suppresses formation of higher self-condensates of both compounds. Decarbonylation was found always to be the primary reaction route [26]. The deoxygenation of methyl octanoate over H-ZSM-5 at 500 °C resulted in lighter hydrocarbon gasses and aromatization, the latter of which proceeded through self-condensation products (tetradecane, 8-pentadecanone, octyl octanoate) [27]. Methyl octanoate was converted to C_6–C_8 alkenes and condensated hydrocarbons (C_{14}–C_{16}) over basic CsNaX without forming aromatics, while weakly acidic NaX resulted in marked production of aromatics before deactivating [28].

Murzin and co-workers have performed seminal studies of the deoxygenation of fatty acids and their derivatives [12–15,29–34]. A range of supported metal catalysts were tested and noble metals on carbon were found most beneficial for the decarboxylation of stearic acid [14]. The conversions of stearic acid, ethyl stearate and tristearine to alkanes were studied in semibatch-reactor between 270 and 360 °C, either in gas-mixture with H_2 or inert gas at up to 40 bars over Pd/C. The products in all cases were almost exclusively *n*-heptadecane [12,13]. and it was shown that stearic acid is an intermediate in the conversion of the ester reactants to *n*-heptadecane [15]. It was furthermore shown that deoxygenation kinetics of other fatty acids proceeds with the same rate [29].

Also in semibatch reaction-mode, Rozmysłowicz et al. studied tall oil fatty acid hydrogenation and decarboxylation [30], while Lestari et al. investigated deoxygenation of stearic acid over Pd on SBA-15 [31] as well as stearic and palmitic acid over Pd on Sibunit carbon [32,33]. The deoxygenation of stearic acid was even performed in a continuous reactor setup [34].

In this work we have focused on linking products to triglyceride and FFA in an idealized model mixture of fat in batch-mode reaction, and thus investigated the hydrodeoxygenation of a feed with a molar ratio of 1:3 between oleic acid and tripalmitin. This approach has made it possible to investigate reactivity and product selectivity of different substrate molecules and product molecules may be related distinctively to molecules in the model mixture.

2. Experimental

2.1. Catalyst preparation

A catalyst metal loading of 5 wt% on alumina was chosen as catalyst to ensure activity and similitude to industrial practice. 5 wt% Pt/γ-Al_2O_3 catalyst was prepared by the incipient-wetness impregnation method [35], where the required amount of the active metal precursor $H_2PtCl_6{\cdot}6H_2O$ (⩾99.0%, Fluka) was dissolved in demineralized water and added to dried and fractionated (<180 μm) γ-alumina powder (brand, BET area 194 m^2/g). The wet catalyst was left at room temperature for 2 h, then dried in an oven at 110 °C for 2 h and finally calcined in air at 400 °C for 8 h with a 100 °C/h ramp. 5 wt% Pd/γ-Al_2O_3 and 5 wt% Ni/γ-Al_2O_3 catalysts were prepared in an analogous way by dissolving respectively $Pd(NO_3)_2{\cdot}2H_2O$ (⩾99.8%, Fluka) or $Ni(NO_3)_2{\cdot}6H_2O$ (⩾99.0%, Aldrich) in water and impregnating alumina, as described above.

2.2. Catalyst characterization

The BET surface areas of the prepared catalysts as well as the γ-alumina support were determined by nitrogen physisorption by measuring adsorption and desorption isotherm at liquid nitrogen temperature on a Micromeritics ASAP 2020 pore analyzer. Before measurement the samples were degassed at 200 °C under vacuum for 4 h.

CO pulse-chemisorption was performed to determine the active metal area, dispersion and particle size. This was done on a Micromeritics Autochem II 2920 with a loop size of 0.366 ml. Ca. 100 mg catalyst sample was flushed with He and then heated and reduced at 150 °C for 2 h in 10% H_2/N_2. Then the sample was flushed with He and cooled, and CO pulse-chemisorption was performed at 25 °C with 5% CO/He using He carrier gas while the CO-concentration in the effluent was continuously measured by a thermal conductivity detector (TCD). For the Ni catalyst, the reduction was also attempted under varying conditions at up to 400 °C for up to 12 h. The stoichiometries for area calculation were Pt:CO = Ni:Co = 1:1 and Pd:CO = 2:1.

2.3. Hydrodeoxygenation

The hydrogenation was carried out in a 50 ml stainless steel autoclave (MicroClave from Autoclave Engineers) by filling the autoclave with 8.1 g *n*-tetradecane (⩾99.0%, Fluka) as solvent, 0.806 g tripalmitin (⩾99.0%, Fluka), 0.094 g oleic acid (⩾99.0%, Fluka) and 0.03 g of *n*-docosane (⩾98.0%, Fluka) as internal standard. A 0.15 ml reference sample was taken out and 0.20 g 5 wt% Pt/γ-Al_2O_3 catalyst added to the remaining 10 wt% model fat mix-

Please cite this article in press as: Madsen AT et al. Hydrodeoxygenation of waste fat for diesel production: Study on model feed with Pt/alumina catalyst. Fuel (2011), doi:10.1016/j.fuel.2011.06.005

ture (consisting of 90 mol% tripalmitin and 10 mol% oleic acid) in *n*-tetradecane.

The autoclave was then sealed at room temperature, charged with 14 bar hydrogen (⩾99.999%, Air Liquide), heated to 325 °C and mechanically stirred at 900 rpm. This procedure effectively resulted in a pressure-rise in the autoclave to 20 bars and also resulted in activation of the catalyst. After 1 h of reaction the autoclave was rapidly cooled to below room temperature in an ice-water bath, opened and a sample of about 0.15 ml withdrawn for analysis. After closing the autoclave again it was purged and recharged with hydrogen and reheated to 325 °C and the procedure repeated to obtain samples after 2, 5 and 20 h of reaction.

In another experimental set the amount of tripalmitin and oleic acid were varied while keeping the *n*-tetradecane amount fixed. Variation of the reaction temperature was also performed to study the dependence on conversion of the reactants, and the influence of hydrogen pressure to examine the preference for decarboxylation, decarbonylation or complete reduction. Furthermore, two other 5 wt% Pd/γ-Al_2O_3 and 5 wt% Ni/γ-Al_2O_3 catalysts were tested for selectivity towards the hydrogenation and decarboxylation reactions.

2.4. Product analysis

The liquid reaction mixtures were quantified by an Agilent Technologies 6890N GC equipped with flame ionization detector (FID), split/splitless injection system and a HP-5 capillary column (J&W Scientific, 30 m × 0.32 mm × 0.25 μm, 5 mol% phenylmethyl polysiloxane). Qualitative analysis was performed by GC–MS with an Agilent Technologies 6850 GC–MS with a HP-5MS column (J&W Scientific, 30 m × 0.25 mm × 0.25 μm, 5 mol% phenylmethyl polysiloxane). A few gas samples of selected runs were taken out from the autoclave in a gas bag and injected with a gas syringe on an Agilent Technologies 6890N GC equipped with thermal conductivity detector (TCD) and flame ionization detector (FID), split/splitless injection system and a DB-1 capillary column (J&W Scientific, 50 m × 0.32 mm × 0.5 μm of dimethylpolysiloxane).

All samples were silylated by addition of 20 μl N-methyl-N-trimethylsilyl-trifluoroacetamide (MSTFA) (⩾97.0%, Fluka) to each 0.15 ml sample, followed by heating to 60 °C for 30 min and cooling to room temperature before running the analysis on GC and GC–MS. Free fatty acids (FFAs) were hereby converted to trimethylsilyl esters which were sufficiently volatile and thermally stable to allow analysis with reduced peak tailing in the gas chromatogram [31]. It should be noted that a split/splitless injector cannot itself be used in directly quantifying the amount of tripalmitin in a given hydrocarbon sample. Discrimination will result when molar masses of the compounds gets too high, which may also make split/splitless GC analyses of fats cumbersome. Instead we used the yield of pentadecane and hexadecane to calculate the tripalmitin conversion, as these alkanes are measured quantitatively with good precision by split/splitless GC injection and FID detection. This assumption could be justified since no other compounds were observed above impurity threshold.

During the experimentation stearic acid was observed as an intermediate by hydrogenation of oleic acid. The sum of oleic acid and stearic acid concentrations calculated from the GC-FID chromatograms has been used to denote the amount of unconverted fatty acid.

3. Results and discussion

3.1. Time series

Results of conversion and yield were plotted against the time of sampling to illustrate time series of each catalytic run. The results obtained for the standard reactions conducted at 325 °C and 20 bars H_2 with 0.2 g 5 wt% Pt/γ-Al_2O_3 are shown in Fig. 2.

As seen in Fig. 2, full conversion of the oleic acid to C_{17} and C_{18} alkanes were achieved within 5 h. In comparison the tripalmitin was converted rather slowly, which is probably related to the larger size of the molecule and more hindered access to the functional group to be reacted for the triester. It was observed that the yields of pentadecane (C_{15}) and heptadecane (C_{17}) were more than an order of magnitude higher than those of hexadecane (C_{16}) and octadecane (C_{18}), respectively. Hence, the pressure of H_2 was 20 bars, the liberation of the carboxylate functionalities from the carbon chains of the feed (decarboxylation and decarbonylation) dominated the reactions for both the oleic acid and tripalmitin, in accordance with the findings of Murzin and co-workers [13,15].

Notably, the hydrogenation and decarboxylation reactions of stearic acid have almost identical Gibbs free energies ($\Delta G \sim -85$ kJ/mol) at about 300 °C, while the Gibbs free energy of decarbonylation is less negative ($\Delta G \sim -68$ kJ/mol) [14]. This strongly support that the product distribution may be effected by catalyst.

It was observed during the experiments that the double bond in oleic acid was rapidly saturated to give stearic acid. This proceeds much faster and at lower temperatures than the ester/acid decarboxylation and the complete saturation of the fatty acid chain was observed in all the experiments.

3.2. Variation and characterization of catalysts

Comparative screening of catalysts with 5 wt% Pd or Ni on γ-Al_2O_3 revealed that these metals were also active for the deoxygenation. Actually it could be observed that the Pd catalyst was more active than the Pt catalyst, and also more selective to the C_{17} and C_{15} products (Table 1). The higher activity is probably related to the higher molar loading of Pd (4.8 mol%) compared to Pt (2.7 mol%) on the support where palladium metal area is double that of platinum, as measured by the CO pulse-chemisorption experiments (Table 2). Nickel, however, was less active than Pt and Pd as well as less selective to decarboxylation reactions, but the catalyst particles were also larger than Pd and Pt particles on average (Table 2) and for this reason may be less reactive. The results obtained after 5 h can be seen in Table 1. The strong tendency towards decarboxylation and decarbonylation for Pd and Pt catalysts as well as the relative tendency in catalyst activity has also been observed by Murzin et al. [13–15], although it was indicated that Ni should favor split-off of CO or CO_2 to a somewhat higher degree. This was also presented by Kubička et al. [21], though a

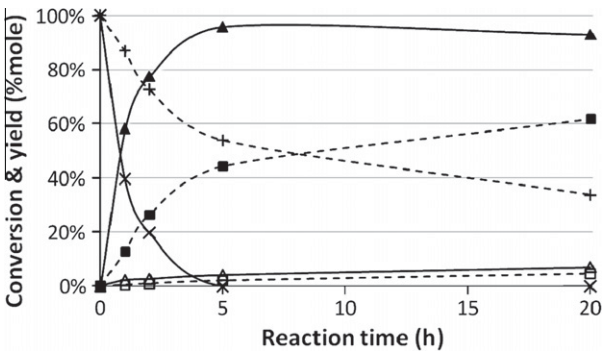

Fig. 2. Hydrodeoxygenation time series conducted at 325 °C and 20 bar H_2 with 0.2 g 5 wt% Pt/γ-Al_2O_3. Legend: Tripalmitin (– × –) and its products pentadecane (–■–) and hexadecane (–□–), oleic acid (– + –) and its products heptadecane (–▲–) and octadecane (–Δ–).

Please cite this article in press as: Madsen AT et al. Hydrodeoxygenation of waste fat for diesel production: Study on model feed with Pt/alumina catalyst. Fuel (2011), doi:10.1016/j.fuel.2011.06.005

Table 1
Catalysts for hydrodeoxygenation at 20 bar H_2, 325 °C, 5 h reaction over 0.2 g catalyst.

Entry	Catalyst	Tripalmitin		Oleic acid	
		$(CO_2 + CO)/H_2$[b]	Conversion (%)	$(CO_2 + CO)/H_2$[b]	Conversion (%)
1	5 wt% Pt/γ-Al_2O_3[a]	21.9	46.2	23.3	100
2	5 wt% Ni/γ-Al_2O_3[a]	4.8	10.4	1.4	76.8
3	5 wt% Pd/γ-Al_2O_3[a]	28.6	71.1	28.5	100

[b] Ratio of decarboxylation + decarbonylation to hydrogenation.

Table 2
Catalyst and support characterization.

Entry	Catalyst	mol% metal[a]	BET-area (m^2/g)	Pore volume (ml/g)	Mean metal particle size (nm)	Metal surf. area (m^2/g)
1	γ-Al_2O_3	—	255	0.607	—	—
2	5 wt% Pt/γ-Al_2O_3	2.68	251	0.575	5.4	2.82
3	5 wt% Pd/γ-Al_2O_3	4.80	236	0.539	4.6	5.69
4	5 wt% Ni/γ-Al_2O_3	8.38	217	0.523	8.2	4.81

[a] Calculated molar percentage of active metal on the γ-Al_2O_3 support.

poorer conversion of carboxylic acids over Ni/Al_2O_3 than over supported Pd catalysts has previously been reported [36].

3.3. Control experiments

A key step in the experimentation was to establish if deoxygenation of the model feed actually resulted in production of linear-chain alkanes only by the mentioned overall schemes in Fig. 1a–d. To examine this, we therefore performed control experiments to elucidate the influence of the support material, the gas atmosphere used, the temperature and the method of preparation of the Pt catalyst.

First a Mason–Boudart-test was made to investigate if diffusion resistance played a role in the catalytic tests. The 5 wt% Pt/γ-Al_2O_3 of <180 μm size was crushed down and sieved to a size of <50 μm and used for deoxygenation of a mixture of tripalmitin and oleic acid. This produced within a few percent the same yields of resulting C_{15}–C_{18} alkanes (not shown) after 1, 2, 5 and 20 h, so diffusion limitation was deemed unimportant.

Then it was investigated whether or not formed alkanes and the substrates underwent C–C scission at positions other than the ester/acid functionality or isomerization, by performing a reference experiment with Pt/Al_2O_3 at 20 bar hydrogen and 325 °C without reactants. From this experiment it was confirmed that less than 1% of *n*-tetradecane was isomerized after treatment for 20 h. It is known that alkanes may undergo C–C-scission or isomerization under these circumstances, and though the degree of isomerization was found to be quite low, it must be noted that alkanes are not completely unaltered by Pt catalysts at these temperatures, which has also been reported previously for similar experiments [14,15]. To evaluate the alteration of the reactants by the temperature a reaction run was also performed with reactants at 325 °C and 20 bar H_2 without added catalyst. This experiment resulted in a conversion of oleic acid of about 3% and of tripalmitin of about 4% after 5 h, thus confirming that a catalyst is necessary to perform the sought reaction (Table 3, entry 5).

As the support material γ-alumina itself could play a role in the reaction, it was also important to establish if such an influence was present. By using only the γ-Al_2O_3 as additive under H_2 atmosphere a total yield of alkanes of 7% was obtained from oleic acid and 6% from tripalmitin after 5 h, while respectively 2% and 5% were obtained under N_2 atmosphere (Table 3, entries 3 and 4). When using Pt/Al_2O_3 as catalyst under N_2 pressure the conversion of oleic acid after 5 h reached 99% (Table 3, entry 2). Thus hydrogen was not directly necessary to convert oleic acid to hydrocarbons with Pt catalyst, but unsaturated compounds were produced instead of linear alkanes. Under these conditions the conversion of tripalmitin was only 4% after 5 h.

3.4. Feed variation

The free fatty acids reacted faster to hydrocarbons than triglycerides, as shown above. However, the ratio of decarboxylation/decarbonylation to hydrogenation was almost identical for both triglyceride and free fatty acid. This implied that triglycerides reacted via an intermediate, which was likely palmitic acid formed by hydrolysis or partial hydrogenation of the triglyceride molecules.

A catalytic run with only oleic acid as reactant was then performed at 325 °C and 20 bar H_2 using 5 wt% Pt/γ-Al_2O_3 catalyst. Here only heptadecane (major product) and octadecane (minor product) was observed as products during the first 5 h of reaction. This observation confirmed that formation of *n*-heptadecane and *n*-octadecane resulted selectively from linear monoacids of 18 C-atoms. No palmitic acid was observed.

The analogous experiment with only tripalmitin was also conducted. Here it was confirmed that the treatment of tripalmitin resulted in the formation of pentadecane (major product) and hexadecane (minor product), and palmitic acid furthermore appeared during the reaction. These results implied that palmitic acid was at least one of the intermediates formed during tripalmitin conversion.

A likely reaction for formation of the intermediate is partial hydrogenation, as shown in Fig. 3. Since the degree of hydrogenation was less pronounced compared to decarboxylation, the partial pressure of water was quite low. On the other hand the hydrogen pressure was high, so it is likely that propandiyl-dipalmitate and palmitic acid are formed (Fig. 3). This behavior and mechanism have previously been described in the literature [13,14].

The hydrogenated di-ester may then have been further hydrogenated to the mono-ester and palmitic acid, and again to finally have released propane and the last acid molecule, while the palmitic acid, parallel to oleic or stearic acid, may have underwent decarboxylation, decarbonylation or hydrogenation to pentadecane or hexadecane.

Table 3
Conversion of oleic acid with supported catalyst, with support and without any catalyst in control experiments at 20 bar gas 325 °C, 5 h reaction over 0.2 g catalyst.

Entry	Catalyst	Gas atmosphere	Oleic acid conversion (%)	Tripalmitin conversion (%)
1	5 wt% Pt/γ-Al_2O_3	H_2	100	46
2	5 wt% Pt/γ-Al_2O_3	N_2	99	4
3	γ-Al_2O_3	H_2	7	6
4	γ-Al_2O_3	N_2	2	5
5	None	H_2	3	4

Please cite this article in press as: Madsen AT et al. Hydrodeoxygenation of waste fat for diesel production: Study on model feed with Pt/alumina catalyst. Fuel (2011), doi:10.1016/j.fuel.2011.06.005

3.5. Variation of the temperature

Experiments were further performed at different temperatures to evaluate the performance of the Pt catalyst with respect to the model feed. The conversions found for oleic acid and tripalmitin after 5 h of reaction are plotted against temperature in Fig. 4.

The conversions of both reactants were below 5% after 5 h at 250 °C and 275 °C. However, at 300 °C about half of the oleic acid was converted while only around one tenth of the tripalmitin was converted to alkanes. At 325 °C the conversion of the oleic acid to alkanes reached 100%, and the conversion of tripalmitin reached 40%. The tripalmitin only reached full conversion after 5 h when using a temperature of 375 °C, clearly showing that the triglyceride was more reluctant to react under the applied conditions.

Murzin and co-workers have showed that not just CO_2 but also CO was formed in the mixture during the reaction of stearic acid and ethyl stearate to alkanes [14,15]. It can thus be suspected that decarbonylation also takes place during the reaction studied here. It should be noted that if either CO or CO_2 are formed exclusively during the course of the reaction it may not necessarily be observed, because the catalysts could be active for the water–gas shift (WGS) equilibrium in presence of hydrogen and water vapor (Table 4a) so that a mixture of CO and CO_2 will always form. According to thermodynamics also methanation of both CO and CO_2 with H_2 (Table 4b and c, respectively) may occur around 300 °C, as also suggested by Murzin et al. [14]. Although platinum is known not to be very active in reactions involving CO due to high dissociation energy of CO [37], methanation does play a role in the studied gas–solid reactions. Hence, gas-phase analysis of reaction mixture from tripalmitin and oleic acid deoxygenation over 5 wt% Pt/γ-Al_2O_3 at 325 °C and 20 bar showed that in all cases about 60% CH_4 was formed and about 40% as a mixture of CO and CO_2. However, here the reactor interior (i.e., stainless steel) may also have contributed since iron is a rather good Fischer–Tropsch catalyst [37]. Some N_2 and Ar was present as well due to leakage of air. No C_3-species (e.g. propane) from the tripalmitin conversion were detected, though. These may be mixed in the liquid tetradecane phase at elevated pressures.

It must be noted that methanation is problematic in this process because methane is not useful as a fuel in the resulting low concentrations, it is a much worse greenhouse gas than CO_2, and methanation consume more hydrogen than full reduction of the fatty acids. If methanation cannot be avoided in an industrial process, it is more attractive to fully reduce the fatty acid chains to alkanes as shown in Fig. 1b and d.

3.6. Variation of hydrogen pressure

The pressure variation experiments are summarized in Fig. 5. Highest yield of heptadecane after 1 h reaction at 325 °C was obtained with 9 bar H_2. When the pressure of H_2 was increased above 9 bars the amount of heptadecane ($C_{17}H_{36}$) formed from oleic acid decreased, while the formed amounts of hexadecane ($C_{16}H_{34}$) and octadecane ($C_{18}H_{38}$) remained low. This implied that the selectivity

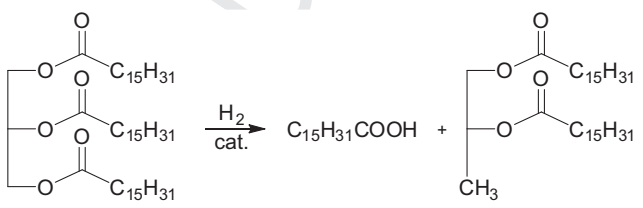

Fig. 3. Partial hydrogenation of tripalmitin to yield intermediates palmitic acid and propandiyl-dipalmitate.

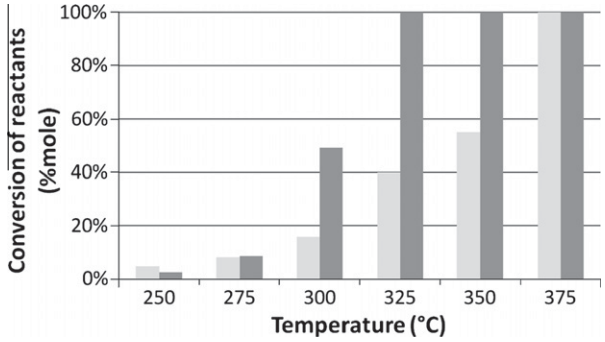

Fig. 4. Conversion as a function of temperature between 250 and 375 °C with 20 bar H_2 over 0.2 g Pt/γ-Al_2O_3 after 5 h. Legend: Oleic acid (light gray) and tripalmitin (dark gray).

Table 4
Thermodynamics of water–gas shift and methanation reactions at 300 °C [14].

	Reaction	$\Delta H_{573\ K}$ (kJ/mol)	$\Delta G_{573\ K}$ (m^2/g)
(a)	$CO + H_2O \leftrightarrow H_2 + CO_2$	−39.2	−17.6
(b)	$CO + 3H_2 \leftrightarrow CH_4 + H_2O$	−216.4	−78.8
(c)	$CO_2 + 4H_2 \leftrightarrow CH_4 + 2H_2O$	−117.2	−61.2

towards full reduction is not improved by adding more H_2, and the oleic acid conversion declined. This behavior is unexpected and may call for a more elaborated study, but possibly the dissolved H_2 in the alkane solvent reached saturation while the higher hydrogen pressure pushed the water–gas shift equilibrium towards increased CO formation from CO_2. CO is known to preferentially adsorb on surfaces and may thus deactivate the surface. Previously it has been observed that stearic acid react via decarboxylation over supported Pd, while esters may react via both decarboxylation or decarbonylation over Pd and Pt depending on the process parameters [12–15] Also competitive adsorption of hydrogen may have hindered the acid adsorption or the hydrogen may have inhibited the decarboxylation of oleic or stearic acid.

As previously mentioned (Section 3.3) H_2 may be necessary to avoid deactivation of the catalyst by scavenging the surface from deactivating species [13,30,38]. Such deactivation is reported to take place over a Pd/C catalyst by formation of aromatics from unsaturated compounds [30,38], and thus likely also over platinum catalysts. Formation of alkenes was observed over a sulphided NiMo-catalyst as part of a deoxygenation mechanism from aldehydes and alcohols in hydrogen [18]. C_{17}-alkenes and heavier ketones have previously been observed to form from methyl

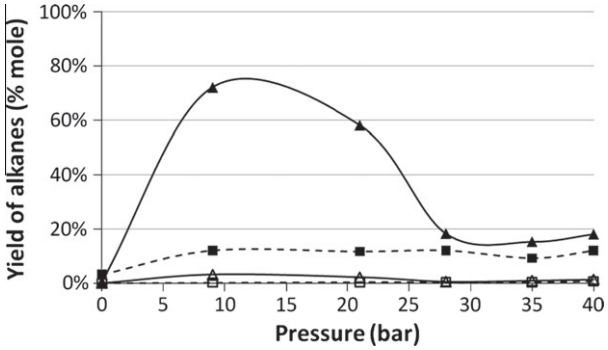

Fig. 5. Yields of C_{15}–C_{18} alkanes after 1 h reaction at 325 °C with 0.2 g 5 wt% Pt/γ-Al_2O_3. Legend: Pentadecane (–■–), hexadecane (–□–), heptadecane (–▲–), octadecane (–Δ–). Dotted lines represent products of tripalmitin conversion and solid lines are products of oleic acid conversion.

Please cite this article in press as: Madsen AT et al. Hydrodeoxygenation of waste fat for diesel production: Study on model feed with Pt/alumina catalyst. Fuel (2011), doi:10.1016/j.fuel.2011.06.005

stearate over Pt/Al_2O_3 in He atmosphere, which was suspected to lead to deactivation [39]. Accordingly, it is likely that the high activity for conversion of oleic acid in inert atmosphere (Section 3.3) yielding unsaturated compounds in turn may cause catalyst deactivation.

The pentadecane ($C_{15}H_{32}$) formation was more or less constant at 12% when the pressure of H_2 increased from 9 to 40 bars of hydrogen. H_2 may not be the rate-limiting component in the conversion of tripalmitin, but some H_2 was necessary for the conversion as no H_2 resulted in a yield of pentadecane of 3%. This could be explained by the mechanistic suggestion in Section 3.4, assuming that hydrogen is needed to split off the fatty acids from the glycerides for further reaction [13]. Thus it appeared that the optimum hydrogen pressure under the examined reaction conditions was around 10 bars in terms of the yields of pentadecane and heptadecane.

4. Conclusion

Hydrodeoxygenation of a model fat mixture composed of oleic acid and tripalmitin has been studied with an alumina-supported platinum catalyst. The conversion of the free fatty acids took place faster than that of triglycerides, a property that may be ascribed to the difference in metal particle sizes and diffusivity of the reactants, besides the intrinsic difference in reactivity for esters and carboxylic acids. By excluding respectively oleic acid and tripalmitin in comparative experiments it was demonstrated that triglycerides reacted to alkanes via their corresponding free fatty acids, and that this reaction determined the overall reaction rate under these conditions.

At reaction temperatures below 300 °C the conversions of both triglycerides and free fatty acids were low, the latter being faster. At 325 °C and above the reaction proceeded fast for both triglyceride and free fatty acid. Gas-phase analysis revealed that methanation and probably also water–gas-shift contribute a role in altering the atmosphere during reaction progression, maybe from interference with the reactor interior. Formation of unsaturated hydrocarbons dominated in absence of hydrogen, while a hydrogen pressure between 9 and 20 bars was found to be optimal for the reaction, depending on the reactant being either free fatty acid or triglyceride.

The hydrodeoxygenation of oils and fats is a promising and flexible way of providing biofuels, and examination on model feeds – such as a mixture of tripalmitin and oleic acid applied in the present work – is a suitable approach to get detailed insight into the factors determining the production of renewable long-chain hydrocarbons.

Acknowledgement

A.T.M is grateful for the funding of his PhD stipend in the Waste-2-Value innovation consortium through the Danish Agency for Science, Technology and Innovation.

References

[1] The European Union Directive. 2009/28/EC, on the promotion of the use of energy from renewable sources. Offic J EU 2003;12:1–20.
[2] Snåre M, Murzin DY. Reply to "comment on 'heterogeneous catalytic deoxygenation of stearic acid for production of biodiesel'". Ind Eng Chem Res 2006;45:6875.
[3] Ma F, Hanna MA. Biodiesel production: a review. Bioresource Technol 1999;70:1–15.
[4] Knothe G, Van Gerpen J, Krahl J. The biodiesel handbook. (Urbana, Illinois, USA): AOCS Press; 2005.
[5] Kulkarni MG, Dalai AK. Waste cooking oil – an economical source for biodiesel: a review. Ind Eng Chem Res 2006;45:2901–13.
[6] Meher LC, Vidya Sagar D, Naik SN. Technical aspects of biodiesel production by transesterification – a review. Renew Sust Energy Rev 2006;10:248–68.
[7] Van Gerpen J. Biodiesel processing and production. Fuel Process Technol 2005;86:1097–107.
[8] Mittelbach M, Remschmidt C. Biodiesel: The comprehensive handbook. 3rd ed. Graz, (Austria), Martin Mittelbach; 2006.
[9] Huber GW, Iborra S, Corma A. Synthesis of transportation fuels from biomass: chemistry, catalysts, and engineering. Chem Rev 2006;106:4044–98.
[10] Stumborg M, Wong A, Hogan E. Hydroprocessed vegetable oils for diesel fuel improvement. Bioresource Technol 1996;56:13–8.
[11] Huber GW, O'Connor P, Corma A. Processing biomass in conventional oil refineries: production of high quality diesel by hydrotreating vegetable oils in heavy vacuum oil mixtures. Appl Catal A 2007;329:120–9.
[12] Kubičková I, Snåre M, Eränen K, Mäki-Arvela P, Murzin DY. Hydrocarbons for diesel fuel via decarboxylation of vegetable oils. Catal Today 2005;106:197–200.
[13] Mäki-Arvela P, Kubičková I, Snåre M, Eränen K, Murzin DY. Catalytic deoxygenation of fatty acids and their derivatives. Energy Fuels 2007;21:30–41.
[14] Snåre M, Kubičková I, Mäki-Arvela P, Eränen K, Murzin DY. Heterogeneous catalytic deoxygenation of stearic acid for production of biodiesel. Ind Eng Chem Res 2006;45:5708–15.
[15] Snåre M, Kubičková I, Mäki-Arvela P, Eränen K, Wärnå J, Murzin DY. Production of diesel fuel from renewable feeds: kinetics of ethyl stearate decarboxylation. Chem Eng J 2007;134:29–34.
[16] Koskinen M, Sourander M, Nurminen M. Apply a comprehensive approach to biofuels. Hydrocarb Process 2006;85:81–6.
[17] Mikkonen S. Catalytic upgrading of biorefinery oil from micro-algae. Hydrocarb Process 2008;87:63–6.
[18] Donnis B, Egeberg RG, Blom P, Knudsen KG. Hydroprocessing of bio-oils and oxygenates to hydrocarbons. Understanding the reaction routes. Top Catal 2009;52:229–40.
[19] Senol O, Viljava T, Krause A. Hydrodeoxygenation of aliphatic esters on sulphided NiMo/γ-AlO and CoMo/γ-AlO catalyst: the effect of water. Catal Today 2005;106:186–9.
[20] Senol OI, Ryymin EM, Viljava T-R, Krause AOI. Reactions of methyl heptanoate hydrodeoxygenation on sulphided catalysts. J Mol Catal A 2007;268:1–8.
[21] Kubička D, Šimáček P, Kolena J, Lederer J, Šebor G. Catalytic transformations of vegetable oils into hydrocarbons. In: ICP2007 proceedings – 43rd international petroleum conference, Bratislava, Slovakia; 2007. p. 1–7.
[22] Kubička D, Kaluža L. Deoxygenation of vegetable oils over sulfided Ni, Mo and NiMo catalysts. Appl Catal A 2010;372:199–208.
[23] Šimáček P, Kubička D, Šebor G, Pospíšil M. Hydroprocessed rapeseed oil as a source of hydrocarbon-based biodiesel. Fuel 2009;88:456–60.
[24] Kubička D, Bejblová M, Vlk J. Conversion of vegetable oils into hydrocarbons over CoMo/MCM-41 catalysts. Top Catal 2010;53:168–78.
[25] Kubička D, Šimáček P, Žilková N. Transformation of vegetable oils into hydrocarbons over mesoporous-alumina-supported CoMo catalysts. Top Catal 2009;52:161–8.
[26] Do PT, Chiappero M, Lobban LL, Resasco DE. Catalytic deoxygenation of methyl-octanoate and methyl-stearate on Pt/Al_2O_3. Catal Lett 2009;130:9–18.
[27] Danuthai T, Jongpatiwut S, Rirksomboon T, Osuwan S, Resasco DE. Conversion of methylesters to hydrocarbons over an H-ZSM5 zeolite catalyst. Appl Catal A 2009;361:99–105.
[28] Sooknoi T, Danuthai T, Lobban LL, Mallinson R, Resasco DE. Deoxygenation of methylesters over CsNaX. J Catal 2008;258:199–209.
[29] Simakova I, Simakova O, Mäki-Arvela P, Murzin DY. Decarboxylation of fatty acids over Pd supported on mesoporous carbon. Catal Today 2010;150:28–31.
[30] Rozmysłowicz B, Mäki-Arvela P, Lestari S, Simakova OA, Eränen K, Simakova I, et al. Catalytic deoxygenation of tall oil fatty acids over a palladium-mesoporous carbon catalyst: a new source of biofuels. Top Catal 2010;53:1274–7.
[31] Lestari S, Mäki-Arvela P, Eränen K, Beltramini J, Lu GQM, Murzin DY. Diesel-like hydrocarbons from catalytic deoxygenation of stearic acid over supported Pd nanoparticles on SBA-15 catalysts. Catal Lett 2009;134:250–7.
[32] Lestari S, Simakova I, Tokarev A, Mäki-Arvela P, Eränen K, Murzin DY. Synthesis of biodiesel via deoxygenation of stearic acid over supported Pd/C catalyst. Catal Lett 2008;122:247–51.
[33] Lestari S, Mäki-Arvela P, Simakova I, Beltramini J, Lu GQM, Murzin DY. Catalytic deoxygenation of stearic acid and palmitic acid in semibatch mode. Catal Lett 2009;130:48–51.
[34] Lestari S, Mäki-Arvela P, Beltramini J, Lu GQM, Murzin DY. Transforming triglycerides and fatty acids into biofuels. ChemSusChem 2009;2:1109–19.
[35] Pinna F. Supported metal catalysts preparation. Catal Today 1998;41:129–37.
[36] Maier WF, Roth W, Thies I, Schleyer PVR. Chem Ber 1982;115:808–12.
[37] Andersson M, Bligaard T, Kustov A, Larsen K, Greeley J, Johannessen T, et al. Toward computational screening in heterogeneous catalysis: Pareto-optimal methanation catalysts. J Catal 2006;239:501–6.
[38] Lestari S, Mäki-Arvela P, Bernas H, Simakova O, Sjöholm R, Beltramini J, et al. Catalytic deoxygenation of stearic acid in a continuous reactor over a mesoporous carbon-supported Pd catalyst. Energy Fuels 2009;23:3842–5.
[39] Do PT, Chiappero M, Lobban LL, Resasco DE. Catalytic deoxygenation of methyl-octanoate and methyl-stearate over Pt/Al_2O_3. Catal Lett 2009;130:9–18.

Please cite this article in press as: Madsen AT et al. Hydrodeoxygenation of waste fat for diesel production: Study on model feed with Pt/alumina catalyst. Fuel (2011), doi:10.1016/j.fuel.2011.06.005

REVIEW

Challenges and perspectives for catalysis in production of diesel from biomass

Biofuels (2011) 2(4), xxx–xxx

Anders Theilgaard Madsen[1], Helle Søndergaard[1], Rasmus Fehrmann[1] & Anders Riisager[†1]

The production of biofuels is expected to increase in the future due to environmental concerns, accelerating oil prices and the desire to achieve independence from mineral oil sources. Of the proposed methods for diesel production from biomass, the esterification and transesterification of plant oils or waste fats with methanol is the most prominent and has been applied industrially for a decade. Homogeneous acid and base catalysis is normally used, but solid acids, solid bases, ionic liquids and lipases are being developed as replacements. Hydrodeoxygenation of vegetable oils has likewise been commercialized. Diesel from biomass may also be produced by catalytic upgrading of bio-oils from flash pyrolysis, by aqueous-phase reforming of carbohydrates into non- or mono-functionalized hydrocarbons via consecutive reduction-condensation reactions, or by gasification of biomass to synthesis gas of CO and H_2 and liquefaction to alkanes via Fischer–Tropsch synthesis. Here, the current challenges and perspectives regarding catalysis and raw materials for diesel production from biomass are surveyed.

Diesel

▪ Biomass raw materials & conversion technologies

The production of diesel from biomass is growing worldwide. This growth is driven by, amongst other factors, capital interests, environmental concerns and the desire to make national fuel supplies more independent of global petroleum supply and price. The EU fuel directive 2003/30/EC mandated in 2003 that a share of 5.75% energy content should derive from biofuels in 2010, rising to 10% by 2020 [1]. At the same time, the EU has opted for a promotion of biofuel production from waste products and a discouragement of 'bad biofuels systems', that is, exclusion of biofuels produced with a low or even negative displacement of carbon dioxide from the atmosphere or biofuels production triggering deterioration of sensitive wildlife habitats and ecosystems [2]. Furthermore, as transportation fuels based on fossil feedstocks are usually the cheapest petroleum products, the production processes for sustainable fuels must also be economically feasible and the feedstock as cheap as possible. As waste products (second-generation resources) represent the cheapest feedstock available and are usually also the most environmentally benign to employ, the use of such feedstock is highly desirable.

Utilization of biomass to produce diesel oils has undergone substantial research in recent years and a number of catalytic methods exists; fats and oils can either be transesterified with alcohol to form FAMEs [3–5], deoxygenated at moderate temperatures with hydrogen to form *n*-alkanes [6–10] or cracked at elevated temperatures to form a hydrocarbon blend [11–13]. Carbohydrates may be converted by aqueous-phase reforming (APR) to form unfunctionalized or monofunctional hydrocarbons [14–16]. Biomass in general may be gasified to syn-gas (a mixture of carbon monoxide and hydrogen) and liquefied via Fischer–Tropsch synthesis (FTS) [17,18]. Thermal depolymerization either by flash pyrolysis or hydrothermal upgrading can yield a **bio-oil** that can be further upgraded by cracking or hydrogenation [19–22]. A graphical overview of these techniques can be seen in **Figure 1**.

The term 'biodiesel' usually refers solely to fatty acid alkyl esters and in particular the fatty acid methyl esters (FAMEs) [23]. The market share of FAMEs is the largest of the available diesel oils from biomass, but it is not the only

[1]Centre for Catalysis and Sustainable Chemistry, Department of Chemistry, Building 207, Technical University of Denmark, DK 2800 Kgs. Lyngby, Denmark
[†]Author for correspondence: Tel.: +45 4525 2233; Fax: +45 4588 3136; E-mail: E-mail: ar@kemi.dtu.dk

10.4155/BFS.11.115 ISSN 1759-7269

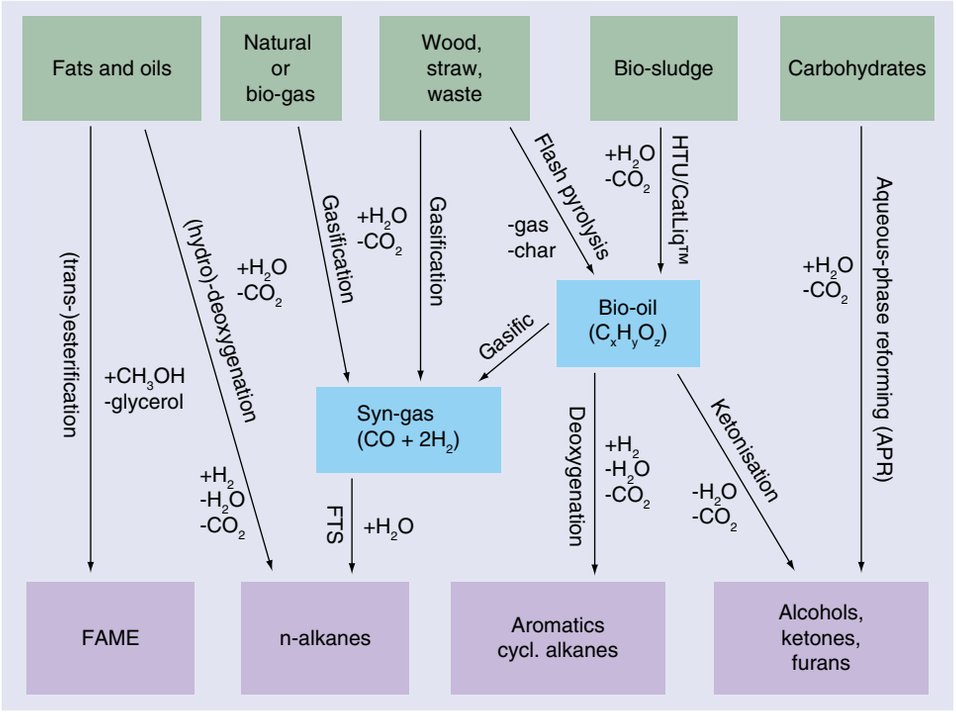

Figure 1. Overview of biomass conversion technologies leading to diesel oils.

Key terms

Bio-oil: Tar fraction from biomass pyrolysis. Contains numerous compounds: ketones, aldehydes, carboxylic acids, aromatic ethers, phenols, alcohols and polyfunctional molecules in emulsified water. It is unsuited for fuelling engines, but may be catalytically hydrodeoxygenated to usable fuels.

Cetane number: Indication of 'ease of ignition' of the diesel measured in a test engine. Diesel is injected in a compression-ignition engine when the piston is approaching the cylinder top dead center (near full compression) and it must ignite immediately. Specifies the percentage of cetane (*n*-hexadecane, *n*-$C_{16}H_{34}$) in a mixture with *iso*´-cetane (2,2,4,4,6,8,8-heptamethylnonane, *i*-$C_{16}H_{34}$) that gives similar engine performance as the test fuel. The cetane number must be > 51 in Europe and > 47 in North America. Linear chained alkanes ignite easier than branched ones and high cetane number gives fast ignition.

Lower heating value: Describes the energy density in the fuel. Usually around 43 MJ/kg or 36 MJ/l for diesel oils.

share. Accordingly, suggestions for wider definitions regarding naming of fuels have been suggested [24–26]. For the sake of clarity, we will refer to the technical–chemical terms for each fuel in this review. Importantly, biodiesel is not pure vegetable oil or fat. Engine and fuel system require modifications to be able to run on such fuels and these changes are often illegal for road vehicles and lead to annulment of engine warranties and specifications for emissions. Combustion of vegetable oil in the engine often becomes incomplete and both particle and NO_x emissions are reported to rise. Plant oils are also often too viscous to be pumped in the fuel and injector systems [3].

A considerable number of reviews on production of diesel from biomass have been published in recent years, especially regarding FAME [27–30], but also on more advanced fuel production [31,32]. Here, however, we highlight the catalytic technologies necessary for the conversion of various biomasses into diesel fuel, and we compare the various catalytic technologies in terms of fuel properties, biomass resources and process intensities.

▪ Diesel properties

Diesel may be defined as liquid fuels that can be used in an unmodified diesel engine and has fuel properties similar to those of a middle distillate (or so-called middle-cut) from petroleum oil refining, from which most of the world's diesel fuel is produced. Another part of it is produced via hydrocracking of vacuum gas oil from the bottom of the distillation column. The number of carbon atoms in the fuel ranges from 12 to 18 and consists primarily of alkanes. The most important properties for diesel oil as well as for characterizing alternative diesel fuel relative to the norm for petroleum diesel fuel are the **cetane number** describing the ignition properties, **lower heating value** (connected with the density) describing the energy content and the cold flow properties described by the **cold filter plugging point**. Other relevant measures for describing the cold properties are **pour point** and **cloud point**.

The contents of unwanted sulfur and aromatics are a measure of the environmental quality of the fuels. The long-term **storage stability** is relevant for refiners and end-users. The **flash point** is a measure of safe handling temperature, while **viscosity** and **lubricity** describes behavior in the fuel system and engine.

Transesterification & esterification of fats & oils

The most applied and studied method for producing diesel from biomass is the alcoholysis or transesterification of fats and oils to yield fatty acid alkyl esters. Usually the alcohol is methanol due to lowest cost, ease of separation and high reaction rate, whereby FAMEs are formed [33]. FAME can be used directly in the engine without modification and be mixed in all ratios with petrochemical diesel fuel. The global production of FAME in 2008 reached 11.1 Mton – of these, the EU countries produced 7.76 Mton and the USA 2.33 Mton [5,201,202].

▪ Industrial production of FAME

Fats and oils consist primarily of triglycerides (TGs). These, as well as mono- and di-glycerides can be transesterified into FAMEs by methanol **(Figure 2A)**. The sources of the TGs are all types of vegetable oils, animal fats or waste greases [34]. A successful transesterification

leads to two phases: glycerol and excess methanol separated from FAME. Notably, equimolar glycerol is obtained as a byproduct for every three FAME molecules produced. The oil and FAME phase (nonpolar) and the alcohol phase (polar) are not directly miscible with each other. In industrial practice, the reaction is normally performed at approximately 60–70°C and with a few wt% of homogeneous alkali metal hydroxides or methoxides as base catalyst. Typically potassium hydroxide is preferred as it is nonhygroscopic and cheap [35,36].

The transesterification is equilibrium driven and in fact reversible. However, due to use of two-three times molar excess of methanol and the immiscibility of FAME and alcohols, the transesterification of oils typically reaches over 99% yield after a few hours of reaction [33].

Initially the reaction is slow and dependent on vigorous mixing of the two phases (e.g., by stirring) to get a large interfacial area between the two phases. During reaction, di- and mono-glycerides are formed and these compounds act as emulsifiers for the reaction mixture. Once the transesterification is nearing completion, the two phases start to separate again (settling). Industrially this reaction is normally done in a stirred batch-reactor with a separate settling-tank, since the settling is often slower than the transesterification reaction [37,38]. However, continuous reactors for FAME synthesis have appeared over the last couple of years using homogeneous catalysts. This is advantageous in terms of process operation and control, labor demand, supervision and optimization of product quality.

The homogeneous, base-catalyzed transesterification works efficiently, but oils and fats may contain free fatty acids (FFAs). Waste fats have especially high amounts of FFAs: 2–7 wt% for used cooking oils, 5–30 wt% for waste animal fats and abattoir waste and some trap greases often above 50 wt% [3]. When the feedstock contains more than approximately 0.5–1 wt% of FFAs, these will react with the basic catalyst and form soap (i.e., FFA salt); whereby:

- Base otherwise intended for transesterification will be consumed;
- The formed soap emulsifies the phases and hinders the settling and separation after reaction;
- Water formed by saponification lead to basic hydrolysis of the glycerides yielding more soap.

For these reasons, the FFAs must first be esterified with methanol to form FAMEs. Esterifications are acid catalyzed and in the biodiesel industry a few wt% sulfuric acid (H_2SO_4) is normally used for this purpose. Sulfuric acid has the advantage of being both cheap, a strong acid and very hygroscopic. The mixture of methanol and fat is esterified at 60–70°C with stirring for a few hours to bring the content of FFAs under 0.5 wt% (as is shown in Figure 2B) prior to transesterification.

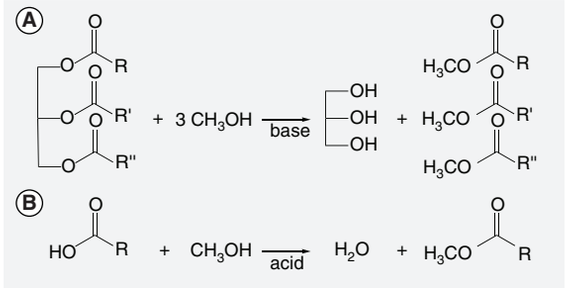

Figure 2. Production of fatty acid methyl esters. (A) Base-catalyzed transesterification of a triglyceride with methanol to form glycerol and fatty acids methyl esters. **(B)** Acid-catalyzed esterification of free fatty acid with methanol to form water and fatty acid methyl esters.

In principle, the transesterification can be catalyzed by both bases and acids, leaving room for a one-step acid-catalyzed process, but the base-catalyzed reaction is several orders of magnitude faster than the acid-catalyzed reaction [33]. Temperatures of at least 150–200°C are needed to perform transesterification with sulfuric acid to get a reasonable space time yield, thus requiring pressurized equipment (due to the vapor pressure of methanol, bp.: 64.6°C) and therefore it is usually considered undesired. The esterification by homogeneous acid also leads to other challenges:

- Neutralization and basification before the transesterification and neutralization before final separation of the alcohol phases must be performed. This yields large amounts of alkali salts as byproducts (usually K_2SO_4 and $KHSO_4$) with no immediate use;
- Water formed during esterification and neutralization lead to saponification in the consecutive basic transesterification reaction;
- Homogeneous catalysts must be added constantly, which can be costly;

Key terms

Cloud point: Temperature where, upon cooling, visible diesel crystals start to form as a cloud wax; cloud point is usually a bit higher than cold filter plugging point.

Storage stability: Arbitrary evaluation of the ease of long-term storage of the diesel fuel.

Flash point: Safety measure indicating the temperature of the liquid fuel at which a flash can ignite vapors over it.

Viscosity: Measure (in mm^2/s) of the 'thickness' of the liquid fuel. Too high viscosity makes pumping difficult.

Lubricity: Lubricating properties of the diesel, measured as the 'wear' imposed when rubbing a steel ball against a steel disk immersed in the fuel.

Cold filter plugging point: Temperature at which a test filter is plugged with diesel wax crystals; the most common way to report cold properties of diesel. Can be lowered by additives, which is generally necessary in cold climates.

Pour point: Measured by first cooling a diesel sample to solid and then heating it up; the temperature within regular intervals at which the diesel starts flowing is the pour point.

- The formed salts ends up partly dissolved in the glycerol and methanol phase, which must be purified by decantation and distillation after reaction and settling [38].

It is of immense interest to substitute the homogeneous catalysts in FAME production with heterogeneous catalysts. This would fit well into a flow reactor with solid catalyst bed, for instance by using statis mixers and it would greatly ease downstream separation, prevent salt byproducts, lower the catalyst inventory cost and prevent corrosion by the acidic H_2SO_4 [39]. An extensive number of organic and inorganic bases and acids have been proposed in literature as catalysts for the two reactions.

Inorganic metal-oxide bases

A range of different inorganic bases have been tested in the transesterification reaction; alkali or earth-alkali metal oxides or hydroxides are generally very basic and thus active, but normally dissolve in methanol [40]. ZnO or Al_2O_3-ZnO mixed oxide were investigated as well as rare-earth oxides, but both required high temperatures (at least 200°C) for conversion of vegetable oils with methanol to FAME [41,42]. Bimetallic oxides of calcium ($Ca_2Fe_2O_5$, $CaMnO_3$, $CaCeO_3$, $CaTiO_3$ and $CaZrO_3$) were found to catalyze transesterification with methanol at 60°C with good reusability of the catalysts [43]. Porous silicates such as zeolite BEA, USY and FAU, and mesoporous silicalites such as KIT-6, ITQ-6, SBA-15 and MCM-41, have been ion-exchanged with La^{3+}, Mg^{2+} or K^+ ions and tested in FAME production as well, however high transesterification activity often requires higher temperatures (>150°C) with these porous materials [44–46]. Hydrotalcites have shown superior transesterification activity to some inorganic porous bases dependent on composition and calcinations conditions [47–51]. Activity has also been enhanced by doping with Cs, Ba, Sr or La, by substituting Al with Fe or Mg with Co, or by embedding hydrotalcite on a polymer support [52–55].

Basic organic amines

A number of different organic amines and derivatives have been shown to be applicable for the transesterification of oils and fats. At an early stage, a number of substituted alkylguanidines or cyclic guanidines have been suggested as very active catalysts for transesterification and substituted tetramethyl guanidine (R-TMG) or substituted 1,5,7-triazabicyclo[4,4,0]dec-5-ene (R-TBD) nested on PS/PVB polymer supported analogoues [56]. Carbon nanotubes doped with amines or gem-diamines have recently shown activity in the transesterification of TG at conditions near normal industrial operating temperatures [57,58]. Synthetic solid bases such as methyl-substituted phosphazenium, either unsupported or linked to silica support, or mesoporous MCM-41 functionalized with tin–triflate or amines have been tested for transesterification with promising results [59–62]. Even base-functionalized metal–organic frameworks and supported quaternary substituted ammonium groups were also shown to be promising organic materials for basic methanolysis of oils and fats [63,64].

Acidic inorganic oxides & derivatives

Supported tungstated catalysts ($WO_3/M(P)O_x$) have been investigated for the esterification of FFA with methanol between 60 and 200°C and at the highest temperatures full conversion of FFA is easily obtained while transesterification of TGs also takes place [65–68]. Related to the solid tungstated oxides are the so-called heteropolyacids based on tungsten or molybdenum phosphate. These are strong acids in their protonated form and can be supported on metal oxide or even carbon [69]. Partial substitution of protons with other cations, for instance as $Zr_{0.7}H_{0.2}PW_{12}O_{40}$, increased the acidity and allowed both esterification and transesterification at 65°C within 4–8 h [70]. The completely protonated heteropolyacids $H_3PW_{12}O_{40}$, $H_4SiW_{12}O_{40}$, $H_3PMo_{12}O_{40}$ and $H_4SiMo_{12}O_{40}$ had different acidities, which correlated with their transesterification activities [71]. $H_3PW_{12}O_{40}$, supported on various materials easily catalyzed the esterification of FFA in waste oils at 25–60°C [72,73]. A multifunctionalized composite of $H_3PW_{12}O_{40}$ supporting Nb_2O_5 or Ta_2O_5 was active for esterification at benign conditions, and activity could be increased by adding nonpolar alkyl functionalities [74,75], although dissolution of the acid in methanol can occur.

Sulfated metal oxides are related to their tungstated analogues and sulfated TiO_2, SnO_2 and ZrO_2 have been suggested as acidic catalysts for the esterification to form FAME as well as for the simultaneous transesterification of the TGs [76–80]. The same oxides were further evaluated supported on or mixed with high surface-area supports of Al_2O_3 or SiO_2 [76,81]. Leaching of sulfate to the methanol from SO_4^{2-}/MO_x is, however, a common problem [80].

Various Brønsted-acidic zeolites have been shown to esterify FFA at 60 °C, whereas higher temperature was required for Brønsted-acidic Al-MCM-41 [82,83]. Functionalization of MCM-41 or SBA-15 via anchoring with acidic WO_3, heteropolyacids and sulfonic acid functionalities also facilitated esterification of FFA with methanol [84,85].

Organic sulfonic acids

Amongst the acidic catalysts for esterification one type of organic acid has been studied extensively, namely sulfonic acids (R-SO_3H). Simple sulfonic acids include $MeSO_3H$ and *p*-toluenesulfonic acid, while solid sulfonic acids can be prepared by anchoring the sulfonic

functionality onto polymeric supports by treatment with sulfuric acid; the resulting acid is often as strong as or stronger than sulfuric acid.

Resin-type sulfonic acid can be bought on a technical scale, for instance ion-exchange resins [86]. Esterification can be performed over various Amberlyst-resins and Dowex HCR-W2 between 30 and 65°C, which yielded a satisfactory esterification of FFA [87]. A comparative study between the sulfonic resins NKC-9, 001x7 and D61 proved the former to be superior in the reaction of FFA and methanol at 60°C [88].

A number of polymer-based sulfonic-acids have been prepared for esterification and studied, for instance starting from polymers such as PVA-PS/PVB, PS, sulfonated PV and PS, mesoporous silica or polyanilines deposited on carbon [89–93]. The incorporation of sulfonic acid groups into the matrixes can be tailored and is usually between 0.6 to 6.0 mmol/g of the total supported catalyst mass. Esterification of FFA may be performed under normal operating conditions of 60°C with one–two times molar excess of methanol.

Another approach for obtaining a sulfonic acid-containing polymer was first proposed by Toda *et al.* [94]. A carbohydrate source, for example, sucrose or cellulose, is carbonized (or pyrolyzed) under inert atmosphere of around 400°C for 4–24 h. The resulting coke consisting of small graphene layers is then sulfonated with sulfuric acid at elevated temperatures (~150°C) also for 4–24 h. Despite low surface areas of the material itself, the catalyst was found to be very active in the esterification of FFA at 60°C and had acid strength comparable to that of H_2SO_4 [95,96]. At 150°C and 17 bars a carbohydrate-based sulfonic acid was also active for transesterification, but leaching of sulfonic acid functionalities resulted [97]. Impregnation upon mesoporous silicas allowed tailoring porosity and hydrophobicity and thereby enhancing the esterification rate [98].

▪ Ionic liquid catalyzed (trans-)esterification

Within the last few years sulfonic acid functionalized acidic ionic liquids (ILs) have been suggested as alternative Brønsted acid catalysts [99]. ILs are salts, usually organic, with a melting point below 100°C and can be used as catalysts and/or solvents for numerous reactions. Although ILs have been reported as reaction media for homogeneous catalysts for transesterification, ILs may further be functionalized by incorporating sulfonic acid functionality, yielding both a liquid reaction medium and a very strong acid as catalyst [100–102]. This approach is attractive for the esterification and transesterification reactions [99]. The cation can be based on substituted imidazolium or pyridinium ions functionalized with sulfonic acid, and anions should preferably be very weak bases, for example, triflate or methyl sulfonate [99,102,103]. The melting point of the ILs must be below the reaction temperature for FAME synthesis, otherwise the activity is too low [102]. By functionalizing the IL with more sulfonic acid functionalities the IL exhibits an even higher catalytic activity [104].

▪ Enzymatic (trans-)esterification

In addition to chemical catalysts, lipases from different microorganisms can also be applied in FAME synthesis. The conditions are often mild, usually around ambient temperature (i.e., 25–50°C), and both transesterification and esterification are catalyzed [33]. For the lipases to be applied in industrial FAME production they must be immobilized on a porous support [105–107]. To date the catalytic activities reported are not of the same magnitude as the chemical catalysts, although the activity can sometimes be enhanced by using a co-solvent [35,108,109]. Some lipases may also be rendered inactive by too high concentrations of methanol and continuous addition of methanol, genetically altering the lipases or switching alcohol can therefore be necessary [110,111].

▪ Super-critical (trans-)esterification

As an alternative to using catalysts, the esterification and transesterification may be performed using supercritical methanol (P_C = 81 bar, T_C = 234.5°C) at very short reaction times. Adding a co-solvent, such as carbon dioxide or hexane, or a base to the supercritical methanol can further improve the reaction rates [112–114]. However, the harsh supercritical conditions require high-pressure equipment and handling, and the energy and economical balance for this may not be advantageous.

▪ Glycerol

The main byproduct of the transesterification is glycerol **(Figure 2A)**. The increasing amount of FAME produced accordingly yields increasing amounts of glycerol, since approximately 100 kg of glycerol is formed per tonne of FAME made. Valorization of glycerol can therefore be an important contribution to the overall economy of the FAME process. A few suggested reactions of glycerol into more valuable chemicals include reduction, dehydration, oxidation, or complete gasification into synthesis gas for production, for example, methanol. Some of these products are shown in **Figure 3**, but we direct readers to the reviews on glycerol conversion by Zhou and co-authors [115] or Johnson and Taconi [116] for more details.

▪ Overview of catalysts for FAME production

An overview of the catalysts for FAME production via esterification and transesterification of fats and oils with alcohol are found in **Table 1**.

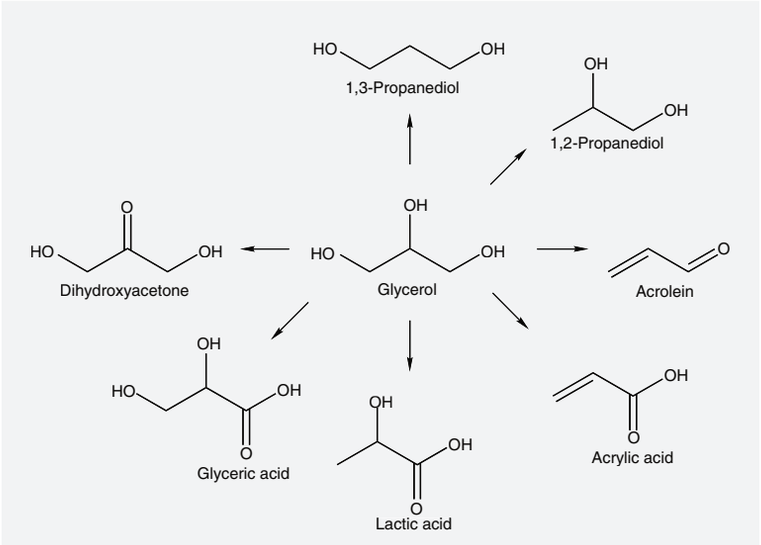

Figure 3. Useful products from oxidation (with molecular O_2 or H_2O_2 over supported noble metal catalysts), reduction (with H_2 over supported transition metal catalysts) and dehydration of glycerol (via acid catalysis).

Hydrodeoxygenation of fats & oils

The hydrodeoxygenation (HDO) of fats and oils is an alternative approach for upgrading fatty feedstock. It was first industrialized by the Finnish company Neste Oil at their refinery in Porvoo, Finland, as described by Koskinen *et al.* [24] and Mikkonen [26]. The approach usually requires hydrogen and may be visualized as shown in **Figure 4**. Based on recent literature the catalysts for deoxygenation of fats and oils can be divided into three categories: supported sulfided metals, supported (noble) metals and micro- or meso-porous acid–base catalysts for cracking-type reactions.

Table 1. Respectively basic, acidic and alternative esterification and transesterification catalysts for use in the production of fatty acid methyl esters.

Catalyst	Advantages	Challenges
Organic amines	Strong bases Porosity via supporting	Water and methanol tolerance
Basic inorganic oxides	Temperature stable	Possibility of dissolution
Organic sulfonic acids	Very acidic Porosity via supporting	Temperature stability
Acidic oxides and heteropolyacids	Very acidic Tailoring of surface properties	Dissolution in methanol
Sulfated metal oxides	Very acidic	Sulfate leaching
Ionic liquids	Reaction medium and catalyst Properties can be tailored Anchoring possible Can catalyze transesterification	Separation problems Possible eco-toxicity issues
Immobilized enzymes	Benign reaction conditions Ease of reuse Both esterification and transesterification	Low activity Tolerance to methanol

Sulfided metal catalysts

Kubička and co-workers evaluated the HDO of rapeseed oil over sulfided CoMo and NiMo supported primarily on Al_2O_3 in a number of studies at 250–350°C and 7–110 bars H_2 [117–120]. Activity of sulfided NiMo/Al_2O_3 superseded that of separate MoS_2/Al_2O_3 and NiS/Al_2O_3 in liquid phase HDO and full conversion in rapeseed oil conversion over three commercial sulfided NiMo/Al_2O_3 catalysts at 70 bar hydrogen was only achieved at > 310°C, while lower temperatures left FFAs and TGs in the product. Using a porous, Brønsted-acidic support of Al-MCM-41 for sulfided CoMo instead of Lewis-acidic Al_2O_3 did not alter activity, but MCM-41-support without Al in the framework was less active at 20–110 bar H_2 and 300–320°C.

Huber *et al.* co-treated sunflower oil and heavy vacuum oil over sulfided NiMo/Al_2O_3 at 300–450°C and 50 bars [121]. Maximal carbon yield of 71% of C_{15}-C_{18} *n*-alkanes were obtained from the mixture, and cracking reactions and isomerization of products became more pronounced at higher temperatures. Šimáček and co-authors observed that a co-desulfurization-deoxygenation of 5% rapeseed oil in vacuum gas oil at 400–420°C yielded similar fuel product properties as pure vacuum gas oil desulfurization [13].

Donnis and co-workers confirmed that both reduction and decarboxylation can take place in the HDO over sulfided NiMo/Al_2O_3 and obtained selectivity to decarboxylation products from rapeseed oil of up to 64% at full deoxygenation in light gas oil at 45 bar H_2 and 350°C [22]. Guzman *et al.* performed HDO of pure palm oil over sulfided NiMo/Al_2O_3 at 40–90 bar H_2 and 350°C and reported that selectivity to *n*-alkanes with even carbon numbers (complete reduction) increased with pressure [8].

Krause *et al.* studied the HDO of heptanoic acid, heptanol, methyl and ethyl heptanoate over sulfided CoMo/Al_2O_3 and NiMo/Al_2O_3 at 250°C and 15 or 75 bar H_2 [122,123]. NiMo, but not CoMo was very sensitive to the sulfidation conditions. Unsulfided catalysts were neither very active nor selective towards C_6 or C_7 alkane formation.

The sulfided catalysts pose the inherent challenge that they deactivate (desulfidize) over time if sulfur is not added periodically, for instance as H_2S or CS_2 or by co-treating with sulfur-containing compounds such as refinery gas oils. The consumption of hydrogen should optimally be minimized to save costs, so higher selectivities for decarboxylation or

decarbonylation, as described by Donnis *et al.*, should be aimed for if methanation can be avoided [22]. A great asset of this procedure is the absence of formed aromatics.

Transition metal catalysts

Most studies of deoxygenation of fatty acids and their derivatives over metal catalysts have been performed by Murzin and co-workers, although others have contributed as well. Especially conversion of stearic acid, ethyl stearate and tristearine to alkanes have been extensively studied and the reaction routes elucidated in semibatch-reactors between 270 and 360°C, either in gas mixture with H_2 or inert gas at up to 40 bars. By screening a range of active catalyst metals and supports, Snåre *et al.* found that platinum or palladium supported on carbon were most active and had the highest selectivities for decarboxylation of stearic acid to *n*-heptadecane [6].

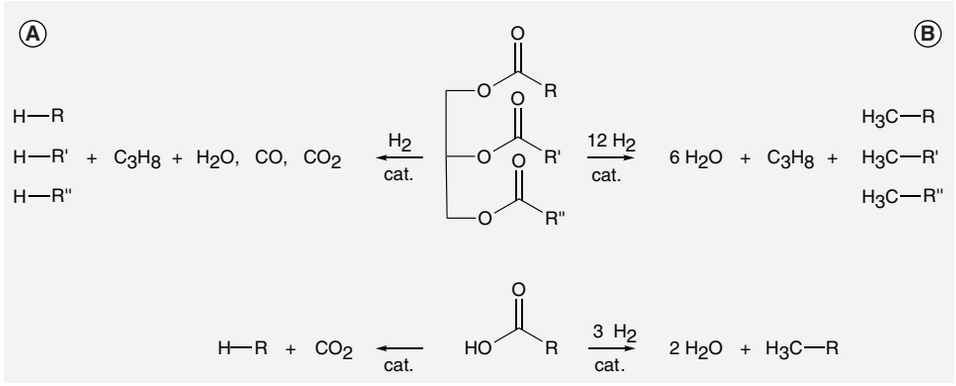

Figure 4. Hydrodeoxygenation of triglycerides and free fatty acids. (A) Decarboxylation and decarbonylation of feedstock, which is the prominent route with supported transition metals. **(B)** Complete reduction with H_2 of the feedstock, which is usually the dominant route over many sulphided catalysts.

In connected work, Pd/C was used as a catalyst to establish kinetic models for deoxygenation of tristearine, ethyl stearate, stearic acid and of other fatty acids to alkanes [9,124,125]. Deoxygenation of the carboxylic acid itself took place almost exclusively via decarboxylation, but ester functionalities underwent more complicated mechanisms [124]. Deoxygenation of methyl octanoate and methyl stearate over Pt/Al_2O_3 at 330°C in He and H_2 gas revealed that H_2 suppressed formation of higher self-condensates of the esters and that decarbonylation was always the primary reaction route [126]. Dehydrogenation of C_{18} tall oil fatty acids and the pressure of hydrogen had a considerable impact on deoxygenation to C_{17}-hydrocarbons over Pd/Sibunit [127]. The deoxygenation of TGs over carbon-supported Ni, Pd and Pt at 350°C without added hydrogen yielded CO_2, CO, CH_4 and lighter hydrocarbons in the gas phase, a range of liquid alkanes and heavier paraffins, and FFAs as intermediates [128].

Palladium and platinum as catalysts have also been investigated on a number of nanoporous and microporous supports. Pd catalysts were investigated supported on SBA-15, mesocellular SiO_2-foam or SAPO-31 for the deoxygenation of stearic acid or sunflower oil [10,129,130]. Hancsók and co-authors deoxygenated saturated vegetable oil over $Pt/H\text{-}ZSM\text{-}22/Al_2O_3$ to isomerized alkanes [131]. Acid functionalities of the support lead to modest isomerization of the formed *n*-alkanes to improve the cold properties of the fuel, but undesired cracking and deactivation also took place if the temperatures were too high.

From literature it appears that deoxygenation of carboxylic acids deoxygenate via decarboxylation ($-CO_2$), while ester undergo decarbonylation (-CO). This selectivity is an advantage, avoiding the immediate use of hydrogen. However, hydrogen may be required to avoid deactivation by aromatization or CO poisoning. This leads to a problem of methanization of CO or CO_2 with H_2, a highly undesirable situation. The methane may be burned for process heat or steam reformed back to H_2 and CO, but this is costly and the separation of the gases alone may be tedious. Deoxygenation of real feedstocks such as vegetable oils or waste fats is sparsely studied and more challenging to convert over noble-metal catalysts. They contain impurities such as salts, sterols and phospholipids. Furthermore, the TGs are always more or less unsaturated, which is believed to cause deactivation by coking via cyclization, dehydrogenations and Diels–Alder reactions. More research is needed to unravel the mechanisms behind deactivation by coking and how to avoid it, but saturation of the double-bonds with H_2 prior to deoxygenation may be a solution [125,127,132].

Cracking-type deoxygenation

Resasco *et al.* studied deoxygenation of methyl octanoate over various zeolites. Using H-ZSM-5 at 500°C, lighter hydrocarbon gases and aromatic products were formed, the latter of which proceeded through self-condensation products such as tetradecane, 8-pentadecanone and octyl octanoate. The aromatization selectivity, as well as the conversion, was much lower at 400°C. Interestingly, with zeolite X, longer hydrocarbons (C_{14}-C_{16}) and no aromatics were formed over basic CsNaX, while the weakly acidic NaX resulted in aromatics before deactivating [133,134].

H-ZSM-5, rare-earth-modified Y-zeolite and MCM-41 have been used to crack palm oil at 400–500°C. The products were mainly gasoline- and diesel-range hydrocarbons, and the selectivity to the latter rose

with decreasing cracking temperature and thereby also decreasing conversion [11,135]. Heptadecane, heptadecene and cracking products, such as alkanes and minor amounts of carboxylic acids, were found during oleic acid decomposition at 400°C over basic hydrotalcites [12]. Analogous products were formed in soybean oil pyrolysis over Al_2O_3-supported tin and zinc oxides at 350–400°C [136].

Both diesel- and gasoline-range products and varying production of gas result from the cracking of fats and oils. Aromatics are also produced, which are undesired in diesel fuel [23]. The aromatization inside micro- and meso-porous catalysts leads to deactivation by coking, especially with acidic porous materials. Regeneration could, however, be performed in a technical FCC system by burning off the coke in a regeneration zone (provided that the catalyst can endure this treatment).

▪ Overview of catalysts for HDO of fats

A comparison of the catalysts for HDO of fats and oils mentioned in the HDO of fats and oils section is given in Table 2.

Alternative technologies for biomass diesel

The potential supply of fats and oils at present can only cover a minor fraction of the diesel demand, although algae farming may provide a supply of more oils on the long term. Utilization of the most abundant biomass resource, namely lignocellulose (e.g., straw, wood and fibers) is therefore imperative. Three potential and complementary strategies are proposed for this, namely thermal depolymerization of biomass and upgrading of the resulting bio-oils, APR of carbohydrate biomass and gasification of biomass followed by FTS.

▪ Upgrading of bio-oils

One auspicious way of dealing with lignocelluloses relevant for diesel production is upgrading bio-oils. These are usually produced through flash pyrolysis, that is, fast heating to 400–650°C of finely ground of wood or straw at short residence time, often under inert gas and with sand or other ceramics as a heat carrier. This protocol produces a gas fraction containing various carbonaceous gases, a residual char fraction and varying amounts of condensable, multifunctional tar called flash pyrolysis-oil or just bio-oil. Another less-explored way is through the conversion of aqueous sludge or dissolved or suspended biomass in near-critical water with inorganic catalysts; so-called hydrothermal upgrading of biomass or the proprietary CatLiq™ process. This harsh treatment also yields a bio-oil fraction after decantation [137,138].

A few of the typical aromatic bio-oil compounds are shown in Figure 5. Depending on the pyrolysis conditions the output of bio-oils may be more than half of the biomass input weight.

Upgrading of bio-oils from flash pyrolysis bears some resemblance to HDO of fatty feedstocks, and the catalysts can also be divided into the same categories, namely cracking-type, supported sulfided metals and supported transition metals, with the notable inclusion that bio-oils may also be treated over a catalyst during the pyrolysis itself – this is known as catalytic pyrolysis. The difference from the well-defined TG molecules largely complicates the HDO of bio-oils. These processes will remove a part or all of the oxygen from the oils (lower the O/C-ratio) and saturate double-bonds (increase the H/C ratio). Removal of much of the oxygen in the bio-oils, as well as water, can be a pretreatment to hydrocracking in conventional refinery operation, for instance together with normal petroleum gas-oil feeds, justifying two-stage processes [139]. Supported metal and sulfided metal catalysts have the advantage of working at lower temperatures than the cracking of acidic or basic catalyst, but they do require hydrogen to function as well as sulfurous compounds in the feed for the catalysts to remain active. However, aromatics in the deoxygenated bio-oils are generally undesired for diesel fuel [23].

Cracking-type upgrading

Zeolites, especially acidic, are suited for cracking bio-oils since they are crystalline and therefore more robust for the harsh conditions in cracking reactions with water vapor present. They can also be easily regenerated by burning away coke. Aho and co-workers studied pyrolysis and cracking, as well as catalytic pyrolysis of pine sawdust at 400–450°C over quartz sand and zeolites H-BEA, H-FAU, H-MFI or H-MOR and some of their Fe-modified counterparts. The highest removal of oxygen was achieved with H-MFI [140,141]. Cracking of bio-oil was studied at 500°C on H-FAU and Ni-FAU zeolites, giving low liquid yields and high yield of C_2-C_4 and C_{5+} gases. Notably, methane formation

Table 2. Comparison of sulfided metals, transition metals and porous ceramics as catalysts for hydrodeoxygenation.

Catalyst	Advantages	Challenges
Supported sulfided metal	Not easily deactivated Co-treating with petrodiesel	Needs sulfur addition H_2 consumption
Supported transition metals	High selectivity towards decarboxylation or decarbonylation	H_2 consumed by side reactions Deactivation Methanation
Micro/mesoporous ceramics	No hydrogen needed Easy regeneration after deactivation	Coking Diverse product range; low diesel selectivity

was avoided [142]. Co-cracking of a distillation residue with 10 wt% of bio-oil at 520°C over a commercial FCC catalyst was found feasible and yielded normal coking behavior due to a low total oxygen concentration in the feed [143]. At temperatures up to 650°C, the catalytic pyrolysis of lignin and glucose over H-MFI and other zeolites resulted mostly in cracking to aromatics, coke and light gases [20,144,145].

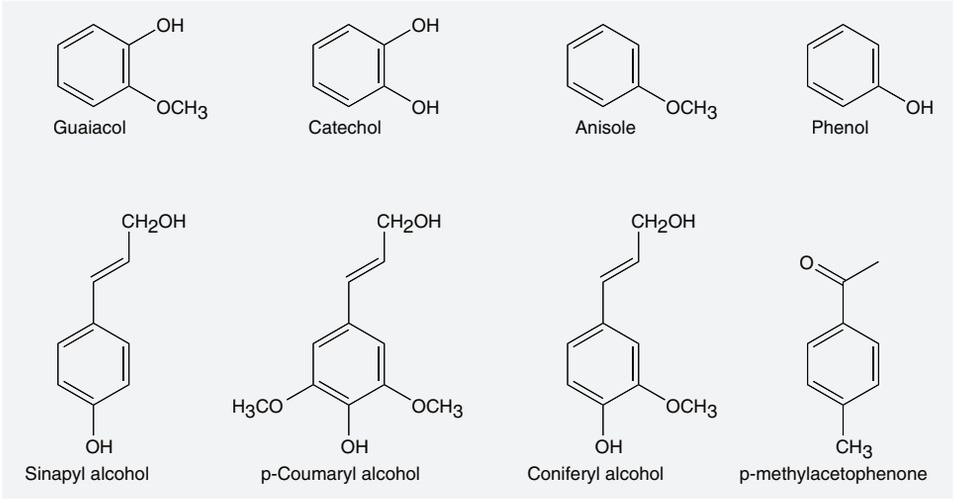

Figure 5. Aromatic monomers in lignin networks and also found as a major part of many bio-oils.

Sulfided metal catalysts

The HDO of bio-oils over supported sulfided catalysts were studied over a decade ago, for instance by Delmon *et al.* [146]. Sulfided CoMo/Al_2O_3 and NiMo/Al_2O_3 are usually the catalysts of choice. More recently, the sulfided CoMo/Al_2O_3 was shown to be less active than sulfided NiMo/Al_2O_3 for the HDO of guaiacol in batch mode at 200–350°C, but the CoMo was more selective to HDO products [147]. Different phenolic and aliphatic oxygenates were converted over supported sulfided CoMo and NiMo catalyst with alcohols, aldehydes and carboxylic acids as intermediates. The acidic γ-Al_2O_3 support also mediated esterification, dehydration and hydrolysis reactions [148]. Bio-oil HDO has been studied in two-step semibatch systems over sulfided NiMo/Al_2O_3. Leaving a few wt% of oxygen as ketones or ethers may be attractive with respect to hydrogen consumption and product properties [149].

Transition metal catalysts

A few reports are available on HDO of bio-oils over supported metal catalysts. The activity of Pd, Pt and Ru with different metal particle sizes supported on for instance carbon, SiO_2 or Al_2O_3 have been tested as catalysts in the HDO of various model oil compounds between 250°C and 350°C and up to 200 bar H_2. An oil yield of 60 wt% with 90 mol% oxygen removal has been achieved from bio-oil, yielding oil with a higher heating value of approximately 40 MJ/kg. Catalysts are reported to deactivate by coking in the pore system [21,139].

▪ Aqueous-phase reforming

An auspicious approach to fuel and chemicals production have been pursued especially by Dumesic and coworkers, who have studied the upgrading of sugars and polyols to hydrocarbons by reforming biomass in water – APR. As shown in **Figure 6A**, the principle behind this approach is the simultaneous catalytic reduction and reforming of sugars and sugar derivatives.

Polyols are very soluble in water, but once they get sufficiently reduced, for instance to monofunctional hydrocarbons, they spontaneously separate and form a nonpolar hydrocarbon-phase. This phase contains a mixture of different monofunctional hydrocarbons – ketones, carboxylic acids, alcohols and more or less saturated furanic heterocycles with a carbon range of C_4-C_6. Gas-phase products are CO_2 and minor amounts of C_1-C_6 alkanes [150,151]. A sweep-stream of hydrocarbons can enhance the separation [15].

Aqueous reforming of polyols

A range of catalysts have been suggested for the APR of sorbitol, but Pt and Pt-Re catalysts supported on ceramics or carbon have been found advantageous and it is suggested that a bifunctional catalyst containing a metal and an acid functionality are needed to facilitate all reactions [150,152]. They facilitate both dehydrogenation and C-C-scissions to liberate adsorbed CO species, which are then water-gas-shifted to CO_2 and hydrogen [150]. APR is usually performed at approximately 200–250°C and at pressures of 18–40 bar, and in an aqueous phase. Aromatization, methanization and CO production are for these reasons minimized.

Condensations prior to reduction

Carbohydrates are built by units of maximally six carbon atoms, meaning that hydrocarbons with more than six atoms require C-C-coupling reactions. This may be done prior to reduction, as carbohydrates may undergo aldol condensation to couple ketones and aldehydes to other carbonyls. This can take place via 5-(hydroxymethyl) furfural by dehydrations and isomerizations from fructose, glucose and cellulose [153]. One or two molecules of 5-(hydroxymethyl)furfural may for instance be reacted

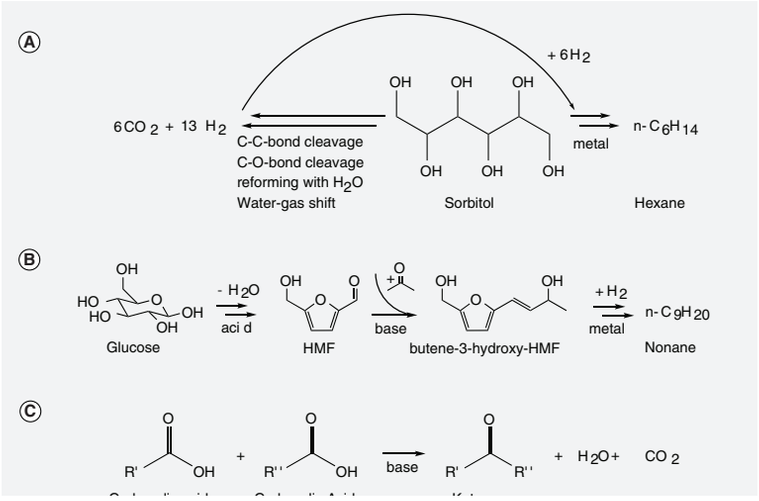

Figure 6. Reforming, reduction and condensations of carbohydrates.
(A) Principle in aqueous-phase reforming of carbohydrates and derivatives over dual-function acid and metal catalyst. **(B)** Acid-catalyzed isomerization and dehydration, base-catalyzed aldol condensation (C-C coupling), and reduction of carbohydrates over supported metal catalysts.
(C) Base-catalyzed ketonization of carboxylic acids.

with acetone over basic catalysts, as seen in **Figure 6B**, yielding either a C_9 or C_{15} building block that can be reduced [154].

Product condensation/reduction reactions

A final step in the biomass conversion is the reduction of remaining single-oxygen-containing compounds and unsaturated carbon-carbon bonds. This processing can involve various types of catalytic reactions.

Cracking can be done over acidic zeolites to yield a mixture of light hydrocarbon gases, *iso*-alkanes and aromatics [150]. Light olefins or alcohols obtained via dehydration could be upgraded to larger olefins by oligomerization yielding for instance diesel-length hydrocarbons; γ-valerolactone upgrading was investigated by aqueous-phase ring-opening and decarboxylation to butene over silica-alumina catalyst at 375°C, followed by oligomerization over an acidic zeolite. This yielded over 75% C_{8+} hydrocarbons [155].

Ketonization can upgrade carboxylic acids migrating to the hydrocarbon phase during the APR. The ketonization merges two carboxylic acids together as seen in **Figure 6C**, for instance over an acidic $CeZrO_x$ catalyst and esterification with alcohols present in the organic phase also takes place [156,157]. Ketonizations have even been achieved with acids in flash pyrolysis oils with reasonable success [158]. Two ketone molecules, directly from APR or from subsequent ketonization, may react under acidic conditions to form an enone as condensate (an unsaturated ketone) by splitting off water and then be reduced, as has been proposed over $Pd/Ce_xZr_{1-x}O_y$ above 300°C [157,159].

Sugars and polyols are not as cheap as waste lignocellulosic biomass, so a greater feedstock tolerance would make this process extremely viable, for instance, such as the cascade-process recently proposed by Serrano-Ruiz *et al.* from cellulose via γ-valerolactone and ketonization to 5-nonanone [160]. Larger water-soluble biomass-derived molecules may pose problems to APR, as they can result in coking.

▪ Gasification & FTS

By gasification of coal or biomass or steam reforming of natural gas, a synthesis gas (syn-gas) consisting of CO and H_2 can be obtained, which can then be used for the FTS yielding primarily linear-chained alkanes. The principle behind this approach is shown in **Figure 7**.

Gasification

The gasification of biomass has been extensively studied, yet a range of technical challenges remain. All types of biomass may in principle be gasified and then converted, but differing reactivities of various raw materials dominate the processes. Usually, the biomass is heated to 700–1100°C in a fixed- or fluidized-bed system, either in inert gas or with minor amounts of oxygen (resulting in combustion reactions to heat the reactions) and usually at low pressures, with steam and/or other recycled process gases. The pyrolysis and gasification is a gradual process in which the biomass particles degases and volatilizes step-wise [161]. Often temperatures of at least 1000°C are necessary for total carbon conversion to gas, depending on the feedstock and the conditions used, as alkali and earth-alkali ions affect the gasification reactivity [162].

Catalytic gasification or gasification in super-critical water may allow conversion at lower temperatures requiring less expensive equipment [163–165]. Through optimization, however, it was found that only at 400°C the noncatalytic gasification efficiency in air-steam mixtures in a bubbling fluidized bed could be as high as 60% [166].

Quenching must be performed to stop gas-phase reactions downstream. However, some tar is still produced during gasification [167], which can clog up pipes downstream upon cooling and form coke on surfaces [168,169]. Sulfur-, phosphorous- and nitrogen-containing compounds or tars contained in the producer gas may also poison the catalysts downstream, and catalytic removal of these compounds has been reviewed [168,170].

Fischer–Tropsch synthesis

A vast amount of research literature is available about FTS catalysis [203], which is usually performed by metal oxide-supported metals at 150–330°C and 50–200 bar. Supported ruthenium has been shown to be the most active metal for FTS, but supported iron and cobalt are used industrially due to lower price [171]. The Co or Fe

may be doped with smaller amounts of other metals, for instance Mn, Ni, Pt, Ru, K or Ce.

Water and straight-chain alkanes **(Figure 7)** are the main FTS products, the latter being ideal for diesel fuels. An important feature of the reaction is that if diffusivities and steric effects are disregarded, the weight fraction of a certain carbon chain length (*i*) is given from the statistical probability of chain growth, α, by the Anderson–Schultz–Flory-distribution: $W_i = i \cdot (1-\alpha)^2 \cdot \alpha^{i-1}$.

Often the selectivity is expressed as the yield of the most desired hydrocarbons, namely those with a chain-length of at least five carbon atoms, C_{5+}. FTS-catalysts always form methane to some degree, and the higher α is, the less methane is formed. Impurities of aldehydes, alcohols and fatty acids are also formed however, which must be reduced if FTS is used for diesel production. Light isomerization might also be necessary to achieve low CFPP [172].

The FTS catalysts are sensitive to poisons, especially sulfur, which form sulfides with the catalyst metal if present above ppm level. The particle sizes and structure of the catalyst metal, as well as the microscopic environment in which they are used, strongly affect activity as well as C_{5+} selectivity [173,174]. The effect on selectivity, activity and catalyst stability of alloying metals or promoting with alkalis are often complex [175–177]. Confinement of active sites can dramatically alter the selectivity [178], while support acidity and microporosity may be used to directly isomerize products [179]. Optimization towards production of longer chain alcohols, aldehydes or ketones is another strategy, since upgrading and drop-in blend for petrol, jet fuel or diesel can then be tailored – or steered towards the production of bulk chemicals via FTS [180,181].

A large part of the carbon from gasification and FTS ends up as CO_2. In terms of carbon capture and storage, this procedure has the advantage of producing concentrated CO_2 – maybe at elevated pressure – a net negative CO_2 emission from gasification and FTS is therefore possible by storing CO_2 from the biomass that was taken up during the growth of the flora [182].

Gasifiers are economy-of-scale equipment – the bigger, the cheaper. On the other hand, biomass from agriculture has a low energy density and needs to be transported a long way to centralized plants, so upgrading the energy density via decentralized pyrolysis plants may be advantageous [183].

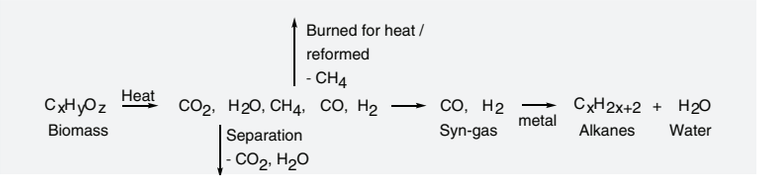

Figure 7. Gasification of biomass to producer gas, consecutive gas cleaning and adjustment, and Fischer–Tropsch synthesis catalyzed by supported Fe or Co catalysts.

Future perspective

▪ Transesterification of fats & oils

The transesterification of oils and fats with alcohol is applied on industrial level today, but the process has a number of drawbacks. The main two disadvantages are the work-intensive batch-mode reaction and the byproduction of salts, which arises due to the use of homogeneous catalysts. A range of both organic or inorganic solid acids and bases have been suggested in literature as heterogeneous catalysts and the most prominent ones are expected to be industrially implemented, especially with fresh vegetable oil feedstock. More advanced continuous flow systems and reusable heterogeneous catalysts for optimized plant economy should also be demonstrated on technical scale. The downstream valorization of glycerol is expected to be a larger contributor to the overall transesterification economy as new glycerol-based commodity chemicals are introduced.

▪ HDO of fats & oils

HDO of fats and oils is performed industrially with sulfided metal catalysts, and these require the addition and presence of sulfur in the feedstock to function. It is therefore relevant to co-treat fats and oils with a sulfur-containing petroleum feedstock to be desulfurized. Nonsulfided catalysts are suitable for treating fatty feedstocks that only contain oxygen functionalities, but their lifetimes should be optimized and deactivation phenomena studied before implementation as they are difficult to regenerate. Cracking of fats and oils over acidic or basic porous materials, which are easier to regenerate, generally yields byproduction of lighter, less valuable gases and poorer selectivities to either of the primary fuels such as gasoline, jet fuel and diesel.

Fats and oils are, however, a sparse resource. The amounts of waste fats or greases from, for example, abattoirs and restaurants are limited and the land use associated with growing vegetable oil resources cannot cope with demand for fuels either. In the coming years, research into routes for biofuels from more abundant biomass waste will become much more important and can be expected to be introduced at an industrial scale as well. The research into flash pyrolysis bio-oils production and aqueous phase reforming and their consecutive upgrading steps can thus become increasingly prominent.

▪ Upgrading of bio-oils

Bio-oils can be considered 'bio-crude oils' due to their chemically complex nature and high oxygen content, which pose challenges in terms of catalytic processing and upgrading. In-depth studies and progress in understanding the catalytic deoxygenation over both sulfided and unsulfided transition metals and porous acids or bases are needed to integrate them in refining. Coupling reactions need to be furnished to yield longer hydrocarbons suitable for different fuel pools, especially for diesel, and maximization of the bio-oil yield must be further studied and implemented. Hydrogen consumption is an issue to be resolved and is dependent on the type of upgrading and the potential ability to reform some of the bio-oil or biomass into hydrogen. The extraction of functional aromatic chemicals instead may be valuable as well. The solid char from the pyrolysis can be gasified or burned for heat, but it can also be used for enhancing or remediating fertility of soils (as 'Terra Preta') and sequestering carbon via the biosphere.

▪ Aqueous-phase reforming

Aqueous-phase reforming is a more benign approach to biomass refining and its ability to reform water-soluble biomass, even cellulose and hemi-cellulose, through acidic hydrolysis is a major asset. The process integration, mild temperatures and pressures makes it possible to conserve a very high energy content of the biomass in the products and facilitate building smaller plants in regional farming districts avoiding long-distance transport of biomass. The methodology circumvents distillation of dilute aqueous solutions of fuel grade compounds (e.g., ethanol). The integrated production and consumption balance described for hydrogen is yet another advantage. It may be expected that multifunctional catalysis gives rise to more selective processes in APR, in turn yielding higher selectivity of targeted classes of hydrocarbons. This is achieved from carbohydrates by catalytic hydrolysis, dehydration, selective condensations and hydrogenations in integrated processes. The catalysts for these reactions are solid acids and bases as well as functional microporous materials, supported transition-metals and their alloys, and multifunctional catalysts.

However, the necessary reactors and separators for different treatments may end up in a vastly complex process layout, which can be complicated to erect in smaller systems.

▪ Gasification & FTS

Gasification may be implemented with all types of biomass, but it faces a number of challenges especially from tar clogging and coking in pipes and unwanted gas-phase reactions in the produced gas. Technical solutions to these issues, as well as furnishing a closer process and heat integration to optimize energy efficiency, should be accomplished. Research into FTS will seek to further optimize selectivity by structural and electronic promotion, encasing or encapsulating active sites; use of meso- and micro-porous materials for synthesis of more advanced and selective catalysts, so as to avoid methane formation and steer selectivity towards a desired range of hydrocarbons. Major logistic challenges also need to be resolved regarding gasification-based biofuels. Dinjus *et al.* described the logistics around collection of biomass for central processing and suggested that residues such as straw or wood are upgraded by flash pyrolysis in small decentralized plants, so that the bio-oil and char fraction, now with a much higher carbon and energy density can be transported to and upgraded at central gasification–FTS plants [183].

Conclusion

In terms of fuel quality, much depends upon the processing and reaction conditions of each process, the feedstock used and mechanistic details of the catalysts, especially from upgraded bio-oils or hydrocarbons from aqueous-phase reformed biomass. However, both the production of FAME or alkanes from oils and fats and the gasification and FTS fuel reached such maturity that the fuels can be compared. This has been attempted by Mikkonen [26] and Knothe [184].

Production of FAME from fats uses the most benign reaction conditions, the cheapest plant design and may be decentralized, for instance in connection with abattoir waste-treatment or food-production plants. More forcing conditions are used for HDO of fats and oils, and it is more suited for traditional refinery infrastructure with possibilities of heat recovery and easy access to hydrogen and isomerization units.

Gasification and FTS may, in principle, be applied to all types of biomass, but the method requires the most forcing reaction conditions and the most extensive plant design. Gasifiers are economy-of-scale plants and usually pose the largest investment in a gasification and FTS plant, so this procedure is only viable for very big plants and thus huge amounts of available biomass.

The APR and the pyrolysis followed by deoxygenation are intermediate technologies compared with the former. They are much more complex than transesterification or HDO of fats and oils, but they enable cost reduction via process integration, beneficial logistics, upgrading energy density and using more abundant feedstocks. In addition, they can also be used in conjunction with existing refining infrastructure or gasification and FTS.

Primary and easily upgradeable feedstock such as plant oils are not and cannot be available in quantities sufficient to replace the entire diesel oil demand, so waste products from agriculture and forestry hold greater perspective for use in the future. It is necessary that in the future biorefineries have sufficient tolerance to use diverse raw materials as feedstock, primarily in the form of waste. New biorefineries employing these raw materials for biochemicals and biofuels will come online over the coming decade.

Financial & competing interests disclosure

Anders Theilgaard Madsen is thankful to the Danish Agency for Research and Innovation for financing his PhD-stipend through the innovation consortium 'Waste-to-Value'. The authors have no other relevant affiliations or financial involvement with any organization or entity with a financial interest in or financial conflict with the subject matter or materials discussed in the manuscript apart from those disclosed.

No writing assistance was utilized in the production of this manuscript.

Executive summary

Transesterification of fats & oils

- Transesterification is the largest source of diesel from biomass today.
- Active heterogeneous catalysts are required for ease of purification, process economy, lowering environmental impact and designing efficient continuous flow systems.
- Already suggested and auspicious heterogeneous catalysts are both organic and inorganic solid acids and bases, ionic liquids, or immobilized enzymes.
- Byproduct glycerol has found a few new industrial uses as raw material.

Deoxygenation of fats & oils

- Deoxygenation can be performed over traditional sulfided metal catalysts, supported noble-metal catalysts and porous acids or bases.
- The sulfided metals are employed industrially today.
- Noble metal catalysts are selective and consume less hydrogen but deactivate fast.
- Acidic or basic catalysts yield a mix of hydrocarbons and coke via cracking, but they are easy to regenerate.
- Side reactions and deactivation behavior must be understood and avoided with most catalysts, especially when using unsaturated fatty feedstock.

Deoxygenation of bio-oils

- Deoxygenation is more demanding than that of fats due to the multifunctional and aromatic nature of bio-oils; however the same catalysts have been studied.
- Catalytic pyrolysis may provide process simplification and higher energy efficiency.
- Net hydrogen consumption must be lowered, for instance by steam reforming of the feedstock, and the production of aromatics must be lowered.
- Primary deoxygenation of bio-oils is necessary before potential co-processing in petroleum refineries.
- Catalysts less prone to coking and deactivation should be developed or a durable regeneration strategy integrated.
- Deoxygenation of bio-oils and contingent hydrogen production should be integrated with the gaseous products from flash pyrolysis for higher process efficiency.

Aqueous-phase reforming, aldol-condensations & ketonization

- Aqueous-phase reforming is a two-phase process for reforming water-soluble carbohydrates into hydrocarbons. Also cellulose and hemicelluloses may be used as raw materials. The preferred catalyst is usually Pt-Re/C.
- High energy efficiency due to integrated heat- and hydrogen use, selective processes and mild reaction conditions.
- Pre- and post-reactions (hydrolysis, aldol-condensations, ketonization) of the aqueous-phase reforming can target the plant layout towards the desired hydrocarbon product range; the yield of diesel-range hydrocarbons should be optimized.

Gasification & Fischer–Tropsch synthesis

- All biomass can be gasified into synthesis gas and 'reconstructed' as hydrocarbons via Fischer–Tropsch synthesis (FTS).
- Gasifiers are economy-of-scale equipment, and logistics of biomass collection and energy efficiency trade-offs are important. Plant and process economy should be optimized for smaller, decentralized units.
- Gasification yield should be optimized for temperatures as low as possible, for instance via catalysis.
- Gas cleaning and cooling must be performed to avoid coking, clogging, corrosion and side-reactions, as well as FTS catalyst deactivation.
- The FTS catalysts are improved by tailoring the active site structure for higher activity and selectivity via promotion, bi-functional catalysts and use of porous materials.
- The FTS catalyst tolerance to impurities of N-, P- or S-containing compounds or alkali salts should be addressed.

Future perspective

- Different types of diesel fuels from biomass will be used together in the near future.
- Waste feedstocks will get a more prominent role due to ecological considerations and their low price. Food versus fuel dilemma will be increasingly controversial. Technologies to convert agricultural and forestry waste of all kinds to fuels will be increasingly important.

Bibliography

Papers of special note have been highlighted as:

- ■ of interest
- ■■ of considerable interest

1 Directive 2003/30/EC of the European Parliament and of the Council. *Offic. J. European Union* 12(2), 1–20 (2003).

2 The European Commission. Renewable Energy Road Map. *Renewable Energies in the 21st Century: Building a More Sustainable Future. Working Paper: COM(2006) 848 Final*. The European Commission, Brussels, Belgium (2007).

3 Meher LC, Vidya Sagar D, Naik SN. Technical aspects of biodiesel production by transesterification – a review. *Renew. Sust. Energy Rev.* 10(3), 248–268 (2006).

4 Mittelbach M, Remschmidt C. *Biodiesel: the Comprehensive Handbook*. Mittelbach M (Ed.). Martin Mittelbach, Graz, Austria (2006).

5 Knothe G. Biodiesel: current trends and properties. *Top. Catal.* 53(11–12), 714–720 (2010).

6 Snåre M, Kubicková I, Mäki-Arvela P, Eränen K, Murzin DY. Heterogeneous catalytic deoxygenation of stearic acid for production of biodiesel. *Ind. Eng. Chem. Res.* 45(16), 5708–5715 (2006).

7 Huber GW, Corma A. Synergies between bio- and oil refineries for the production of fuels from biomass. *Angew. Chem. Int. Ed.* 46(38), 7184–7201 (2007).

■■ **Review on the possibilites for producing biofuels in existing refinery infrastructure, with emphasis especially on catalytic cracking and hydrotreatment**

8 Guzman A, Torres JE, Prada LP, Nuñez ML. Hydroprocessing of crude palm oil at pilot plant scale. *Catal. Today.* 156(1–2), 38–43 (2010).

9 Simakova I, Simakova O, Mäki-Arvela P, Murzin DY. Decarboxylation of fatty acids over Pd supported on mesoporous carbon. *Catal. Today.* 150(1–2), 28–31 (2010).

10 Kikhtyanin OV, Rubanov AE, Ayupov AB, Echevsky GV. Hydroconversion of sunflower oil on Pd/SAPO-31 catalyst. *Fuel* 89(10), 3085–3092 (2010).

11 Tamunaidu P, Bhatia S. Catalytic cracking of palm oil for the production of biofuels: optimization studies. *Bioresour. Technol.* 98(18), 3593–3601 (2007).

12 Na J-G, Yi BE, Kim JN *et al.* Hydrocarbon production from decarboxylation of fatty acid without hydrogen. *Catal. Today.* 156(1–2), 44–48 (2009).

13 Šimáček P, Kubička D. Hydrocracking of petroleum vacuum distillate containing rapeseed oil: evaluation of diesel fuel. *Fuel* 89(7), 1508–1513 (2010).

14 Huber GW, Chheda JN, Barrett CJ, Dumesic JA. Production of liquid alkanes by aqueous-phase processing of biomass-derived carbohydrates. *Science* 308(5727), 1446–1450 (2005).

15 Chheda JN, Huber GW, Dumesic JA. Liquid-phase catalytic processing of biomass-derived oxygenated hydrocarbons to fuels and chemicals. *Angew. Chem. Int. Ed.* 46(38), 7164–7183 (2007).

16 Serrano-Ruiz JC, Wang D, Dumesic JA. Catalytic upgrading of levulinic acid to 5-nonanone. *Green Chem.* 12(4), 574–577 (2010).

17 Abatzoglou N, Dalai A, Gitzhofer F. Green diesel from Fischer–Tropsch synthesis: challenges and hurdles. Presented at: *3rd IASME/WSEAS international conference on energy, environment, ecosystems and sustainable development*. Greece, 24–26 July 2007.

18 Zhang W. Automotive fuels from biomass via gasification. *Fuel Process. Technol.* 91(8), 866–876 (2010).

19 Stöcker M. Biofuels and biomass-to-liquid fuels in the biorefinery: catalytic conversion of lignocellulosic biomass using porous materials. *Angew. Chem., Int. Ed.* 47(48), 9200–9211 (2008).

20 Carlson TR, Jae J, Lin Y-C, Tompsett GA, Huber GW. Catalytic fast pyrolysis of glucose with HZSM-5: the combined homogeneous and heterogeneous reactions. *J. Catal.* 270(1), 110–124 (2010).

21 Wildschut J, Mahfud FH, Venderbosch RH, Heeres HJ. Hydrotreatment of fast pyrolysis oil using heterogeneous noble-metal catalysts. *Ind. Eng. Chem. Res.* 48(23), 10324–10334 (2009).

22 Donnis B, Egeberg RG, Blom P, Knudsen KG. Hydroprocessing of bio-oils and oxygenates to hydrocarbons. Understanding the reaction routes. *Top. Catal.* 52(3), 229–240 (2009).

23 Knothe G. Analyzing biodiesel: standards and other methods. *J. Am. Oil Chem. Soc.* 83(10), 823–833 (2006

24 Koskinen M, Sourander M, Nurminen M. Apply a comprehensive approach to biofuels. *Hydrocarb. Process.* 85(2), 81–86 (2006

25 Snåre M, Murzin DY. Reply to 'Comment on heterogeneous catalytic deoxygenation of stearic acid for production of biodiesel'. *Ind. Eng. Chem. Res.* 45(20), 6875–6875 (2006).

26 Mikkonen S. Second-generation renewable diesel offers advantages. *Hydrocarb. Process.* 87(Feb), 63–66 (2008).

27 Sharma YC, Singh B, Korstad J. Advancements in solid acid catalysts for ecofriendly and economically viable synthesis of biodiesel. *Biofpr.* 5(1), 69–92 (2011).

28 Yan S, DiMaggio C, Mohan S, Kim M, Salley SO, Ng KYS. Advancements in heterogeneous catalysis for biodiesel synthesis. *Top. Catal.* 53(11–12), 721–736 (2010).

29 Melero JA, Iglesias J, Morales G. Heterogeneous acid catalysts for biodiesel production: current status and future challenges. *Green Chem.* 11(9), 1285–1308 (2009).

30 Semwal S, Arora AK, Badoni RP, Tuli DK. Biodiesel production using heterogeneous catalysts. *Bioresour. Technol.* 102(3), 2151–2161 (2010).

31 Choudhary TV, Phillips CB. Renewable fuels via catalytic hydrodeoxygenation. *Appl. Catal. A* 397(1–2), 1–12 (2011)

32 Bulushev DA, Ross JHR. Catalysis for conversion of biomass to fuels via pyrolysis and gasification: a review. *Catal. Today* DOI: 10.1016/j.cattod.2011.02.005 (2011) (Epub ahead of print).

33 Huber GW, Iborra S, Corma A. Synthesis of transportation fuels from biomass: chemistry, catalysts, and engineering. *Chem. Rev.* 106(9), 4044–4098 (2006).

■ **Description and comparison of feedstocks and methods for the production of biofuel, especially emphasizing the catalytic chemistry involved.**

34 Jacobson K, Gopinath R, Meher LC, Dalai AK. Solid acid catalyzed biodiesel production from waste cooking oil. *Appl. Catal. B* 85(1–2), 86–91 (2008).

35 Casanave D, Duplan J-L, Freund E. Diesel fuels from biomass. *Pure Appl. Chem.* 79(11), 2071–2081 (2007).

36 Sivasamy A, Cheah KY, Fornasiero P, Kemausuor F, Zinoviev S, Miertus S. catalytic applications in the production of biodiesel from vegetable oils. *ChemSusChem* 2(4), 278–300 (2009).

37 Lotero E, Liu Y, Lopez DE, Suwannakarn K, Bruce DA, Goodwin Jr JG. Synthesis of biodiesel via acid catalysis. *Ind. Eng. Chem. Res.* 44(14), 5353–5363 (2005).

38 Demirbas A. Biodiesel production from vegetable oils via catalytic and non-catalytic supercritical methanol transesterification methods. *Progress Energ. Combust. Science* 31(5–6), 466–487 (2005).

39 Mo X, Lotero E, Lu C, Liu Y, Goodwin JG.

A novel sulfonated carbon composite solid acid catalyst for biodiesel synthesis. *Catal. Lett.* 123(1–2), 1–6 (2008).

40 Liu X, He H, Wang Y, Zhu S. Transesterification of soybean oil to biodiesel using SrO as a solid base catalyst. *Catal. Comm.* 8(7), 1107–1111 (2007).

41 Pugnet V, Maury S, Coupard V *et al.* Stability, activity and selectivity study of a zinc aluminate heterogeneous catalyst for the transesterification of vegetable oil in batch reactor. *Appl. Catal. A* 374(1–2), 71–78 (2010).

42 Russbueldt BME, Hoelderich WF. New rare earth oxide catalysts for the transesterification of triglycerides with methanol resulting in biodiesel and pure glycerol. *J. Catal.* 271(2), 290–304 (2010).

43 Kawashima A, Matsubara K, Honda K. Development of heterogeneous base catalysts for biodiesel production. *Bioresour. Technol.* 99(9), 3439–3443 (2008).

44 Shu Q, Yang B, Yuan H, Qing S, Zhu G. Synthesis of biodiesel from soybean oil and methanol catalyzed by zeolite beta modified with La^{3+}. *Catal. Comm.* 8(12), 2158–2164 (2007).

45 Macario A, Giordano G, Onida B, Cocina D, Tagarelli A, Giuffrè AM. Biodiesel production process by homogeneous/heterogeneous catalytic system using an acid–base catalyst. *Appl. Catal. A* 378(2), 160–168 (2010).

46 Li E, Rudolph V. Transesterification of vegetable oil to biodiesel over mgo-functionalized mesoporous catalysts. *Energy Fuels* 22(1), 145–149 (2008).

47 Georgogianni KG, Katsoulidis AP, Pomonis PJ, Kontominas MG. Transesterification of soybean frying oil to biodiesel using heterogeneous catalysts. *Fuel Process. Technol.* 90(5), 671–676 (2009).

48 Georgogianni KG, Katsoulidis AK, Pomonis PJ, Manos G, Kontominas MG. Transesterification of rapeseed oil for the production of biodiesel using homogeneous and heterogeneous catalysis. *Fuel Process. Technol.* 90(7–8), 1016–1022 (2009).

49 Liu Y, Lotero E, Goodwin Jr JG, Mo X. Transesterification of poultry fat with methanol using Mg-Al hydrotalcite derived catalysts. *Appl. Catal. A* 331(), 138–148 (2007).

50 Brito A, Borges ME, Garín M, Hernández A. Biodiesel production from waste oil using Mg-Al layered double hydroxide catalysts. *Energy Fuels.* 23(6), 2952–2958 (2009).

51 Kim MJ, Park SM, Chang DR, Seo G. Transesterification of triacetin, tributyrin, and soybean oil with methanol over hydrotalcites with different water contents. *Fuel Process. Technol.* 91(6), 618–624 (2010).

52 Chuayplod P, Trakarnpruk W. Transesterification of rice bran oil with methanol catalyzed by Mg(Al)La hydrotalcites and metal/MgAl oxides. *Ind. Eng. Chem. Res.* 48(9), 4177–4183 (2009).

53 Macala GS, Robertson AW, Johnson CL *et al.* Transesterification catalysts from iron doped hydrotalcite-like precursors: solid bases for biodiesel production. *Catal. Lett.* 122(3), 205–209 (2008).

54 Li E, Xu ZP, Rudolph V. MgCoAl-LDH derived heterogeneous catalysts for the ethanol transesterification of canola oil to biodiesel. *Appl. Catal. B* 88(1–2), 42–49 (2009).

55 Guerreiro L, Pereira PM, Fonseca IM *et al.* PVA embedded hydrotalcite membranes as basic catalysts for biodiesel synthesis by soybean oil methanolysis. *Catal. Today* 156(3–4), 191–197 (2010).

56 Schuchardt U. Transesterification of soybean oil catalyzed by alkylguanidines heterogenized on different substituted polystyrenes. *J. Mol. Catal. A: Chem.* 109(1), 37–44 (1996).

57 Villa A, Tessonnier J-P, Majoulet O, Su DS, Schlögl R. Amino-functionalized carbon nanotubes as solid basic catalysts for the transesterification of triglycerides. *Chem. Comm.* (29), 4405–4407 (2009).

58 Cerro-Alarcón M, Corma A, Iborra S, Martínez C, Sabater MJ. Methanolysis of sunflower oil using gem-diamines as active organocatalysts for biodiesel production. *Appl. Catal. A* 382(1), 36–42 (2010).

59 Cerro-Alarcón M, Corma A, Iborra S, Gómez JP. Biomass to fuels: a water-free process for biodiesel production with phosphazene catalysts. *Appl. Catal. A* 346(1–2), 52–57 (2008).

60 Kim M-Y, Seo G, Kwon OZ, Chang DR. The exceptional activity of a phosphazenium hydroxide catalyst incorporated onto silica in the transesterification of tributyrin with methanol. *Chem. Comm.* (21), 3110–3112 (2009).

61 Verziu M, El Haskouri J, Beltran D *et al.* Mesoporous tin–triflate based catalysts for transesterification of sunflower oil. *Top. Catal.* 53(11–12), 763–772 (2010).

62 Saravanamurugan S, Han D, Koo J, Park S. Transesterification reactions over morphology controlled amino-functionalized SBA-15 catalysts. *Catal. Comm.* 9(1), 158–163 (2008).

63 Savonnet M, Aguado S, Ravon U *et al.* Solvent free base catalysis and transesterification over basic functionalised metal–organic frameworks. *Green Chem.* 11(11), 1729–1732 (2009).

64 Liu Y, Lotero E, Goodwinjr J, Lu C. Transesterification of triacetin using solid Brønsted bases. *J. Catal.* 246(2), 428–433 (2007).

65 Sunita G, Devassy BM, Vinu A, Sawant DP, Balasubramanian VV, Halligudi SB. Synthesis of biodiesel over zirconia-supported isopoly and heteropoly tungstate catalysts. *Catal. Comm.* 9(5), 696–702 (2008).

66 Park Y-M, Lee JY, Chung S-H *et al.* Esterification of used vegetable oils using the heterogeneous WO_3/ZrO_2 catalyst for production of biodiesel. *Bioresour. Technol.* 101(Suppl. 1), S59–S61 (2010).

67 Komintarachat C, Chuepeng S. Solid acid catalyst for biodiesel production from waste used cooking oils. *Ind. Eng. Chem. Res.* 48(20), 9350–9353 (2009).

68 Ngaosuwan K, Mo X, Goodwin Jr JG, Praserthdam P. Effect of solvent on hydrolysis and transesterification reactions on tungstated zirconia. *Appl. Catal. A* 380(1–2), 81–86 (2010).

69 Kulkarni MG, Gopinath R, Meher LC, Dalai AK. Solid acid catalyzed biodiesel production by simultaneous esterification and transesterification. *Green Chem.* 8(12), 1056–1062 (2006).

70 Zhang X, Li J, Chen Y *et al.* Heteropolyacid nanoreactor with double acid sites as a highly efficient and reusable catalyst for the transesterification of waste cooking oil. *Energy Fuels.* 23(9), 4640–4646 (2009).

71 Morin P, Hamad B, Sapaly G *et al.* Transesterification of rapeseed oil with ethanol. I. Catalysis with homogeneous Keggin heteropolyacids. *Appl. Catal. A* 330, 69–76 (2007).

72 Oliveira CF, Dezaneti LM, Garcia FAC *et al.* Esterification of oleic acid with ethanol by 12-tungstophosphoric acid supported on zirconia. *Appl. Catal, A.* 372(2), 153–161 (2010).

73 Cardoso AL, Augusti R, Silva MJ. Investigation on the esterification of fatty acids catalyzed by the $H_3PW_{12}O_{40}$ heteropolyacid. *J. Am. Oil Chem. Soc.* 85(6), 555–560 (2008).

74 Srilatha K, Lingaiah N, Devi BLAP, Prasad RBN, Venkateswar S, Prasad PSS. Esterification of free fatty acids for biodiesel production over heteropoly tungstate

supported on niobia catalysts. *Appl. Catal. A* 365(1), 28–33 (2009).

75 Xu L, Wang Y, Yang X, Hu J, Li W, Guo Y. Simultaneous esterification and transesterification of soybean oil with methanol catalyzed by mesoporous Ta_2O_5/SiO_2–[$H_3PW_{12}O_{40}$/R] (R = Me or Ph) hybrid catalysts. *Green Chem.* 11(3), 314–317 (2009).

76 Lam MK, Lee KT, Mohamed AR. Sulfated tin oxide as solid superacid catalyst for transesterification of waste cooking oil: an optimization study. *Appl. Catal. B* 93(1–2), 134–139 (2009).

77 Suwannakarn K, Lotero E, Goodwin Jr JG, Lu C. Stability of sulfated zirconia and the nature of the catalytically active species in the transesterification of triglycerides. *J. Catal.* 255(2), 279–286 (2008).

78 Du Y, Liu S, Ji Y *et al.* Synthesis of sulfated silica-doped tin oxides and their high activities in transesterification. *Catal. Lett.* 124(1–2), 133–138 (2008).

79 López DE, Goodwin Jr JG, Bruce DA, Furuta S. Esterification and transesterification using modified-zirconia catalysts. *Appl. Catal. A* 339(1), 76–83 (2008).

80 Rattanaphra D, Harvey A, Srinophakun P. simultaneous conversion of triglyceride/free fatty acid mixtures into biodiesel using sulfated zirconia. *Top. Catal.* 53(), 773–782 (2010).

81 JC, Zhang J, Yarmo MA. Structure and reactivity of silica-supported zirconium sulfate for esterification of fatty acid under solvent-free condition. *Appl. Catal. A* 332(2), 209–215 (2007).

82 Chung K-H, Chang D-R, Park B-G. Removal of free fatty acid in waste frying oil by esterification with methanol on zeolite catalysts. *Bioresour. Technol.* 99(16), 7438–7443 (2008).

83 Carmo Jr A, Desouza L, Dacosta C, Longo E, Zamian J, Darochafilho G. Production of biodiesel by esterification of palmitic acid over mesoporous aluminosilicate Al-MCM-41. *Fuel* 88(3), 461–468 (2009).

84 Jiménez-Morales I, Santamaría-González J, Maireles-Torres P, Jiménez-López A. Zirconium doped MCM-41 supported WO_3 solid acid catalysts for the esterification of oleic acid with methanol. *Appl. Catal. A* 379(1–2), 61–68 (2010).

85 Dhainaut J.; Dacquin J-P, Lee AF, Wilson K. Hierarchical macroporous–mesoporous SBA-15 sulfonic acidcatalysts for biodiesel synthesis. *Green Chem.* 12(2), 296–303 (2010).

86 Shibasaki-Kitakawa N, Tsuji T, Chida K, Kubo M, Yonemoto T. Simple Continuous production process of biodiesel fuel from oil with high content of free fatty acid using ion-exchange resin catalysts. *Energy Fuels.* 24(6), 3634–3638 (2010).

87 Özbay N, Oktar N, Tapan NA. Esterification of free fatty acids in waste cooking oils (WCO): Role of ion-exchange resins. *Fuel* 87(10–11), 1789–1798 (2008).

88 Feng Y, He B, Cao Y *et al.* Biodiesel production using cation-exchange resin as heterogeneous catalyst. *Bioresour. Technol.* 101(5), 1518–1521 (2010).

89 Caetano CS, Guerreiro L, Fonseca IM, Ramos AM, Vital J, Castanheiro JE. Esterification of fatty acids to biodiesel over polymers with sulfonic acid groups. *Appl. Catal. A* 359(1–2), 41–46 (2009).

90 Soldi RA, Oliveira ARS, Ramos LP, César-Oliveira MAF. Soybean oil and beef tallow alcoholysis by acid heterogeneous catalysis. *Appl. Catal. A* 361(1–2), 42–48 (2009).

91 Okayasu T, Saito K, Nishide H, Hearn MTW. Preparation of a novel poly(vinylsulfonic acid)-grafted solid phase acid catalyst and its use in esterification reactions. *Chem. Comm.* (31), 4708–4710 (2009).

92 Melero JA, Bautista LF, Iglesias J, Morales G, Sánchez-Vázquez R, Suárez-Marcos I. Biodiesel production over arenesulfonic acid-modified mesostructured catalysts: optimization of reaction parameters using response surface methodology. *Top. Catal.* 53(11–12), 795–804 (2010).

93 Zięba A, Drelinkiewicz A, Konyushenko E, Stejskal J. Activity and stability of polyaniline sulfate-based solid acid catalysts for the transesterification of triglycerides and esterification of fatty acids with methanol. *Appl. Catal. A* 383(1–2), 169–181 (2010).

94 Toda M, Takagaki A, Okamura M *et al.* Biodiesel made with sugar catalyst. *Nature* 438(7065), 178 (2005).

95 Hara M. Biodiesel production by amorphous carbon bearing SO_3H, COOH and phenolic OH groups, a solid Brønsted acid catalyst. *Top. Catal.* 53(11–12), 805–810 (2010).

96 Dehkhoda AM, West AH, Ellis N. Biochar based solid acid catalyst for biodiesel production. *Appl. Catal. A* 382(2), 197–204 (2010).

97 Lien Y-S, Hsieh L-S, Wu JCS. Biodiesel synthesis by simultaneous esterification and transesterification using oleophilic acid catalyst. *Ind. Eng. Chem. Res.* 49(5), 2118–2121 (2010).

98 Nakajima K, Okamura M, Kondo JN *et al.* Amorphous carbon bearing sulfonic acid groups in mesoporous silica as a selective catalyst. *Chem. Mater.* 21(1), 186–193 (2009).

99 Wu Q, Chen H, Han M, Wang D, Wang J. Transesterification of cottonseed oil catalyzed by brønsted acidic ionic liquids. *Ind. Eng. Chem. Res.* 46(24), 7955–7960 (2007).

100 Lapis AAM, de Oliveira LF, Neto BAD, Dupont J. Ionic liquid supported acid/base-catalyzed production of biodiesel. *ChemSusChem* 1(8–9), 759–762 (2008).

101 DaSilveira Neto B, Alves M, Lapis A *et al.* 1-n-butyl-3-methylimidazolium tetrachloro-indate (BMI.$InCl_4$) as a media for the synthesis of biodiesel from vegetable oils. *J. Catal.* 249(2), 154–161 (2007).

102 Han M, Yi W, Wu Q, Liu Y, Hong Y, Wang D. Preparation of biodiesel from waste oils catalyzed by a Brønsted acidic ionic liquid. *Bioresour. Technol.* 100(7), 2308–2310 (2009).

103 Li K-X, Chen L, Yan Z-C, Wang H-L. Application of pyridinium ionic liquid as a recyclable catalyst for acid-catalyzed transesterification of jatropha oil. *Catal. Lett.* 139(3–4), 151–156 (2010).

104 Liang X, Yang J. Synthesis of a novel multi-SO_3H functionalized ionic liquid and its catalytic activities for biodiesel synthesis. *Green Chem.* 12(2), 201–204 (2010).

105 Nassreddine S, Karout A, Lorraine Christ M, Pierre AC. Transesterification of a vegetal oil with methanol catalyzed by a silica fibre reinforced aerogel encapsulated lipase. *Appl. Catal. A* 344(1–2), 70–77 (2008).

106 Shakeri M, Kawakami K. Effect of the structural chemical composition of mesoporous materials on the adsorption and activation of the *Rhizopus oryzae* lipase-catalyzed trans-esterification reaction in organic solvent. *Catal. Comm.* 10(2), 165–168 (2008).

107 Dizge N, Aydiner C, Imer DY, Bayramoglu M, Tanriseven A, Keskinler B. Biodiesel production from sunflower, soybean, and waste cooking oils by transesterification using lipase immobilized onto a novel microporous polymer. *Bioresour. Technol.* 100(6), 1983–1991 (2009).

108 Keng PS, Basri M, Ariff AB, Abdul Rahman MB, Abdul Rahman RNZ, Salleh AB. Scale-up synthesis of lipase-catalyzed palm esters in stirred-tank reactor. *Bioresour. Technol.* 99(14), 6097–6104 (2008).

109 Fu B, Vasudevan PT. Effect of organic

solvents on enzyme-catalyzed synthesis of biodiesel. *Energy Fuels* 23(8), 4105–4111 (2009).

110 Xiao M, Mathew S, Obbard JP. Biodiesel fuel production via transesterification of oils using lipase biocatalyst. *GCB Bioenergy* 1(2), 115–125 (2009).

111 Hernández-Martín E, Otero C. Different enzyme requirements for the synthesis of biodiesel: novozym 435 and lipozyme TL IM. *Bioresour. Technol.* 99(2), 277–286 (2008).

112 Yin J, Xiao M, Song J. Biodiesel from soybean oil in supercritical methanol with co-solvent. *Energ. Convers. Manage.* 49(5), 908–912 (2008).

113 Hegel P, Mabe G, Pereda S, Brignole E. Phase transitions in a biodiesel reactor using supercritical methanol. *Ind. Eng. Chem. Res.* 46(19), 6360–6365 (2007).

114 Saka S, Isayama Y, Ilham Z, Jiayu X. New process for catalyst-free biodiesel production using subcritical acetic acid and supercritical methanol. *Fuel* 89(7), 1442–1446 (2010).

115 Zhou C-HC, Beltramini JN, Fan Y-X, Lu GQM. Chemoselective catalytic conversion of glycerol as a biorenewable source to valuable commodity chemicals. *Chem. Soc. Rev.* 37(3), 527–549 (2008).

116 Johnson DT, Taconi KA. The glycerin glut: options for the value-added conversion of crude glycerol resulting from biodiesel production. *Environm. Progress.* 26(4), 338–348 (2007).

117 Kubička D, Kaluža L. Deoxygenation of vegetable oils over sulfided Ni, Mo and NiMo catalysts. *Appl. Catal. A* 372(2), 199–208 (2010).

118 Šimáček P, Kubička D, Šebor G, Pospíšil M. Hydroprocessed rapeseed oil as a source of hydrocarbon-based biodiesel. *Fuel* 88(3), 456–460 (2009).

119 Kubička D, Bejblová M, Vlk J. Conversion of vegetable oils into hydrocarbons over CoMo/MCM-41 catalysts. *Top. Catal.* 53(3–4), 168–178 (2010).

120 Kubička D, Šimáček P, Žilková N. Transformation of vegetable oils into hydrocarbons over mesoporous-alumina-supported CoMo catalysts. *Top. Catal.* 52(1–2), 161–168 (2009).

121 Huber GW, O'Connor P, Corma A. Processing biomass in conventional oil refineries: production of high quality diesel by hydrotreating vegetable oils in heavy vacuum oil mixtures. *Appl. Catal. A* 329, 120–129 (2007).

122 Şenol O, Viljava T-R, Krause AOI. Effect of sulphiding agents on the hydrodeoxygenation of aliphatic esters on sulphided catalysts. *Appl. Catal. A* 326(2), 236–244 (2007).

123 Ryymin E-M, Honkela ML, Viljava T-R, Krause AOI. Insight to sulfur species in the hydrodeoxygenation of aliphatic esters over sulfided NiMo/γ-Al_2O_3 catalyst. *Appl. Catal. A* 358(1), 42–48 (2009).

124 Snåre M, Kubičková I, Mäki-Arvela P, Eränen K, Wärnå J, Murzin DY. Production of diesel fuel from renewable feeds: Kinetics of ethyl stearate decarboxylation. *Chem. Eng. J.* 134(1–3), 29–34 (2007).

125 Mäki-Arvela P, Kubičková I, Snåre M, Eränen K, Murzin DY. Catalytic deoxygenation of fatty acids and their derivatives. *Energy Fuels* 21(1), 30–41 (2007).

126 Do PT, Chiappero M, Lobban LL, Resasco DE. catalytic deoxygenation of methyl-octanoate and methyl-stearate on Pt/Al_2O_3. *Catal. Lett.* 130(1–2), 9–18 (2009).

127 Rozmysłowicz B, Mäki-Arvela P, Lestari S *et al.* Catalytic deoxygenation of tall oil fatty acids over a palladium-mesoporous carbon catalyst: a new source of biofuels. *Top. Catal.* 53(15–18), 1274–1277 (2010).

128 Morgan T, Grubb D, Santillan-Jimenez E, Crocker M. Conversion of triglycerides to hydrocarbons over supported metal catalysts. *Top. Catal.* 53(11–12), 820–829 (2010).

129 Lestari S, Mäki-Arvela P, Eränen K, Beltramini J, Max Lu GQ, Murzin DY. diesel-like hydrocarbons from catalytic deoxygenation of stearic acid over supported Pd nanoparticles on SBA-15 catalysts. *Catal. Lett.* 134(3–4), 250–257 (2009).

130 Ping EW, Wallace R, Pierson J, Fuller TF, Jones CW. Highly dispersed palladium nanoparticles on ultra-porous silica mesocellular foam for the catalytic decarboxylation of stearic acid. *Microporous Mesoporous Mater.* 132(1–2), 174–180 (2010).

131 Hancsók J, Krár M, Magyar S, Boda L, Holló A, Kalló D. Investigation of the production of high cetane number bio gas oil from pre-hydrogenated vegetable oils over Pt/HZSM-22/Al_2O_3. *Microporous Mesoporous Mater.* 101(1–2), 148–152 (2007).

132 Lestari S, Mäki-Arvela P, Bernas H *et al.* catalytic deoxygenation of stearic acid in a continuous reactor over a mesoporous carbon-supported Pd catalyst. *Energy Fuels* 23(8), 3842–3845 (2009).

133 Danuthai T, Jongpatiwut S, Rirksomboon T, Osuwan S, Resasco DE. Conversion of methylesters to hydrocarbons over an H-ZSM5 zeolite catalyst. *Appl. Catal. A* 361(1–2), 99–105 (2009).

134 Sooknoi T, Danuthai T, Lobban LL, Mallinson R, Resasco DE. Deoxygenation of methylesters over CsNaX. *J. Catal.* 258(1), 199–209 (2008).

135 Sang OY. Biofuel production from catalytic cracking of palm oil. *Energy Sourc. A.* 25(9), 859–869 (2003).

136 Quirino RL, Tavares AP, Peres AC, Rubim JC, Suarez PAZ. Studying the influence of alumina catalysts doped with tin and zinc oxides in the soybean oil pyrolysis reaction. *J. Am. Oil Chem. Soc.* 86(2), 167–172 (2008).

137 Knežević D, Schmiedl D, Meier D, Kersten S, van Swaaij W. High-throughput screening technique for conversion in hot compressed water: quantification and characterization of liquid and solid products. *Ind. Eng. Chem. Res.* 46(6), 1810–1817 (2007).

138 Hammerschmidt A, Boukis N, Hauer E *et al.* Catalytic conversion of waste biomass by hydrothermal treatment. *Fuel* 90(2), 555–562 (2011).

139 Elliott DC, Hart TR, Neuenschwander GG, Rotness LJ, Zacher AH. Catalytic hydroprocessing of biomass fast pyrolysis bio-oil to produce hydrocarbon products. *Environ. Prog. Sust. Energ.* 28(3), 441–449 (2009).

■ **Meticulous investigation of various upgrading procedures for bio-oils, especially concerning the resulting liquid composition of upgraded fast pyrolysis oils from various sources.**

140 Aho A, Kumar N, Lashkul AV *et al.* Catalytic upgrading of woody biomass derived pyrolysis vapours over iron modified zeolites in a dual-fluidized bed reactor. *Fuel* 89(8), 1992–2000 (2010).

141 Aho A, Kumar N, Eränen K, Salmi T, Hupa M, Murzin DY. Catalytic pyrolysis of woody biomass in a fluidized bed reactor: influence of the zeolite structure. *Fuel* 87(12), 2493–2501 (2008).

142 Valle B, Gayubo AG, Alonso A, Aguayo AT, Bilbao J. Hydrothermally stable HZSM-5 zeolite catalysts for the transformation of crude bio-oil into hydrocarbons. *Appl. Catal. A* 100(1–2), 318–327 (2010).

143 de MiguelMercader F, Groeneveld MJ, Kersten SRA, Way NWJ, Schaverien CJ, Hogendoorn J. Production of advanced biofuels: co-processing of upgraded pyrolysis oil in standard refinery units. *Appl. Catal. B* 96(1–2), 57–66 (2010).

144 Mullen CA, Boateng AA. Catalytic pyrolysis-GC/MS of lignin from several sources. *Fuel Process. Technol.* 91(11), 1446–1458 (2010).

145 Carlson TR, Tompsett GA, Conner WC,

Huber GW. Aromatic production from catalytic fast pyrolysis of biomass-derived feedstocks. *Top. Catal.* 52(3), 241–252 (2009).

146 Ferrari M, Maggi R, Delmon B, Grange P. Influences of the hydrogen sulfide partial pressure and of a nitrogen compound on the hydrodeoxygenation activity of a CoMo/carbon catalyst. *J. Catal.* 198(1), 47–55 (2001).

147 Gutierrez A, Domine M, Solantausta Y. Co-processing of upgraded bio-liquids in standard refinery units – fundamentals. Presented at: *15th European Biomass Conference & Exhibition*. Berlin, Germany, 7–11 May 2007.

148 Şenol O, Ryymin E-M, Viljava T-R, Krause AOI. Effect of hydrogen sulphide on the hydrodeoxygenation of aromatic and aliphatic oxygenates on sulphided catalysts. *J. Mol. Catal. A Chem*. 277(1–2), 107–112 (2007).

149 French RJ, Hrdlicka J, Baldwin R. Mild hydrotreating of biomass pyrolysis oils to produce a suitable refinery feedstock. *Environ. Prog. Sustainable Energy.* 29(2), 142–150 (2010).

150 Kunkes EL, Simonetti DA, West RM, Serrano-Ruiz JC, Gärtner CA, Dumesic JA. Catalytic conversion of biomass to monofunctional hydrocarbons and targeted liquid-fuel classes. *Science* 322(5900), 417–421 (2008).

151 West RM, Kunkes EL, Simonetti DA, Dumesic J. Catalytic conversion of biomass-derived carbohydrates to fuels and chemicals by formation and upgrading of mono-functional hydrocarbon intermediates. *Catal. Today.* 147(2), 115–125 (2009).

152 Li N, Huber GW. Aqueous-phase hydrodeoxygenation of sorbitol with Pt/SiO2-Al2O3: Identification of reaction intermediates. *J. Catal.* 270(1), 48–59 (2010).

153 Román-Leshkov Y, Barrett CJ, Liu ZY, Dumesic J. Production of dimethylfuran for liquid fuels from biomass-derived carbohydrates. *Nature* 447(7147), 982–985 (2007).

154 Chheda J, Dumesic J. An overview of dehydration, aldol-condensation and hydrogenation processes for production of liquid alkanes from biomass-derived carbohydrates. *Catal. Today* 123(1–4), 59–70 (2007).

■ **Outline of aqueous-phase reforming reactions to biofuels from sugars, with emphasis on carbon yields, catalysts and selectivities.**

155 Bond JQ, Alonso DM, Wang D, West RM, Dumesic JA. Integrated catalytic conversion of g-valerolactone to liquid alkenes for transportation fuels. *Science* 327(5969), 1110–1114 (2010).

156 Gärtner CA, Serrano-Ruiz JC, Braden DJ, Dumesic JA. Catalytic coupling of carboxylic acids by ketonization as a processing step in biomass conversion. *J. Catal.* 266(1), 71–78 (2009).

157 Gürbüz EI, Kunkes EL, Dumesic JA. Dual-bed catalyst system for C-C coupling of biomass-derived oxygenated hydrocarbons to fuel-grade compounds. *Green Chem*. 12(2), 223–227 (2010).

158 Gärtner CA, Serrano-Ruiz JC, Braden DJ, Dumesic J. Catalytic upgrading of bio-oils by ketonization. *ChemSusChem* 2(12), 1121–1124 (2009).

159 Gürbüz EI, Kunkes EL, Dumesic J. Integration of C-C coupling reactions of biomass-derived oxygenates to fuel-grade compounds. *Appl. Catal. B* 94(1–2), 134–141 (2010).

160 Serrano-Ruiz JC, Braden DJ, West RM, Dumesic J. Conversion of cellulose to hydrocarbon fuels by progressive removal of oxygen. *Appl. Catal. B* 100(1–2), 184–189 (2010).

161 McKendry P. Energy production from biomass (part 3): gasification technologies. *Bioresour. Technol.* 83(1), 55–63 (2002).

162 Moilanen A, Nasrullah M, Kurkela E. The effect of biomass feedstock type and process parameters on achieving the total carbon conversion in the large scale fluidized bed gasification of biomass. *Environ. Prog. Sust. Energ.* 28(3), 355–359 (2009).

163 Kunkes E, Simonetti D, Dumesic J *et al.* The role of rhenium in the conversion of glycerol to synthesis gas over carbon supported platinum-rhenium catalysts. *J. Catal.* 260(1), 164–177 (2008).

164 Rass-Hansen J, Christensen CH, Sehested J, Helveg S, Rostrup-Nielsen JR, Dahl S. Renewable hydrogen: carbon formation on Ni and Ru catalysts during ethanol steam-reforming. *Green Chem.* 9(9), 1016–1021 (2007).

165 Matsumura Y, Minowa T, Potic B *et al.* Biomass gasification in near- and super-critical water: Status and prospects. *Biomass Bioenergy* 29(4), 269–292 (2005).

166 Campoy M, Gómez-Barea A, Villanueva AL, Ollero P. Air-steam gasification of biomass in a fluidized bed under simulated autothermal and adiabatic conditions. *Ind. Eng. Chem. Res.* 47(16), 5957–5965 (2008).

167 Wolfesberger U, Aigner I, Hofbauer H. Tar content and composition in producer gas of fluidized bed gasification of wood-Influence of temperature and pressure. *Environ. Prog. Sust. Energ.* 28(3), 372–379 (2009).

168 Zwart RWR, Van der Drift A, Bos A, Visser HJM, Cieplik MK, Könemann HWJ. Oil-based gas washing-flexible tar removal for high-efficient production of clean heat and power as well as sustainable fuels and chemicals. *Environ. Prog. Sust. Energ.* 28(3), 324–335 (2009).

169 Pope CJ, Marrone PA, Yeh BV. Thermodynamic driving forces for postgasification carbon deposition. *Environ. Prog. Sus. Energ.* 29(2), 151–162 (2010).

170 Torres W, Pansare S, Goodwin Jr JG. Hot gas removal of tars, ammonia, and hydrogen sulfide from biomass gasification gas. *Catal. Rev.* 49(4), 407–456 (2007).

171 Simonetti DA, Rass-Hansen J, Kunkes EL, Soares RR, Dumesic JA. Coupling of glycerol processing with Fischer–Tropsch synthesis for production of liquid fuels. *Green Chem*. 9(10), 1073–1083 (2007).

172 Gamba S, Pellegrini La, Calemma V, Gambaro C. Liquid fuels from Fischer–Tropsch wax hydrocracking: isomer distribution. *Catal. Today.* 156(1–2), 58–64 (2010).

173 Tavasoli A, Trépanier M, Dalai AK, Abatzoglou N. Effects of confinement in carbon nanotubes on the activity, selectivity, and lifetime of Fischer–Tropsch Co/carbon nanotube catalysts. *J. Chem. Eng. Data*. 55(8), 2757–2763 (2011).

174 Tavasoli A, Trépanier M, MalekAbbaslou RM, Dalai AK, Abatzoglou N. Fischer–Tropsch synthesis on mono- and bimetallic Co and Fe catalysts supported on carbon nanotubes. *Fuel Process. Technol.* 90(12), 1486–1494 (2009).

175 Ma W, Kugler EL, Wright J, Dadyburjor DB. Mo- Fe catalysts supported on activated carbon for synthesis of liquid fuels by the Fischer–Tropsch process: effect of mo addition on reducibility, activity, and hydrocarbon selectivity. *Energy Fuels* 20(6), 2299–2307 (2006).

176 Herranz T, Rojas S, Perezalonso F, Ojeda M, Terreros P, Fierro J. Genesis of iron carbides and their role in the synthesis of hydrocarbons from synthesis gas. *J. Catal.* 243(1), 199–211 (2006).

177 Trepanier M, Tavasoli A, Dalai A, Abatzoglou N. Co, Ru and K loadings effects on the activity and selectivity of carbon nanotubes supported cobalt catalyst in Fischer–Tropsch synthesis. *Appl. Catal. A* 353(2), 193–202 (2009).

178 Chen W, Fan Z, Pan X, Bao X. Effect of confinement in carbon nanotubes on the activity of Fischer–Tropsch iron catalyst. *J. Am. Chem. Soc.* 130(29), 9414–9419 (2008).

179 Liu S, Gujar AC, Thomas P, Toghiani H, White MG. Synthesis of gasoline-range hydrocarbons over Mo/HZSM-5 catalysts. *Appl. Catal. A* 357(1), 18–25 (2009).

180 Christensen JM, Mortensen PM, Trane R, Jensen PA, Jensen AD. Effects of H_2S and process conditions in the synthesis of mixed alcohols from syngas over alkali promoted cobalt-molybdenum sulfide. *Appl. Catal. A* 366(1), 29–43 (2009).

181 Durham E, Zhang S, Roberts C. Diesel-length aldehydes and ketones via supercritical Fischer Tropsch synthesis on an iron catalyst. *Appl. Catal. A* 386(1–2), 65–73 (2010).

182 Kintisch E. The greening of synfuels. *Science* 320(5874), 306–308 (2008).

183 Henrich E, Dahmen N, Dinjus E. Cost estimate for biosynfuel production via biosyncrude gasification. *Biofuels Bioprod. Biorefin.* 3(1), 28–41 (2009).

■ **Evaluation of costs, energy balance and logistic challenges with Germany as a case for synthetic fuel production via decentral pyrolysis and central gasification and Fischer–Tropsch synthesis.**

184 Knothe G. Biodiesel and renewable diesel: a comparison. *Progress Energ. Combust. Science* 36(3), 36, 364–373 (2010).

■■ **Thorough comparison of Renewable Diesel and FAME with respect to production, fuel properties and engine performance.**

■ Websites

201 Emerging Markets Online. www.emerging-markets.com/PDF/Biodiesel2020Study.pdf (Accessed 11 May 2011)

202 European Biodiesel Board. www.ebb-eu.org/prev_stats_production.php (Accessed 11 May 2011)

203 Fischer–Tropsch archive. www.fischer-tropsch.org (Accessed 11 May 2011)